Designing more sustainable thermosetting non-isocyanate polyurethane foams: from greener blowing agents to functional applications

Katherine Arlete Gouveia Jovel

April 21st, 2026

A thesis presented for the degree of
Doctor of Philosophy in Chemical Sciences

European Joint Doctorate
University of Mons (Belgium)
Faculty of Sciences, Chemical sciences
&
University of Montpellier (France)
CNRS-ICGM, Sciences Chimiques Balard Doctoral School
Academic year 2025-2026

Jury Members:

Pr. Jean-Marie Raquez	University of Mons, Belgium	Thesis Director
Pr. Sylvain Caillol	University of Montpellier, France	Thesis Director
Pr. Vincent Ladmiral	University of Montpellier, France	Thesis Co-director
Pr. Pascal Gerbaux	University of Mons, Belgium	Examiner
Dr. Anne Goldberg	University of Mons, Belgium	Invited member
Dr. Giada Lo Re	Chalmers University of technology, Sweden	Examiner
Pr. Christophe Detrembleur	University of Liege, Belgium	Reviewer
Pr. Henri Cramail	University of Bordeaux, France	Reviewer

To you, Mom. You taught me to be brave, to be strong and the power of big dreams.

Para ti mami, por haberme enseñado a ser valiente, fuerte y soñar en grande.

Acknowledgments

I would like to begin this section with some context, and what this project meant in my life. Thanks to this thesis, I came from Venezuela, my home country, to Belgium and France without knowing a single word of French and without really grasping what I was accepting or what would await me in the coming years. But, as with everything in life, if you don't take risks, you don't win, and I believe that in these 4 years I have personally gained far more than I could have ever remotely imagined. I leave this written here, so that if I ever want to reread my thesis in a few years, I can remember with the same emotion what I experienced and learned. But above all, remember that limits only exist in our minds.

After having moved 5 times throughout this project (approximately once a year) between coming to Mons, going to Montpellier, returning to Mons, and spending about 3 months in Ghent, I met incredible people who, beyond being colleagues, became friends. After many hours of classes, and many nights ending with headaches, I was able to learn French -despite still having my latin accent and the fact that, for me, *au-dessus* and *au-dessous* still sound the same; my Francophone colleagues understand me, speak to me in French, and I can even crack a joke or two. So, for me, that is already winning and more than enough.

I would like to begin by thanking primarily my supervisors, Jean-Marie Raquez and Sylvain Caillol, for giving me the opportunity to be part of this ambitious project and for seeing the potential in me to carry it out. For allowing me to work in their laboratories and giving me the freedom to develop my ideas. Jean-Marie, thank you especially for challenging me throughout these thesis years -although sometimes a bit more than I would have liked -and for believing in me and pushing me until the end during this challenging final year. Thank you for your advice, for caring about me, and for making me laugh with your jokes in French -which I didn't always understand. Sylvain, thank you for the support, for the good humor, for your availability, for being so considerate, for your humanity, and for finding the right words of encouragement at every moment.

Likewise, I would like to thank all the members of the jury: Henri Cramail, Christophe Detrembleur, Giada Lo Re, Pascal Gerbaux, Anne Goldberg, Vincent Ladmiral, Sylvain Caillol, and Jean-Marie Raquez, for having accepted to review and discuss this work.

I would like to thank my colleagues from the SMPC lab, who became friends and welcomed me during my first year of the thesis. Caro, thank you for always being willing to help me from

day 1, for teaching me French, and for your human warmth. I fondly remember the months we spent in Montpellier, the dinners, and the conversations we had about life. Sylvie, one of the most empathetic, big-hearted, passionate, and fun people I have ever met. Thank you for motivating me, listening to me, and advising me during my breakdowns and existential crises- let's say every other day. I loved being your desk neighbour and being able to laugh and understand each other just by exchanging glances. Noemi and Sebastien, thank you so much for your good humor, your jokes, and for always finding a little time to chat during lunch with coffee and teaching me so much French. Thanks also to the lab boys: Guillem, we arrived in Mons on the same day, not knowing that many rainy days awaited us! But we made it, we survived. Thank you for your willingness to help -especially when we had to cook foams at 'Show your PhD'- for your kindness and warmth. I admire your determination to keep improving yourself every day. Gabriel, for your nice vibes, for all our random and fun conversations, almost always next to the extruders. Thanks also to my girl friends Esra, Nazli, Emma, and Pavithra, for being so kind, for talking about everything and nothing, for distracting us, laughing, and spending such good times together. I will miss the girls' nights out! Pavi, it was super nice to have shared a year in the lab together and to learn from each other about our projects. Alma, Adrian and Louis, thanks for your party spirit.

Dear Anne, infinite thanks for your help in the final stage of my thesis. Thank you for being that ray of light I needed, for the unconditional support, for your time, for the advice, the right words, for your kindness, for your humanity, and for all those deeper conversations about life, beyond the scientific discussions. After each meeting, my energy tank was refilled again!

Next, I want to thank my second lab in Montpellier. I never imagined that I would find, meet, and become friends with such fun people. From day 1, you were willing to help me, teach me French, and welcome me at lunches in the cafeteria. Neymara and Elena, my latin soulmates in France! Elena, although you are Italian, you have a very latin heart -fun, huge, noble, and warm. Thank you for becoming an unconditional friend and for doing crazy things with me inside and outside the laboratory. Neymara, my favorite Brazilian, obviously. We connected from the moment we met. I cherish the beautiful memories of all the moments we shared, the coffee breaks, the trips to the gym, the nights out, and our conversations. Phillibert, Dimitri, and Joshua, thank you for making every day in the lab and office fun. Joshua, special thanks for helping me in the $scCO_2$ lab and for the fun scientific discussions and teamwork. Dim, for teaching me so much about synthesis and chemistry, for all the jokes (light and not so light), and the bad words you taught me in French -no comments. Phillibert and Camille, for the great

atmosphere in the office and for teaching me NMR (almost every day). To Nouha, Logan, and Yoan, for your kindness and camaraderie. Patrick, thank you so much for your diligence, for allowing me to carry out my experiments in the $scCO_2$ laboratory, for following my work closely, and for helping me. Thank you all for making my year in Montpellier unparalleled. You exceeded my expectations. It was a pleasure to have been part of such a collaborative, warm and human team.

To my colleagues from the NIPU-EJD project -obviously, we all went through the same frustrations, uncertainties, moves, challenges, and travels. Thank you all for making this project much more bearable, for creating a community, and for supporting each other both scientifically and personally. Federico, Francesca, Luca, Nicholas, Florent, Maliheh, Pauline, Christy, Guillem, Marco, and Pavithra. Christy, I will always remember your witty and well-timed jokes. Pauline, for your warmth and kindness. Maliheh, for your wisdom and empathy. Luca, Guillem, and Marco, for being the active team after the conferences and workshops.

Now I want to thank my closest friends, who have been there for me despite the distance that separates us. I want to tell you that you have been an essential part of this stage of my life, and even though life has led us to be apart in 6 different countries and 3 different continents, we remain as close as if we had just had coffee together yesterday. Thank you for always being on the other side of the phone and for your unconditional friendship. This is for you, my best friends: Katerin, Gretel, Estefania, Maria Jose, Yessibeth, and Jorgelis. You have been my rock in my most difficult moments. I am fortunate to have grown, lived, and celebrated so many moments by your side. Majo, I am so grateful that life brought us together in Mons! Thank you for all the meals, the conversations about everything, for your sound advice, for helping me with all my moves, for offering me your home whenever I needed it, and obviously and most importantly, for keeping me company during my compulsive shopping sprees! Words fall short. Thanks also to my smartest friends: Alejandro, for believing in me, for motivating me, for infinite hours in the phone and for always finding pragmatic solutions together. Thank you, Ben, for your friendship, your constant support, and for always believing so much in me.

Alejandro, thank you for always being there for me, for taking care of me, supporting me, and listening to me. Thank you for being the calm and peace to my intense whirlwinds. Thank you for so many beautiful moments. Thank you for making me smile every day. I cannot imagine having achieved this without you.

Thank you to my family, mami, papa, and hermana. Thank you for raising me in a home filled with love, for your unconditional love and care. For being my greatest example of discipline, resilience, strength, and courage. Hermana, thanks for your caring heart, for your generous spirit and for putting family always first. I admire your courage to speak up. Papi, you have always been my best example of hard work, discipline, and intelligence. Thanks for your generosity and for spoiling me so much! Mami, especially to you, thank you for instilling your bravery in me, for always staying strong, for wanting the best for me, for your guidance, and for teaching me to see life with joy. I am certain that all of this makes you very proud in heaven. I will carry you always in my heart.

Abstract

Polyurethane (PU) foams are among the most widely used polymeric materials, but their conventional production presents significant drawbacks: the synthesis relies on toxic isocyanates, while the foaming process employs environmentally harmful physical blowing agents (PBAs) such as chlorofluorocarbons (CFCs) and hydrofluorocarbons (HFCs), with high ozone depletion potential (ODP) and global warming potential (GWP). Polyhydroxyurethanes (PHUs), also known as non-isocyanate polyurethanes (NIPU), synthesized via aminolysis of five-membered cyclic carbonates, have emerged as a safer alternative. However, research on NIPU foams toward industrial applications remains limited. This thesis aims to bridge this gap by developing thermosetting NIPU foams through two sustainable foaming strategies: (i) Rigid foams using supercritical carbon dioxide ($scCO_2$) as a greener PBA, non-toxic, non-flammable, with zero ODP and negligible GWP, and (ii) Flexible foams using water as a chemical blowing agent (CBA).

The first part establishes an innovative approach for $scCO_2$-blown rigid NIPU foams through a batch process involving pressure-induced CO_2 absorption followed by temperature-induced desorption and simultaneous curing. This strategy, scarcely explored for thermosetting NIPU systems, yielded foams with tunable densities (270–451 kg/m^3), compression moduli (16–350 kPa), and cell sizes (0.33–0.99 mm). Notably, these foams exhibited humidity-triggered shape memory behavior with recovery ratios over 99%, expanding their potential for stimuli-responsive applications.

Building upon this platform, flame-retardant NIPU foams were developed by incorporating a phosphorus-containing diamine (DOPO-diamine) as a reactive flame retardant (RFR). Covalently bonded phosphorus (0.5–2 wt%) foams achieved a 66% reduction in total heat release compared to phosphorus-free foams and V-0 classification in UL-94 testing, addressing a critical limitation for building applications where fire safety is paramount.

To further expand the NIPU foam portfolio, water-blown flexible foams containing renewable bio-based nanofillers were developed and investigated. The incorporation of chitin nanocrystals (ChNC), chitin nanofibers (ChNF), and cellulose nanofibers (CNF) revealed an unexpected plasticizing effect on the PHU matrix, with glass transition temperatures decreasing from 23°C to 7–18°C. Despite this, mechanical characterization demonstrated concentration-

dependent enhancement, with ChNF achieving a 165% increase in compressive modulus at 2 wt% loading, following a performance hierarchy of ChNF > CNF > ChNC.

By addressing the ongoing challenges toward industrially relevant NIPU foams, this thesis establishes versatile strategies for sustainable thermosetting foams with tailored properties, bridging the gap between emerging PHU foam technology and industrial applications while contributing to greener alternatives aligned with sustainability goals, circular economy principles, and European regulatory frameworks.

Keywords: Non-isocyanate polyurethanes, polyhydroxyurethanes, supercritical CO_2, water-blown foams, reactive flame retardants, bio-based nanofillers, chitin, cellulose, sustainable foams.

Résumé

Les mousses de polyuréthane (PU) comptent parmi les matériaux polymères les plus utilisés, mais leur production conventionnelle présente des inconvénients majeurs : la synthèse repose sur des isocyanates toxiques, tandis que le procédé de moussage utilise des agents d'expansion physiques nocifs pour l'environnement, tels que les chlorofluorocarbones et les hydrofluorocarbones, présentant un potentiel élevé d'appauvrissement de la couche d'ozone et de contribution au réchauffement climatique). Les polyhydroxyuréthanes (PHUs), également appelés polyuréthanes sans isocyanate (NIPUs), synthétisés par aminolyse de carbonates cycliques à cinq chaînons, se sont imposés comme une alternative plus sûre. Cependant, la recherche sur les mousses NIPU, orientée vers les applications industrielles, reste limitée. Cette thèse vise à combler ce fossé en développant des mousses NIPU thermodurcissables à travers deux stratégies de moussage durables : (i) des mousses rigides utilisant le dioxyde de carbone supercritique ($scCO_2$) comme agent d'expansion physique plus écologique, non toxique, ininflammable, avec un avec un potentiel de destruction de la couche d'ozone nul et une contribution au réchauffement climatique négligeable, et (ii) des mousses flexibles utilisant l'eau comme agent d'expansion chimique .

La première partie établit une approche innovante pour les mousses NIPU rigides expansées au $scCO_2$ via un procédé discontinu impliquant une absorption de CO_2 induite par la pression, suivie d'une désorption induite par la température et d'une réticulation simultanée. Cette stratégie, peu explorée pour les systèmes NIPU thermodurcissables, a permis d'obtenir des mousses aux propriétés modulables : densités (270–451 kg/m³), modules de compression (16–350 kPa) et tailles de cellules (0,33–0,99 mm). Ces mousses ont notamment présenté un comportement de mémoire de forme induit par l'humidité avec des taux de récupération atteignant 99%, élargissant leur potentiel pour des applications stimulo-sensibles.

En s'appuyant sur cette plateforme, des mousses NIPU ignifuges ont été développées en incorporant une diamine contenant du phosphore (DOPO-diamine) comme retardateur de flamme réactif (RFR). Le phosphore lié de manière covalente (0,5–2 % en masse) a permis une réduction de 66% du dégagement total de chaleur par rapport aux mousses sans phosphore et une classification V-0 au test UL-94, répondant ainsi à une limitation critique pour les applications dans la construction où la sécurité incendie est primordiale.

Afin d'élargir davantage le portefeuille de mousses NIPU, des mousses flexibles expansées à l'eau contenant des nanocharges biosourcées renouvelables ont été développées et étudiées. L'incorporation de nanocristaux de chitine, de nanofibres de chitine et de nanofibres de cellulose a révélé un effet plastifiant inattendu sur la matrice PHU, avec des températures de transition vitreuse diminuant de 23°C à 7–18°C. Malgré cela, on a pu démontrer, par le biais de caractérisations mécaniques, que le module de compression dépendait de leur concentration, atteignant par exemple une augmentation de 165% dans le cas des ChNF à 2 % en masse. On obtient ainsi la hiérarchie $E_{ChNF} > E_{CNF} > E_{ChNC}$.

En répondant aux défis actuels liés à la conception de mousses NIPU industriellement pertinentes, cette thèse établit des stratégies polyvalentes pour produire des mousses thermodurcissables durables aux propriétés taillées sur mesure. Elle comble ainsi le fossé entre la technologie émergente des mousses PHU et les applications industrielles, tout en contribuant à des alternatives plus écologiques alignées sur les objectifs de durabilité, les principes de l'économie circulaire et les cadres réglementaires européens.

Mots-clés : Polyuréthanes sans isocyanate, polyhydroxyuréthanes, CO_2 supercritique, mousses expansées à l'eau, retardateurs de flamme réactifs, nanocharges biosourcées, chitine, cellulose, mousses durables

.

Table of Contents

List of Abbreviations

5CC	Five-membered cyclic carbonate
6CC	Six-membered cyclic carbonate
APP	Ammonium polyphosphate
ATH	Aluminium trihydrate
ATR	Attenuated total reflectance
Bis(AEE)	1,2-bis(2-aminoethoxy)ethane
$CaCO_3$	Calcium carbonate
CAGR	Compound annual growth rate
CANs	Covalent adaptable networks
CBA	Chemical blowing agent
CC	Cyclic carbonate
CFC	Chlorofluorocarbon
ChNC	Chitin nanocrystals
ChNF	Chitin nanofibers
CNC	Cellulose nanocrystals
CNF	Cellulose nanofibers
CO_2	Carbon dioxide
DABP	Diaminobenzophenone
DBTDL	Dibutyltin dilaurate
DBU	1,8-Diazabicyclo[5.4.0]undec-7-ene
DCC	Dynamic covalent chemistry
DDA	Degree of deacetylation
DMA	Dynamic mechanical analysis
DMC	Dimethyl carbonate
DOPO	9,10-Dihydro-9-oxa-10-phosphaphenanthrene-10-oxide
DSC	Differential scanning calorimetry
Ec	Compressive modulus
EDA	Ethylenediamine
EG	Expandable graphite
EJD	European Joint Doctorate
EPS	Expanded polystyrene
ESR	Early-stage researcher

EU	European Union
FR	Flame retardant
FTIR	Fourier transform infrared spectroscopy
GC	Gel content
GWP	Global warming potential
HCFC	Hydrochlorofluorocarbon
HCs	Hydrocarbons
HDI	Hexamethylene diisocyanate
HFC	Hydrofluorocarbon
HMDA	Hexamethylenediamine
HRR	Heat release rate
H_2O	Water
IPDA	Isophorone diamine
IPDI	Isophorone diisocyanate
LCST	Lower critical solution temperature
LDI	L-Lysine diisocyanate
LOI	Limiting oxygen index
MDI	Methylene diphenyl diisocyanate
MSCA	Marie Skłodowska-Curie Actions
MXDA	m-Xylylenediamine
NIPU	Non-isocyanate polyurethane
NMR	Nuclear magnetic resonance
ODP	Ozone depletion potential
PBA	Physical blowing agent
PDI	Pentamethylene diisocyanate
PEG	Polyethylene glycol
pHRR	Peak heat release rate
PHU	Polyhydroxyurethane
PMHS	Polymethylhydrosiloxane
PPOBC	Polypropylene oxide biscarbonate
PU	Polyurethane
PUF	Polyurethane foam
REx	Reactive extrusion
RFR	Reactive flame retardant
ROP	Ring-opening polymerization

Rr	Recovery ratio
SAOS	Small amplitude oscillatory shear
$scCO_2$	Supercritical carbon dioxide
SEM	Scanning electron microscopy
SME	Shape memory effect
SMM	Shape memory material
SMP	Shape memory polymer
TBAB	Tetrabutylammonium bromide
T_d	Degradation temperature
T_{d5}	Temperature at 5% mass loss
TDI	Toluene diisocyanate
TGA	Thermogravimetric analysis
T_g	Glass transition temperature
THR	Total heat release
Tm	Melting temperature
TMPTC	Trimethylolpropane triscarbonate
TMPTE	Trimethylolpropane triglycidyl ether
TREN	Tris(2-aminoethyl)amine
TTI	Time to ignition
UL94	Underwriters Laboratories 94 (flammability standard)
UNEP	United Nations Environment Programme
WC	Water content
XPS	Extruded polystyrene
XRD	X-ray diffraction

Chapter I

General Introduction

The rapid growth of the global economy over the past century has been fueled by various industrial expansion and technological breakthroughs. However, this progress has reached out at a significant environmental cost, particularly from the chemical industry, which relies heavily on resource extraction and energy use. As a result, several planetary boundaries have been pushed beyond their limits, evidenced by climate change, biodiversity loss, land degradation, and chemical pollution, each posing risks to both the planet and human well-being.[1,2]

Within this broader context, the production of plastics has steadily increased, and polyurethane (PU) foams account for a significant portion of the global polymer market, contributing to the environmental burden[3]. In 2023, overall PU foam production was estimated at around 13.3 million tonnes,[4] a figure projected to grow in response to rising demand for thermal insulation, cushioning, and automotive applications.[5,6] This widespread use has made PU foams one of the most consumed classes of synthetic polymers, thanks to their versatility and wide range of applications, from flexible foams in furniture and automotive seating to rigid foams in construction and refrigeration.[7–10]

Despite their utility, the conventional production of PU foams presents serious drawbacks. The process relies on petrochemical-based polyols and toxic isocyanates, raising significant environmental and health concerns.[11,12] In addition, many PU foams are produced using hydrocarbons as blowing agents, which pose further environmental challenges. In line with the principles of green chemistry, namely, the use of renewable feedstocks, reduction of hazardous substances, and minimization of waste and energy consumption throughout the life cycle [13], there is a clear need to rethink PU foam production.

A promising route to align PU foam manufacturing with these principles is the development of Non-Isocyanate Polyurethanes (NIPUs). Unlike traditional PUs, One type of NIPUs, specifically polyhydroxyurethanes (PHU) are synthesized from cyclic carbonates and amines, thereby eliminating the need for toxic isocyanates and reducing the associated health and environmental risks.[14] In parallel, the integration of more sustainable physical blowing agents, such as supercritical carbon dioxide ($scCO_2$), could provide a greener alternative to hydrocarbons, HFCs, and HCFCs.[15] Being non-toxic, non-flammable, and readily available, $scCO_2$ is an attractive candidate for producing NIPU foams without contributing to ozone depletion,[16] yet its potential in thermosetting NIPU foams has not been fully exploited. Additionally, water-blown NIPU foams represent another environmentally friendly option,

resembling conventional isocyanate-based foaming processes while avoiding hazardous chemistry.[17]

Although progress has been made in developing NIPU foams, further research is still required to optimize their synthesis and foaming processes, to control morphology, and to enhance their functional properties so they may compete with conventional isocyanate-based PU foams already well established in the market. Encountering these challenges would significantly contribute to the 2030 sustainability goals by promoting materials that are environmentally responsible across their entire life cycle, from raw materials and greener synthesis routes to improved end-of-life management. This holistic approach is needed to shift from linear, disposable models toward circular ones, highlighting the need to rethink and redesign the way materials are conceived and produced.

In line with these sustainability goals, the European Union (EU) funds multidisciplinary scientific programs that foster the transition toward a more sustainable and environmentally responsible chemical industry. This PhD thesis is thereby conducted within the framework of the Non-Isocyanate Polyurethanes European Joint Doctorate (NIPU-EJD), a project funded under the Horizon 2020 program through the Marie Skłodowska-Curie Actions (MSCA). The consortium brings together 12 early-stage researchers (ESRs) across seven universities, with the goal of advancing in green chemistry for polyurethanes, covering the design of greener monomers, development of materials with industrial applications, and management of end-of-life pathways.

Therefore, this PhD thesis aims to (1) develop thermosetting non-isocyanate polyurethane (NIPU) foams through a more sustainable synthesis approach, utilizing the aminolysis of various 5-membered cyclic carbonates with greener physical and chemical blowing agents, and (2) evaluate their performance for potential applications across diverse fields.

The forthcoming Chapter II will provide a comprehensive overview of recent advancements in greener strategies for PU-based materials, with particular focus on the transition to NIPU foams, innovative foaming processes, and their applications in areas such as building insulation, flame retardancy, biomedical devices, and sensor technologies. Chapter III will outline the overall research strategy and objectives that conducted the experimental work. Chapter IV, and V will present the synthesis and characterization of thermosetting NIPU foams fabricated integrating reactive flame retardants and supercritical CO_2 as physical blowing agent, while Chapter VI focuses on water-blown NIPU foams as chemical blowing agent with

bio-based nanofillers. Finally, Chapter VII will provide the overall conclusions and future perspectives of this work.

Chapter II

State of Art

1. Polyurethane foams: Importance and general aspects

Polymer foams have become essential materials among various applications due to their unique combination of properties. They exhibit low-density, high-energy absorption, thermal insulation and mechanical resilience. These materials are characterized by cellular structures that confers lightweight properties while presenting superior structural integrity. The specific polymer composition and cellular morphology dictate their physical, thermal, and mechanical performance, making them indispensable in construction, packaging, automotive, aerospace, biomedical, and cushioning applications.[18,19]

Among polymeric materials, polyurethanes (PU) foams stand out for their high versatility, existing in two main categories: flexible and rigid polyurethane foams. Flexible PU foams that exhibit high elasticity and impact absorption, are widely used in seating, bedding, and automotive interiors.[11,20,21] Their structure enables long-term comfort and durability, making them ideal for mattresses, furniture and vehicle cushioning. In the case of rigid PU foams, they are known for their high thermal insulation performance and are extensively employed in refrigeration systems, industrial insulation panels, and energy efficient materials.[22,23]

The global polymer foam market continues to exhibit steady growth, valued at USD 103 billion in 2024, with projections to reach USD 142 billion by 2030, reflecting a compound annual growth rate (CAGR) of 5.6%. Within this market, polyurethane foams hold a significant share, accounting for USD 47 billion in 2024, with an anticipated CAGR of 6.27% by 2030.[24] The increasing demand for energy-efficient solutions, particularly in the construction sector, for thermal insulation in the construction industry is a primary driver of PU foam market expansion as shown in Figure II. 1.

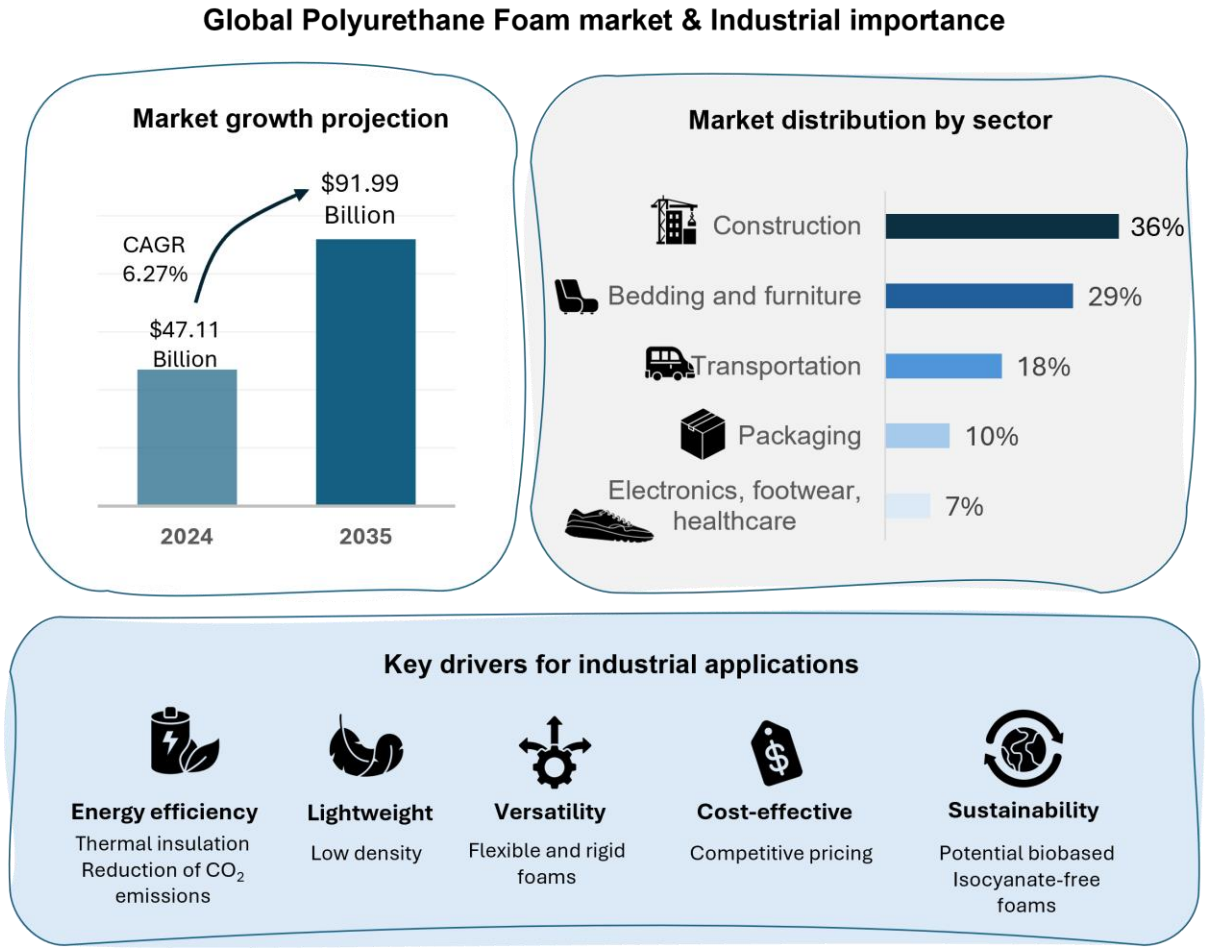

Figure II. 1. Global PU market and industrial importance

Indeed, polyurethane foams (PUF) have emerged as key materials to address sustainability challenges in our modern society due to their extraordinary thermal insulation properties. Their extensive use in building insulation is essential for reducing energy consumption and enhancing heating and cooling efficiency. This is attributed to their low thermal conductivity (20-30 mW/mK), which surpasses that of PS, mineral wool, and cellulose in thermal performances.[25] As a result, they contribute to reduced greenhouse gas emissions by minimizing energy loss. PU foams are recognized for their high durability, which significantly extends service life and reduces the frequency of material replacement, raw material consumption, and energy demand.[26]

These properties are fundamentally based on their chemical composition and synthesis process. The dominance of polyurethane foams in these applications derives from their versatile chemistry. Based on the polyaddition reaction between the hydroxyl (-OH) groups of a polyol

with the isocyanate (-NCO) groups of a polyisocyanate, the synthesis of polyurethane (PU) foams begins with the precise selection and formulation of key components, including polyols, polyisocyanates, blowing agents (BAs), additives, such as catalysts, surfactants, pigments, flame retardants (FRs), plasticizers. The high reactivity of isocyanate groups with hydrogen-labile species that results in the formation of carbamate (urethane) linkages facilitates rapid polymerization under mild conditions, yielding a broad range of material properties (Figure II.2).

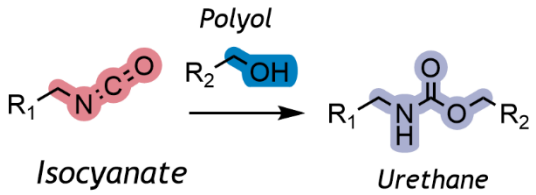

Figure II. 2 Urethane linkage formation from isocyanate reaction with polyols

The relative proportions of these components strongly influence foam density, cellular morphology and therefore performances upon the targeted application. Depending on the precursor functionality, PU chemistry can result into thermoplastic (non-crosslinked) or thermosets (crosslinked) networks. Among them, thermosetting PU foams dominate the commercial market due to their superior dimensional stability, solvent resistance, and mechanical strength.

Polyols are one of the main constituents of PU formulations and are usually viscous liquid containing at least two or more hydroxyl (-OH) groups per molecule to ensure the formation of a crosslinked material. The most used polyols are polyfunctional polyethers like polyethylene glycol, polypropylene glycols, acrylic polyols and polyester polyols.[25] Polyethers are obtained via alkoxylation in the presence of basic catalyst, where ethylene oxide (EO) or propylene oxide (PO) typically react with a starting molecule containing hydroxyl or amine functional groups. Among the most common polyols, initiators molecules include ethylene glycol (f =2), glycerine (f = 3), pentaerythritol (f =4), sorbitol (f = 6) and among the polyamine initiators are ethylene diamine (f = 4) and diethylene triamine (f = 5).[27] In contrast, polyesters polyols are synthesized through polycondensation or polyaddition reactions between dicarboxylic acid or anhydrides with a polyol initiator starter molecule.

The molecular weight of polyols clearly influences the final properties of PU foams. Polyols with low molecular weight usually form rigid PUFs, due to the higher number of urethane groups formed per unit volume. On the contrary, high molecular weight polyols yield flexible PU foams as fewer number of urethane groups and more aliphatic chains are formed.[11,28,29]

Isocyanates serve as the source of –NCO functional groups within these PU foams and typically contain two reactive functional groups per molecule. They react with polyols, water and cross-linkers in the formulation, forming a three-dimensional polymer network. The main used isocyanates include aromatic isocyanates like toluene diisocyanate (TDI), and methylene diphenyl 4,4'-diisocyanate (MDI), which collectively account for 90% of global isocyanate consumption.[6] Aliphatic isocyanates such as hexamethylenediisocyanate (HDI), and isophorone diisocyanate (IPDI) are also used (Figure II. 3). The most popular industrial pathway for isocyanate synthesis involves the phosgenation of a primary amines.[11] However, this process presents significant both safety and health concerns due to the extreme toxicity of phosgene.

Aromatic isocyanates exhibit higher reactivity than their aliphatic counterparts due to the delocalization of the negative charge on the aromatic ring. This high reactivity makes them suitable for foam production, where rapid polymerization is required.[30] Furthermore, their chemical structure contributes to superior mechanical and flame retardant properties.

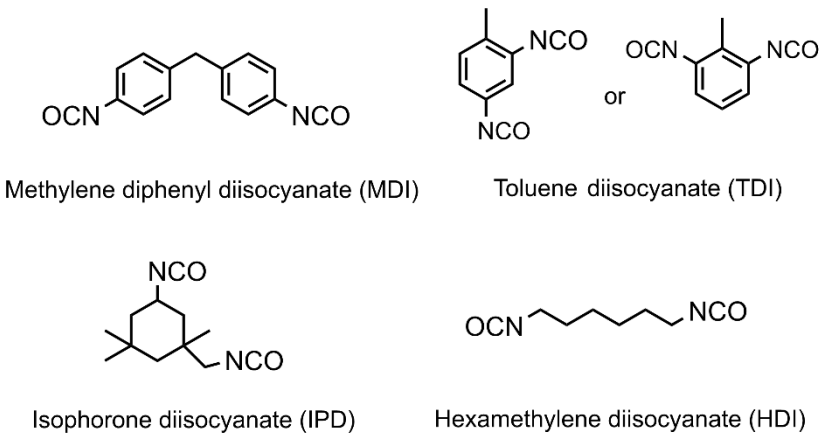

Figure II. 3. Chemical structure of the main diisocyanates used in PU foams production

Foam formation in polyurethanes (PU) systems requires the expansion of the polymer matrix through the introduction of gas and bubbles.[27] This process is typically facilitated by the generation of carbon dioxide CO_2, which is produced *in situ* via the reaction between

isocyanate groups and water (Figure II. 4). When CO_2 is released, it expands the polymeric material, forming a well-stablished cellular material. This mechanism mainly produces soft foams with open cells.[31] In addition to chemical blowing, PU foam expansion can be also achieved through physical foaming, where low-boiling non-reactive liquids are incorporated into the formulation. In the past, the most commonly used physical blowing agents (PBAs) included chlorofluorocarbons (CFCs), hydrochlorofluorocarbons (HCFCs), and hydrofluorocarbons (HFCs). Nowadays, pentane has remained as the most predominant PBA in Europe. The polymer expansion occurs due to the vaporization of these low-boiling liquids induced by the reaction exotherm, affording a better control over PU foaming.[11,32]

Even whether PU foams are widely used thanks to their versatile formulations with polyols, isocyanates, blowing agents, and additives, most of these components remain fossil-based, and their production often involves hazardous processes such as phosgenation for isocyanates. In addition, traditional physical blowing agents like CFCs, HCFCs, and HFCs have contributed significantly to greenhouse gas emissions. These issues highlight the need to rethink PU chemistry and processing toward safer and more sustainable alternatives.

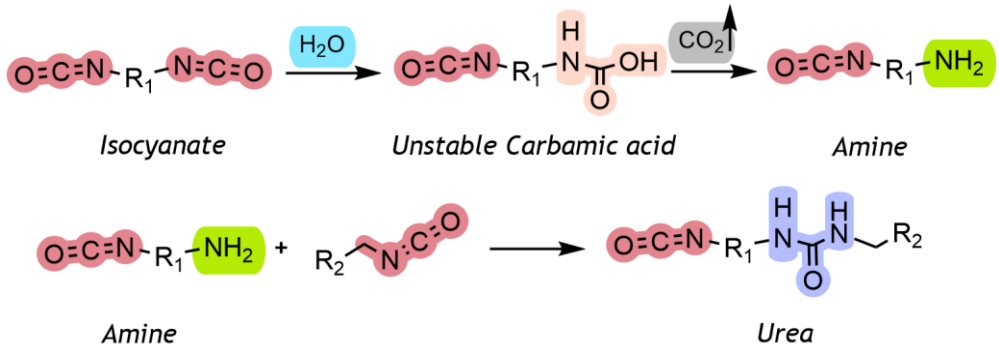

Figure II. 4. Reaction mechanism between isocyanate and water producing CO_2, serving as blowing agent in PU foams

2. Toward more sustainable PU materials

Despite the advantages of PU foams in modern society, they face major sustainability challenges due to their fossil-based origin, the use of hazardous reactants, and their contribution to greenhouse gas emissions. According to the United Nations Environment Programme (UNEP), over 90% of biodiversity loss and water stress worldwide can be attributed to resource extraction, material processing, fuels and food.[33] Furthermore, nearly half of global greenhouse gas emissions arise from the unsustainable use of raw materials, particularly fossil-based ones.

Therefore, to address these issues, advancing toward circular economy and resource-efficient industrial practices are fundamental to decouple economic growth from environmental degradation and ensure long-term resource availability.

2.1.Sustainability challenges and strategies

Polyurethane (PU) foams can become more sustainable by implementing greener polymer synthesis and foaming processes. A cradle-to-grave approach could be utilized to identify critical variables requiring improvement and ensuring a more comprehensive sustainability assessment. Beyond their energy-saving applications, PU foams should align with the principles of green chemistry and sustainable goals, which include: (1) increasing the use of renewable feedstocks to reduce dependence on petro-based resources, (2) optimizing monomer design and functionalization to improve performance during consumer utilization, (3) minimizing hazardous chemicals such as toxic solvents and reactants, (4) reducing greenhouse gas emissions during manufacturing, and (5) mitigating waste generation through process efficiency.[13] These actions are the core to transition toward a more environmentally responsible manufacturing. In addition, improving end-of-life management strategies through, e.g., recyclability, material durability, and the design of reprocessable materials, enabled by dynamic covalent chemistry (DCC), support the transition to a circular and more sustainable economy (i.e.: Cradle to cradle) (Figure II. 5).[34]

2.2. Bio-based raw materials & greener blowing agents

Research has increasingly focused on developing new bio-based reagents and alternative synthetic routes for PU foams production. Polyols, one of the primary reactants in PU synthesis, can be derived from diverse renewable sources such as vegetable oils, starch, chitosan, lignocellulose, tannin, among others.[35] In parallel, research on bio-based and phosgene-free routes is continuously raising to reduce fossil dependence and mitigate safety concerns associated to phosgenation. Another critical point is the adoption of more environmentally friendly blowing agents. Historically, high-global warming (GWP) gases, such as Chlorofluorocarbons (CFCs), Hydrochlorofluorocarbons (HCFCs), or Hydrofluorocarbons (HFCs) were extensively used. However, due to their negative environmental impact, these compounds have been progressively phased out and banned under international protocols.

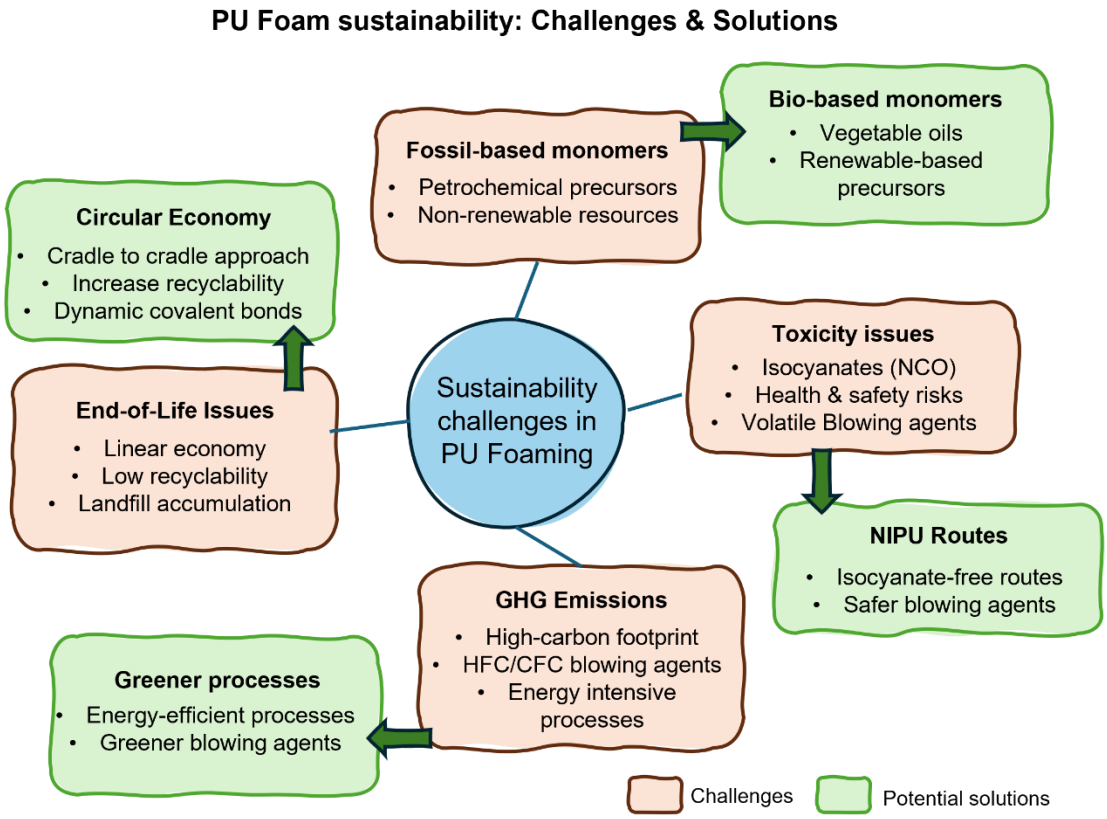

Figure II. 5. Sustainability challenges in PU foams production: from monomers selection to end of life management.

2.3. Recyclability and recovery methods

Due to large annual production (13.3 Mt/y) and associated waste generation of PU foams, recycling and reprocessing are key points in sustainability. PU foams can be recycled through chemical or mechanical processes. Mechanical recycling involves the regrinding of PU foams for reuse in new products. Chemical recycling methods such as glycolysis, hydrolysis and pyrolysis aim to recover polyols to a certain extent. Glycolysis has already been implemented at industrial scale to obtain recycled polyols for new foam production. However, economic and environmental challenges limit a widespread adoption and the most privileged end-life scenario remain the energy recovery through incineration.

2.4. End-of-life management

Dynamic covalent chemistry (DCC) represents a transformative approach for sustainable PU materials. Unlike conventional crosslinked polymer networks, which exhibit irreversible covalent bonding and limited end-of-life processing, DDC introduces exchangeable covalent

bonds that allow materials to undergo bond reformation, stress relaxation and reprocessability under external stimuli.[34] A prominent example in polyurethane systems is transcarbamoylation, an exchange reaction that can proceed through either associative mechanisms involving hydroxyl-mediated exchange or dissociative mechanisms involving direct urethane–urethane exchange, both of which can be catalytically promoted.[36] This dynamic behaviour allows to engineer materials with precise tuneable properties, with self-healing capabilities and ability to reprocess into new forms without significant loss of mechanical integrity.

3. Toward more sustainable PU chemistry

As previously mentioned, the sustainability of conventional PU chemistry can be improved through the substitution of fossil derived monomers with bio-based alternatives. In this regard, significant research has been devoted to the development of bio-based polyols (Figure II.6), which today represent the largest share of the bio polyols market, valued at USD 8.74 billion in 2024 and projected to reach USD 9.3 billion by 2025.[37] Their diversity stems from a wide

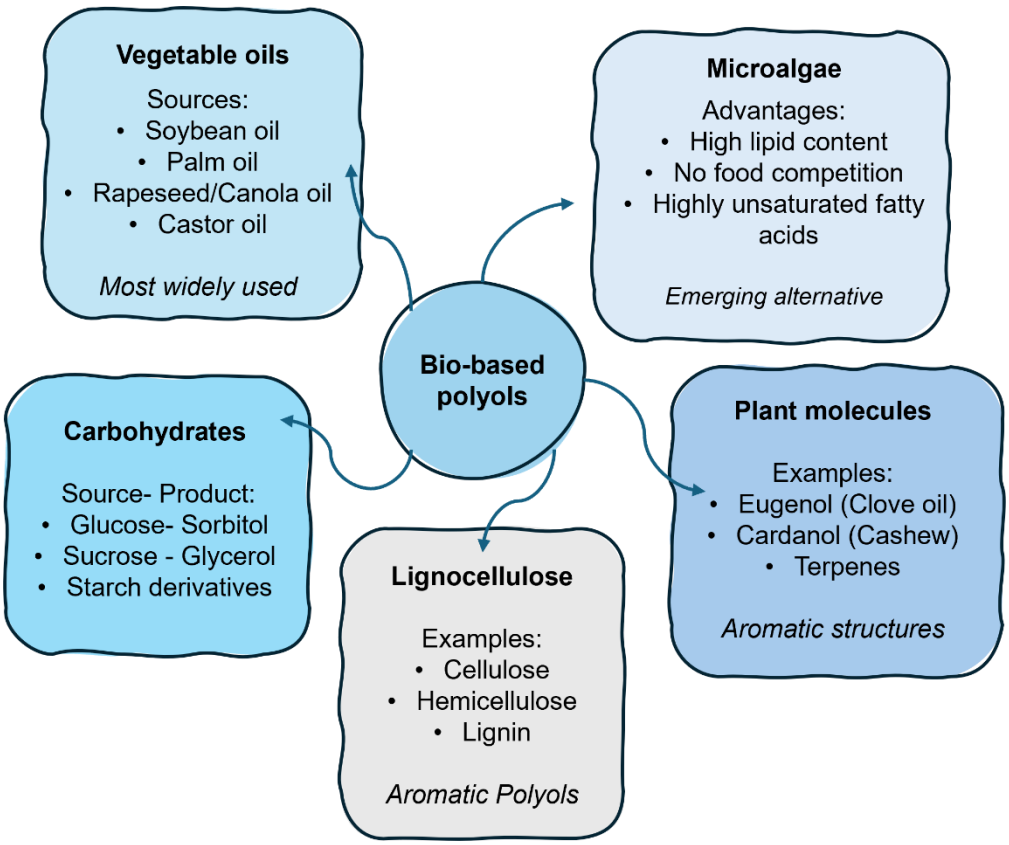

Figure II. 6. Main bio-based polyols resources used for the production of partially bio-based polyurethanes.

range of renewable feedstocks, including vegetable oils, lignocellulosic biomass, carbohydrates, microalgae, and other plan derived materials (Figure II. 6). [38–40] Each source provides polyols with different chemical structures, functionalities, and molecular weight, ultimately determining their performances in specific PU applications.

3.1. Biobased polyols:

Vegetable oils are the most widely used feedstock due to the availability and cost efficiency, particularly palm, rapeseed, and soybean oils.[41] Their triglyceride structure can be chemically modified through processes such as epoxidation and ring opening, hydroformylation, or transesterification, introducing hydroxyl groups along fatty acid chains.[42]

The resulting polyols are suitable for flexible PU foams, combining mechanical performances and partial biodegradability. Castor oil, with its naturally hydroxylated ricinoleic acid, represents a special case for further functionalization and viscosity tunability.[43,44]

Microalgae oils have emerged as an alternative, mitigating competition with the food chain. Their triglycerides exhibit longer fatty acid chains with higher unsaturation levels, making them attractive for PU foam applications. Nevertheless, industrial scalability remains a challenge, and their market is still very limited compared to conventional vegetable oils.[35]

Lignocellulosic biomass (cellulose, hemicellulose, lignin) is another promising source, particularly for aromatic polyols. Methods such as liquefaction, oxypropylation and hydroxymethylation allow the conversion of biomass into polyols with both aliphatic and aromatic hydroxyl groups.[35,43] Lignin, which constitutes up to 45% of biomass, is especially interesting due to its natural aromatic structure, contributing to rigidity, thermal resistance, and even flame-retardant properties when incorporated into PU networks.[42,45] However, the heterogeneity of lignin, poor solubility, and limited hydroxyl reactivity significantly restrict its large-scale use.

Other plant-derived molecules, such as eugenol (from clove oil) and cardanol (from cashew nutshell liquid), have been converted into polyols via Mannich or thiol-ene reactions. These aromatic polyols are particularly valuable for high performance coating, adhesives, and rigid foams.[46–50]

Carbohydrate-based polyols are obtained from sugars (glucose, sucrose, starch) mainly through catalytic hydrogenation, yielding compounds like sorbitol. These polyols provide high hydroxyl density, water solubility, and biodegradability, making them appropriate for rigid PU

foams.[51–53] Polysaccharides such as starch, chitosan, and alginate have attracted attention for their natural biocompatibility and capacity to introduce microbial activity. [51,54,55]

3.2. Phosgene-free and biobased isocyanates:

While bio-based polyols have reached industrial maturity, the development of bio-based isocyanates has remained limited, slowing down the full transition to sustainable polyurethane chemistry. The main reason is the efficiency of the conventional industrial process, which still relies on phosgene, a highly toxic compound that poses severe health and environmental hazards.[56] This dependence has motivated research into phosgene-free synthetic routes and biobased alternatives, although their large-scale application remains scarce.

Several phosgene-free strategies have been explored, such as reductive carbonylation of nitro compounds, Curtius rearrangement of fatty acid derived azides, or multi step catalytic processes from lignin-derived phenols.[57–60] These approaches demonstrate the technical feasibility of replacing phosgene, but issues of safety, cost, and scalability still hinder industrial implementation. In parallel, bio-based isocyanates have been synthesized from renewable feedstock, including amino acids, fatty acids, and lignin derivatives. Examples include L-lysine diisocyanate (LDI), investigated for biomedical applications, and guaiacol/vanillin-based isocyanate derived from lignin. [60,61]

On the commercial side, recent years have witnessed incremental adoption of sustainable isocyanates. Companies such as Covestro, Vencorex, and Henkel have launched partially or fully bio-based alternatives including Pentamethylene Diisocyanate (PDI), Tolonate™ X FLO 100, and Dimer Acid Diisocyanate, applied in foams, coatings, adhesives, and optical fibers. [62–66] Despite being synthesized through phosgenation in some cases, these materials reduce the carbon footprint by incorporating significant fractions of renewable carbon (up to 70%).

In general, bio-based polyols and isocyanates mitigate the carbon footprint and enhance biodegradability with non-toxic compound degradation. Nevertheless, significant challenges remain. Phosgenation continues to dominate due to its incomparable industrial efficiency. Furthermore, isocyanates themselves are classified as CMR substances (carcinogenic, mutagenic, and toxic for reproduction), raising occupational health and safety concerns that cannot be resolved merely through renewable sourcing. Their intrinsic toxicity and high reactivity drive the search for Non-Isocyanate Polyurethanes (NIPU) routes, which aim to combine safer monomers, safer synthesis, and comparable performance.

4. Non-isocyanate polyurethane routes (NIPU)

The toxicity and environmental concerns associated with isocyanate-based polyurethane (PU) synthesis have driven research into Non-Isocyanate Polyurethanes (NIPU) routes, which aim to retain the desirable properties of conventional PUs while eliminating hazardous reagents. Several alternative synthesis methods have been developed, some of them include the copolymerization of aziridines with carbon dioxide, ring-opening polymerization (ROP) of cyclic carbamates, transurethanization, carbamate-aldehyde reactions, and aminolysis of carbonates. Each method presents advantages and limitations regarding, precursors, synthetic feasibility, reaction efficiency, and final material properties.

4.1. Copolymerization of Aziridines with Carbon Dioxide

One of the routes to synthesize Non-Isocyanate Polyurethanes (NIPU) is through the copolymerization of aziridines with carbon dioxide (CO_2) as shown in Figure II. 7. This reaction produces polyurethane-amine oligomers without the use of phosgene or isocyanates. However, this route yields low carbamate linkages, as aziridine primarily undergoes homopolymerization, which represents a significant drawback. A notable example of this synthesis route was conducted by Kuran et al.,[67] who synthesized PU oligomers (500 $g \cdot mol^{-1}$) in the presence of an organozinc catalyst. Ihata et al.,[68] also investigated this method using supercritical CO_2 with a pressure of 22 MPa, obtaining an increase of carbamate content from 30 to 62%.[68] These oligomers exhibited thermal responsive properties with Lower critical solution temperatures (LCST) between 40-85°C.

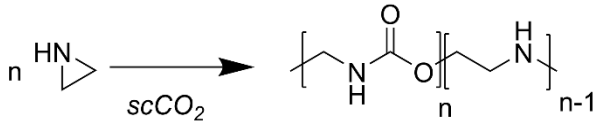

Figure II. 7. Copolymerization of aziridines with carbon dioxide. [67,68]

4.2. Ring-Opening Polymerization (ROP) of Cyclic Carbamates

ROP of cyclic carbamates affords another approach to synthesize NIPUs, maintaining high atom economy, low energy consumption, and reduced waste generation (Figure II. 8).[69] Zhang et al.,[69] demonstrated the potential of this route. They obtained aliphatic polyurethanes by polymerizing 5-membered cyclic carbamates substituted with vinyl groups via anionic ring-opening polymerization under mild conditions. Furthermore, Neffgen et al.,[70] also demonstrated the polyurethane synthesis by the cationic ring-opening of trimethylene urethane

using methyl trifluoromethanesulfonate as catalyst. Interestingly, they reported the depolymerization of the polymer by ring closure at high temperatures (140°C) under vacuum using titanium tetraisopropoxide ($Ti(OiPr)_4$) as catalyst.

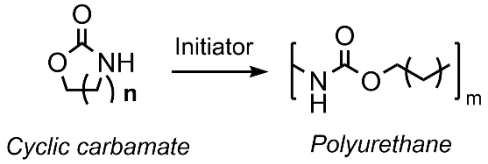

Figure II. 8. Ring-opening polymerization of cyclic carbamates.[69]

The main drawback of ROP lies on the use of hazardous and toxic reagents for monomer synthesis. For instance, the production of cyclic carbamate monomers often requires ethyl chloroformate, a phosgene-based reagent, dibutyltin dimethoxide as catalyst, or releases phenol as by product, which raise significant health concerns.

4.3. Carbamate-Aldehyde Reaction (CA): A VOC-Free Alternative

The carbamate-aldehyde reaction has recently gained renewed interest for NIPU synthesis in crosslinked polyurethane materials with potential coating applications.[71,72]This reaction involves the condensation of a primary carbamate with an aldehyde under acidic catalysis, resulting in the formation of two urethane groups attached to the same carbon atom, releasing water as byproduct as shown in Figure II. 9.

Figure II. 9. Carbamate-aldehyde reaction to produce polyurethanes.[71]

A significant advancement in this field was made by David Gerard et al.,[71] who optimized the carbamate-aldehyde reaction by employing monoaldehydes instead of polyaldehydes to reduce toxicity. Specifically, they used bio-based aldehydes, such as 5-methyl furfural and vanillin, to synthesize PU thermosets in solvent-free conditions. Similarly, Silbert et al.[72] synthesized bio-based coatings from soybean oil-derived polycarbamate, reacting with 1,4-cyclohexanedicarboxaldehyde or 2,5-diformylfuran at 120°C, significantly reducing reaction times compared to room temperature curing (2 h vs. 180 days).

These studies confirm that the carbamate-aldehyde reaction is a promising pathway for bio-based PUs, since there is only water release as byproduct. However, this could be seen as a drawback as well.

4.4. Transurethanization

Transurethanization, also known as transcarbamoylation, enables the formation of carbamate linkages where an alcohol reacts with an existing urethane bond, leading to a new urethane moiety, releasing a low-molecular-weight alcohol as a byproduct (Figure II. 10). This method allows the synthesis of NIPUs without using isocyanates.[73] The synthesis of carbamates can be also enhanced beyond traditional phosgene-based routes. Some examples include the synthesis of bio-based carbamates derived from dimethyl carbonate (DMC) and diamines,[74] or the synthesis of carbamates from amines, alcohols and CO_2.[75]

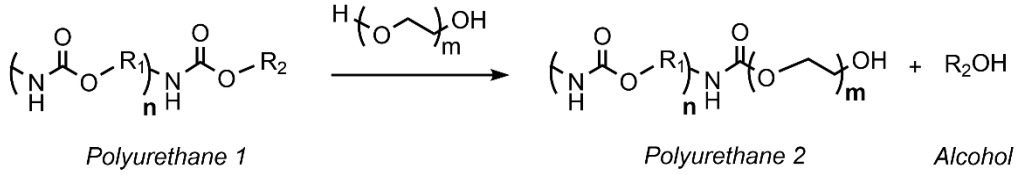

Figure II. 10. Transurethanization of a polyurethane with a polyol to produce another polyurethane.[73]

Indeed, Kebir et al.,[76] demonstrated the use of carbamates derived from DMC and amines (1,6-hexadiamine, 1,10-decanediamine, and Priamine 1074) to synthesize thermoplastic NIPUs. These polymers were modified by introducing polyethylene glycol (PEG) segments, exhibiting soft segments with low T_g (-49 to 1 °C) and varied melting temperatures (39-49 °C). The resulting NIPUs displayed superior thermal stability compared to conventional PUs.

Transurethanization could be considered one of the most sustainable routes to substitute conventional PU synthesis, by using bio-based carbamates and polyols, and avoiding the use of toxic reagents.

4.5. Aminolysis of 5-membered-Carbonates:

This synthesis route involves in the polyaddition of 5-membered-cyclic carbonates and amines, leading to the formation of polyhydroxyurethanes (PHU).[77,78] They are distinguished by their pendant hydroxyl groups, which have been reported to enhance some polymer properties such as adhesion, chemical resistance, mechanical properties and further functionalization (Figure

II. 11).[79–81] This approach has gained remarkable attention in sustainable polymer chemistry due to several key advantages.

Firstly, it eliminates the use of phosgene and isocyanates during the synthesis process. Secondly, the reaction exhibits high efficiency since it does not generate any byproduct like methanol or water, and the reaction can be conducted in solvent-free conditions. Additionally, 5-membered cyclic carbonates can be synthesized from CO_2- and bio-based feedstocks.

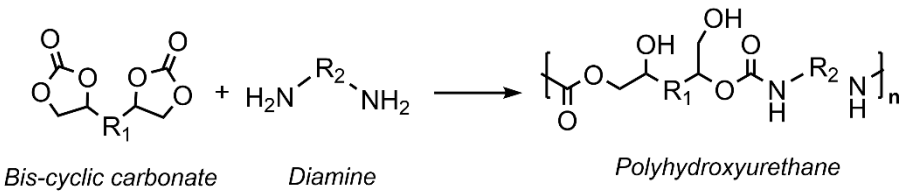

Figure II. 11. Synthesis of polyhydroxyurethanes from 5-membered cyclic carbonates and amines.[77,78]

Importantly, this aminolysis route using 5CC has become the most widely adopted synthesis pathway for producing NIPU foams, owing to its simplicity, versatility and compability with a wide range of amines, which are commercially available. In this context, the present thesis will focus on the aminolysis of 5CC as the key route to design new PHU-based foams, with particular attention to some cyclic carbonates and amine molecules that will be explored experimentally in the following chapters. To this basis, the next section will review in more detail the synthesis, properties and renewable sources of 5-membered cyclic carbonates and amines employed in this chemistry.

5. 5-membered Cyclic carbonates (5CC)

5 membered cyclic carbonates (5CC) have attracted academic and commercial attention in the last decades and have emerged as new key precursors in the synthesis of NIPUs due to its alternative sustainable synthesis process and inherent good properties. Among its interesting properties include thermal stability, low-volatility and relative non-toxicity. Several synthesis routes have been reported in the literature, including diols and epoxides as the main precursors.[82–85]

The conventional approach to synthesize 5CC consists in the phosgenation of diols, using phosgene or its derivatives, such as triphosgene. Burk and Roof reported the synthesis of 5CC from 1,2 diols and triphosgene in dichloromethane under mild conditions with high yields (87-99%).[84] However, the inherent toxicity of phosgene-based compounds significantly restrict the feasibility of this method for sustainable applications. A greener alternative involves the direct cycloaddition of carbon dioxide (CO_2) to epoxides, forming cyclic carbonates with high atom efficiency (Figure II. 12).[86–88] Indeed, it was demonstrated that this reaction exhibited the most favorable E-factor. This means that it is the best proportion between the reactants used in the reaction, such as monomers, solvents and catalysts in comparison with generated waste.[89] This reaction has been extensively studied using various catalytic systems including calcium-based catalysts combined with DBU (1,8-diazabicyclo[5.4.0]undec-7-ene), tetrabutylammonium bromide (TBAB), calcium iodide and crown ether, as well as aluminum-based catalysts. The use of these catalysts have enabled the reaction to proceed under mild conditions and atmospheric CO_2 pressure.[90–92] The CO_2 fixation strategy not only eliminates the use of toxic reagents but also contributes to greenhouse gas valorisation.

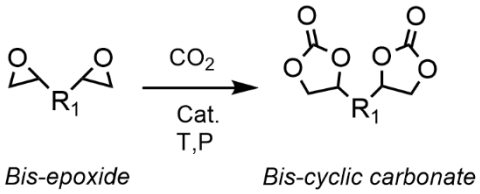

Figure II. 12. Cyclic carbonate formation from CO_2 fixation in epoxides.[86–88]

The synthesis of polyfunctional cyclic carbonates (5CC) is necessary to produce both non-crosslinked (thermoplastic) and crosslinked (thermosetting) NIPUs. Among the most commonly employed polyfunctional 5-membered cyclic carbonates are trimethylolpropane tricarbonate (TMPTC),[93,94] a trifunctional carbonate, and poly(propylene oxide) biscarbonate (PPOBC),[95–99] a bifunctional carbonate.

A widely adopted synthesis route for these 5CC involves the fixation of CO_2 onto the epoxide precursors, specifically trimethylpropane triglycidyl ether (TMPTE) or poly(propylene oxide)glycidyl ether (PPOBC). This reaction is catalyzed by TBAB in ethyl acetate under 20 bars of CO_2 for 72 hours (Figure II. 13).[93,99] Alternatively to this, the synthesis of poly functional 5CC could be conducted under supercritical CO_2 in order to avoid the use of solvents.[100]

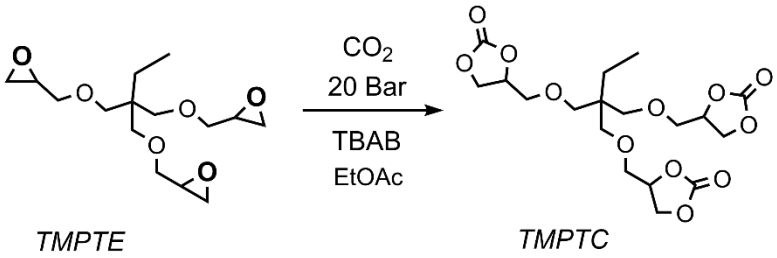

Figure II. 13. Synthesis of TMPTC from the CO_2 fixation in TMPTE.[93,99]

The use of renewable feedstock for the synthesis of 5CC has been also studied to avoid the use of petrochemical-based reagents. Vegetables oils are among the most promising candidates due to their abundant availability, diverse chemical structures and the presence of unsaturated bonds in their aliphatic chains, which facilitates epoxidation though peroxidation, and subsequent CO_2 fixation.[101]

Among vegetable oil-derived 5CCs, soybean oil-based cyclic carbonate is the most widely studied and utilized.[100,102–110] It has been incorporated into various NIPU applications, including adhesives,[111] antibacterial membranes,[112] and anticorrosion coatings.[113] Other vegetable oils explored include linseed oil,[114–118] sunflower oil,[119–121] castor oil,[122,123] rubber seed oil and jatropha oil.[124,125] Lignocellulosic biomass-derivatives, such as creosol, vanillin and ferulic acid,[126–128] are other sources of renewable feedstock, gaining increasing attention due to their aromatic structure and hydroxyl functionalities. Other bio-based sources found in the literature include polyols, such as glycerol, trimethylolpropane, sorbitol, mannitol, and terpenes, such as limonene.[129–131]

6. Amines

Amines are the other key reactants in the aminolysis of 5-membered cyclic carbonates, acting as hardening agents in the formation of polyhydroxyurethane (PHU) linkages. One of the primary advantages of this route is the wide commercial availability (yet petro-based) of

amines, which enables broad applicability in Non-Isocyanate Polyurethane (NIPU) synthesis. Various types of amines have been extensively investigated and reported in the literature, including diamines, triamines, and polyamines with either aliphatic or aromatic structures as shown in Figure II. 14. In terms of reactivity, primary amines exhibit the highest reactivity, followed by secondary amines and tertiary.[132]

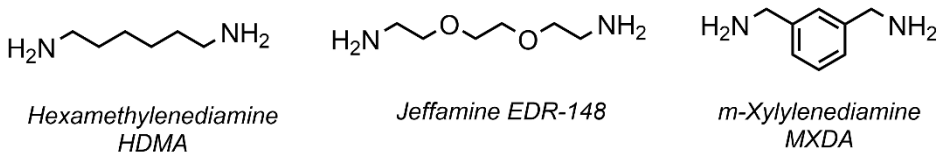

Figure II. 14. Chemical structure of diamines mainly used in the production of polyhydroxyurethanes (PHU).

Similar to cyclic carbonates, amines can also be synthesized from renewable feedstocks. Common bio-based sources include vegetable oil derivatives,[133,134] such as sunflower[135] and cardanol-based amines,[136] lignin-derived amines,[126] amino acid-derived amines, such as lysine and lysinol-based polyamines,[137,138] sugar-derived amines,[139,140], terpene-derived amines[141] and in combination via polycondensation. However, bio-based amines are not yet widely commercially available, which brings limitations to expand bio-based PHU materials.

7. NIPU Foaming process based on physical and chemical blowing agents

Following the discussion about Non-Isocyanate Polyurethanes (NIPU) chemistry in the previous section, another critical aspect to discuss in foam production is the expansion mechanism and the associated foaming chemistry, as summarized in Figure II. 15. In general, the formation of cellular materials requires the controlled release of a gas, which is typically derived from blowing agents (BAs). These agents play a crucial role in both the manufacturing and performance of polymeric foams, determining key properties such as density, cellular microstructure, and morphology (open vs. closed pores).

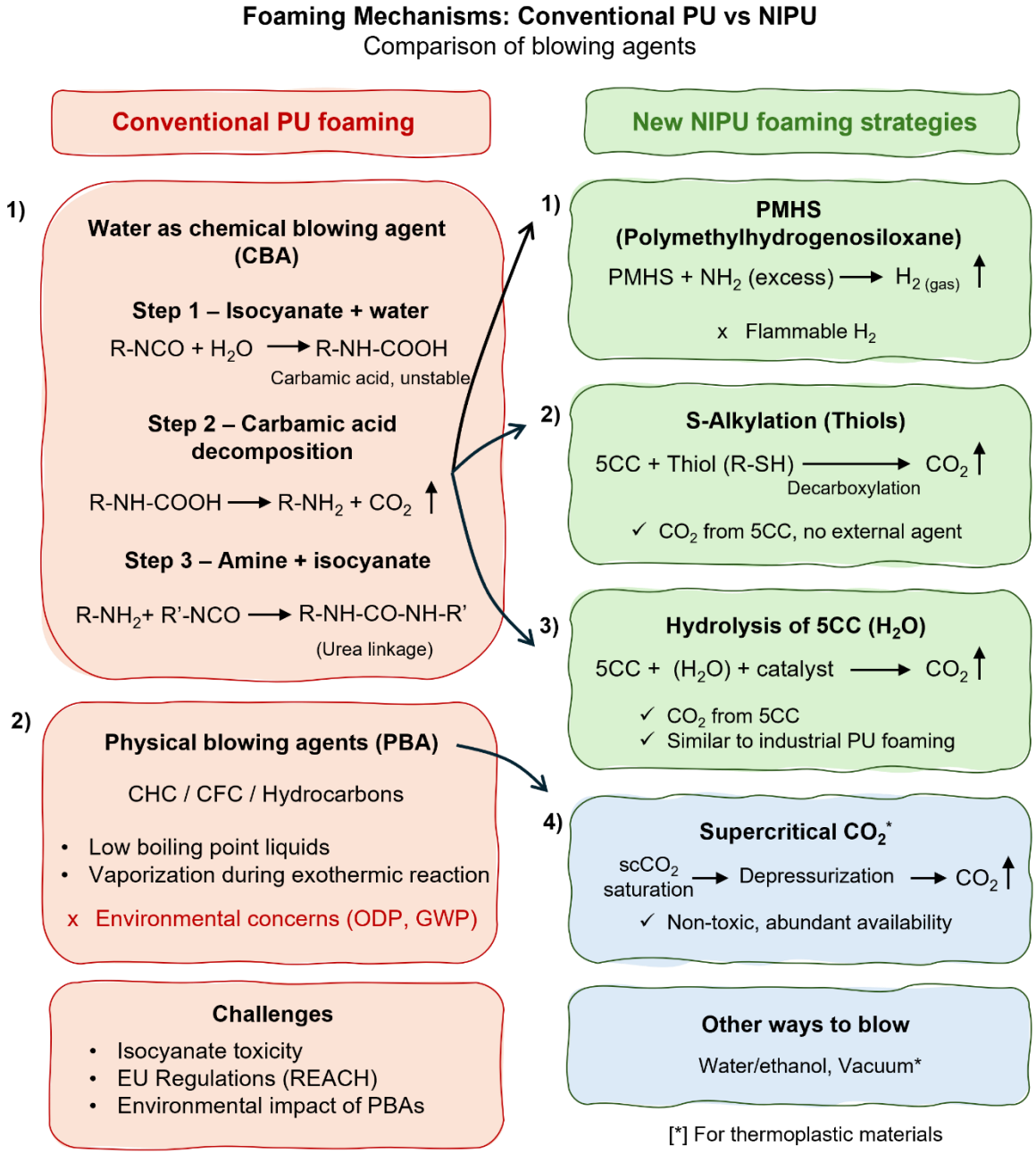

Figure II. 15. Comparison of conventional PU vs new NIPU strategies for foaming.

7.1. Chemical blowing agents

In conventional self-blowing PU foam chemistry, foams are expanded through the incorporation of water, which plays the key role in the foaming reaction. Initially, water rapidly reacts with isocyanate, forming an intermediate carbamic acid that quickly decomposes, releasing carbon dioxide (CO_2) and generating an amine. This amine then undergoes a secondary reaction with another isocyanate molecule, leading to the formation of urea.

Although highly effective, as already mentioned, this process relies on the use of toxic isocyanates, which has motivated the search for safer alternatives such as NIPU foam mechanisms.

In this context, the development of NIPU thermosetting foams has experienced significant growth, with notable breakthroughs in the field over the past decade. Most academic research efforts have been focused on the self-blowing approach, exploring various strategies to achieve foam expansion. These strategies primarily involve the incorporation of a third compound that reacts with one of the NIPU monomers, either the cyclic carbonate or amine, to generate and release gas, therefore inducing the foaming process. Among these strategies, the first self-foaming NIPU reported was due to the reaction between poly(methylhydrogenosiloxane) (PMHS) and amine precursors to produce H_2 as blowing agent. Later on, the decarboxylation and hydrolysis of 5-membered cyclic carbonate was exploited through aliphatic or cyclic carbonate thioles and water, respectively. More recently, amine-CO_2 adducts have been explored as reactive blowing comonomers, releasing CO_2 in situ upon aminolysis with cyclic carbonates under mild temperatures. Self-blowing NIPU foams aim to eliminate isocyanate-based chemistry by developing alternative gas-generation strategies that can effectively produce gas in a controlled manner, while maintaining the functional properties of the foam. The following sections will provide a detailed discussion of the major strategies used for chemical blowing agents used in NIPU foams, highlight their mechanisms, advantages and limitations.

7.1.1. PMHS

As an initial approach, NIPU foams were successfully produced using poly(methylhydrogenosiloxane) (PMHS), also known as Momentive MH15. In this strategy, PMHS is incorporated into the formulation, where it reacts with amine groups (NH_2) currently added in excess, to generate hydrogen gas (H_2) as a blowing agent (Figure II.16).

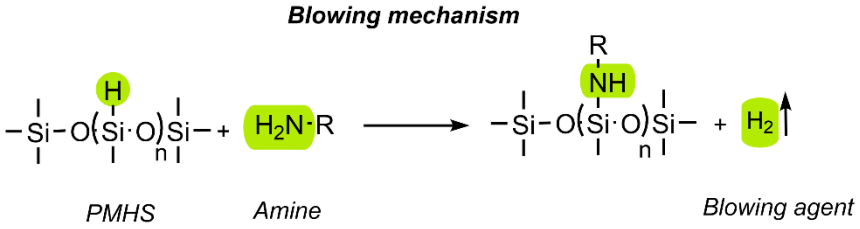

Figure II. 16. Blowing mechanism between PMHS and amines to generate H_2 as blowing agent. [142]

Following this strategy, Cornille et al.,[142] synthesized flexible foams using a mixture of trifunctional 5-membered cyclic carbonate (trimethylolpropane tris cyclic carbonate, TMPTC) and difunctional 5CC (polypropylene oxide bis cyclic carbonate, PPOBC380 or PPOBC640), combined with an aliphatic amine (Jeffamine EDR-148 or Priamine 1073) and TBD as a catalyst as shown in Figure II. 17. Initially, they investigated different cyclic carbonate ratios. The carbonate mixture was first combined with the catalyst, followed by the addition of the amine, and finally, PMHS was incorporated into the formulation. The foaming process was then carried out at 80°C for 12 hours, followed by post-curing at 120°C for 4 hours. Using the same PMHS-based approach, a variation in cyclic carbonate ratios, along with the use of thiourea as a catalyst and jeffamine EDR-148 as the amine, enabled the production of NIPU foams at room temperature after three days.[143] The foams obtained with TBD and foamed at 80–120°C exhibited glass transition temperatures (T_g) ranging from -18 to 19°C, with densities

between194 and 295 kg/m³. Similarly, the foams produced at room temperature had slightly higher T_g values (0 to 11°C), densities between 271 and 303 kg/m³, and gel contents (GC) of 91–95%.

Coste et al.,[99] also reported the fabrication of NIPU foams using 5-membered cyclic carbonates (5CC) with different chemical structures, covalently grafted with DOPO to impart fire-retardant properties. The various 5CC compounds were reacted with Jeffamine EDR-148, using thiourea as a catalyst and PMHS as the blowing agent, at 80°C for 24 hours, followed by a post-curing step at 150°C for 2 hours. The resulting foams exhibited glass transition temperatures (T_g) ranging from 3 to 39°C, densities between 301 and 832 kg/m³, and gel contents (GC) between 81 and 90%.

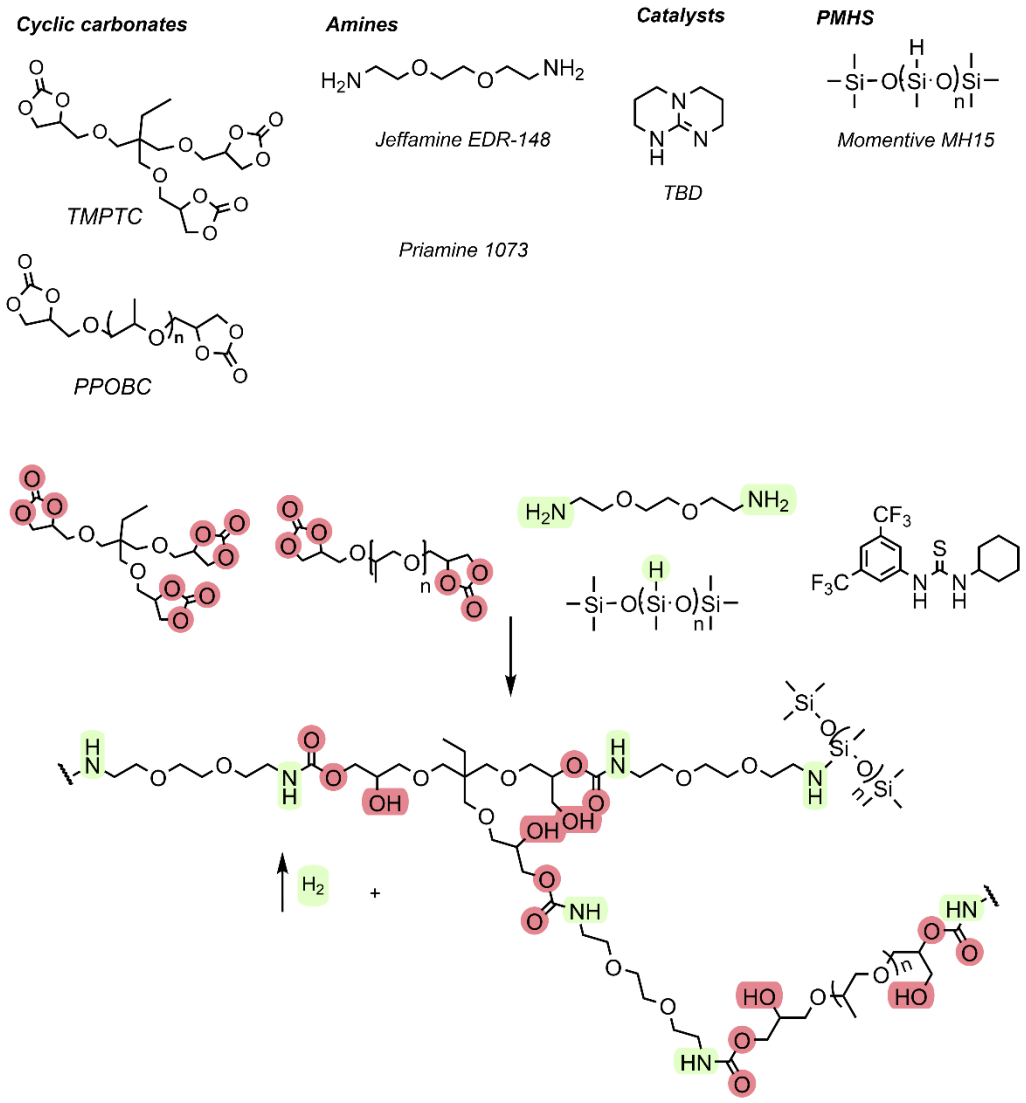

Figure II. 17. PHU foaming strategy using PMHS to produce H_2 as blowing agent.[129]

Using PMHS, NIPU foams were also recently obtained through the polyaddition of 6-membered cyclic carbonates (6CC) with amines of different chemical structures, without the use of a catalyst. In this study, cadaverine, m-xylylenediamine (m-XDA), and isophorone diamine (IPDA) were used (shown in Figure II. 18). The reactivity of the amines was analyzed in bulk through rheological studies, revealing that cadaverine exhibited the highest reactivity, followed by m-XDA, and IPDA as the least reactive. The foaming process was induced at low temperatures (50°C) overnight, followed by post-curing at 120°C for 2 hours. Additionally,

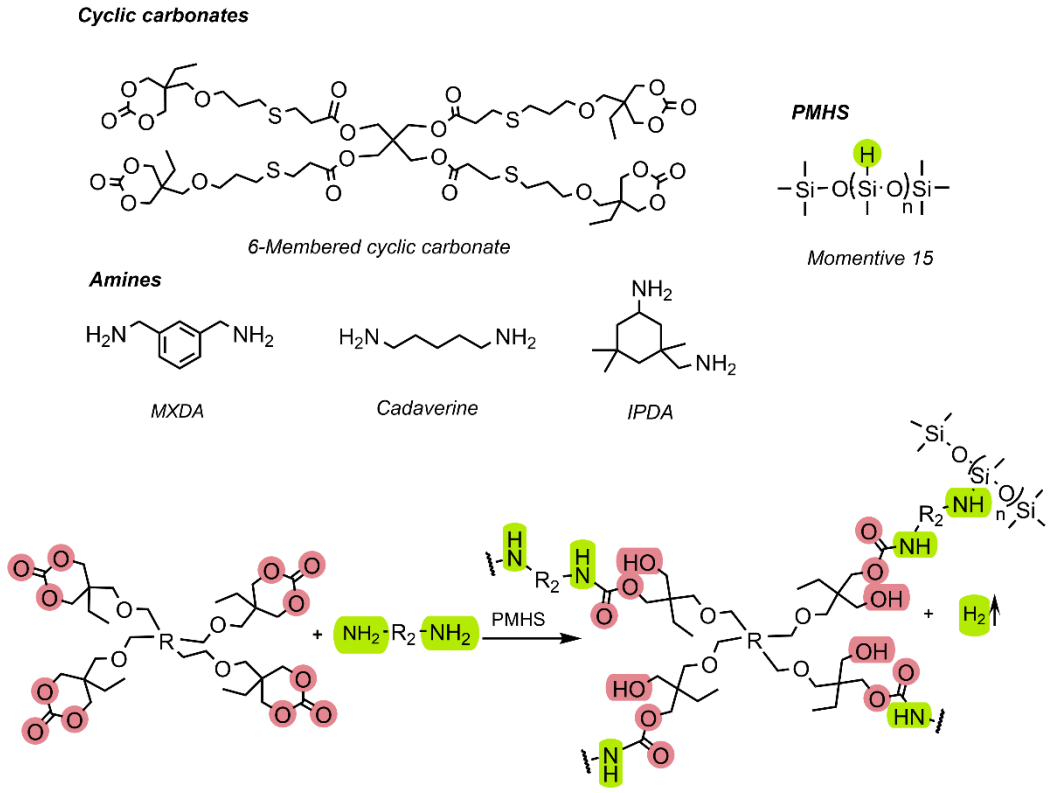

Figure II. 18. PHU foaming strategy using 6CC, different diamines and PMHS to generate H_2 as blowing agent.[144]

surfactants were incorporated to enhance foams morphology. The resulting foams exhibited glass transition temperatures (T_g) ranging from 7 to 27°C, densities between 530 and 170 kg/m³, and gel contents (GC) of 80–82%.[144]

Subsequently, NIPU foams derived from bio-based precursors were also synthesized using PMHS as a CBA. In this approach, a kraft lignin-based cyclic carbonate was employed as the 5CC precursor, in combination with a fatty acid-based diamine (Priamine 1074). The foams were prepared by first dissolving the kraft lignin-based cyclic carbonate in DMSO, followed by the addition of Priamine 1074, and finally, incorporating PMHS into the formulation. The

foaming process was carried out at 150°C for 12 hours, resulting in foams with high glass transition temperatures (T_g) ranging from 84 to 94°C, and densities between 241 and 337 kg/m³.[145]

7.1.2. S-alkylation

As a second approach for synthesizing self-foaming NIPU foams, the S-alkylation reaction of 5-membered cyclic carbonates (5CC) was exploited to generate CO_2 directly from 5CC by incorporating thiols into the formulation with 5CC and amines. These thiols act as soft nucleophiles, enabling the decarboxylation of 5CC, therefore releasing CO_2 as a blowing agent (Figure II.19).

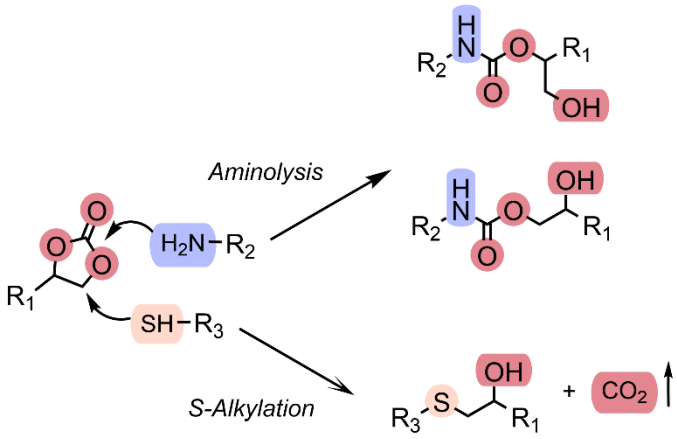

Figure II. 19. S-Alkylation strategy using thiols to generate CO_2 as blowing agent in PHU foaming.[146]

Monie et al.[146] synthesized self-blowing NIPU foams exploiting this strategy, by using 5CC, amines, and thiols. Initially, they investigated the reactivity of aminolysis toward 5CC, as well as the S-alkylation of thiols with 5CC. Through a screening study using reaction models, various catalysts and temperatures were evaluated. Their results demonstrated that DBU was the most effective catalyst for promoting both reactions. This efficiency was attributed to the fact that aminolysis of 5CC occurred slightly faster than the decarboxylation, which is crucial for achieving a proper balance between polymer network formation and CO_2 release to ensure successful foam expansion. Thermosetting NIPU foams were successfully synthesized using trifunctional cyclic carbonate (TMPTC), Jeffamine EDR-148, and EDT, an aliphatic thiol, with DBU as catalyst (Figure II. 20). To enhance foam homogeneity, various surfactants and additives (Laponite and Tegomer Si-C 2230) were incorporated. The foams were obtained by

mixing the precursors and letting them to react at room temperature for 16 hours, followed by foaming and curing at 100°C for 2 hours, with a post-curing step at 120°C for 30 minutes.

This same procedure was then applied using other diamines, such as 1,6-hexamethylene diamine (HMDA) and m-xylylenediamine (MXDA). The resulting foams exhibited glass transition temperatures (T_g) ranging from 2 to 8°C, with densities between 166 and 207 kg/m^3.

Following this work, Purwanto et al.[94] utilized the same precursors (5CC, diamine and dithiols) to synthesize NIPU foams. This study focused on exploring the effect of thiol concentration on the final foam properties and conducting a rheological study to optimize and reduce foaming and curing time. To achieve this, the network-forming precursors (5CC and amine) with the

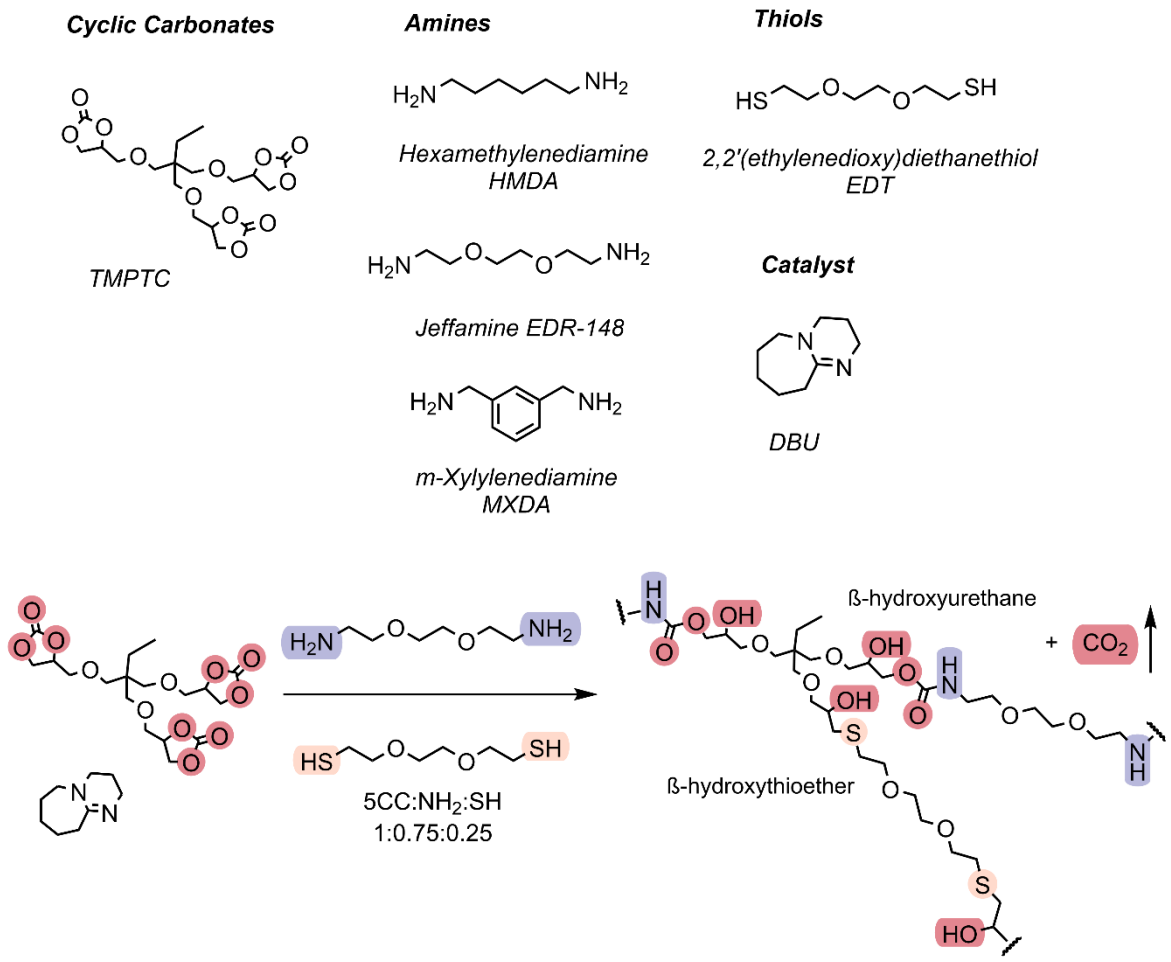

Figure II. 20. PHU foaming strategy using TMPTC, aliphatic amines and EDT to generate CO_2 as blowing agent.[146]

catalyst were pre-reacted at 80°C for 4 minutes. Subsequently, the thiol was added to the mixture, inducing the foaming process at 120°C for 30 minutes. The foams obtained exhibited a range of T_g between 3 y 23°C, with densities between 510 and 210 Kg.m^{-3}. This strategy,

involving the use of aliphatic thiols, has also inspired the development of other types of foams. For example, Khezraji et al.,[147] reported the synthesis of poly(thioether) foams at room temperature by reacting bis-cyclic carbonates with two thiol compounds, trimethylolpropane tris(3-mercaptopropionate) (f = 3) and pentaerythritol tetrakis(3-mercaptopropanoic acid) (f = 4), at varying concentrations in the presence of DBU as a catalyst. The resulting foams exhibited medium densities (113–194 kg/m³) and glass transition temperatures (T_g), ranging from 18 to 28°C.

Monie et al.,[148] reported the synthesis of self-foaming NIPU foams incorporating 5-membered cyclic carbonates (5CCs), thiolactones, and diamines. In this study, they took advantage of the reactivity of amines with 5CCs to form the polyhydroxyurethane (PHU) polymer network, while simultaneously, thiolactones undergo aminolysis, generating thiols that subsequently reacted via S-alkylation with 5CCs, leading to CO_2 release as a blowing agent. Several formulations were investigated, combining TMPTC (trimethylolpropane tris cyclic carbonate) as the 5CC precursor and N-acetylhomocysteine thiolactone (NAHcT) as the thiol precursor, to determine the optimal foaming conditions. Two different amines were employed, m-xylylenediamine (MXDA) and Jeffamine EDR-148. The resulting foams exhibited glass transition temperatures (T_g) between 27 and 56°C in their dry state, with densities ranging from 167 to 185 kg/m³ and a gel content (GC) of 94–95%.

Similarly, Coste et al.,[149] reported the use of dithiocarbonates (DTCs), specifically polypropylene oxide bis-thiocarbonate (PPOTC), as a thiol precursor, with TMPTC as the 5CC component and EDR-148 as the diamine, to synthesize self-blowing NIPU foams. In this approach, the DTC undergoes aminolysis to generate thiols, which subsequently decarboxylated 5CCs, releasing CO_2 to drive foam expansion (Figure II. 21). The foams were synthesized using 5CC, DTC, EDR-148, and DBU as a catalyst, with the foaming process conducted at 90°C for 24 hours. To improve foam morphology, Tegomer and Laponite (5 wt%) were incorporated as additives. Interestingly, the foams exhibited two glass transition

temperatures (T_g): T_{g1} ranging from -45 to -31°C and T_{g2} ranging from 11 to 19°C. The foam densities ranged from 249 to 445 kg/m³, with a gel content (GC) of approximately 82–83%.

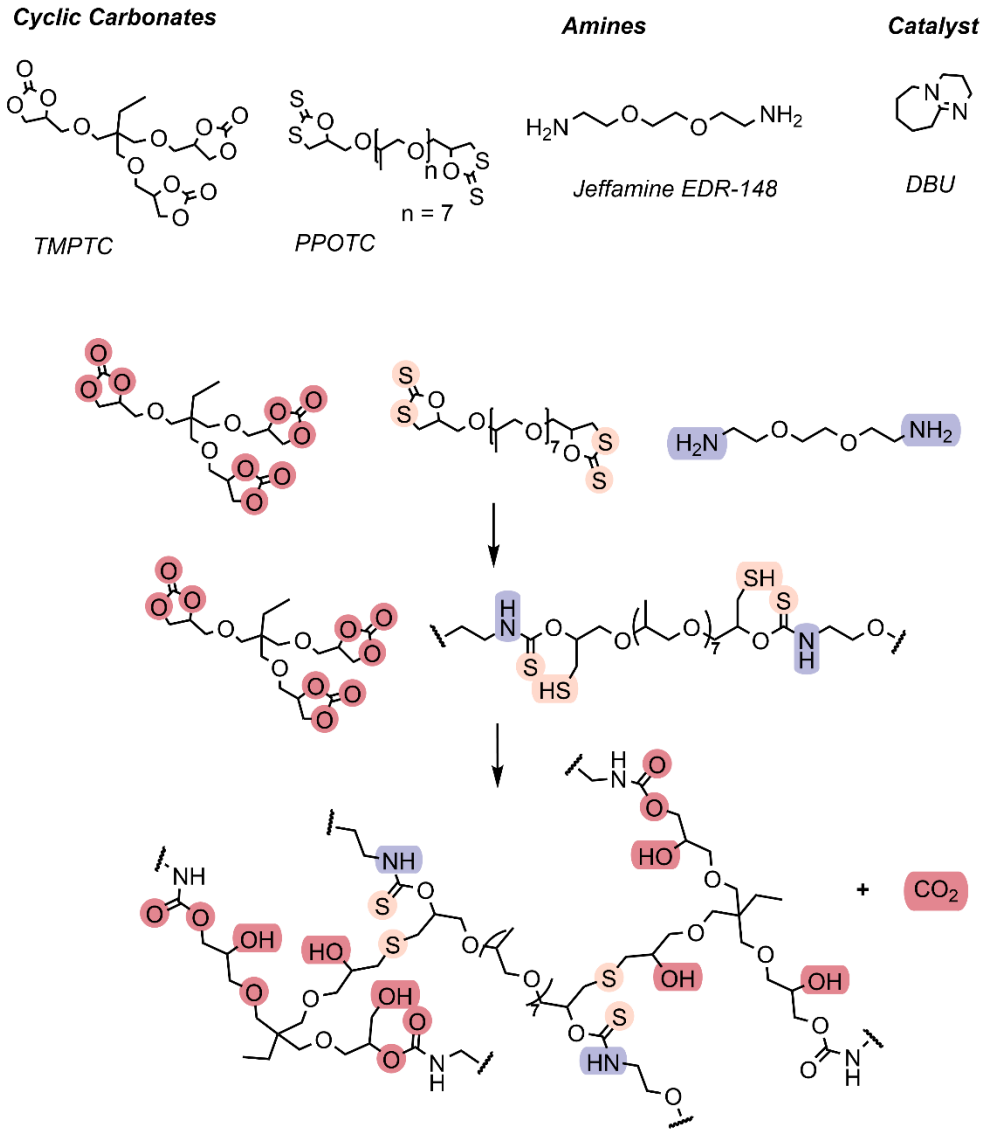

Figure II. 21. PHU foaming strategy using dithiocarbonates (PPOTC) as thiol to generate CO_2 as blowing agent.[149]

More recently, this strategy has also been explored using bio-based precursors derived from plant sources, such as cashew nutshell and linseed oil cyclic carbonates. Purwanto et al.,[150] reported the use of cashew nutshell-derived NC-514 cyclic carbonate in combination with a trifunctional poly(propylene glycol)-based amine (T-403) as a crosslinker, and ethylene dithiol (EDT) as a thiol precursor in different concentrations to explore the effect of the final properties. Moreover, to enhance foam morphology, Tegomer E-Si 2330 (2 mol%) was incorporated into the formulation. The foaming process was conducted in two steps: first, the

cyclic carbonate was reacted with the amine and DBU as catalyst at 120°C to achieve a suitable viscosity, followed by the addition of EDT to induce foaming at the same temperature. The pre-curing and foaming times varied depending on the thiol concentration used in the formulation. The resulting bio-based NIPU foams exhibited glass transition temperatures (T_g) between -2 and 6°C, with densities ranging from 320 to 550 kg/m³. A higher thiol concentration led to greater CO_2 release, resulting in a reduction in foam density, an increase in cell size, a decrease in cell density, and a lower crosslinking density. The foams exhibited gel content (GC) between 82 and 85%.

Expanding on this strategy, the same group further investigated the influence of different thiol chemical structures, employing three thiols of distinct functionalities: 2,2-(ethylenedioxy)diethanethiol (f = 2), trimethylolpropane tris(3-mercaptopropionate) (f = 3), and pentaerythritol tetrakis(3-mercaptopropionate) (f = 4). For the synthesis of these foams, they used dimer acid-derived cyclic carbonate (GS-120) in combination with a trifunctional amine (T-403), DBU as the catalyst, and Tegomer E-Si 2330 (1 mol% relative to cyclic carbonate groups) as an additive. Initially, the cyclic carbonate, amine, additive, and DBU were pre-reacted at 120°C, followed by the addition of the thiol to induce foaming at the same temperature. The resulting foams exhibited T_g values between -28 and -17°C, with densities ranging from 290 to 310 kg/m³ and a gel content between 85 and 89%. This study demonstrated that foam morphology was independent of the thiol type, as all formulations exhibited similar densities, cell sizes, and cell densities. However, crosslinking density increased with the functionality of the thiol, indicating higher-functional thiols contributed to a more interconnected polymeric network.[151]

Finally, Wang et al.,[117] reported the synthesis of NIPU foams using linseed oil derived cyclic carbonate (CLSO). This study examined the effect of thiols with different functionalities (f = 2, 3, 4) as previously reported by Purwanto et al., in combination with different diamines, specifically Jeffamine EDR-148, hexamethylene diamine (HMDA), and m-xylylene diamine (MXDA), in the presence of DBU as a catalyst. NIPU foams were synthesized by mixing CLSO, thiol, amine, and DBU at 90°C for 2 minutes, followed by curing at 140°C for 1 hour. The foams then underwent two post-curing steps at 170°C for 1 hour and 180°C for 2 hours. The resulting foams exhibited low glass transition temperatures (T_g) between -5 and 9°C, with similar densities across all formulations, ranging from 130 to 170 kg/m³.

7.1.3. 5CC hydrolysis

In addition to the previously mentioned strategies, Bourguignon et al.[17] reported a significant advancement in self-blowing NIPU foams, resembling the conventional foaming mechanism of polyurethane using water. In a prior study on NIPU hydrogels, the same research group demonstrated that 5-membered cyclic carbonates (5CC) undergo hydrolysis in the presence of water at pH 12.5.[152] Leveraging this secondary reaction, they exploited 5CC hydrolysis to generate self-blowing NIPU foams by introducing water into the formulation (Figure II.22)

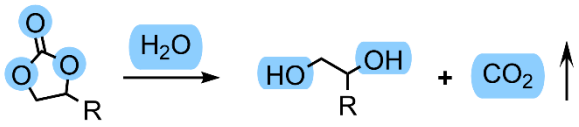

Figure II. 22. Hydrolysis of 5-membered cyclic carbonates to generate CO_2 as blowing agent.[17]

In this study, the optimal conditions for hydrolysis and curing, varying temperature, water content, and catalyst concentration, were investigated to ensure that the formation of the polyhydroxyurethane (PHU) network occurred slightly faster than the 5CC hydrolysis, allowing for the controlled release of CO_2 as a blowing agent (BA). The foams were synthesized using trimethylolpropane tris(cyclic carbonate) (TMPTC) as the 5CC precursor, along with various amines, including Jeffamine EDR-148, MXDA, and HMDA, in the presence of water (H_2O), DBU as a catalyst, and hydrotalcite (12 wt% relative to TMPTC) (Figure II. 23). The foaming process was carried out at 80–100°C for 3–5 hours, yielding foams with densities ranging from 153 to 429 kg/m³ and high gel content values (93–94%), despite the fact that the alcohols formed during 5CC hydrolysis did not contribute to the polymer network formation.

Notably, the incorporation of additives such as hydrotalcite contributed to reducing pore size and density in most cases. Additionally, foams synthesized using MXDA as the amine precursor exhibited the lowest densities (154 kg/m³), emphasizing the influence of precursor selection on final foam morphology and performance.[17]

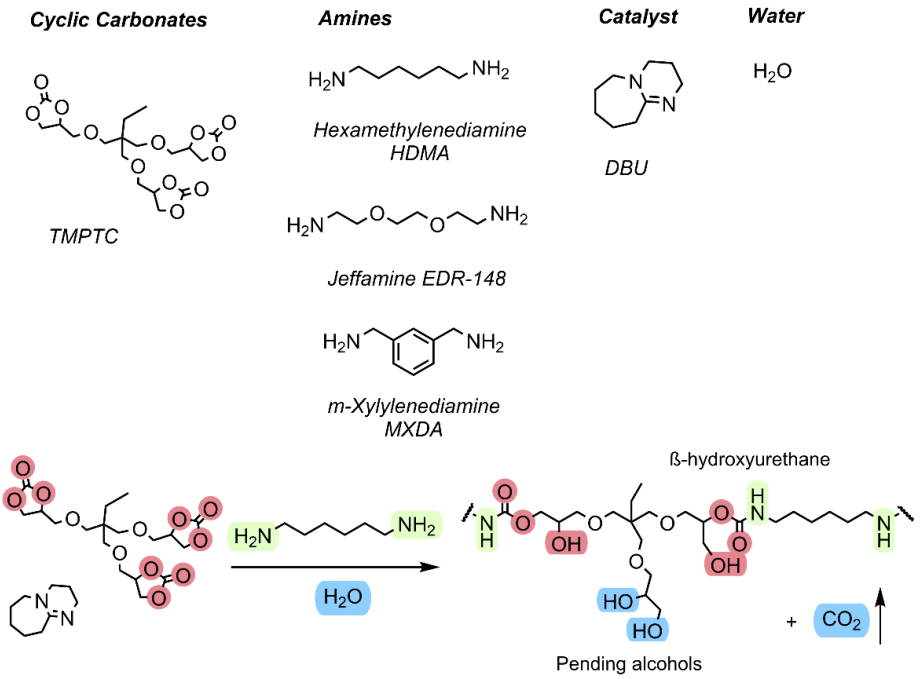

Figure II. 23. PHU foaming strategy using TMPTC, different amines, and water to produce CO_2 as blowing agent.

Lastly, taking a further step toward emulating water-blown conventional polyurethane foams, the hydrolysis of 5CC was further refined to enable NIPU foam production at room temperature. This was achieved by incorporating epoxidized precursors (TMPTE) alongside 5CC (TMPTC), a diamine mixture (MXDA) and tris(2-aminoethyl)amine (TREN)), water (H_2O) as a blowing agent, and KOH as a catalyst. The exothermic aminolysis of epoxides rapidly increased the formulation temperature, subsequently triggering the decarboxylation of 5CC, facilitating foam expansion. This process allowed for the rapid production of hybrid-NIPU foams in just 5 minutes at room temperature. The resulting foams exhibited densities ranging from 211 to 294 kg/m³ and glass transition temperatures (T_g) between 2 and 47°C, depending on the tunability of the monomers. The foams also demonstrated high gel content values of 88–96%.[153]

7.1.4. CO_2-amine adducts

Lastly, another chemical blowing mechanism was recently reported by Choong et al.,[154] using various amine-CO_2 adducts as an in situ CO_2 source. Among the adducts investigated, the TETA-DBN adduct (TC3) was preferred due to the highest CO_2 adsorption (60.4%) and an

effective CO_2 desorption (87%) at 60 °C via aminolysis with cyclic carbonates. The adduct served a dual role as both blowing agent and reactive comonomer in formulations based on a tris(cyclic carbonate) (TMPCC) and a bis(cyclic carbonate) (FBC), with two diamines: 1,2-bis(2-aminoethoxy)ethane (BisAEE) and 1,5-diaminopentane (DAP). Optimal foaming conditions were established at 60 °C for 24 h with a reactive group molar ratio of [TMPCC]/[FBC]/[BisAEE]/[TC3] = 1/0.18/1.05/0.13, as lower temperatures (50 °C) led to incomplete curing and higher foam densities, while higher temperatures (80 °C) caused cell rupture and foam shrinkage. Under these conditions, foams with densities ranges of 0.203–0.239 $g \cdot cm^{-3}$ were obtained with homogeneous cell size (cell diameters of 232 ± 97 and 314 ± 116 µm for BisAEE- and DAP-based foams, respectively), with DAP-containing foams exhibiting higher glass transition temperature (Tg = 24 °C vs. 16 °C for BisAEE), attributed to the shorter, more rigid aliphatic chain of DAP. All formulations showed high gel contents (89–93%), confirming an advanced degree of crosslinking. This approach represents a promising low-temperature, isocyanate-free foaming strategy, though long curing times (24–48 h) remain a limitation to address.

The latest studies have demonstrated significant progress in the development of self-blowing non-isocyanate polyurethane (NIPU) foams. These advancements range from the use of polymethylhydrosiloxane (PMHS) and thiols at moderate temperatures (80-100°C), as well as using amines-CO_2 adducts at 60 °C to the more recent breakthroughs in water-blown foams that can be synthesized at room temperature. This latter is closed to the synthesis methods traditionally employed in isocyanate-based polyurethane chemistry. However, this emerging synthesis also encompasses the production of hybrid foams derived from cyclic carbonates, epoxies, and amines used as curing agents. This hybrid foams present the potential for a new class of foams, that would serve as either direct replacements for conventional polyurethane foams or as new materials. Further thermos-mechanical characterization would be necessary to have new perspectives on these hybrid foams.

7.2. Physical blowing agents: New opportunities for NIPU foams

While chemical blowing agents have enabled significant advances in self-foaming NIPU systems, alternative approaches involving physical blowing agents (PBAs) have also gained attention for their industrial scalability and advantages in foam structure and cost-efficiency.

Physical blowing agents (PBAs) are either gases or low-boiling-point liquids introduced into the polymer matrix during processing. These agents expand when pressure is reduced or temperature is increased, forming the foam structure. Common PBAs for the production of polyurethane (PU) foams include short-chain aliphatic hydrocarbons (C_5–C_7) and halogenated hydrocarbons (C_1–C_4) in liquid form, as well as gaseous CO_2, N_2, and hydrocarbons. These PBAs are widely used in the PU industry due to their low cost and broad applicability to both thermoplastic and thermosetting foams.[15,155]

Economically, PBAs have significant advantages. They enable the production of low-density foams (≤50 kg/m³) at a fraction of the cost compared to chemical blowing agents (CBAs). Comparative analyses suggest that producing foams of equivalent density with CBAs can be up to ten times more expensive. Furthermore, PBAs generally produce closed-cell foams with superior mechanical strength and insulation, while CBAs tend to favor open-cell structures with smaller pore sizes. However, PBA-based processes require investment in specialized high-pressure equipment, balancing their economic and structural benefits with higher initial setup costs.[15,155,156]

Historically, physical blowing agents such as chlorofluorocarbons (CFCs) and hydrofluorocarbons (HFCs) were extensively employed in rigid polyurethane (PU) foams, beginning in the 1960s. These agents offered low thermal conductivity (e.g., CFC-11 reaching 17 mW/m·K), enabling the production of closed-cell foams with excellent insulation properties. Optimization of formulations even reduced final thermal conductivities to approximately 15 mW/m·K. However, CFCs and HFCs were later identified as ozone-depleting substances and greenhouse gases with high global warming potential (GWP). **Figure II. 24** summarizes the evolution of physical blowing agents over time. Following the Montreal

Protocol, their use was phased out in Europe and other developed countries by 1996, with complete discontinuation between 2003 and 2015.[11,15,155]

Today, the demand is for PBAs that minimize ozone depletion and health risks while maintaining foam performance. Ideal PBAs should exhibit high solubility with precursors, low solubility in the final polymer matrix, low thermal conductivity, low gas diffusion rates, zero

Physical Blowing Agents (PBA): Classification & Evolution

Environmental impact and regulatory timeline

Category	Examples	ODP/GWP	Status	Comments	Period
CFC Chlorofluoro-carbons	CFC-11 (CCl_3F) CFC-12 (CCl_2F_2) CFC-113	ODP: 0.6-1.0GWP: 4,750-10,900	Banned	Excellent insulation but severe ozone depletion Montreal Protocol 1987	1960s-1990s
HCFC Hydrochloro-fluorocarbons	HCFC-141b HCFC-142b HCFC-22	ODP: 0.02-0.1GWP: 600-2,400	Phased out	Lower ODP than CFCs Transition solution Kigali Amendment 2016	1990s-2020
HFC Hydrofluoro-carbons	HFC-134a HFC-245fa HFC-365mfc	ODP: 0 GWP: 950-3,500	Being restricted	No ozone depletion but high GWP (climate change) F-gas regulation EU	1990s-Present
Hydrocarbons HC	Pentane (C_5H_{12}) Cyclopentane Isopentane	ODP: 0 GWP: ~3-2 Very low	Approved	Low environmental impact Flammable (safety concern) Widely used in EU	2000s-Present
CO_2/scCO_2 Carbon dioxide (supercritical)	CO_2 (liquid/gas) scCO_2 (P>73.8 bar, T>31°C)	ODP: 0 GWP: 1 Minimal impact	Green ideal	Non-toxic, non-flammable Excellent cell control High pressure equipment Growing research interest	2010s-Future NIPU foams

Figure II. 24. Classification and evolution of physical blowing agents over time.

ozone depletion potential (ODP), low flammability, and chemical inertness. Hydrocarbons, particularly pentanes (cyclopentane, isopentane, and n-pentane), have been adopted in Europe

as alternatives due to their zero ODP and good insulation properties, despite their inherent flammability that requires strict safety measures.

7.2.1. Hydrocarbons, Hydrofluorocarbons (HFC), Hydrochlorofluorocarbon HCFC, chlorofluorocarbons (CFC)

In this context, the use of physical blowing agents (PBAs) has also been explored for the development of non-isocyanate polyurethane (NIPU) foams through various batch processes. The evolution of PBAs in NIPU foam synthesis encompasses a progression from conventional agents, such as hydrocarbons, HFCs, HCFCs, and CFCs, to more environmentally benign alternatives, including Solstice® LBA, Solkane® 365/227, supercritical CO_2, water, including also ethanol. These agents differ widely in flammability, global warming potential (GWP), and ozone depletion potential (ODP), highlighting the growing preference for less toxic materials that align with green chemistry principles. Notably, their successful integration into a wide range of NIPU formulations, ranging from thermosetting and thermoplastic systems to reactive extrusion routes, has enabled the production of foams with varying densities, pore sizes, and thermal performance characteristics.

In 2012, hybrid polyurethane spray foams were developed using PBAs, incorporating epoxy and/or acrylic resins with rheology modifiers. Urethane formation in this case involved a combination of isocyanate-based chemistry (polyols and isocyanates) and non-isocyanate chemistry. The non-isocyanate pathway relied on the polyaddition of cyclic carbonates and polyamines. Mixtures of PBAs are used to blow these foams. These include HFCs, HCFCs, CFCs, pentanes, azodicarbonamide, and other PBA compounds such as alkylsiloxanes (Xiameter and MHX-1107) and FEA-1110, a fourth-generation fluorocarbon reported by DuPont to have low global warming potential (GWP), zero ODP and non-flammability.[157]

Subsequently, other non-isocyanate hybrid polymer foams utilizing physical blowing agents (PBAs) were further explored in 2013. These foams were formulated through the reaction of epoxies and amines, incorporating additional components such as acrylates, methacrylates, and polycyclic carbonates. Key CCs include soybean oil cyclic carbonates (CSBO), polyoxypropylene trimethylol propane with terminal cyclic carbonate groups (Cycloat® A), and trimethylolpropane tricyclic carbonate (TMPTC). The blowing agents used in this case primarily consisted HFCs (FM-200, SUVA® 236fa, Solkane® 365mf, among others), HCFCs (Solstice® LBA), alkylhydrogensiloxane (Dow Corning 1107®), and hydrocarbons (n-

pentane, iso-pentane, and cyclopentane). The resulting foams exhibited low densities, ranging from 25 to 40 kg/m³.[158]

In 2016, Blattmann et al.,[159] reported the synthesis of thermosetting foams entirely based on non-isocyanate polyurethane (NIPU) chemistry, utilizing Solkane 365/227 as the physical blowing agent. This PBA is a low-boiling-point liquid and is classified as non-flammable and has no ozone depletion potential (ODP). The NIPU chemistry was based on the aminolysis of an aliphatic amine, hexamethylene diamine (HMDA), with a mixture of cyclic carbonates. Initially, the study focused on optimizing the ratio between two cyclic carbonates: trimethylolpropane tricyclic carbonate (TMPTC) and ethoxylated TMP tricyclic carbonate (EO-TMPGC) (Figure II. 25). The optimal composition was determined to be 60 wt% TMPTC and 40 wt% EO-TMPGC, due to its favorable viscosity, short gelation time (871 seconds) and pot life (410 seconds). Following this optimization, the cyclic carbonate mixture was combined with HMDA and DABCO as a catalyst at room temperature for 4 to 6 minutes. Subsequently,

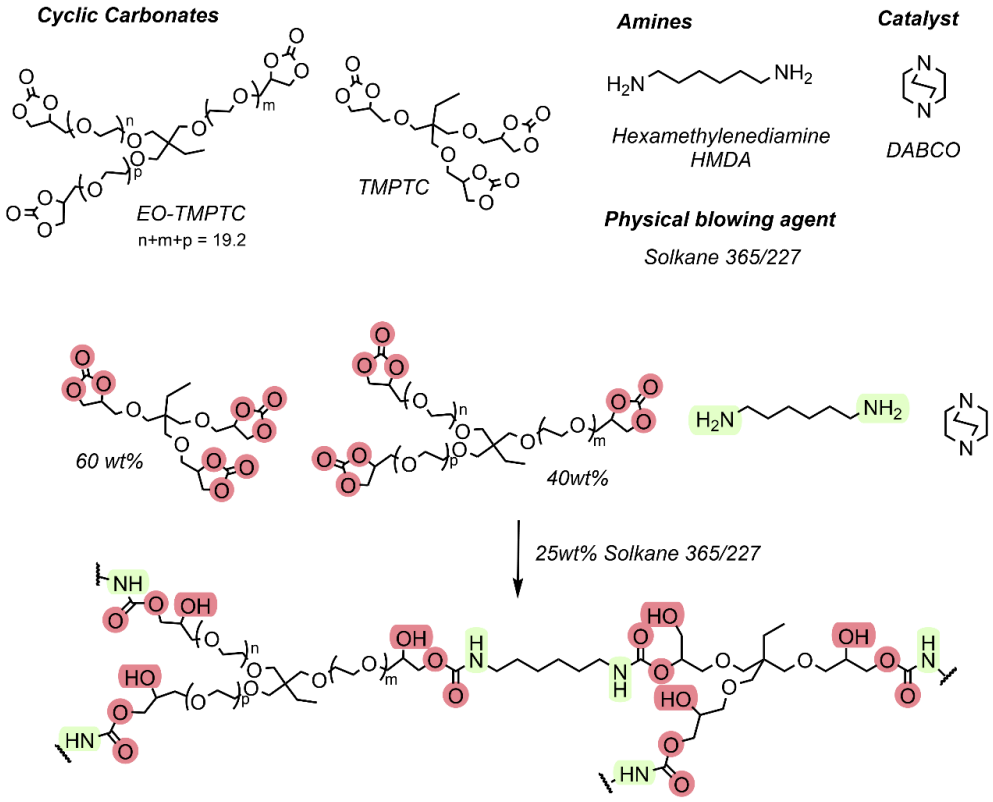

Figure II. 25. Strategy implemented to produced PHU foams with solkane 365/227 as physical blowing agent.[159]

25 wt% of Solkane 365/227 was incorporated into the formulation and mixed for 10 seconds. The resulting blend was then poured into a preheated aluminum mold (50–80°C), where

foaming and curing were induced over 14 hours at 80°C. The foams exhibited densities ranging from 83 to 219 kg/m³ and a T_g of approximately -13°C. This method proved for the first time the synthesis of thermostable NIPU foams with PBAs.

7.2.2. Supercritical CO_2

In the pursuit of more sustainable physical blowing agents beyond hydrocarbons and mix of hydrofluorocarbons without ODP such as solkane, a more ecological option to hydrocarbons such pentane, HFC, CFC and HCFC, CO_2 has also emerged as a promising physical blowing agent option. In fact, supercritical CO_2 ($scCO_2$) is gaining increasing attention in both academic and industrial fields, particularly for polymeric foams, including polyurethane (PU) foams, due to its advantageous characteristics.[160–163] CO_2 is abundantly available and considered as a zero ozone-depletion substance. Although it is a greenhouse gas, its global warming potential (GWP =1) is significantly lower than the traditional PBA (Figure II.24), and its used doesn't contribute to net emissions when sourced from industrial waste streams or carbon capture processes. Furthermore, its recyclability, non-toxicity, and non-flammability render it highly attractive in industrial applications, being aligned with the principles of eco-friendly applications and processes.

In this context, Grignard et al.[164] successfully fabricated microcellular thermoplastic NIPU foams from bio-based and CO_2-sourced NIPU films using supercritical CO_2 ($scCO_2$). Initially, the NIPU films were synthesized from two cyclic carbonates: poly(ethylene glycol) biscyclic carbonate (PEGBC) or partially carbonated (50%) soybean oil cyclic carbonate (CSBO), which was reacted with a bio-sourced amine derived from Pripol 1013, a dimeric fatty acid combined with an aliphatic diamine as shown in Figure II.26. Following an optimization process, the films were saturated under $scCO_2$ conditions at different critical pressures (100 and 300 bar) at 40°C for 3 hours. The cell was quickly cooled down to 0°C and a rapid depressurization step was then applied to prevent foaming from being dependent on the depressurization rate. Blowing was induced at two different temperatures (80 and 100°C) for 1 minute, followed by a cooling step to stabilize the foam structure. The resulting foams exhibited densities ranging from 110 to 176 kg/m³, pore sizes between 3 and 11 μm, and thermal conductivity values

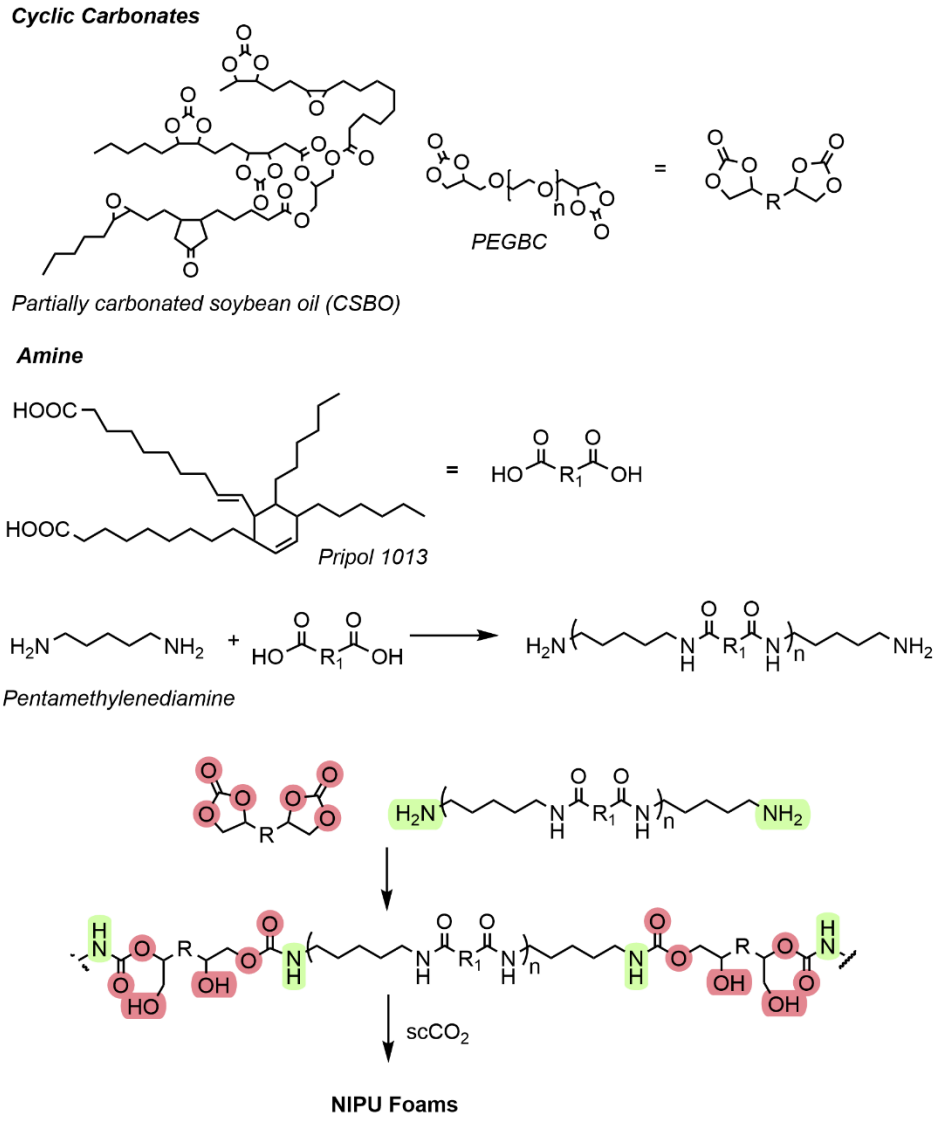

Figure II. 26. Foaming strategy using $scCO_2$ as physical blowing agent to produce thermoplastic PHU. [164]

between 50 and 65 $mW \cdot mK^{-1}$ and T_g ranging from -2 to -7°C.

In another study as reported by Mao et al.,[165] the synthesis and investigation of thermoplastic NIPU foams were conducted through the polyaddition of bio-based bis(cyclic carbonates) and dimer diamines, utilizing supercritical CO_2 ($scCO_2$) as a physical blowing agent. Thermoplastic NIPU films were synthesized by reacting ethylene carbonate bisphenol A (ECBPA) with a mixture of diamines, specifically hexamethylenediamine (HMDA) and C36-alkylenediamine (C36DDA). Additionally, ethylenediamine (EDA) was introduced as a chain extender, to react with 1,2,4,5-benzenetetracarboxylic acid (PMA) to partially form a 3D network, which

enhances the mechanical properties of the material to improve the foaming process. NIPU films were synthesized in the presence of DMF as a solvent at 100 °C for 24 hours. The resulting materials were then saturated with $scCO_2$ at 150 bar and 80 °C for 6 hours. Unlike Grignard's previous work, in which foam expansion was pressure-dependent, this study employed a rapid pressure drop to induce foaming, followed by a cooling step to stabilize the structure. The resulting foams exhibited high glass transition temperatures (T_{gs}) of approximately 30°C, with densities ranging from 215 to 432 kg/m³ and microcellular pores measuring 10–20 µm.

In a similar approach, Kirchberg et al.,[166] reported the synthesis of thermoplastic poly(ester urethane) foams using supercritical CO_2 ($scCO_2$) as a PBA through the polycondensation of carbamates (**Figure II. 27**). In this study, cyclic carbonates were synthesized from dimethyl carbonate (DMC) and various diols, including butanediol, propylene glycol, and ethylene glycol. These cyclic carbonates were subsequently reacted with an amino ester, specifically 11-amino undecanoic acid methyl ester, to form carbamates. The resulting poly(urethane esters) were obtained via bulk polycondensation of these carbamates. As a proof of concept, the foaming behavior of the material under $scCO_2$ conditions was investigated. The poly(ester urethane) was first saturated in $scCO_2$ at 120°C and 500 bar for 8 hours. In accordance with the

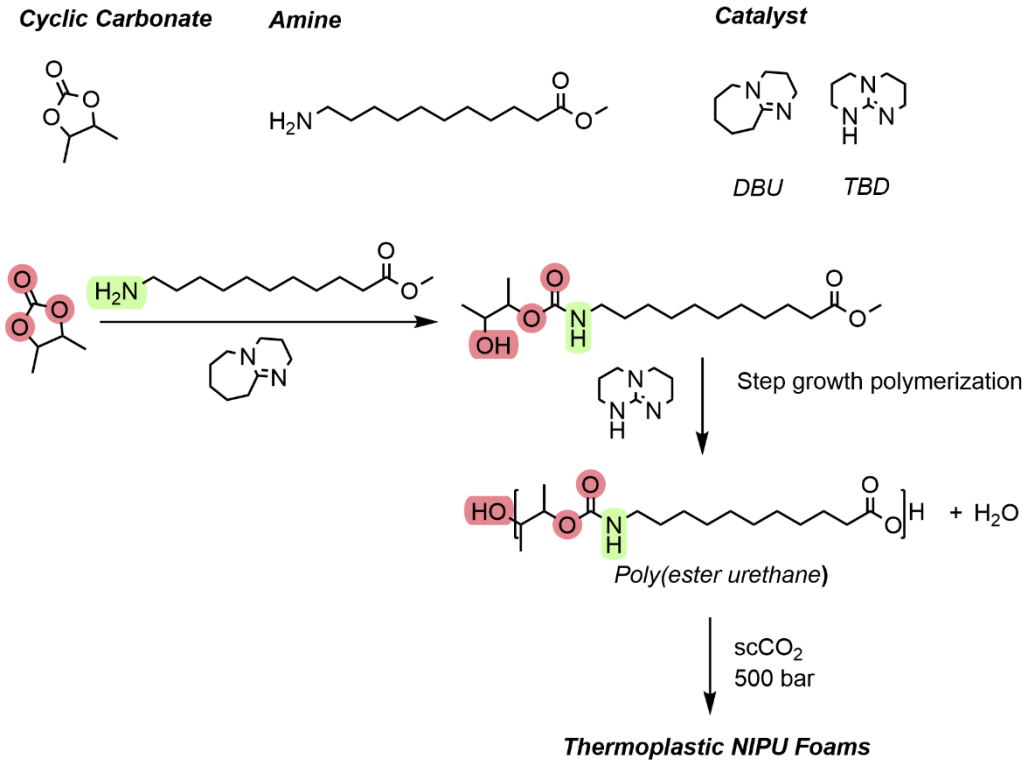

Figure II. 27. Foaming strategy using scCO2 to produce PHU by the step-growth polymerization of a carbamate.[166]

previous work done by Mao, foaming was induced by rapid depressurization of the cell at a rate of 200 bar s^{-1}. This foaming process yielded a closed-cell foam with microcellular pores ranging from 1 to 4 μm, a final foam density of 160 kg/m³ and T_g of -16°C.

Surprisingly, this foaming technology has not been yet applied to other NIPU foams and more importantly, it has not been used for the fabrication of thermosetting foams, which are of greater interest in terms of volume and market demand in PU materials.

7.2.3. Water/Ethanol

Broadening the range of physical blowing agents for NIPU foams, researchers have explored new strategies utilizing water and ethanol as PBAs. Unlike previous studies where water acted as a CBA by reacting with NIPU precursors, in this new approach, water and methanol are incorporated into the formulation at temperatures where evaporation occurs, inducing foam expansion. Valette et al.,[167] reported the synthesis of NIPU foams via transurethane polycondensation, employing water/methanol as physical blowing agents. In this study, inspired by their previous work,[168] NIPU foams were produced from NIPU oligomers synthesized in two steps: first, dimethyl carbonate (DMC) was reacted with bio-based diamines, followed by the incorporation of diols. The resulting NIPU oligomer was then further crosslinked using an epoxide-based crosslinker (DENACOL EX512) and an amino-terminated PDMS as a soft segment. The precursors were mixed with varying water/methanol ratios and foamed within a temperature range of 85 to 120°C. The resulting foams exhibited low glass transition temperatures (T_gs) ranging from -20 to 0°C and densities between 55 and 950 kg/m³.

7.2.4. Other ways to blow

An alternative foaming approach, without the incorporation of any CBA or PBA, was recently reported by Sarma et al.,[169] first the synthesis of thermoplastic NIPUs through the aminolysis of cyclic carbonates via reactive extrusion (REx) was investigated. In this study, various formulations were synthesized using three types of aromatic cyclic carbonates (5CC): bisphenol A bis(cyclic carbonate), bisphenol AF bis(cyclic carbonate), and phenolphthalein bis(cyclic carbonate). These 5CCs were reacted with diamines of different chemical structures, including hexamethylenediamine (HMDA), Priamine 1075, p-xylylenediamine (P-XDA), 3,3′-diamino-N-methyldipropylamine (DNDPA), and isophorone diamine (IPDA). NIPU materials were obtained through reactive extrusion (REx) with 30 wt% DMSO as a hydrogen bond disruptor (HBD), varying the reaction time up to 4.5 hours. Subsequently, only the materials obtained from p-XDA and the three different 5CCs were used to investigate the foaming

process. The thermoplastic materials were foamed under vacuum at elevated temperatures, specifically 5°C below their respective T_gs, for 4-6 hours. The resulting foams exhibited low densities (60–70 kg/m³) with micropores ranging from 123 to 157 μm. Additionally, their thermal conductivity values, ranged between 43 and 47 mW/m·K. These values were comparable to those obtained by Grignard using $scCO_2$ as a PBA.

7.3. Conclusion of CBA and PBA

Over the past decade, there has been an increasing focus on developing new materials and emerging technologies that meet modern societal demands while respecting the planet's physical limits. As previously discussed, efforts in polyurethane (PU) foam production have aimed to transition toward renewable precursors for both polyols and isocyanates (e.g., biomass, carbohydrates, vegetable oils) and to develop synthetic routes that eliminate phosgene in isocyanate production. However, the toxicity of isocyanates and regulatory restrictions, such as those imposed by REACH, have exerted significant pressure on European industries and scientific community to explore alternative chemical pathways and safer technologies for both the environment and labor force's workers.

Despite progress in this field, the complete elimination of isocyanates remains a major challenge. Significant advances have been made in synthesizing non-isocyanate polyurethane (NIPU) foams, blown using either chemical (CBA) or physical (PBA) blowing agents. Regarding the use of CBAs, numerous studies have reported the use of five-membered cyclic carbonates (5CCs) derived from CO_2 fixation, as well as bio-based and commercially available amines and 5CCs. Indeed, aminolysis of 5CC has emerged as the most extensively studied route for generating urethane linkages within the polymeric matrix of NIPU foams. Notably, most foams produced using CBAs are thermosetting materials.

In contrast, the use of PBAs for NIPU foaming has been comparatively less explored. Various synthetic approaches have been reported, ranging from hybrid foams incorporating partial 5CC and amine fractions in PU formulations to fully isocyanate-free formulations relying on the synthesis via carbamate polycondensation, 5CC aminolysis, and transurethanization for the generation of urethane linkages. However, certain foaming processes, such as $scCO_2$ and vacuum foaming at elevated temperatures, have only been applied to the production of thermoplastic foams. This limitation restricts their potential industrial applicability and does not align with the high demand for thermosetting foams, which continue to dominate the commercial PU foam market.

Once foam production is achieved and proven feasible by different strategies, other key factors determining their industrial potential applicability is their final properties and functionality. Therefore, efforts must focus on providing and enhancing the material's properties at the same time to replace conventional materials with more sustainable and high-performance alternatives. However, given the relatively recent development of NIPU foams, their applications remain less explored and limited. This knowledge gap represents new research and development opportunities, allowing for the design and evaluation of these materials while considering their end-of-life scenarios.

Table II. 1. Summary of the foaming mechanisms using chemical blowing agents (CBAs) to produce NIPU foams

Reference	CBA Type	Precursors	T_g (°C)	Density (kg/m³)	Observations
Cornille et al. [142]	PMHS	TMPTC + PPOBC + Jeffamine/Priamine + TBD	-18 to 19	194-295	Foaming: 80°C/12h + 120°C/4h
Cornille et al. [143]	PMHS	TMPTC + PPOBC + Jeffamine 148 + thiourea	0 to 11	271-303	RT/3 days. GC: 91-95%
Coste et al. [99]	PMHS	5CC-DOPO + Jeffamine EDR-148 + thiourea	3 to 39	301-832	GC: 81-90%. Flame retardant
Coste et al. [144]	PMHS	6CC + cadaverine/m-XDA/IPDA	7 to 27	170-530	50°C + 120°C/2h. GC: 80-82%
Sternberg& Pilla [145]	PMHS	Kraft lignin 5CC + Priamine 1074	84 to 94	241-337	150°C/12h. Bio-based
Monie et al. [146]	Thiol	TMPTC + amines + EDT + DBU	2 to 8	166-207	RT/16h + 100°C/2h
Purwanto et al. [94]	Thiol	TMPTC + diamine + dithiol + DBU	3 to 23	210-510	80°C/4min +120°C/30min
El Khezraji et al.[147]	Thiol	Bis-CC + thiols (f=3,4) + DBU	18 to 28	113-194	Poly(thioether) at RT
Monie et al. [148]	Thiol	TMPTC + thiolactone + amines + DBU	27 to 56	167-185	GC: 94-95%
Coste et al.[149]	Thiol	TMPTC + PPOTC + EDR-148 + DBU	T_g1: -45 to -31. T_g2: 11 to 19	249-445	90°C/24h. GC: 82-83%
Purwanto et al. [150]	Thiol	NC-514 (cashew) + T-403 + EDT	-2 to 6	320-550	Bio-based. GC: 82-85%
Purwanto et al. [151]	Thiol	GS-120 (dimer acid) + T-403 + thiols	-28 to -17	290-310	GC: 85-89%
Wang et al. [117]	Thiol	CLSO (linseed) + amines + thiols	-5 to 9	130-170	Bio-based from linseed oil
Bourguignon et al.[17]	Water	TMPTC + amines + H2O + DBU	-7 to 44	153-429	80-100°C/3-5h. GC: 93-94%
Bourguignon et al.[153]	Water	TMPTE + TMPTC + amines + H2O + KOH	2 to 47	211-294	RT/5min. Hybrid. GC: 88-96%

Choong et al. [154]	Amine-CO_2 adducts	TMPTC+FBC+amine-CO2 adducts+amine	14 - 24	239 -462	Foaming: 60°C/24h GC: 89-95%

Table II. 2. Summary of the foaming mechanisms using Physical blowing agents (PBAs) to produce NIPU foams

Reference	PBA Type	Precursors	T_g (°C)	Density (kg/m³)	Observations
Olang [157]	HFCs/HCFCs/CFCs/Pentanes	Hybrid PU spray	NR	25-40	2012 study
Figovsky et al. [158]	HFCs/HCFCs/Hydrocarbons	Hybrid with epoxies	NR	25-40	2013 study
Blattman et al. [159]	Solkane 365/227	TMPTC + EO-TMPGC + HMDA	~-13	83-219	First full NIPU with PBA
Grignard et al. [164]	Supercritical CO_2	PEGBC + CSBO + bio-amine	-2 to -7	110-176	λ: 50-65 mW/m·K
Mao et al. [165]	Supercritical CO_2	ECBPA + HMDA + C36DDA	~30	215-432	150 bar, 80°C
Kirchberg et al.[166]	Supercritical CO_2	DMC + diols + amino ester	-16	160	500 bar, 120°C
Valette et al.[167]	Water/ Ethanol	NIPU oligomers + crosslinker	-20 to 0	55-950	Transurethanization
Sarma et al. [169]	Vacuum	Aromatic 5CC + p-XDA (REx)	NR	60-70	λ: 43-47 mW/m·K

8. NIPU Foams applications

Polyurethane foams (PUF) are widely recognized for its versatility across various applications. Rigid polyurethane foams, in particular, are extensively used in the construction and appliance sectors, serving as thermal insulators and refrigerator liners.[10,170] Beyond thermal performance, safety regulations in construction and other industries necessitate compliance with fire protection standards to ensure human safety, making flame retardancy a critical requirement for such materials. In this context, for NIPU foams to achieve industrial relevance,

their development must go beyond mere synthesis and fabrication. Indeed, it is needed to engineer these materials with enhanced functional properties to position them as viable alternatives to conventional PU foams.

As previously discussed, the applications of NIPU foams remain relatively unexplored compared to the well-established used of PU foams found in literature and at industrial level. However, recent advances have demonstrated promising potential, particularly in thermal insulation and fire retardancy, indicating their suitability for broader industrial adoption. Additionally, other applications inspired by conventional PU such as shape memory are gaining interest, particularly for biomedical and other fields. These advances will be discussed in the following sections.

8.1.Thermal insulation

Polyurethane (PU) foams significantly contribute to energy efficiency and reducing the negative environmental impact.[26,171] Rigid polyurethane foams (PUFs) are among the most widely used insulation materials in the construction industry, alongside mineral wool (glass and rock wool), extruded polystyrene (XPS), and phenolic foams[172]. They are extensively applied in walls, roofs, and attics to minimize heat transfer between indoor and outdoor environments, aiding in thermal building modernization.[173] Moreover, rigid foams are essential for industrial refrigeration and storage applications.[174] In contrast, flexible polyurethane foams are used in insulation where rigid foams are unsuitable, such as in pipes, ventilation ducts, and automotive interiors. They provide both thermal and acoustic insulation. Polyurethane foams are considered one of the best thermal insulation materials, due to their low thermal conductivity in comparison to the other ones.

PU rigid foams offer key advantages that make them highly valuable in the building construction. These properties are: high insulation efficiency with minimal thickness, lightweight and strong mechanical properties, chemical resistance and durability. However, PUFs are inherently flammable and release toxic fumes (such as HCN) upon combustion. This needs compliance with fire regulations, which typically requires the incorporation of flame retardant additives to mitigate these hazards (further discussed in the flame retardancy section). The insulating performance of PU foams is determined by three factors. Firstly, the morphology of the foams, specifically the ratio of open-cell to closed-cell structures, secondly, the thermal conductivity of the gases used as blowing agents, filling the foam cells, and lastly,

the chemical composition of the polymeric material. Typically, the use of physical blowing agents, such as CFC, HFCF, HFC and $scCO_2$ produce closed-cell foams with higher thermal insulation properties, due to the low thermal conductivity (8 to 15 mW/m.K) of these gases and higher gas retention over time.

The outstanding thermal insulation performance of petro-based and partially bio-based PU[8,175] foams has driven the investigation of analogous properties in NIPU foams. To date, only two studies have reported the thermal conductivity of thermoplastic NIPU foams fabricated using physical blowing agents and vacuum blowing techniques. Grignard et al.,[164] examined the insulating properties of thermoplastic closed-cell NIPU foams produced with supercritical CO_2 ($scCO_2$) as the physical blowing agent. The thermal conductivity values of the foams ranged from 50 to 64 mW/m·K, which is comparable to the conductivity of glass wool (λ = 40–45 mW/m·K) and wood (λ = 55 mW/m·K). Notably, these values remained stable after 12 months, suggesting that CO_2 is rapidly replaced by air with no significant aging effects. More recently, Sarma et al.,[169] fabricated three rigid thermoplastic foams through a two-step process: first, the NIPU polymeric matrix was synthesized via reactive extrusion (REx), followed by vacuum foaming at high temperatures, resulting in low-density foams (60–70 kg/m³). The thermal conductivity values ranged between 43 and 47 mW/m·K, which are lower than those reported by Grignard et al.,[176] and comparable to those of expanded polystyrene and certain rigid PU foams.[177] Unlike the previous study, Sarma et al., did not investigate water absorption or aging effects. Overall, the reported thermal conductivity of NIPU foams manufactured using $scCO_2$ and vacuum foaming falls within the range of 43–65 mW/m·K^{-1}.[169]

To gain a comprehensive understanding of the thermal conductivity behavior of NIPU foams, it is important to investigate the influence of precursor chemical structures and the differences between thermoplastic and thermosetting foams. Additionally, assessing the performance of these materials under humid conditions is crucial, as NIPUs are generally more hydrophilic than conventional PU foams, due to the presence of OH groups. Increased water absorption can negatively impact thermal insulation, as absorbed moisture elevates thermal conductivity values (see Table II.3.). Another key aspect to explore is the long-term ageing behaviour of NIPU foams. Over time, the gases initially trapped within the foam cavities diffuse out and are replaced by air, which has a higher thermal conductivity than CO_2 or other physical blowing agents. This process leads to a gradual decline in insulation efficiency, a phenomenon well-documented in conventional PU foams. Therefore, studying the aging effects on NIPU foams could be fundamental to determining their long-term viability in insulation applications.

Table II. 3. Thermal conductivity of thermal insulation materials in dried and moist state.

Material	Thermal conductivity (mW/m.K) [dried]/[moist]
Mineral wool	30-40 / 37-50
Expanded polystyrene (EPS)	37-50 / 30-40
Extruded polystyrene (XPS)	30-40 / 34-44
Polyurethane (PUR)	20-30 / 25-46

By gathering this information, a more comprehensive technical perspective can be obtained on whether NIPU foams are suitable candidates for insulation applications and capable of competing with conventional PU, expanded polystyrene (EPS), and extruded polystyrene (XPS) foams. In this context, further studies could explore potential chemical functionalization of the precursors or the incorporation of specific additives to enhance the insulation properties of NIPU foams, thereby optimizing their performance for thermal insulation properties.

8.2.Flame retardant properties

PU materials are flammable due to their composition, which primarily consists of hydrocarbons chains. In particular, PUFs exhibit a highly porous structure that promotes flammability and increases the combustion. Additionally, the degradation of urethane linkages during combustion releases hydrogen cyanide (HCN), a toxic and harmful fume.[178,179] This intrinsic fire risk brings safety concerns in industries such as construction, thermal insulation and automotive, where strict safety standards are required to protect final consumers. Therefore, to comply with safety regulations and performance standards, it is crucial to develop new strategies that reduce fire load by incorporating fire-resistant elements.

The most common industrial approach for imparting fire-retardant properties to PU foams is through the incorporation of additives, which are physically blended into the formulation during the polymerization process. This method allows for flexibility in modifying the flame-retardant performance without significantly altering the fundamental chemistry of the polymer matrix. The most commonly flame retardant used in PUFs include organic and inorganic additives. Among the organic FR include halogenated (brominated and chlorinated) compounds,[180] phosphorus- and nitrogen-based molecules.[181] Among the inorganic expandable

graphite (EG),[182] aluminium trihydrate (ATH)[183] and ammonium polyphosphate (APP).[184] While additives are effective and easy to incorporate, they can unfavourably alter the physical and mechanical properties of the material. Moreover, since they are not chemically bonded to the polymers, they can migrate from the polymer matrix reducing their long-term efficiency, but more importantly, they can leach into dust, water, food and air, bringing health concerns, due to the direct exposure to people.[10,50,178]

On the other hand, reactive flame retardants (RFR) are chemically bonded to the polymer through co-polymerization with well-designed molecules that contain specific functional groups. RFR not only prevents the volatilization or migration of the additives but also show higher thermal stability and efficiency in long-term.[178] The use of reactive flame retardants in PUs normally lies on the design and modification of compatible monomers such as polyols, that later on will react with isocyanates to produce polyurethanes.[185,186] The primary compounds used in these FRs include halogen, nitrogen and phosphorous-based. However, nowadays the use of halogen-based flame retardants have been banned due to the harmful environmental effects and the release of corrosive and toxic fumes, such as hydrogen bromide (HBr) and hydrogen chlorine (HCl).[187] In this context, the development and innovative design of organophosphorus compounds has emerged as a safer alternative due to their high efficiency and low production of toxic gases.

In different studies, the addition of organophosphorus compounds has significantly improved the fire retardant properties of PU foams.[186,188–190] Notably, among phosphorus-based flame retardants, 9,10-dihydro-9-oxa-10-phosphaphenanthrene-10-oxide (DOPO) is considered one of the most versatile due to its high reactivity, superior flame-retardant efficiency, and compatibility with various functional groups, including aldehydes, epoxides, acrylates, and double bonds,[191–197] Given the proven effectiveness of DOPO-containing polyols in enhancing the fire-retardant properties of PU foams,[194 198–200] this molecule has now also served as inspiration for the development of new reactive flame retardants (RFRs). These novel RFRs can be integrated as precursors in the synthesis of NIPU foams, offering a promising avenue for improving their fire resistance.

Interestingly, the only reported study to date on the use of reactive flame retardants (RFRs) in NIPU foams was conducted by Coste et al.,[99] thermosetting NIPU foams were fabricated incorporating RFRs by grafting DOPO onto various epoxides, followed by CO_2 fixation to generate five-membered cyclic carbonates. These modified DOPO-containing cyclic

carbonates were then used as co-monomers in different proportions to achieve phosphorus content of up to 2 wt% in the final material (Figure II.28).

The resulting foams were systematically analyzed for their thermal and fire-retardant properties, demonstrating the potential of DOPO-functionalized precursors in enhancing the flame resistance of NIPU foams. In general, formulations with phosphorus content, exhibited improved thermal stability, with a significant reduction in total heat release (THR) up to 30% compared to their phosphorus-free counterparts. These results suggest that the incorporation of DOPO-functionalized cyclic carbonates effectively enhances the flame resistance of NIPU foams.

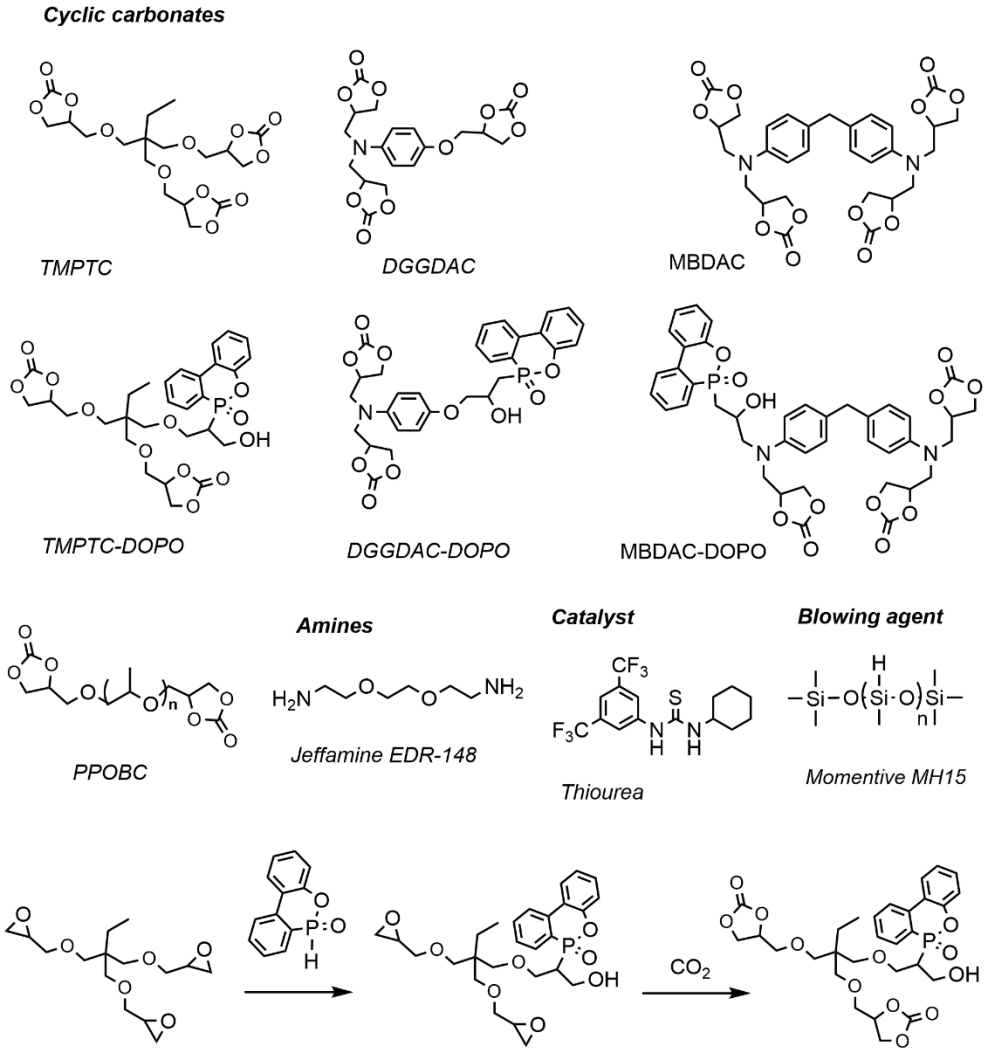

Figure II. 28. Chemical structure of DOPO-containing cyclic carbonates, used as reactive flame retardant (RFR) in the production of PHU foams. Chemical structure of 5CC, amines, catalysts and Momentive MH15.[99]

The use of this approach opens new research avenues for investigating the thermal and morphological properties of NIPU foams incorporating these reactive flame retardants (RFRs). Key aspects to be explored include the impact of phosphorus incorporation on properties such as glass transition temperature (T_g), thermal stability, UL-94 rating, and cone calorimetry performance. Additionally, understanding the reactivity of these RFR molecules is fundamental as it is well-established that the aminolysis of 5-membered cyclic carbonates (5CCs) is relatively slow. The introduction of aromatic moieties from DOPO may further reduce reactivity, necessitating optimization of foaming conditions, curing temperature, catalyst concentration, and other processing parameters.

Beyond processing considerations, this research direction could also provide deeper insights into the fire-retardant mechanisms within the NIPU polymer matrix. Unlike traditional flame-retardant additives that can migrate and lose efficiency over time, covalently bonded RFRs may exhibit superior long-term performance. In conclusion, the work of Coste et al. represents a promising advancement in developing flame-retardant NIPU foams, while eliminating the need for isocyanate-based chemistry, aligning with the growing demand for safer and more sustainable polymeric materials.

8.3.Shape memory

The functionality of PU foams has also been expanded beyond their traditional passive function profiles in thermal insulation, flame retardant and cushioning. The utility of PU foams has significantly evolved, positioning them within a growing class of functional materials finding applications in biomedicine,[201,202] aerospace,[203] robotics,[204,205] packaging,[201] sensing[206–209] and agriculture.[210–212] One of these major advancements is largely attributed to the discovery and utilization of the shape memory effect (SME) in PU foams, making them adaptative to morphological transformations.[213] SME is a phenomenon in which a material, after being temporarily deformed/programmed, can recover its original shape upon exposure to an external stimulus. Common external stimuli include temperature, light, electric or magnetic fields, and humidity.[213] Among these, temperature remains the most widely used trigger in PUFs, owing to its practicality and ease of control in real-world conditions.

In the biomedical field, several noteworthy applications of shape memory polyurethane foams (PUFs) have been reported. Singhal et al.,[214] developed low-density shape memory PUFs with potential use in embolization devices for minimally invasive procedures, demonstrating shape recovery ratios between 94–98%, triggered thermally within a range of 45–70 °C. In another

recent and significant study, shape memory PU foams were explored for breast tissue repair and reconstruction,[215] exhibiting excellent responsiveness at body temperature (37 °C) and achieving recovery rates of up to 98%, while maintaining their mechanical integrity and biocompatibility even after exposure to 40 Gy of radiotherapy. Additionally, other thermally activated shape memory PUFs have been reported with the ability to recover their original shape after almost complete compression, highlighting their potential for applications in the treatment of cerebral aneurysms and as drug delivery platforms.[216] Another clear example of SM PU foams in robotics and programmable materials is the synthesis of PU foams that serve as actuator to open and close air slots depending on the environment temperature.[205]

Due to the remarkable capabilities of conventional PU foams as smart materials mentioned before, there has been growing interest from the scientific community in exploring these functionalities on NIPU foams. This interest is based on the close chemical structural similarity that NIPUs exhibit with traditional PUs, as well as their ease of functionalization attributed to the presence of hydroxyl (–OH) groups in their chemical structure.[217,218]

To date, only few NIPU foams have been reported in the literature to exhibit adaptive functionalities, such as the shape memory effect (SME) triggered by temperature.[145] Notably, some authors have demonstrated the presence of SME in thermoset and elastomer NIPU, which also respond to thermal activation.[219] Interestingly, the biocompatibility of NIPUs has been also confirmed in various biomedical applications, including heart valves and implants.[218,220]

Considering these previously studied properties, along with the well-established applications of conventional PU foams, the exploration of SME in NIPU foams represents a promising research direction. This approach could lead to the development of a more sustainable version of scaffolds for tissue regeneration, featuring high compressibility, capable of recovering their original shape once implanted at the targeted anatomical site, as well as smart systems for controlled fertilizer release in agriculture. Furthermore, their inherent hydrophilicity opens the possibility of exploring new external stimuli for activating SME, such as moisture, either by absorbing water to expand and function as an actuator or sensor, or to modulate their mechanical properties.

9. End life-scenario

Rigid and flexible polyurethane (PU) foams, exhibit mainly a thermoset nature that makes their end-of-life management particularly challenging. Their crosslinked chemical structure provides high stability and durability but also renders them inherently non-reprocessable by conventional methods, posing a major obstacle to their integration into efficient and sustainable recycling schemes aligned with circular economy principles (Figure II.29).

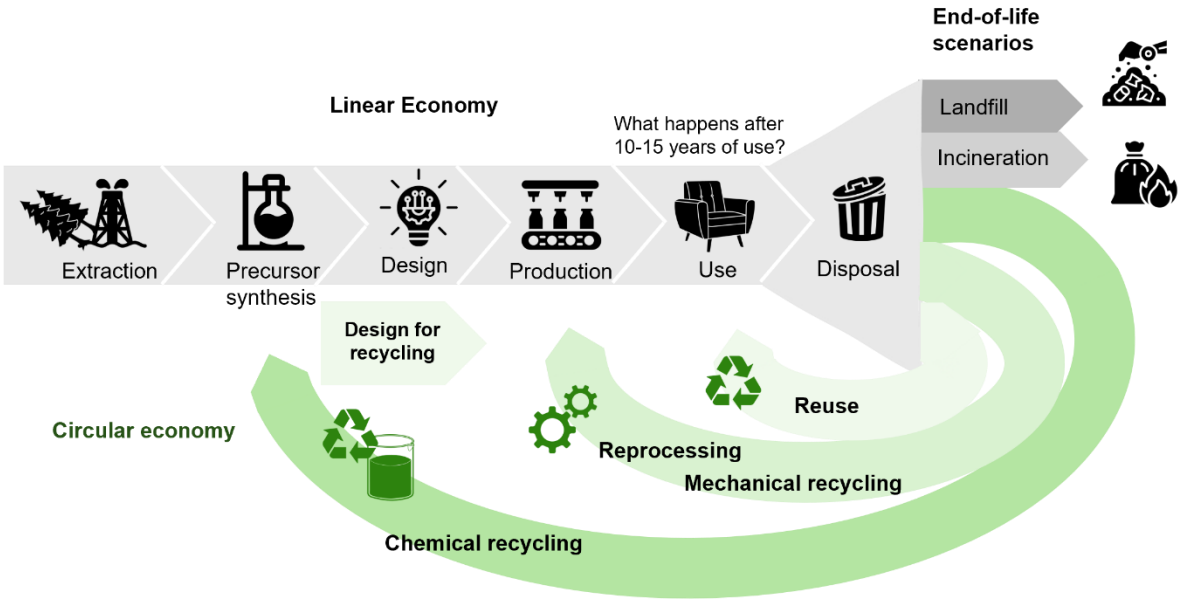

Figure II. 29. End-of-Life scenarios in a linear economy (gray) vs potential solutions for circular economy (green).

Mechanical, chemical, and thermochemical recycling strategies have been developed to manage PU waste, yet each has important limitations: mechanical recycling, based on the physical grinding, downgrades the material's functionality and it is used for lower-value products. This recycling method is used for the production of rebounded foams such as carpet padding, acoustic insulation, sport mats and non-structural components in the automotive industry.[221–223] Chemical recycling such as glycolysis, hydrolysis or aminolysis, recovers valuable fragments like polyols or amines that can be reused in new formulations, but involves harsh conditions, high temperatures, use of catalysts, solvents and purification steps.[224] Additionally, the use of recyclable polyols is limited up to 30% for new PU foams to obtain comparable properties to virgin-polyol-contaning foams. If more quantity of recycled polyols is added, they may unfavorably alter some final properties such as decreasing mechanical strength, irregular foam cells, among others. Therefore, changing the characteristic properties

of the foams for already well-stablished applications.[222] Lastly, thermochemical methods, such as pyrolysis, gasification and hydrogenation transform PU foams into gas that can be used as raw material or as fuel. However, this recycling technique has not succeed at industrial scale yet.[225]

To overcome these limitations and bring new solutions to the management of end-life scenario, the study and incorporation of dynamic covalent bonds into the polyurethane network has emerged as a disruptive strategy.[226] This approach enables reprocessing of PU materials and extends their applicability to rigid and flexible PU foams. This approach transforms the irreversible nature of thermosets into an adaptable network that can respond to external stimuli, such as heat, allowing reshaping, repairing, or recycling without significant degradation of material properties.

Although, polyurethanes are not inherently covalent adaptable network (CANs), they can be engineered to exhibit such dynamic behavior. Some key enablers include the use of suitable catalysts [227](e.g. DBTDL, Bi(III), DBU, TBD), heat (typically temperatures above 120°C) and functional group design, such as the incorporation of tertiary amines, free hydroxyl groups, and the careful selection of polyol and isocyanate components. When these features are combined, Pu can undergo reversible bond exchange reactions, including transcarbamoylation, transesterification or urethane exchange. These dynamic processes allow direct recovery of the material in its functional form while maintaining structural integrity across multiple reuse cycles. This approach preserves structural integrity over multiple reuse cycles and supports low-impact, sustainable processing. Such strategies represent a significant advancement in the reprocessing of PUF foams, with some examples already reported in the literature.[228]

In this context, and based on similar transcarbamoylation reactions, polyhydroxyurethane (PHU) foams have also shown potential for reprocessing, recycling, and reused, leading to the production of high-value materials. Polyhydroxyurethanes (PHU) are synthesized via the polyaddition between 5-membered cyclic carbonates and amines, resulting in a polymer network that inherently contains free hydroxyl (-OH) groups. These groups facilitate transcarbamoylation reactions and contribute to the dynamic nature of the network. Such reactions can be promote by using specific catalysts like DBU, TBD, DABCO, KOH, NaOH, among others, or even without any catalyst load at elevated temperatures (120-250°C).[229]

The reprocessing mechanism in PHU is mostly based on associative covalent exchange, meaning that the crosslinking density remains constant during reprocessing.[100,230–233] However,

some studies have reported the retroformation of 5CC and amines, suggesting that dissociative exchange mechanisms may also occur under certain conditions (Figure II.30.).

However, these mechanisms have not been fully rationalized yet. This associative covalent exchange contrasts with conventional isocyanate-based PU chemistry, because dissociative covalent exchange dominates, resulting in a reduction of the crosslinking density and a viscosity drop during reprocessing.[36]

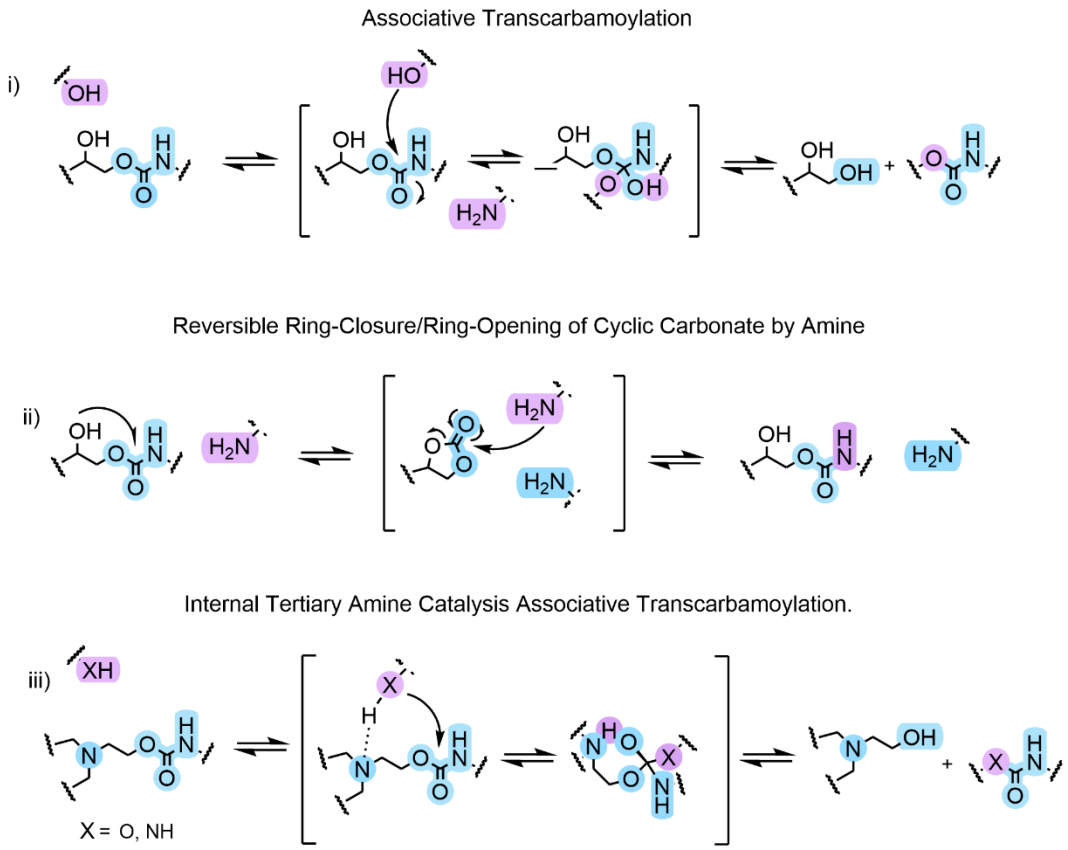

Figure II. 30. Exchange reactions that could possibly occur in PHU networks (i) Associative Transcarbamoylation, (ii) Ring-Opening or Ring-Closure of Cyclic Carbonate by Amine, and (iii) Auto-catalysis by Tertiary Amine in Associative Transcarbamoylation.[36]

The reprocessability of PHU foams has gained attention in recent years due to the contribution to the circular economy and sustainability, particularly for those synthesized via the polyaddition of five-membered cyclic carbonates (5CC) and amines, using chemical blowing agents (CBAs) such as thiols and water. Recently, Detrembleur and co-workers reported,[148] for the first time, the successful reprocessing of PHU foams generated with latent thiols as blowing agents, into PHU films, enabling the fabrication of structural composites. PHU foams were

reprocessed by hot-pressing at 160°C, 10 MPa for 2 hours without any external catalyst. The reprocessing films remained with high gel content (>95%), confirming the crosslinked nature of the film. The glass transition and FTIR analyses of the reprocessed films are similar to PHU foams, suggesting that no degradation or modification of the chemical structure occurred during reprocessing. Interestingly, 2 reprocessed PHU films were compressed with a nylon fabric in the middle, for 2h at 160°C at 20MPa to broaden the application of the PHU materials, confirming the good adhesion between the fabric and PHU films. Notably, these findings highlighted the intrinsic potential of PHU networks for reprocessing, attributed to the presence of hydroxyl functional groups that promote dynamic covalent exchange reactions.

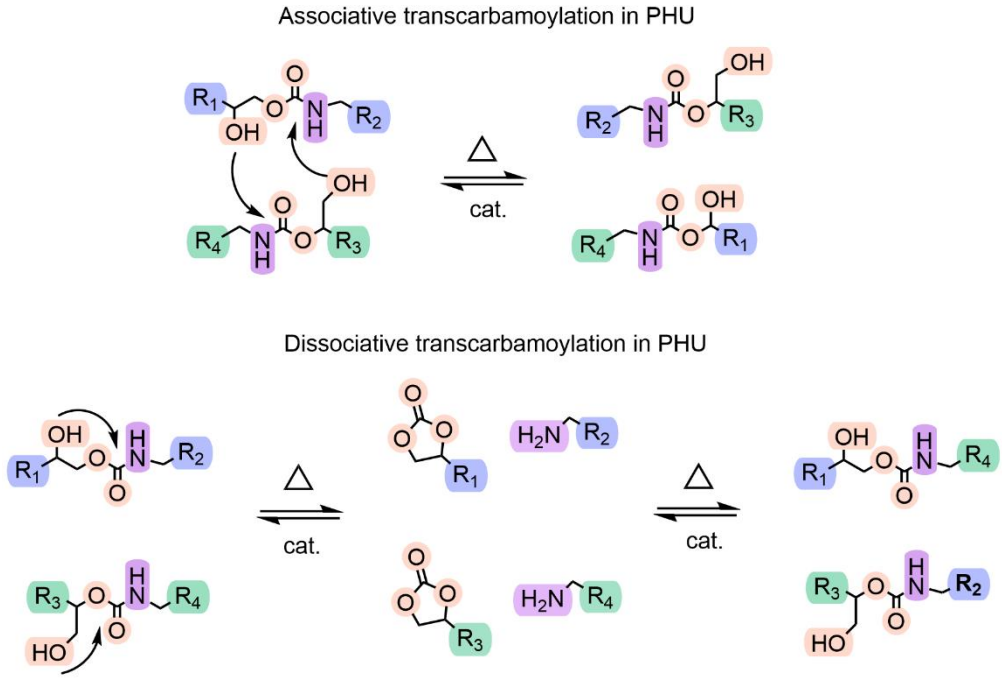

Figure II. 31. Possible transcarbamoylation reactions in PHU networks for reprocessing PHU foams reported in the literature.[94,148,150,151]

Later on, Torkelson et al.,[94] also reported the reprocessability of PHU foams chemically-blown with an aliphatic thiol (EDT) into PHU films. The PHU were cut into pieces and then reprocessed 3 times without any external catalyst at 160°C for 3 hours under compression at 16 MPa. Notably, DMA analyses confirm the high-degree of crosslinking density above the T_g, the *E'* values of the PHU films remained approximately constant after 3 reprocessing cycles and it was also reported that the T_g of the reprocessed PHU films increased by 6-15°C after reprocessing. This was attributed to the further reaction of the unreacted 5CC observed by

FTIR. Interestingly, for both previous studies, even if hydroxythioethers crosslinks are present in the polymer network, the dynamicity of the hydroxyurethanes is not affected.

In the same context, Torkelson et al.,[150,151] also demonstrated the reprocessability of bio-based PHU foams produced by cashew nutshell (NC-514) blown by S-alkylation of thiols (EDT). NIPU foams were also reprocessed into bulk films 3 times by cutting PHU foams into pieces and then hot-pressing at 140°C under 10 MPa for 2 hours. As previously observed, the high-degree of crosslinking density remains in the reprocessed films and E' values slightly increased by each reprocessing cycle. In this study, it was also demonstrated that increasing hydroxythioether linkages led to longer relaxation times (τ), attributed to a rise in permanent (non-crosslinking) linkages and a reduction in dynamic crosslinking content (hydroxyurethane linkages). Stress-relaxation times ranged from 5000 to 200 seconds, depending on the temperature (150-180°C) and thiol/amine concentration. Additionally, the activation energy (E_a) of bond exchange reactions also ranged between 77 and 130 kJ.mol^{-1} for these networks. Followed this study, the same group also studied the relationship of the thiol functionality (f = 2,3,4) for the fabrication of the foams and its direct role in the reprocessability properties. The foams were cut into pieces and hot-compressed at 150°C for 1 hour under 10MPa to obtain bulk films. The reprocessed films showed high retention of crosslinked density and mechanical properties after 3 reprocessing cycles, consistent with findings from the previous work. Notably, an increase in the activation energy (E_a) of bond exchange reactions from 122 to 155kJ/mol and a corresponding rise in (τ) were observed when increasing thiol functionality. This behaviour was attributed to a greater density of permanent crosslinks, which restricts the mobility of the dynamic hydroxyurethane exchange. At elevated temperatures (T = 180°C), the relaxation times (τ) converged to similar values likely due to the presence of ester bonds within the thiol molecules that can undergo transesterification. However, this exchange reaction was suppressed at lower temperatures. The occurrence of transesterification was further supported by experiments involving the epoxide precursor (GSE) and the same thiol molecule (f = 4), confirming that the reaction only proceeds at elevated temperatures (180 °C).

More recently, Detrembleur et al.,[153] reported the feasibility of reprocessing a water-blown hybrid PHU foam as well, synthesized from bio-based 5-membered cyclic carbonates, epoxides and amines. The resulting bio-based foam was reprocessed by hot-pressing into bulk film at 160°C for 2 hours under 2 tons of pressure. The reprocessed film exhibited a similar T_g compared to the original foam ($T_{g\ film}$: -3°C vs T_{gfoam}: -7°C) and retained its chemical structure, indicating that no significant degradation occurred during reprocessing. Although this was a

preliminary study without process optimization, it clearly demonstrated that dynamic covalent exchange reactions can take place despite the hybrid nature of the foam. Indeed, Raquez et al.,[234] have recently reported that hybrid thermosetting networks between epoxides, 5-membered cyclic carbonates and amines, exhibit improved reprocessing performance. This enhancement is attributed to the autocatalytic effect of tertiary amines generated in the polymer network through the aminolysis of epoxides, which in turn promote transcarbamoylation reactions. These findings suggest that previously reported hybrid PHU foams could be further optimized by considering the catalytic behavior of tertiary amines within the network.

These previous studies demonstrated that PHU foams can be successfully reprocessed into bulk films, making them suitable for applications such as adhesives, composite materials, and sports mats. This reprocessability is primarily attributed to the presence of hydroxyl groups that are inherently generated during the polyaddition of cyclic carbonates and amines. These functional groups enable dynamic covalent exchange reactions, allowing the material to be reprocessed without the need for solvent-based catalyst uptake. This characteristic represents a clear advantage over conventional polyurethanes, which typically require immersion in solvent–catalyst systems to initiate network rearrangement.

However, current reprocessing methods for PHU foams rely on hot-pressing, which limits their suitability for continuous or large-scale processing applications. In contrast, conventional PUs have shown compatibility with continuous recycling methods such as reactive extrusion (REx) in the literature, due to their ability to undergo dissociative carbamate bond cleavage, forming again isocyanates and alcohols. This mechanism reduces viscosity and enhances flow, making conventional PUs more processable under such conditions. PHUs, on the other hand, tend to retain their crosslink density during reprocessing, maintaining high viscosity and hindering their use in continuous-based methods. Addressing this limitation remains key to expanding the industrial applicability of PHU foams. The search of new catalysts or incorporation of co-monomers that could promote dissociative mechanism reactions and reduce relaxation time could lead to a big step in the industrialization of reprocessability of PHU foams.

Chapter III

Objectives and Strategy

The main objective of this thesis is to develop thermosetting non-isocyanate polyurethane (NIPU) foams through sustainable synthesis routes and innovative foaming processes. By relying on safer chemistry and greener blowing agents, the work seeks to reduce the environmental and health burdens associated with conventional isocyanate-based foams, while promoting the broader adoption of circular and sustainable materials. Within the framework of the NIPU-EJD project, the thesis specifically focuses on thermoset foams, addressing inherent reactivity, foam processing with both physical and chemical blowing agents, and functional applications. In doing so, it aims to contribute not only to the fundamental understanding of NIPU foams but also to their industrial relevance, ultimately establishing a scientific and technological foundation for the next generation of non-isocyanate polyurethane foams.

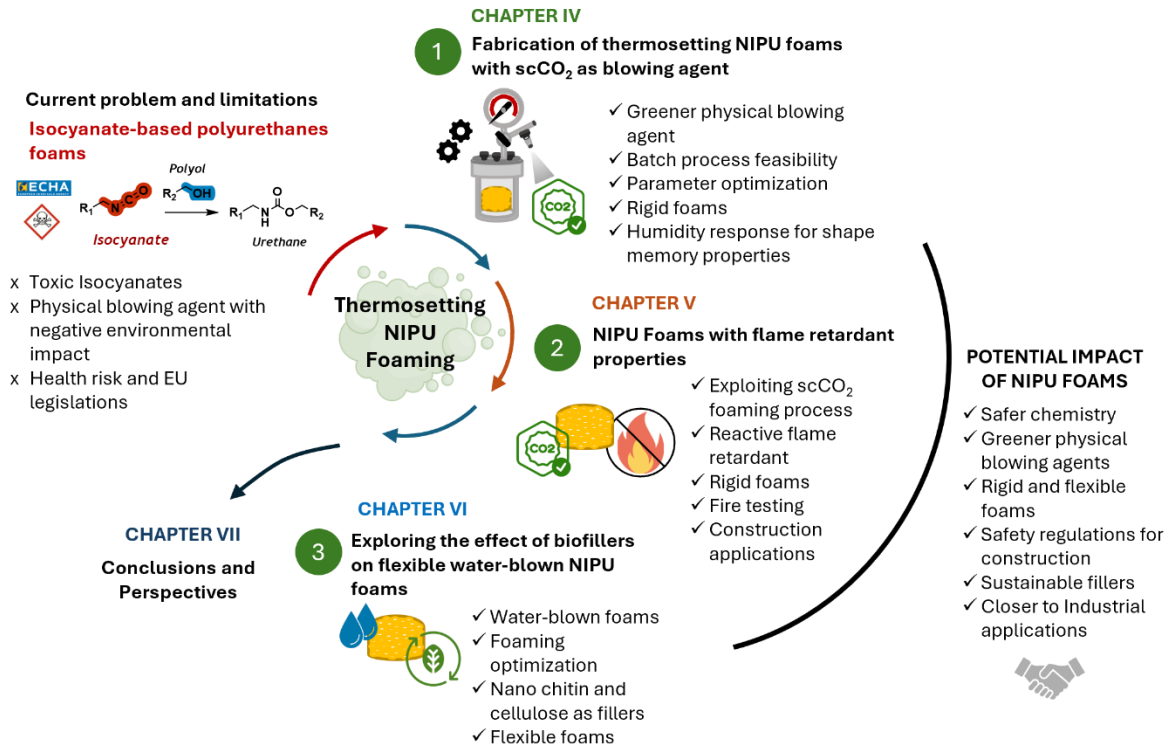

Figure III. 1. General strategy of this thesis

Therefore, **Chapter IV** is dedicated to the development of thermosetting NIPU foams using supercritical CO_2 as a blowing agent, which offers a greener and safer alternative to hydrocarbon-based foaming agents and has not yet been fully exploited in the context of thermosetting NIPUs. The first step is to study the reactivity of cyclic carbonates and amines at low temperatures in order to mimic the conditions applied during the initial stage of foam synthesis (CO_2 absorption). The feasibility of producing thermosetting foams under $scCO_2$ in

a batch process is then demostrated. Following this, several key parameters are varied to investigate their effect on the morphology and mechanical properties of the foams, including the ratio of two different cyclic carbonates, the foaming temperature, and the use of various additives. The final part of this chapter explores the humidity-activated shape memory properties of the foams for further applications.

Later on, **Chapter V** builds upon the promising $scCO_2$ foaming process and explores how the $scCO_2$ platform can serve as a basis for functional foams with improved properties. In particular, a phosphorus-containing amine molecule is synthesized to provide flame-retardant properties to NIPU foams and is used as a co-monomer within the crosslinked network, rather than being incorporated as an additive. This could otherwise lead to migration and reduced long-term performance. Once the foams are synthesized at mild temperature (100°C), this chapter also studies the flame retardant properties of the foams with different phosphorous content using calorimetry and UL-94 tests. This key functionality in NIPU foams aims to bridge the gap between novel materials and practical applications in construction and insulation, where safety regulations are strictly required.

To broaden the research beyond rigid foams produced with physical blowing agents, **Chapter VI** focuses on water-blown flexible NIPU foams and examines the incorporation of renewable nano-additives such as chitin, cellulose, and clay, which are abundantly available. The morphology and key properties, such as density and mechanical performance, are investigated to assess the influence of these bio-fillers on the final properties of the foams. This chapter highlights the importance of bio-based nanofillers as renewable alternatives and emphasizes the importance of anticipating future regulatory requirements and designing materials aligned with circular economy principles.

Finally, **Chapter VII** presents the general conclusions of the thesis and outlines future perspectives arising from the research conducted in the previous chapters.

Chapter IV

Sustainable CO_2 Utilization as a Blowing Agent in Thermoset PHU Foam Production with Humidity-Responsive Shape Memo

Adapted from:

Gouveia, K., Vauloup, J., Colpaert, M., Ocando, C., Lacroix-Desmazes, P., Ladmiral, V., Caillol, S., & Raquez, J.-M.. Sustainable CO_2 Utilization as a Blowing Agent in Thermoset PHU Foam Production with Humidity-Responsive Shape Memory. *ACS Appl. Polym. Mater.* **7**, 6113–6124 (2025)

1. Introduction

As described in Chapter II, research on Non-Isocyanate Polyurethane (NIPU) foams has so far relied on the predominant use of chemical blowing agents, including polymethylhydrosiloxane (PMHS),[142,143] water,[17] and thiols,[148,149] where gas generation occurs through *in situ* chemical reactions during polymerization/crosslinking. In contrast, the application of physical blowing agents (PBA) in thermoset NIPU foams has remained unexplored. Conventional polyurethane technology depends on hydrocarbons (HCs) and hydrofluorocarbons (HFCs) as physical blowing agents (PBAs), despite their flammability, toxicity, and high environmental impact in terms of global warming potential and ozone depletion.[11,15,155] Supercritical carbon dioxide ($scCO_2$) represents an interesting sustainable alternative, being non-flammable, non-toxic, abundantly available, and industrially attractive for foaming processes. However, its use in NIPU foams has been scarcely demonstrated to date, and, more critically, no reports exist on its application to thermosetting NIPU foams, knowing that it could represent in a near future the dominant segment of the polyurethane foam market due to their superior thermal and mechanical performance. Closing this gap would demonstrate the feasibility of coupling NIPU chemistry with a more sustainable physical foaming process, therefore providing a safer alternative to conventional PBAs in the largest class of PU foams.

In this respect, the aim of Chapter IV is to validate and establish a new foaming process for the fabrication of thermosetting NIPU foams using $scCO_2$ as physical blowing agent in a batch process. **The first part of this chapter** focuses on assessing the viability and compatibility of $scCO_2$ foaming process with NIPU chemistry. This first part includes exploring the reactivity of a five-membered cyclic carbonate, Trimethylolpropane triscarbonate (TMPTC) with an aromatic primary diamine *m*-xylylenediamine (MXDA), under conditions that resemble $scCO_2$ processing and impregnation. Using this model reaction, rheological analyses are conducted to investigate the gel point and elucidate the key parameters governing successful foam formation. Once the experimental conditions are established, the feasibility of the foaming process is demonstrated. Foaming temperature, curing time and the addition of Laponite are also studied to further optimize the foaming process at this stage.

The second part of this chapter focuses on optimization strategies aimed at tailoring the properties of the foams. To this end, the formulation scope is extended by varying the ratio between two different five-membered cyclic carbonates, TMPTC and PPOBC. Rheological measurements, such as gelation time and viscosity build-up are studied. In addition, additives

such as Laponite (nanoclay) and surfactants are introduced to enhance bubble stabilization and morphology control. The influence of curing and foaming temperature is also examined. Beyond structural characterization parameters such as density, cell size, and gel content, the resulting foams are further assessed in terms of their thermal and mechanical performance.

Building on our previous results, a particular emphasis is placed on the behavior of the foams under both dry and humid conditions. Therefore, **the third part of this chapter** examines water uptake and the changes in the glass transition temperature (T_g), identifying these parameters as key functional properties that drive the humidity-responsive shape memory behavior.

Demonstrating this fabrication pathway highlights the feasibility of using $scCO_2$ as a physical blowing agent in NIPU chemistry, specifically in the aminolysis of five-membered cyclic carbonates, and establishes it as a promising platform for the sustainable development of thermoset NIPU foams. Moreover, this process serves as a platform to open new avenues for designing and engineering foams with advanced technical properties that are increasingly demanded in industrial applications.

2. Results and Discussion

2.1. NIPU Foam Preparation

As outlined in the introduction of this chapter, a key objective was to demonstrate the feasibility of coupling NIPU chemistry with a sustainable foaming route exploiting supercritical CO_2 ($scCO_2$). To achieve this, it was first necessary to validate the process under controlled conditions using a model formulation. For this purpose, a solvent-free and catalyst-free thermoset system was selected, composed of the trifunctional cyclic carbonate trimethylolpropane triscarbonate (TMPTC) and the aromatic diamine m-xylylenediamine (MXDA) (Scheme IV.1). TMPTC was carefully purified to remove residual tetrabutylammonium bromide (TBAB), the catalyst used for CO_2 fixation, since its presence could interfere by accelerating aminolysis during curing. A 1:1 molar ratio of carbonate to amine functional groups was employed to ensure balanced reactivity. Both monomers are viscous liquids, which facilitated homogeneous mixing and reproducibility of the formulations.

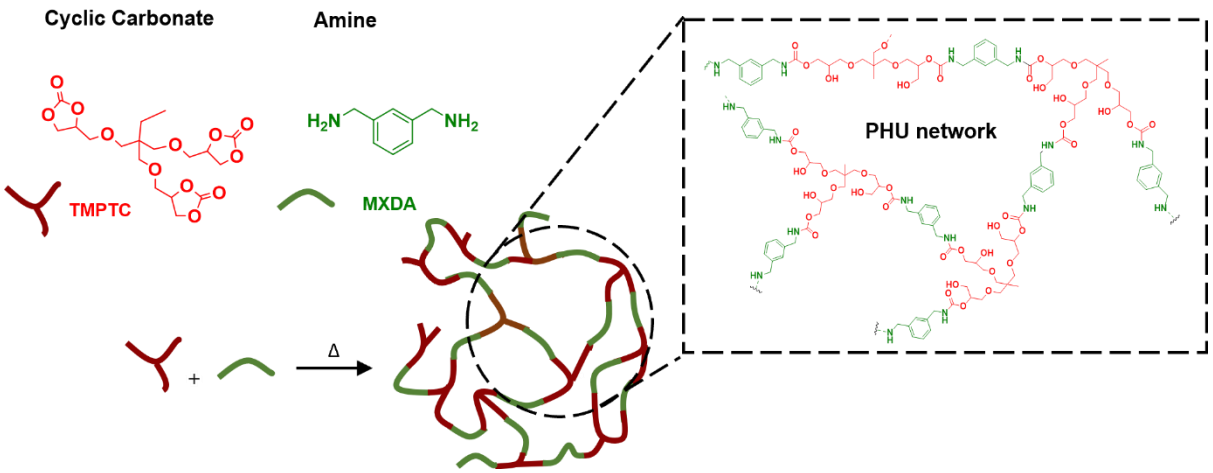

Scheme IV.1. Chemical structures of TMPTC and MXDA monomers and the aminolysis reaction leading to polyhydroxyurethane (PHU) formation.

One of the main challenges identified in the introduction was the difficulty of synchronizing curing and foaming in thermosetting systems. This section addresses this challenge by highlighting the complexity of the foaming process. Successful foam preparation depends critically on the interplay between viscosity build-up and crosslinking degree. In thermosets, two phenomena occur simultaneously at elevated temperatures: *(i)* crosslinking of the PHU network and *(ii)* formation of the cellular structure by gas release. If these processes are not properly balanced, undesired scenarios arise: either excessive crosslinking before gas release, leading to dense solids, or premature gas release before sufficient network formation, resulting in foam collapse.[146] Previous studies on self-blown NIPUs have shown that precise rheological control is essential for overcoming these limitations.[17,142,146,149] In our case, this meant focusing on the conditions of the high-pressure CO_2 absorption step, since they determine whether the subsequent foaming and curing stages can be controlled.

To establish whether the chosen TMPTC/MXDA formulation encounters these conditions, its reactivity was analyzed by rheology under scCO_2-compatible conditions. As emphasized in the introduction, selecting an operating window where the resin remains uncured during saturation is essential for efficient gas impregnation. Accordingly, rheological experiments were conducted at 45 °C, a temperature above the CO_2 critical point. The evolution of storage (G') and loss (G'') moduli over 10 h (Figure IV.1) showed no gel point, confirming that the mixture remains liquid and uncured under these conditions. This result validated that the formulation possesses the necessary rheological window to absorb CO_2 effectively before crosslinking dominates. Thus, rheology provided the first confirmation that scCO_2 impregnation can be compatible with NIPU chemistry and sets the stage for the subsequent foaming experiments.

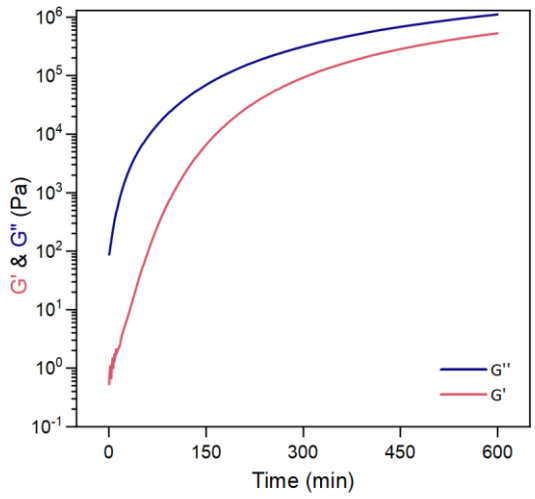

Figure IV.1. Rheological behavior of the TMPTC/MXDA formulation at 45°C showing the evolution of storage modulus (*G′*) and loss modulus (*G″*) over time. The absence of gel point after 10 h confirms the formulation remains processable under scCO₂ saturation conditions.

Guided by this rheological evidence, we implemented a two-step strategy (Figure IV.2): *(i)* CO_2 pressure-induced absorption under supercritical conditions (45 °C, 100 bar, 90 min) followed by *(ii)* CO_2 temperature-induced desorption during curing (100–140 °C). During saturation, CO_2 not only dissolves in the liquid mixture but also reversibly reacts with primary amines to form carbamate salts and carbamic acid, which enhance CO_2 uptake and subsequently contribute to gas release upon heating (> 100 °C).[154]

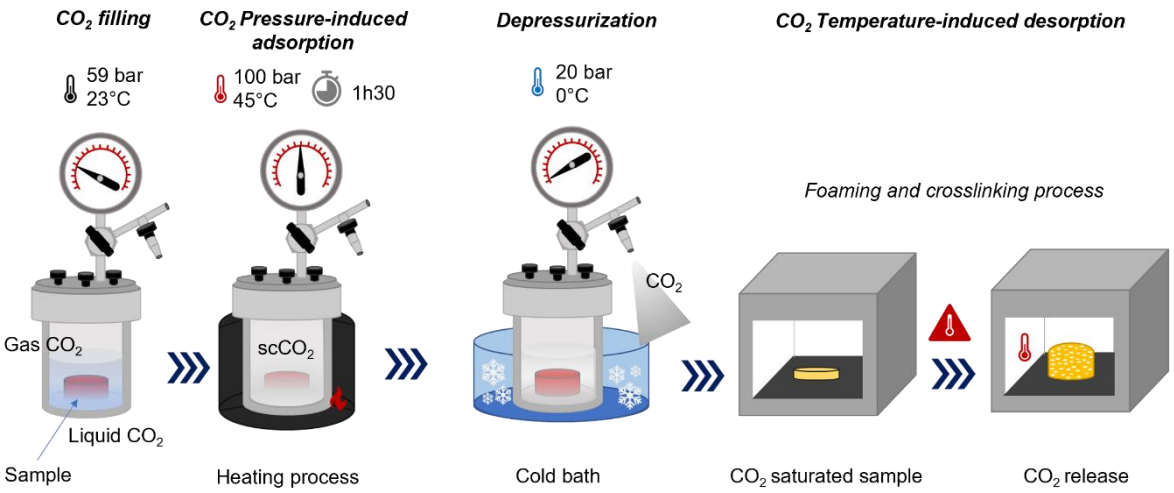

Figure IV.2. Schematic representation of the two-step foaming strategy: (A) CO_2 pressure-induced absorption under supercritical conditions followed by (B) CO_2 temperature-induced desorption during curing, including the mechanism of carbamate decomposition and regeneration of free amines that drive network formation.

We directly verified this amine-CO_2 complexation by visual inspection and FTIR: neat MXDA, initially a clear liquid at room temperature, turned into a white solid after exposure to $scCO_2$ (45 °C, 100 bar, 90 min) (Figure IV.3A). The corresponding FTIR spectrum of this solid displays diagnostic bands at 1545 cm^{-1} (vas COO^- of carbamate), 1664 cm^{-1} (ν C=O of carbamic acid), and ~2206 cm^{-1} (physically adsorbed CO_2), absent in MXDA (Figure IV.3B-C).[235,236]

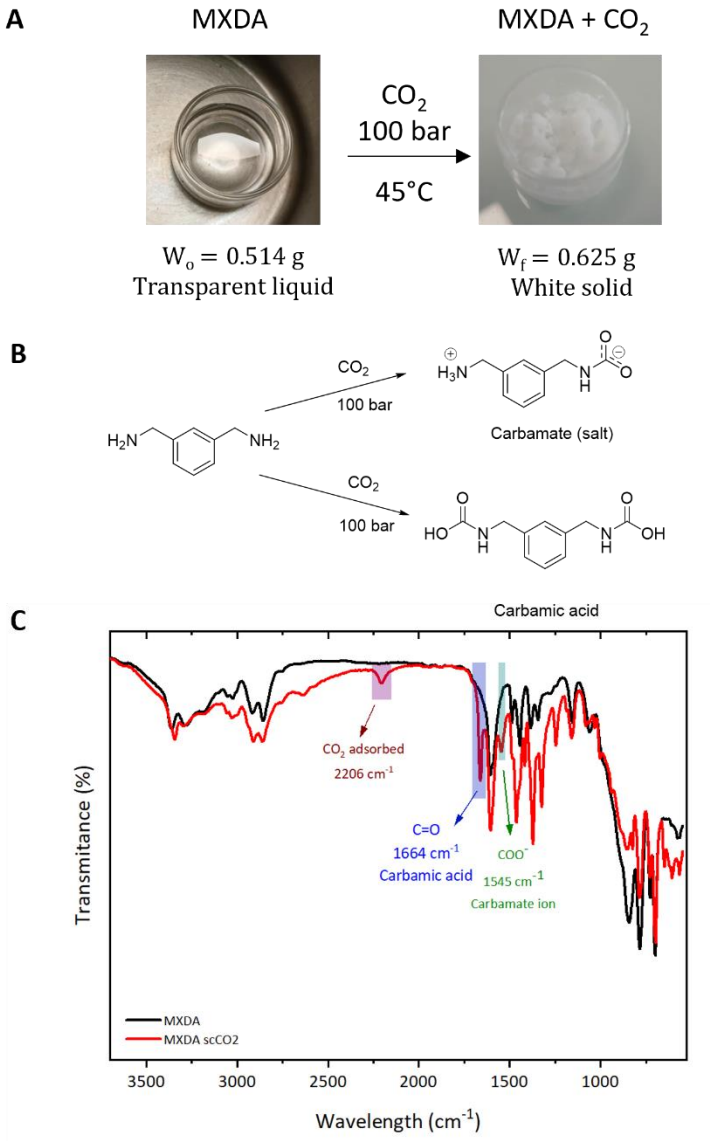

Figure IV.3. Amine-CO_2 complexation evidence: (A) Visual appearance of MXDA before and after $scCO_2$ conditions (Tc = 45°C, Pc = 100 bar). Initial weight, W_0 = 0.514 g and final weight after $scCO_2$ saturation, Wf = 0.625 g. (B) Scheme of carbonatation reaction of MXDA. (C) FTIR spectra of MXDA before and after $scCO_2$ saturation (Tc = 45°C, Pc = 100 bar, t = 1h30).

After saturation, the reactor was cooled to 0 °C (CO_2 in liquid state, vapor pressure ≈ 35 bar) and rapidly depressurized to retain CO_2 within the sample, decoupling expansion from depressurization rate as previously described for thermoplastic NIPUs.[164] A subsequent thermal step at moderate temperature (100–140 °C) was required to obtain a stable cellular structure: heating triggers CO_2 desorption and simultaneously promotes curing of the 5CC/amine resin. Figure IV.4 shows the foaming process over time during the desorption of CO_2.

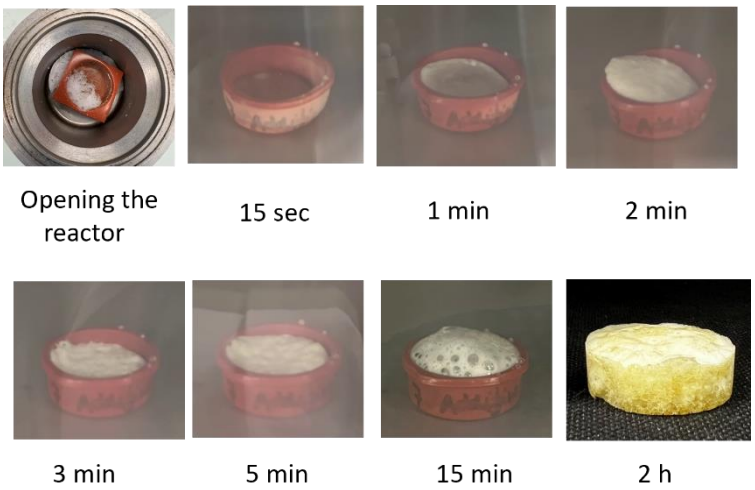

Figure IV.4. Foaming process over time when the foaming process is induced at moderate temperatures (100°C). From the moment the reactor is depressurized to the final stabilized foam after 2 hours at 100°C in the oven.

To validate the feasibility of this approach within the processing map outlined in the introduction, four foams were prepared from TMPTC/MXDA under identical $scCO_2$ saturation (45 °C, 100 bar, 1 h 30 min) and foamed at either 100 or 140 °C, with and without Laponite (Table IV.1; Figure IV.5A). During foaming, CO_2 desorbs from both physically absorbed reservoirs and reversibly bound carbamates, initiating bubble nucleation at the surface (due to localized heating) and propagating inward. The initially translucent film turns white within a few minutes, indicating early cell formation and growth while the matrix is still of low crosslink density. Thermal carbamate decomposition regenerates amines, sustaining curing and viscosity build-up; the increasing crosslink density ultimately traps gas and stabilizes the cellular architecture.

Table IV.1. Foaming conditions for the fabrication of NIPU foams using TMPTC and MXDA. Conditions: [TMPTC]/[MXDA] = 1/1 (expressed in equivalent functions of cyclic carbonates and amines), $scCO_2$ saturation conditions: Tsc = 45°C and Psc = 100 bar.

Entry	Foaming temperature (°C) / Time (h)	Additives
1	140 / 2h	-
2	100 / 3h	-
3	140 / 2h	5 wt% Laponite
4	100 / 3h	5 wt% Laponite

Incorporating 5 wt% Laponite (Entries 3–4) markedly refined the cellular morphology via viscosity increase at early curing and heterogeneous nucleation. At 140 °C, the average cell size decreased from 1.58 ± 0.73 mm (no Laponite, Entry 1) to 0.58 ± 0.39 mm (with Laponite, Entry 3), accompanied by a visible reduction in apparent density (greater foam height, Figure IV.5A). This beneficial effect was even more pronounced at 100 °C, the foam with Laponite (Entry 4) showed no large voids or wall collapse, in contrast to Entry 2 (no Laponite). As already reported elsewhere, 5wt% of Laponite significantly enhanced the quality of the foams and led to a reduction of density of the material.[149] FTIR of all foams confirmed urethane formation (C=O at 1694 cm^{-1}) and disappearance of the cyclic carbonate band at 1790 cm^{-1} (Figure IV.5B).

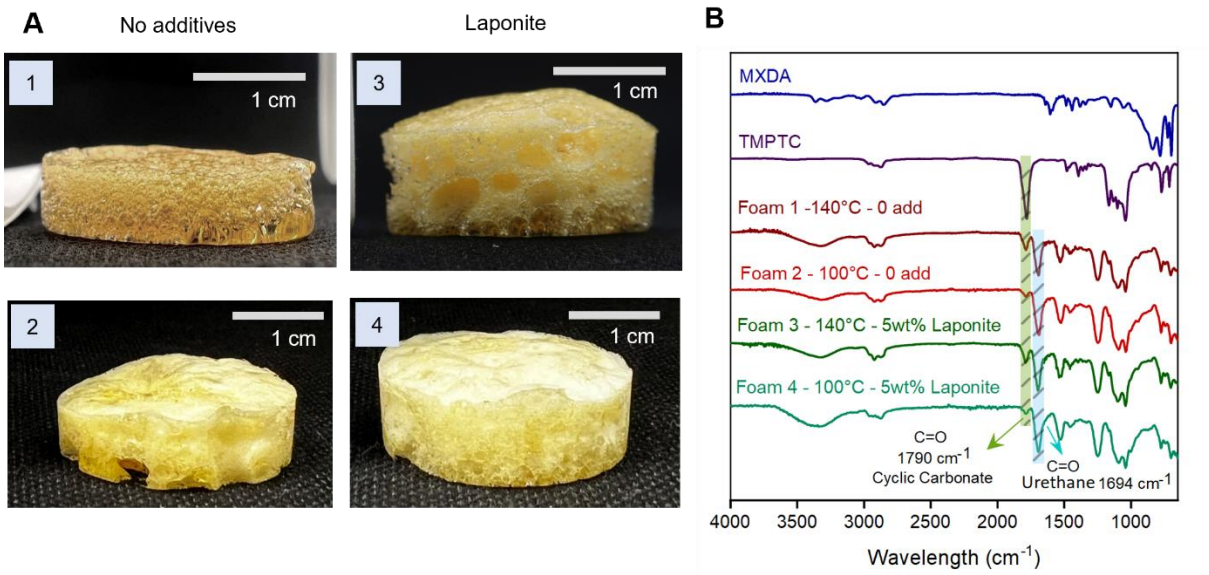

Figure IV.5. NIPU foam characterization: (A) Optical images of NIPU foams prepared at different foaming temperatures with and without Laponite. (B) FTIR spectra of the foams confirming PHU formation.

To monitor diamine effects, the same protocol was applied to TMPTC with an aliphatic hardener (Jeffamine EDR-148), with and without 5 wt% Laponite, at 100/120/140 °C. The resulting foams were heterogeneous; visual inspection suggested that gelation occurred before effective CO_2 release, preventing uniform expansion (Figure IV.6). Hence, MXDA was retained for subsequent optimization.

Based on the experimentally observed sequence under $scCO_2$ foaming (Figure IV.4), the mechanism proceeds as follows: upon heating, CO_2 desorbs both from the physically absorbed fraction in the 5CC/amine matrix and from carbamate/carbamic-acid reservoirs formed with primary amines. Localized heat transfer at the surface triggers bubble nucleation and whitening, with inward propagation. While crosslink density remains low, bubbles expand and the matrix accommodates growth. Concomitantly, thermal decomposition of carbamate/carbamic-acid species releases additional CO_2 and regenerates free amines, which react with 5CC to advance curing and increase viscosity. The rising crosslink density ultimately traps the gas and stabilizes the cellular architecture, rationalizing the observed improvements with Laponite (early viscosity/nucleation control) and the less favorable outcomes with the aliphatic hardener (premature gelation vs. gas release).

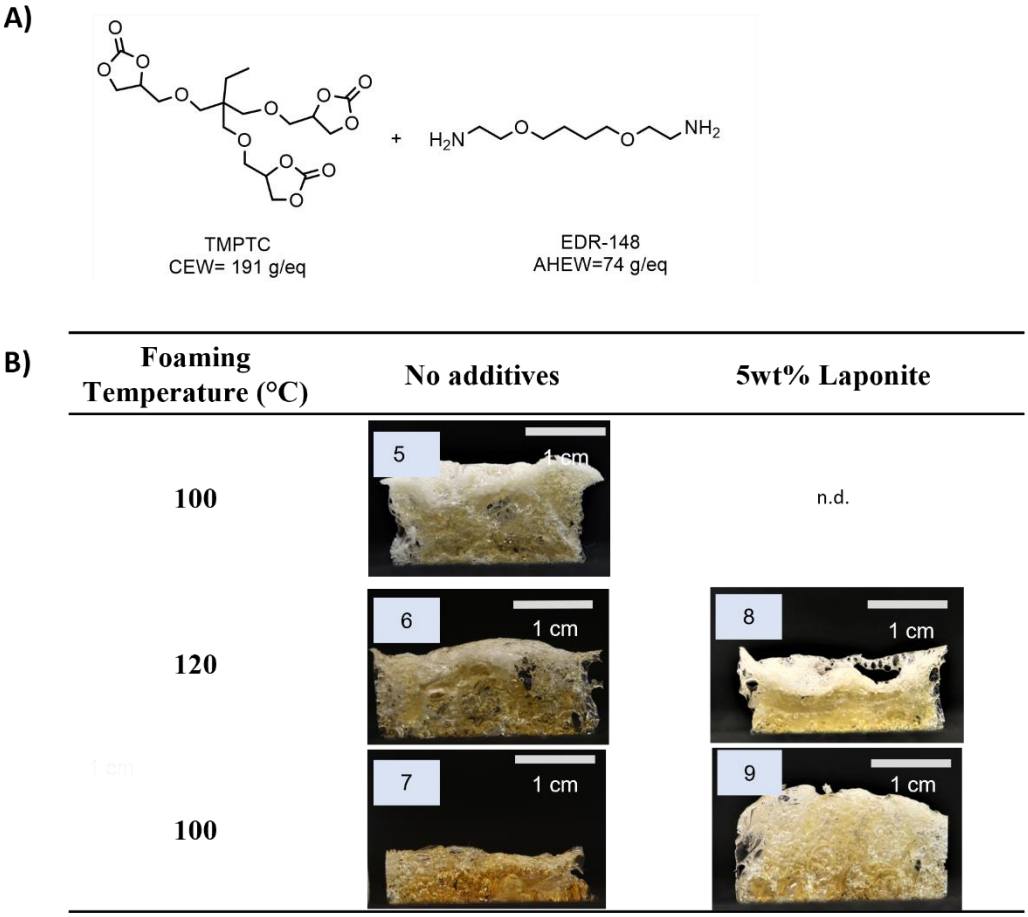

Figure IV.6. Foaming trials with aliphatic amine: (A) Chemical structure of monomers TMPTC and Jeffamine (EDR-148). (B) Optical characterization of thermoset NIPU foams synthesized under $scCO_2$ in a batch process. Conditions: [TMPTC]/[EDR-148] = 1/1. All foams were saturated under $scCO_2$ for 1h30min at Tsc = 45°C and Psc = 100 bar. Foams 15, 16, 17 were foamed without additives. Foams 18, 19 were foamed with 5 wt% Laponite. The foaming process was induced at 100, 120, 140°C for 1h30.

2.2. Monomer Choice for Foaming Control

To better control the foaming process and enhance the morphology of the cellular materials, it is crucial to carefully select the reactants in the formulation. Indeed, the nature of monomers has a significant influence on the resin mixture viscosity, curing rate, crosslinking density, thermal and mechanical properties. The use of a crosslinking monomer is essential for obtaining homogeneous and well-structured foams. The tris(5-membered cyclic carbonate), TMPTC, used in the previous section results in highly compact crosslinked rigid foams due to the short aliphatic chains of the TMPTC monomer. Caillol et al. demonstrated that bis(cyclic carbonates) can impart flexibility to self-blown non-isocyanate polyurethane foams, thereby

enhancing their morpho-structural properties.[143] We thus decided to introduce a bis(5-membered cyclic carbonate), poly(propylene oxide) biscarbonate (PPOBC), with a polyether backbone to confer flexibility to the foams (Figure IV.7A). A series of different formulations was accordingly prepared by varying the mass ratio of the trifunctional (TMPTC) and bifunctional cyclic carbonates (PPOBC), while keeping the equivalence of functions between cyclic carbonates and amines constant and equal to 1 (i.e. ([TMPTC] + [PPOBC])/([MXDA]) = 1/1 (Table IV.2).

Table IV.2. NIPU foam formulations with 5 wt% of Laponite and main characteristics of thermoset NIPU foams obtained by $scCO_2$ saturation at Tsc = 45 °C and Psc = 100 bar for 1.5 h and foaming at 100°C for 3 h. [a]TMPTC: Trimethylolpropane triscarbonate; [b]PPOBC: Poly(propylene oxide) biscarbonate; [c]GC: Gel content.

Entry	[TMPTC][a]	[PPOBC][b]	Density ($g.cm^{-3}$)	T_g (°C)	GC[c] (%)
4	1	0	0.227 ± 0.047	49	97
10	0.9	0.1	0.296 ± 0.048	44	96
11	0.8	0.2	0.285 ± 0.025	40	94
12	0.6	0.4	0.491 ± 0.004	34	88
13	0.5	0.5	0.338 ± 0.037	28	85

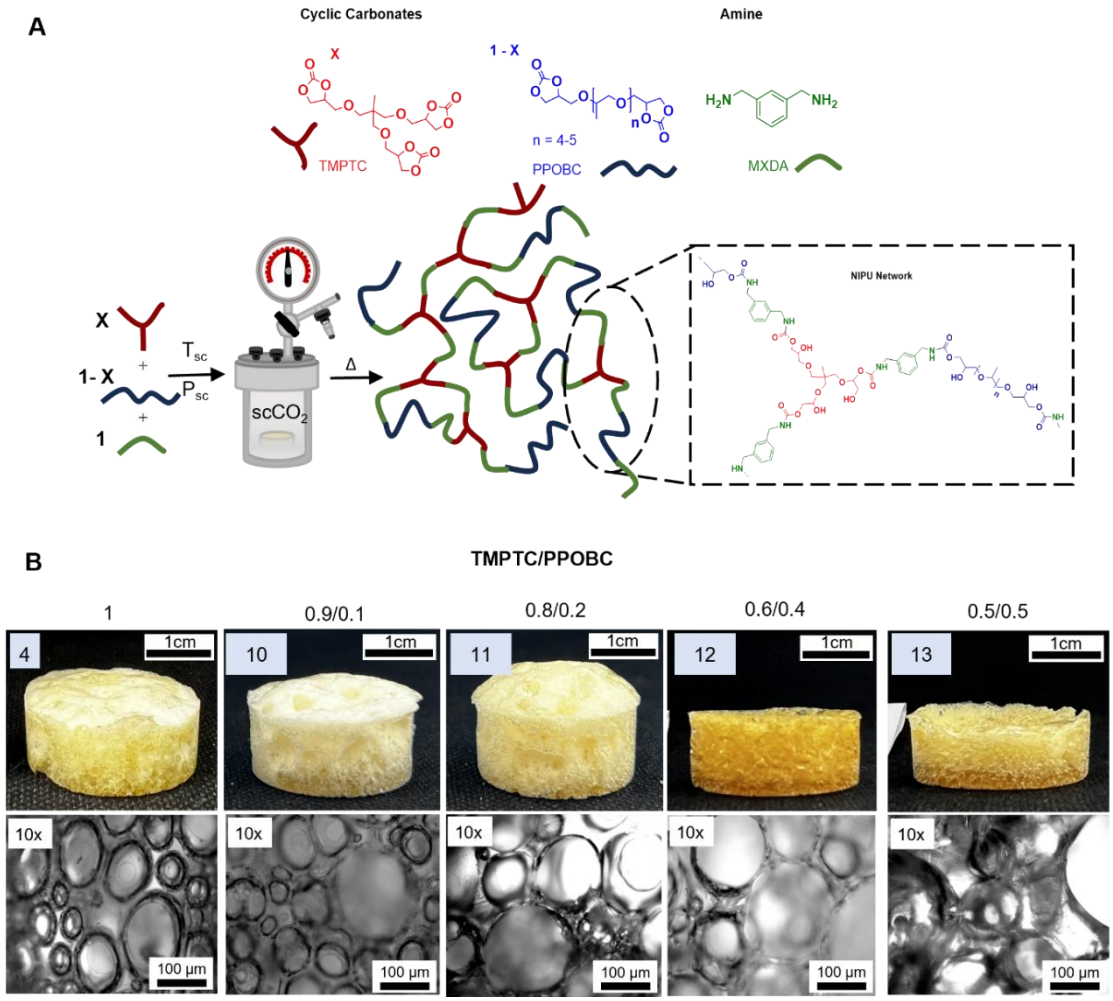

Figure IV.7. Effect of monomer ratio on foam properties. A) Chemical structures of TMPTC and PPOBC. B) Optical images of NIPU foams prepared with different TMPTC/PPOBC ratios, all loaded with 5 wt% Laponite and foamed at 100°C for 3h.

Consistent with previous studies, incorporating PPOBC into the formulation altered the morphology and properties of the foams. The glass transition temperature (T_g) of the foams exhibited a decrease when the content of bis(cyclic carbonate) (PPOBC) was increased. DSC thermograms are depicted in Figure IV.8A. Employing only TMPTC in the formulation (Entry 4) yielded a T_g of 49°C, in contrast to the T_g of 28°C observed for a 0.5/0.5 TMPTC/PPOBC ratio (Entry 13).

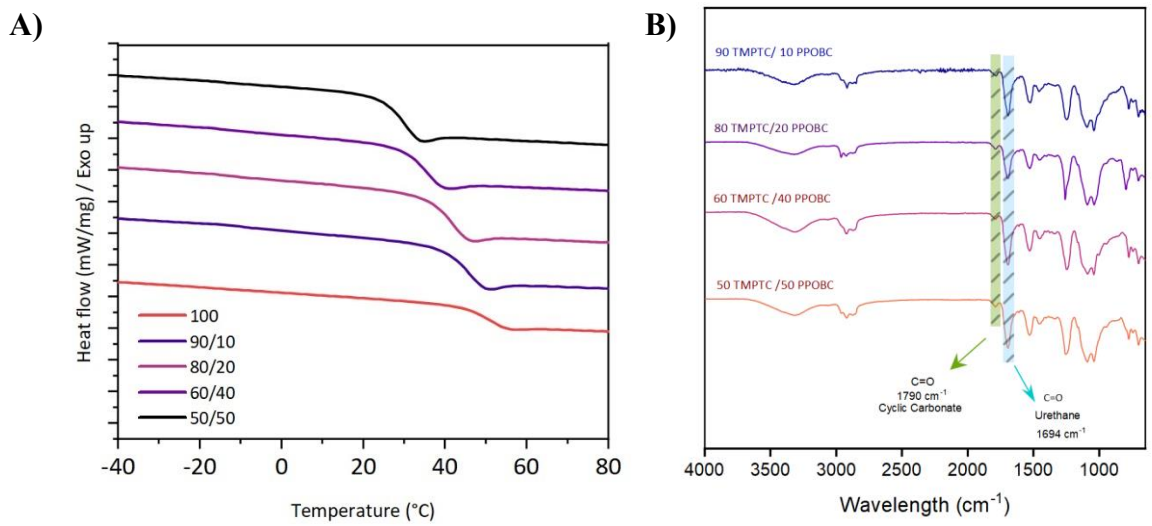

Figure IV.8. DSC thermograms of the NIPU Foams synthesized by varying the ratio between two different 5-membered cyclic carbonates, TMPTC and PPOBC, ([TMPTC]/[PPOBC]) with MXDA using supercritical CO_2 (T = 45°C; P = 100 bar; t = 1h30min) foamed at 100°C with 5 wt% Laponite.

The gel content (GC) of these foams was also assessed (Table IV.2). The gel content of the foams prepared with a TMPTC mass fraction higher than 0.8 were rather high (GC > 94%), indicating highly insoluble networks and confirming the crosslinking process between the triscarbonates and diamines. Indeed, gel content values of 97, 96, and 94% were obtained with 100% TMPTC (Entry 4), 0.9/0.1 TMPTC/PPOBC (Entry 10) and 0.8/0.2 TMPTC/PPOBC (Entry 11), respectively. When a higher quantity of PPOBC biscarbonate was added, a decrease in gel content was noticed. For instance, gel contents decreased to 88 and 85% for 0.6/0.4 TMPTC/PPOBC (Entry 12) and 0.5/0.5 TMPTC/PPOBC (Entry 13), respectively. The material density was also measured to complement the visual characterizations. The foam densities ranged from 0.227 to 0.491 $g.cm^{-3}$. Entries 7 and 8 exhibited the highest density values, 0.491 ± 0.004 $g.cm^{-3}$ and 0.338 ± 0.037 $g.cm^{-3}$, respectively. FTIR spectra confirmed the presence of the urethane group at 1694 cm^{-1} as shown in Figure IV.8B.

In this case, a higher amount of PPOBC decreases the viscosity of the reactive mixture and extends the gelation time (defined as the crossover of G' and G"). With 100% TMPTC at 80°C, gelation occurred in 48 min, however, when 0.2 mass fraction of PPOBC was added, the gelation time increased to 75 min and with 0.5 mass fraction of PPOBC, the gelation point was delayed significantly to 319 min. This slower crosslinking rate and reduced viscosity hinder the effective trapping of the blowing agent (CO_2) during the curing process (Figure IV.9).

Entries 5 and 6 (Table IV.2) resulted in densities of 0.296 ± 0.048 and 0.285 ± 0.025 g.cm^{-3}, respectively. Based on this assessment, a 0.8/0.2 TMPTC/PPOBC formulation (Entry 11) was selected as the most promising candidate for further foaming investigation.

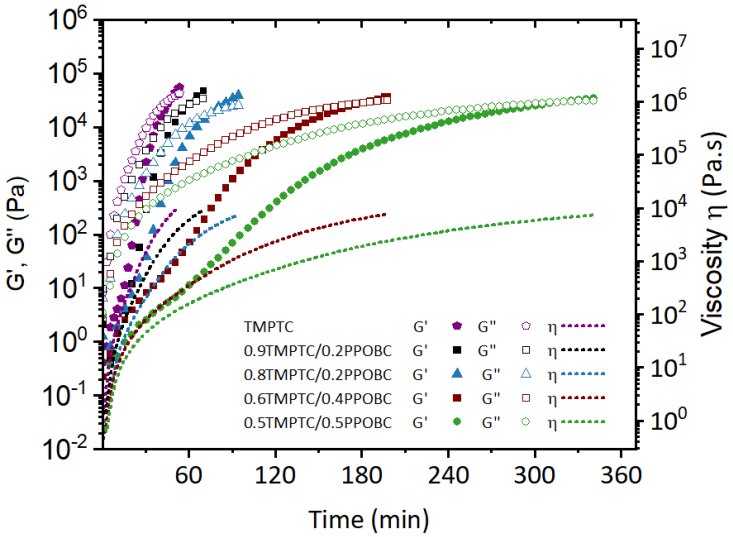

Figure IV.9. Rheological behaviour (*G′*, *G″* and viscosity) of the different formulations between TMPTC, PPOBC and MXDA at 80°C, showing the effect of PPOBC content on gelation time and viscosity build-up.

2.3. Tuning NIPU Foam Properties

Additives are essential for manufacturing tunable foams and precisely controlling the foaming process. They offer various advantages including enhanced overall morphological stability and influencing mechanical properties through viscosity, cell size and density adjustment.[31,237] These benefits allow for precise control over the final foam's characteristics and applications. In the production of morphologically stable thermosetting NIPU foams using supercritical CO_2 ($scCO_2$) as a PBA, it is necessary for the 5CC/amine formulation to exhibit sufficient reactivity and viscosity during the foaming stage. This reactivity is essential for both trapping CO_2 and facilitating crosslinking. Given the rapid CO_2 thermal-induced desorption observed in our study, the incorporation of additives became fundamental for enhancing the cellular expansion and avoiding the coalescence of the cellular material.

To demonstrate the robustness of the foaming process and evaluate the characteristics and properties of the final foams, various additives were incorporated to the foam containing 0.8/0.2 TMPTC/PPOBC (Entry 11). Alongside the synthetic clay (Laponite), two other additives, Tegostab E-8930 and Tegostab E-8158 were selected. Tegostab additives are surface

active agents with cell-regulating properties that reduce the interfacial tension generated during cell expansion, contributing to the stabilization of the foam.[31] The foam formulation characteristics are summarized in Table IV.3. For this series of NIPU foams, the $scCO_2$ foaming protocol used for 0.8/0.2 TMPTC/PPOBC formulation (Foam 6) was again employed. All the formulations (0.8/0.2 TMPTC/PPOBC) with and without additives resulted in thermoset NIPU foams as illustrated in Figure IV.10.

Table IV.3. Properties and morphological characterization of thermoset NIPU foams with different additives and foaming temperatures. All foams were formulated with 0.8 TMPTC / 0.2 PPOBC / MXDA. CO_2 saturation conditions: Tsc: 45 °C and Psc: 100 bar for 90 minutes.

Entry	Foaming T/time	Additives	GC (%)	Density ($g.cm^{-3}$)	Cell size (mm)	Td5% (°C)
14	100°C / 3h	-	90	0.274 ± 0.048	0.42 ± 0.26	251
15	100°C / 3h	5wt% Laponite	94	0.285 ± 0.034	0.33 ± 0.16	260
16	100°C / 3h	0.5wt% E-8158	93	0.360 ± 0.014	0.59 ± 0.22	268
17	100°C / 3h	0.5wt% E-8930	94	0.451 ± 0.023	0.99 ± 0.37	260
18	140°C / 2h	5wt% Laponite	99	0.387 ± 0.010	0.91 ± 0.35	260
19	80°C/1h - 120°C/2h	5wt% Laponite	93	0.294 ± 0.032	n.d.	260

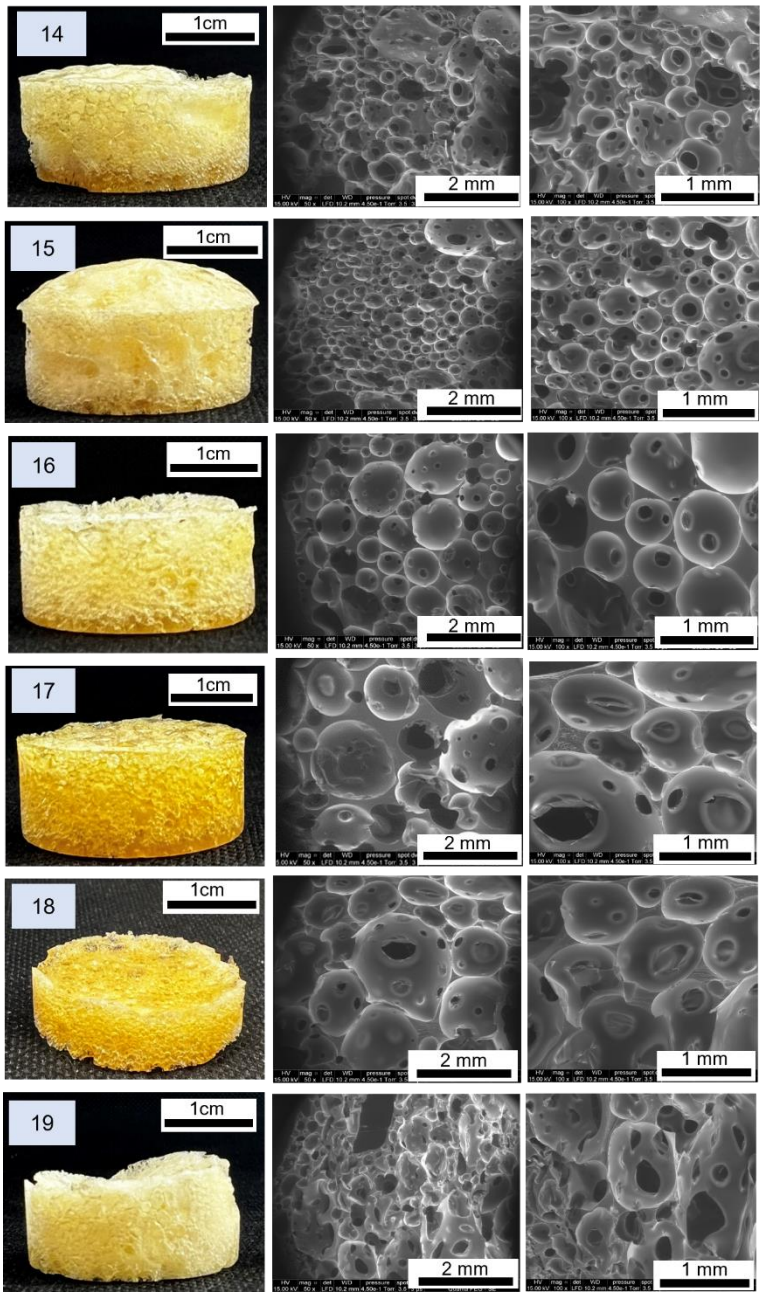

Figure IV.10. Optical images and SEM micrographs of thermoset NIPU foams (0.8/0.2 TMPTC/PPOBC formulation) prepared with different additives and foaming temperatures. Scale bars indicate 1 mm.

The morphology of the foams and cell sizes were determined by scanning electron microscopy (SEM) to assess the impact of these additives on the morpho-structural properties. All foams presented microcellular spherical closed pores with small localized cavities on the faces of the foams. To better showcase the effect of these additives on the formulation, a reference foam

(Entry 14) was designed without any additives. As observed in Figure IV.10, a material of relatively poor structural quality was formed.

As expected, adding 5 wt% of Laponite to the formulation (Entry 15) resulted in a decrease of the cell size, from 0.42 ± 0.26 (without additives) to 0.33 ± 0.16 mm (with Laponite) with a limited increase of the density, from 0.274 to 0.285 g.cm^{-3}. The formulation loaded with Tegostab E-8158 (Entry 16) resulted in a high-density foam (0.360 ± 0.014 g.cm^{-3}) with higher average cell size (0.59 ± 0.22 mm). When Tegostab E-8930 was incorporated into the formulation (Entry 17), the cell size was significantly increased (0.99 ± 0.37 mm) and a high-density foam (0.451 ± 0.023 g.cm^{-3}) was formed. This behavior can be explained by the production of thicker walls between the large cavities and less cell density (Figure A.IV.2). Importantly, the addition of these additives was able to tune the cell size of the foams.

The temperature effect on the CO_2 induced-temperature desorption step was further studied on formulation containing 0.8/0.2 TMPTC/PPOBC, loaded with 5 wt% of Laponite and foamed at 100 °C (Foam 10). Two foams were synthesized at 140 and 80°C, Entry 18 and Entry 14, respectively. The foams obtained are shown in Figure IV.10. Increasing the foaming temperature to 140 °C (Entry 18) resulted in a denser foam (0.387 ± 0.010 g.cm^{-3}) with twice the average cell size (0.91 ± 0.35 mm) in comparison to Entry 15, foamed at 100°C. When the foaming temperature is decreased to 80 °C (Entry 14), the cellular material was of poor quality with a density of 0.294 ± 0.032 g.cm^{-3}. For the latter foam, the average cell size was not measured due to the heterogeneity of the cells, which might be caused by difference rates of CO_2 release and curing.

The gel contents (GC) were also evaluated (Table IV.3). The NIPU foams synthesized at a foaming temperature of 100°C had high gel content ranging from 90 to 94%, confirming the effective crosslinking of the 5CC/amine mixture into a PHU network. The urethane group formation was also confirmed by FTIR analysis (Figure A.IV.3 and 4). When the foam was produced at higher temperature, i.e. 140 °C (Entry 18), the gel content was over 99%.

The glass transition temperature (T_g) of the dried foams (dried overnight) was determined by DSC. All the results are summarized in Figure IV.11. and the DSC thermograms are presented in Figure IV.12 The glass transition temperatures of all the NIPU foams were all within 35 and 42°C and were not significantly affected by the additives or by the foaming temperature used

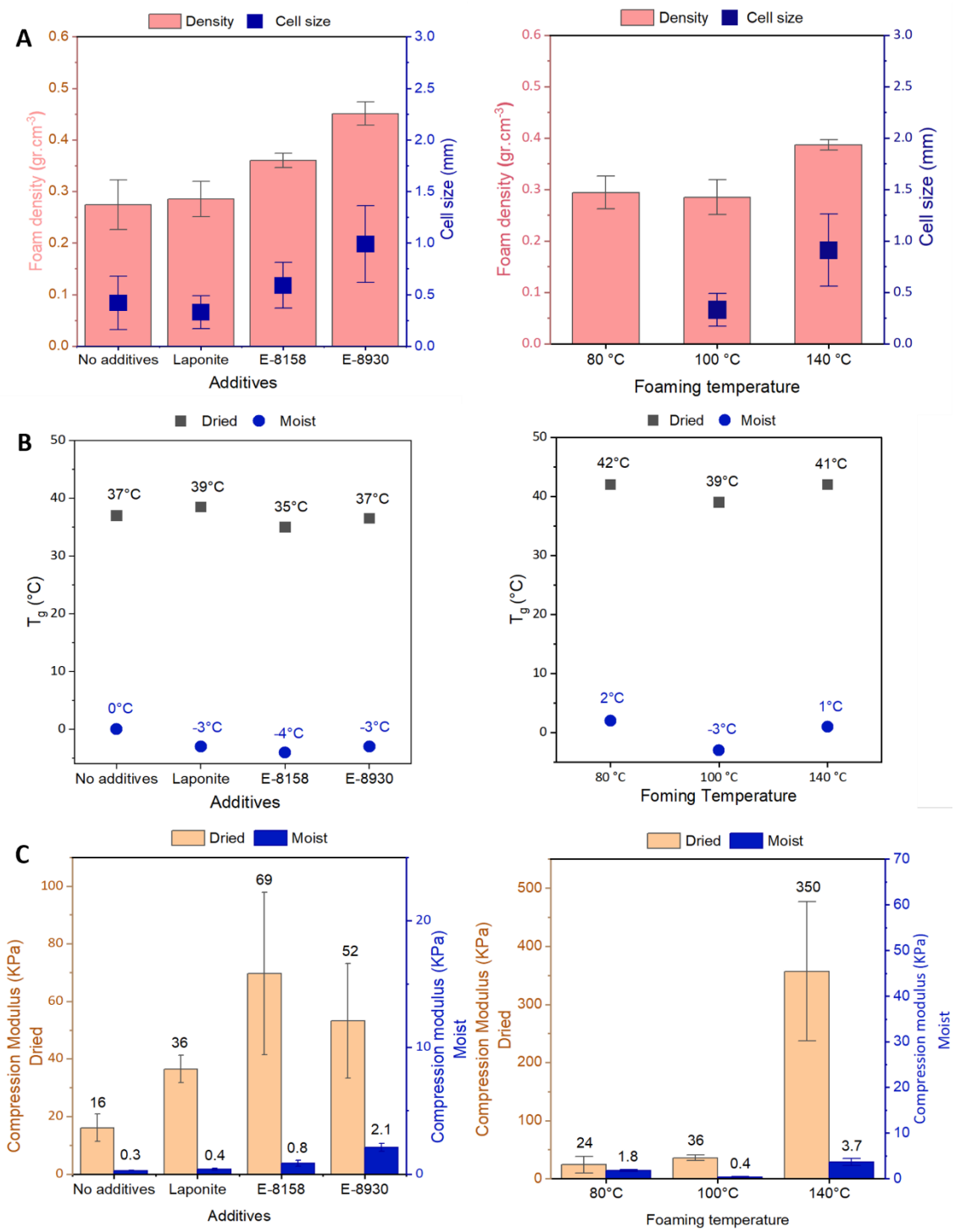

Figure IV.11. Summary of NIPU foam properties synthesized with various additives and foamed at 100°C (Left) and foamed at different temperatures (80°C, 100°C and 140°C) with Laponite (Right). A) Comparison of foam density and cell size. B) T_g in dried and moist state. C) Mechanical properties (compression modulus) in both: dry and moist conditions.

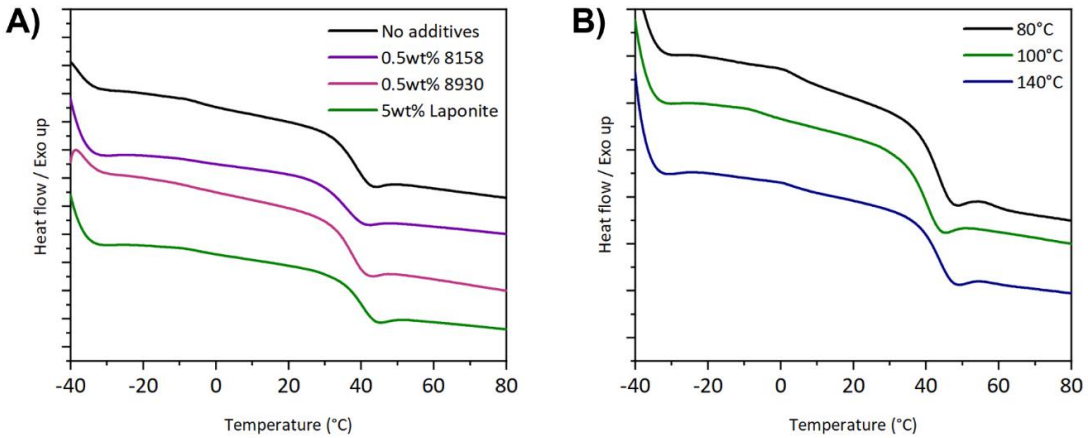

Figure IV.12. DSC thermograms of the dried foams: A) Foams produced at 100°C using different additives. B) Foams produced at different temperatures (80, 100, 140°C) using 5 wt% Laponite.All foams were produced using supercritical CO_2 (T = 45°C; P = 100 bar; t = 1h30min).

However, the polyaddition of cyclic carbonates and amines results in PHU networks containing hydroxyl groups due to the formation of hydroxyurethanes, rendering the foams hygroscopic.[17,148] To further explore the hydrophilic behavior, the water uptake of the foams was thereby determined. Overall, the NIPU foams scarcely absorbed 3-7 wt% of water, which is consistent with previous studies on PHU foams and thermosets exposed to 50% RH.[17,238]

Despite this small water content, there was a significant impact on the thermal properties. For instance, the T_g of the NIPU foam, employing 0.8/0.2 TMPTC/PPOBC, loaded with 5 wt% of Laponite and foamed at 100°C (Entry 15), significantly decreased from 35 °C (dried) up to -4 °C (moist). All the NIPU foams followed the same trend with a T_g of the moist foams ranging from -4 to 2 °C as shown in Figure IV.13. This highlights the significant plasticizing effect of water on PHU networks by using only a small amount of water. Remarkably, when the foams were dried again, they recovered their initial T_g.

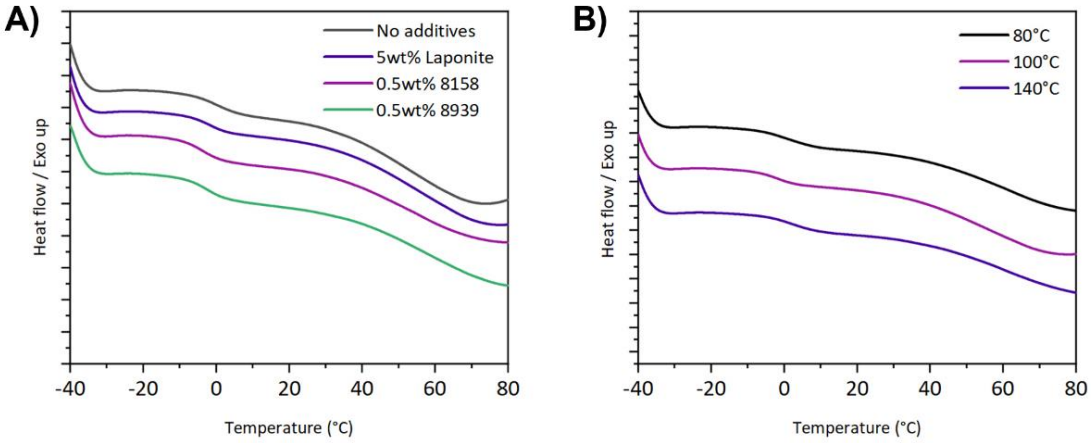

Figure IV.13. DSC thermograms of the moist foams: A) Foams produced at 100°C using different additives. B) Foams produced at different temperatures (80, 100, 140°C) using 5 wt% Laponite. All foams were produced using supercritical CO_2 (T = 45°C; P = 100 bar; t = 1h30min).

To evaluate the impact of additives on the properties of NIPU foams, additional thermogravimetric analyses and compression testing were conducted. In the case of thermogravimetric analyses (Figure IV.14), all samples presented similar degradation temperatures (Td5%) around 260 °C (Table IV.3), confirming that the additives did not influence the degradation temperature of the foams. This degradation temperature is even in the same range (250-300 °C) as previously reported in self-blown and physically blown PHU foams.[17,143,146,148,159]

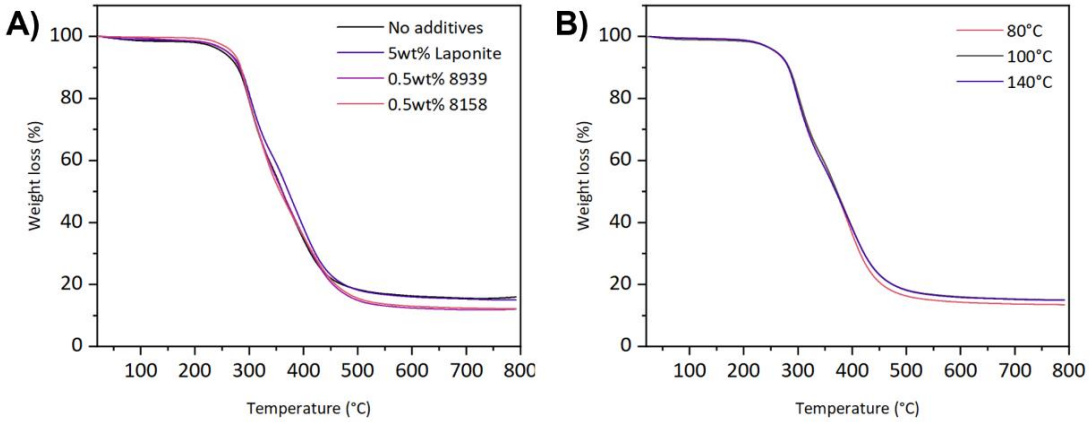

Figure IV.14. Thermogravimetric analysis (TGA) of the foams: A) Foams produced at 100°C using different additives. B) Foams produced at different temperatures (80, 100, 140°C) with 5 wt% Laponite. The analyses were performed at a heating rate of 10°C/min under N_2 flow from room temperature to 800°C.

The impact of these additives was more highlighted in the case of the mechanical properties of NIPU foams using compression tests (Figure IV.12C). The foam synthesized without additives (Foam 9, dried) and characterized by the lowest density (0.274 $g.cm^{-3}$), exhibited the lowest compression modulus (16 kPa). When the foam was added with 5 wt% of Laponite (Entry 15, dried) with a similar density (0.285 $g.cm^{-3}$), the compression modulus raised to 36 kPa. Importantly, the addition of the synthetic nanoclay to the formulation notably reinforced the mechanical strength of the cellular material under compression at comparable densities. When Tegostab E-8158 and E-8930 were used as surfactants in the foams produced at 100°C, it resulted in compression moduli of 69 and 52 kPa, respectively. However, due to the considerable variation in foam densities (0.274-0.451 $g.cm^{-3}$), direct comparison of the compression modulus across all foams is not feasible. For instance, when the foaming temperature was modified to 80 and 140°C for the foams containing 5 wt% of Laponite, the compression moduli were measured at 350 kPa (Entry 18, dried) and 24 kPa (Entry 19, dried). All stress-strain curves are shown in Figure A.IV.5.

As anticipated from the thermal properties, the mechanical properties were significantly influenced by the water uptake and its plasticization effect. All the moist foams exhibited a significant decrease in compression moduli by comparison to their dried counterparts. For instance, the compression modulus of moist foams (Entries 9 and 10) was 0.03 and 0.04 kPa, respectively. Similarly, Entries 11 and 12, in their moist state, exhibited reduced compression moduli from 69 to 0.8 kPa and from 52 to 2.1 kPa, respectively. Foam 18 also showed a decrease in compression moduli from 350 to 3.7 kPa when moist. Stress-strain curves are presented in Figure A.IV.6

These results demonstrate that water uptake leads to significant plasticization, which greatly reduces both the T_g and compression moduli compared to the dried foams. Even whether this plasticization might be perceived as a drawback, it could be actually beneficial when these rigid foams are deemed as shape memory materials triggered by humidity. This affords an interesting approach to span the range of NIPU applications into advanced applications such as heart valves in the biomedical realm.[239]

2.4. Humidity-Responsive Shape Memory Properties

To control the performance and behavior of these humidity-responsive foams, the relationship between T_g, water uptake and the shape recovery with time must be better understood, particularly by investigating the recovery of their original shape when exposed to moisture. To demonstrate the humidity-triggered shape-memory effect, the NIPU foam, without any additive (Entry 14) was dried overnight under vacuum to remove any remaining water at 50 °C. This additive-free foam was selected to study only the neat polymer behavior. The foam was heated at 60 °C and temporarily compressed followed by a rapid cooling to fix the shape (compressed) (see Figure IV.15A). The temporarily deformed foam was exposed to 85% relative humidity and the T_g, water uptake and recovery ratio were measured with time.

Figure IV.15B illustrates the evolution of these parameters with time. During the initial 3-hour exposure of the NIPU foam to humidity, the water uptake reached 5 wt%, the T_g significantly decreased from 45°C to 6°C; and the foam recovered only 3% of its height. After 24 hours, the water uptake increased to 7 wt%, the T_g remained stable (6°C) and the foam recovered its initial height, reaching a recovery ratio of 99% as depicted in Figure IV.15C.

This experiment showed that the recovery ratio rapidly evolves once the T_g goes below room temperature, indicating the material's excellent ability to recover its original shape. This behavior is consistent with the mechanism of shape memory polymers, where the external stimulus is moisture absorption, and the glass transition temperature (T_g) serves as the switching parameter. In the dry state, the foam exhibits a T_g above room temperature, making the material rigid and capable of fixing a temporary shape. When the foam is exposed to humidity, water molecules are absorbed into the polymer matrix, forming hydrogen bonds with hydroxyl (-OH) and amino (-NH-) groups present in the PHU matrix.[240,241] These interactions act as plasticizer, lowering the T_g below room temperature. As a result, the foam transitions from a glassy to a rubbery state, allowing the polymer chains to regain flexibility and mobility. This enables the material to recover its original shape.

Notably, similar humidity-triggered shape memory mechanism has been reported in starch-based films, where the absorbed water also depresses the T_g and facilitates shape recovery.[241,242] These moisture-triggered shape memory materials (SMM) are particularly advantageous because they do not require any external energy source and are responsive to common environmental conditions.

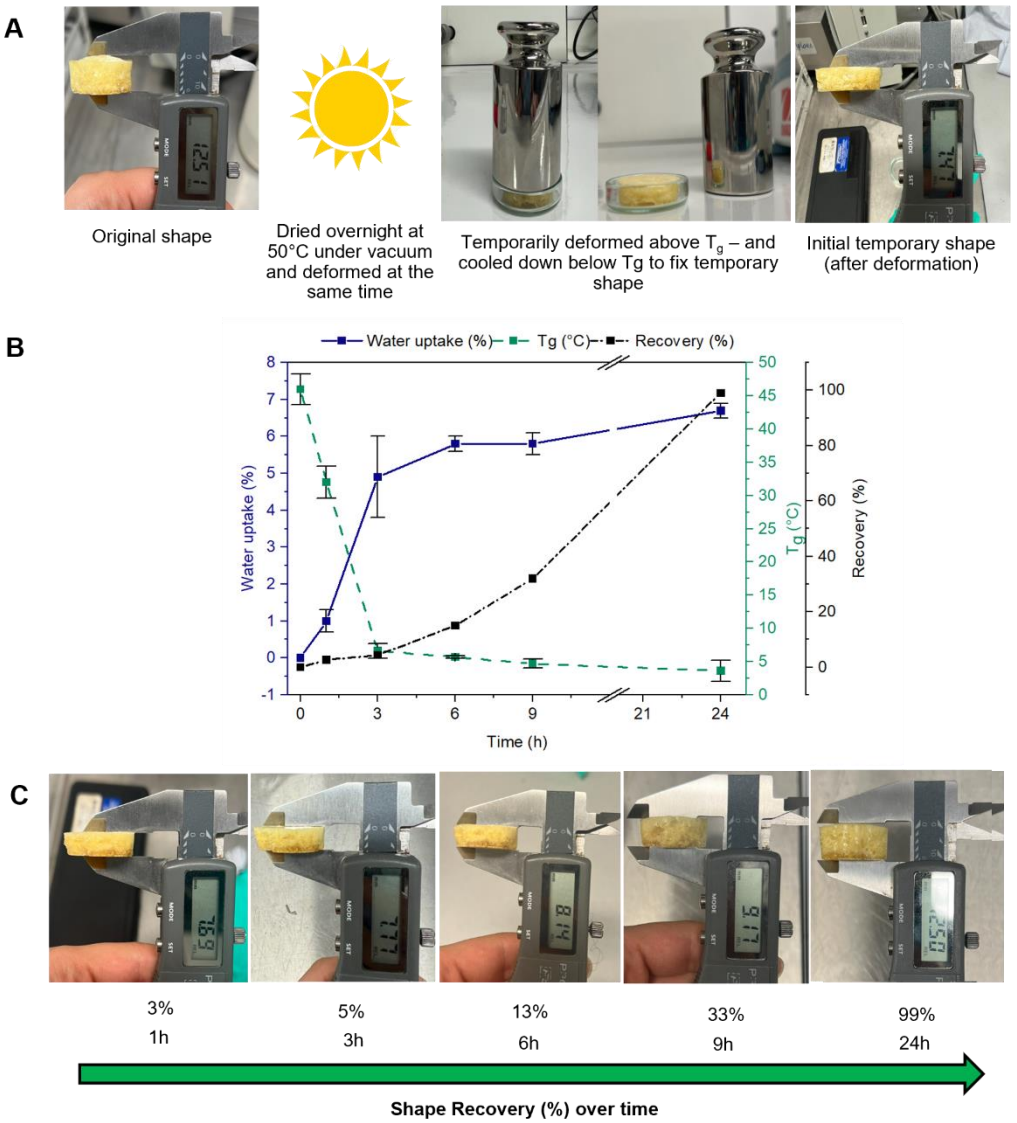

Figure IV.15. Humidity-triggered shape memory behavior of NIPU foams: (A) Schematic representation of the shape memory cycle showing the original shape, temporary compressed shape, and recovered shape upon humidity exposure. (B) Evolution of T_g, water uptake, and recovery ratio over time during exposure to 85% relative humidity. (C) Photographs showing the progressive shape recovery of the compressed foam over 24 hours of humidity exposure.

3. Conclusions

This chapter demonstrated the successful development of an innovative strategy for the eco-friendly preparation of Non-Isocyanate Polyurethane (NIPU) thermoset foams using supercritical CO_2 ($scCO_2$) as a physical blowing agent, offering a safer and greener alternative to conventional blowing agents.

The foaming strategy was based on a two-step batch process combining pressure-induced CO_2 absorption followed by temperature-induced desorption concurrent with curing. Rheological analysis confirmed that the aminolysis of MXDA by TMPTC at low temperatures (45°C) proceeded slowly enough to maintain a slightly crosslinked resin before CO_2 release, enabling controlled foam expansion and cellular structure formation. The proof of concept was successfully validated through the fabrication of rigid foams at different foaming/curing temperatures.

Formulation optimization revealed that incorporating 0.2 mass fraction equivalent of 5-membered bis(cyclic carbonate) (PPOBC) enhanced foam homogeneity and structural integrity. Furthermore, the addition of additives such as nanoclays (Laponite) and surfactants (Tegostab E-8158, E-8930) enabled the production of foams with widely tuneable morphological and mechanical properties. Beyond structural properties, these rigid NIPU foams exhibited shape memory behavior triggered by humidity at room temperature, attributed to the water-induced plasticization of the hydroxyl-rich PHU network.

Overall, this work highlights the versatility and feasibility of $scCO_2$ as a blowing agent for thermoset NIPU foams, representing a dual valorization strategy where CO_2 serves both as a building block for cyclic carbonate synthesis and as a physical blowing agent during foam processing. Future investigations should focus on the influence of $scCO_2$ conditions (pressure, temperature) during the impregnation step, as higher CO_2 uptake may affect resin viscosity through plasticization, potentially influencing foam expansion and stability.

Appendix A.IV

Figures

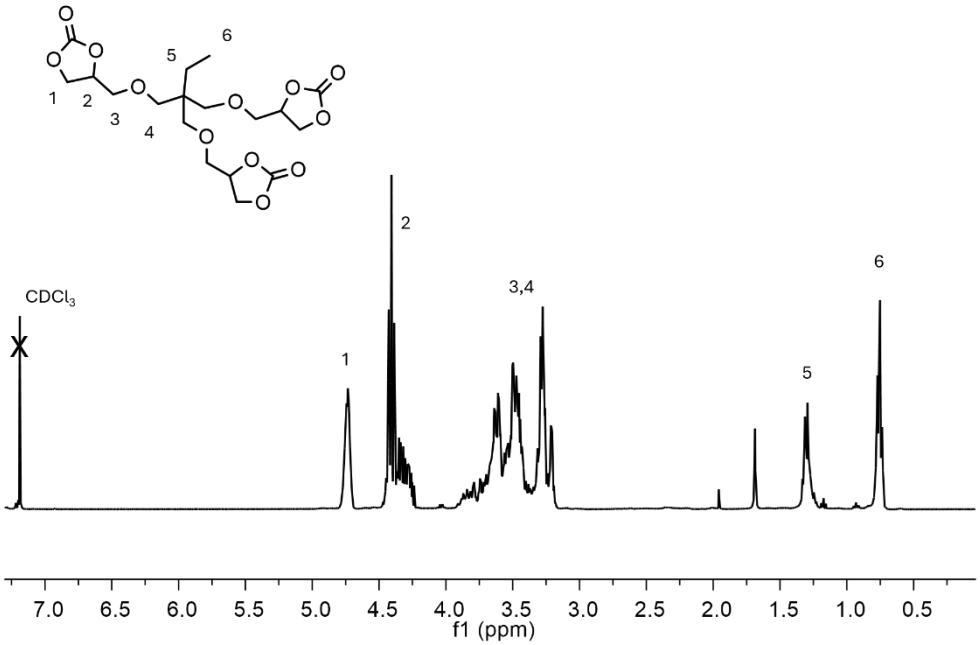

Figure A.IV.1 ^{1}HNMR Spectrum of TMPTC in $CDCl_3$ at room temperature

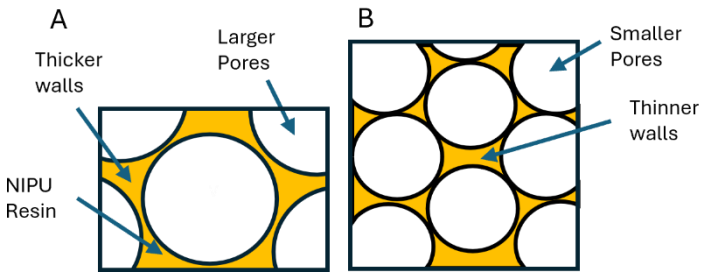

Figure A.IV.2. Schematic representation of two cellular structures. A) High density foam with large pores and thick structural walls. B) Low or medium density foam with smaller pores and thinner structural walls.

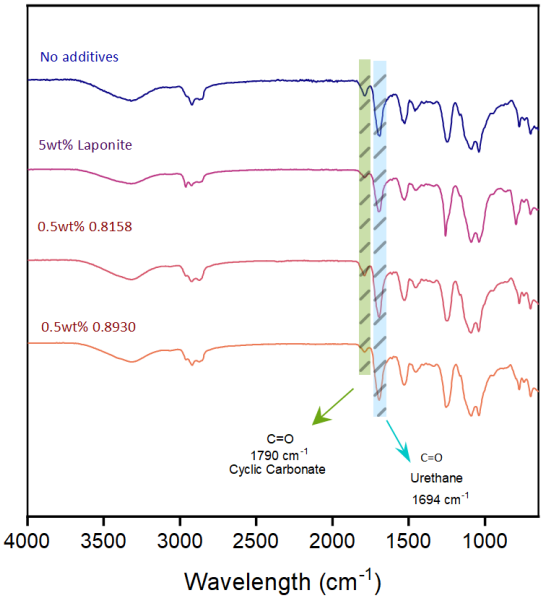

Figure A.IV.3. FTIR spectra of the NIPU Foams synthesized with a ratio of [TMPTC]/[PPOBC] = [0.8]/[0.2] with MXDA produced using supercritical CO_2 (T= 45°C; P = 100 bar; t = 1h30min) and inducing foaming at different temperatures using 5wt% Laponite

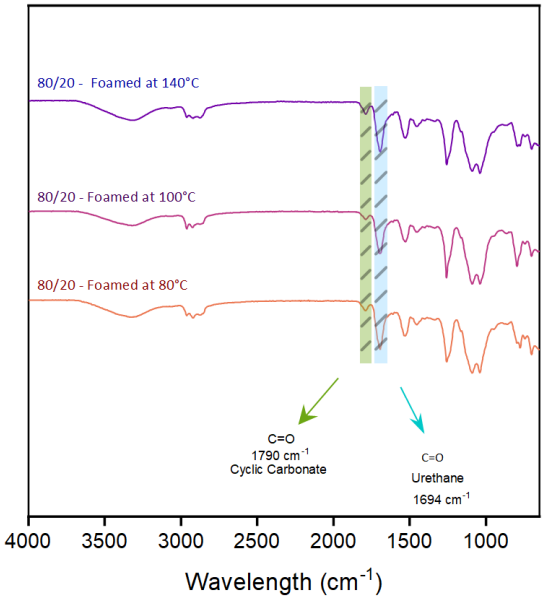

Figure A.IV.4. FTIR spectra of the NIPU Foams synthesized with a ratio of [TMPTC]/[PPOBC] = [0.8]/[0.2] with MXDA produced using supercritical CO_2 (T= 45°C; P = 100 bar; t = 1h30min) and inducing foaming at different temperatures using 5wt% Laponite.

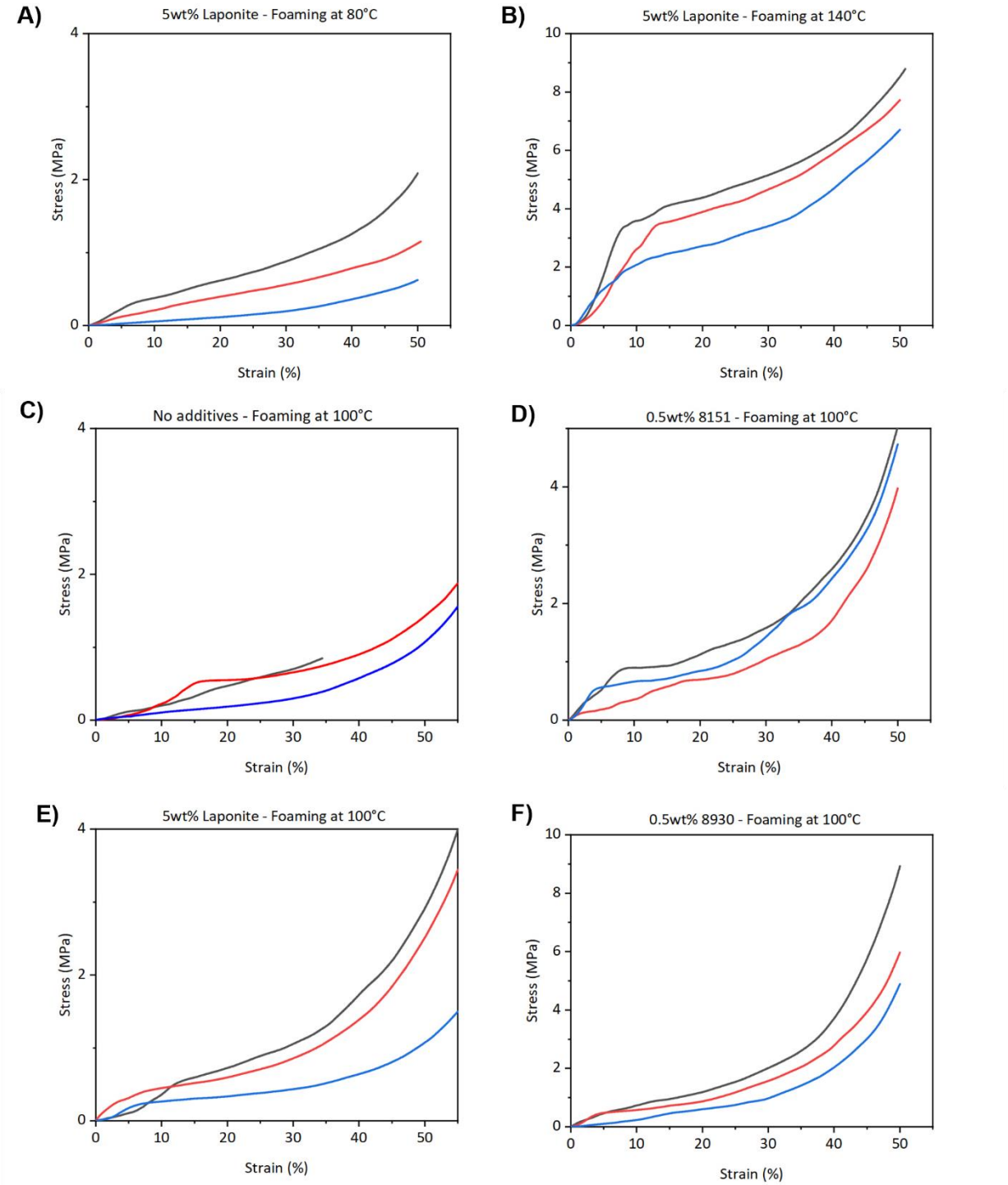

Figure A.IV.5. Compression Stress-Strain curves for the dried foams fabricated using supercritical CO_2 (T= 45°C; P = 10 bar; t = 1h30min): **A)** 5 wt% Laponite, 80°C. **B)** 5 wt% Laponite, 140°C. **C)** 5 wt% Laponite, 100°C. **D)** 0.5 wt% E-8158, 100°C. **E)** 5 wt% Laponite, 100°C. **F)** 0.5 wt% E-8930, 100°C. Conditions: See experimental part (Chapter VIII).

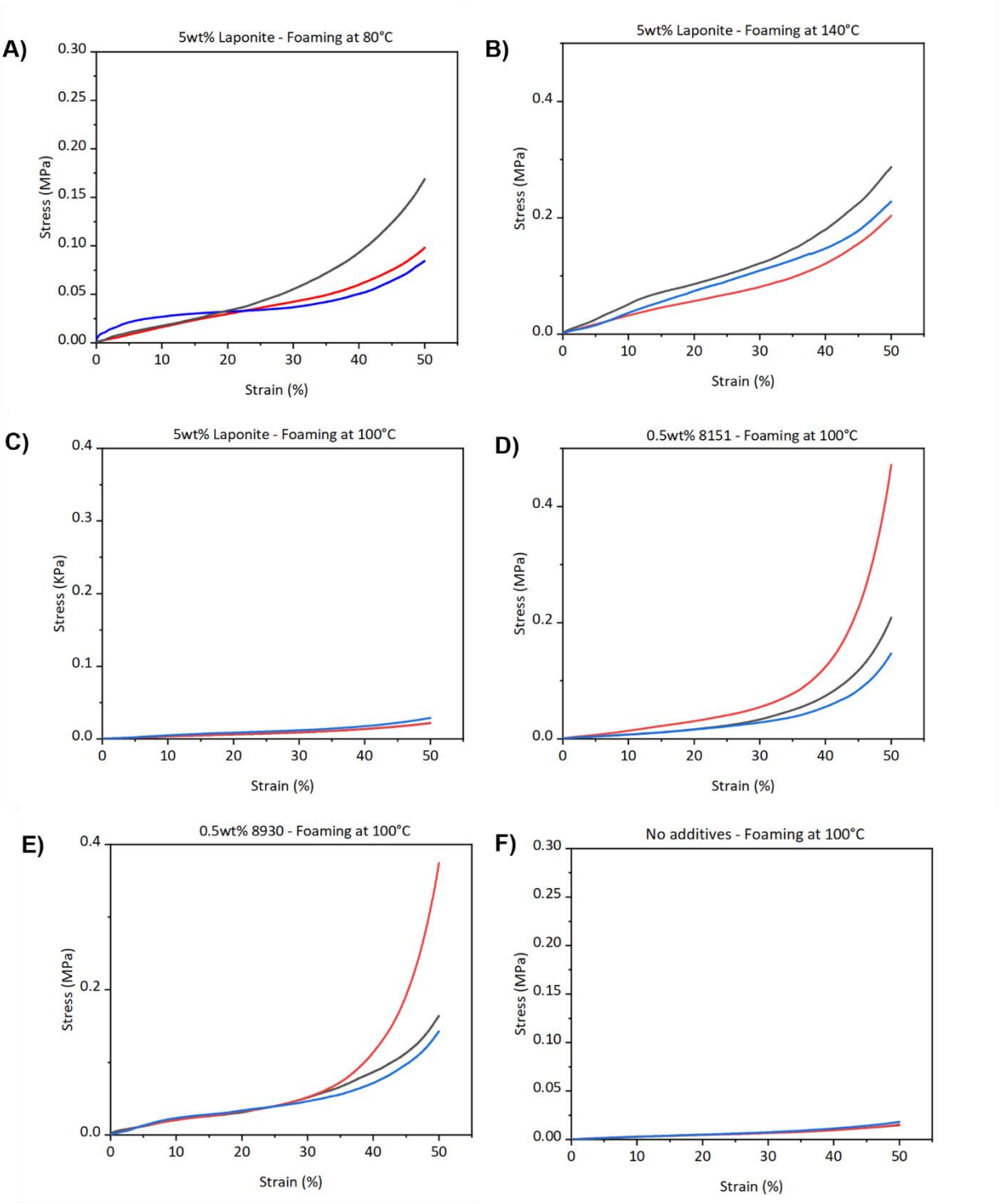

Figure A.IV.6. Compression Stress-Strain curves for the moist foams fabricated using supercritical CO_2 (T= 45°C; P = 10 bar; t = 1h30min): **A)** 5 wt% Laponite, 80°C. **B)** 5 wt% Laponite, 140°C. **C)** 5 wt% Laponite, 100°C. **D)** 0.5 wt% E-8158, 100°C. **E)** 5 wt% Laponite, 100°C. **F)** 0.5 wt% E-8930, 100°C. Conditions: See experimental part (Chapter VIII)

Chapter V

Sustainable production of flame retardant $scCO_2$-blown NIPU Foams

1. Introduction

In Chapter IV, the feasibility of using supercritical carbon dioxide ($scCO_2$) as a sustainable physical blowing agent for NIPU foams was demonstrated, establishing the processing conditions and fundamental parameters required for the successful foam formation. These promising results provide a platform and an interesting opportunity to expand NIPU foams beyond conventional formulations, opening the way to engineer new foams and incorporate additional functionalities directly into the polymer network.

One of the most critical performance limitations about polyurethane foams, both conventional and non-isocyanate based ones, is their high flammability. The development of foams with improved fire resistance is required to expand their potential applications in construction, insulation, and other safety-critical areas. To address this challenge and counterbalance these limitations, reactive flame retardants (RFRs) offer a particularly attractive strategy. Since they are covalently bonded into the network, they avoid migration issues and ensure long-term stability. Among them, phosphorus-based compounds, and especially 9,10-dihydro-oxa-10-phosphaphenanthrene-10-oxide (DOPO) derivatives, have proven to be highly effective in reducing flammability across different thermoset foams. However, their integration in NIPU chemistry has been underexplored.

This chapter builds directly on the $scCO_2$ foaming platform introduced in Chapter IV, extending its application to the development of rigid NIPU foams with flame-retardant properties. A DOPO-containing diamine derived from 4,4′-diaminobenzophenone (DABP) is synthesized in a single step under solvent-free conditions and subsequently employed as a reactive co-monomer, enabling the covalent incorporation of phosphorus into the polymer backbone during network crosslinking and foam formation.

The first part of this chapter investigates the synthesis and reactivity of the DOPO-diamine with five-membered cyclic carbonates, specifically TMPTC, with an emphasis on its selective incorporation into the NIPU network and on proposing the underlying reaction mechanism. **The second part of this chapter** addresses the fabrication of rigid foams under $scCO_2$ batch conditions, using as a reference the formulation established in the previous chapter and incorporating increasing phosphorus loadings up to 2 wt%. The resulting materials are characterized in terms of morphology, density, and gel content. Finally, the flame-retardant performance of the foams is evaluated through thermal stability analyses and fire testing (cone calorimetry and UL-94), providing a comprehensive assessment of their potential as safer and functional alternatives to conventional rigid PU foams.

Overall, this chapter demonstrates how the $scCO_2$ foaming process can be combined with reactive phosphorus-containing monomers to yield rigid, sustainable NIPU foams with enhanced flame-retardant properties, thereby addressing one of the key limitations of NIPU foams and further advancing the strategy of designing NIPU foams with industry-relevant functionalities.

2. Results and discussion

2.1 Synthesis and chemical structure of DOPO-diamine / Reactivity of DOPO-diamine towards 5 membered cyclic carbonate (TMPTC)

Following the strategy outlined in the introduction, the first part of this chapter focuses on the synthesis and reactivity of a DOPO-containing diamine with a 5-membered cyclic carbonate (TMPTC) to determine if the amine can be effectively incorporated into the NIPU network. To this end, the synthesis route and chemical structure of the DOPO-containing diamine were first examined, followed by an investigation of its reactivity towards the five-membered cyclic carbonate, trimethylolpropane triscarbonate (TMPTC). Indeed, this step is crucial to confirm that the DOPO-diamine can act as a co-monomer, playing the role of reactive flame retardant (RFR) and therefore propose the mechanism by which it becomes covalently bonded to the polymer backbone.

The DOPO-diamine was successfully synthesized in bulk under solvent-free conditions at 180 °C for 4 hours via the reaction between 9,10-dihydro-oxa-10-phosphaphenanthrene-10-oxide (DOPO) and 4.4'-diaminobenzophenone (DABP), yielding a phosphorous-containing amine with two primary amine groups. The synthesis route of DOPO-diamine is presented in scheme V.1. The formation of the P-C bond was confirmed by ^{31}P NMR. In this spectrum, the disappearance of the characteristic DOPO chemical shift at 16 ppm and the appearance of the new signals around 31 and 29 ppm (attributed to stereoisomers) indicated the successfully formation of the P-C bond. The corresponding ^{31}P NMR spectra are presented in Figure V.1.A. Complementary TGA analysis further characterized the thermal properties of the molecule. The curves are presented in figure V.1.B. TGA analysis revealed excellent thermal stability with a $Td_5\%$ of 344°C and no significant mass loss below 300°C and the char residue is approximately 20% at 550°C.

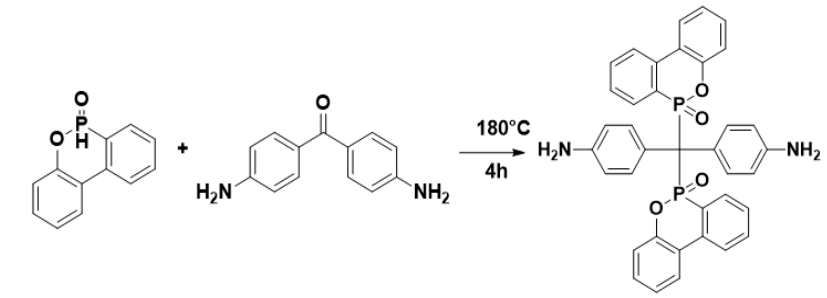

Scheme V.1. Scheme reaction of DOPO-diamine synthesis

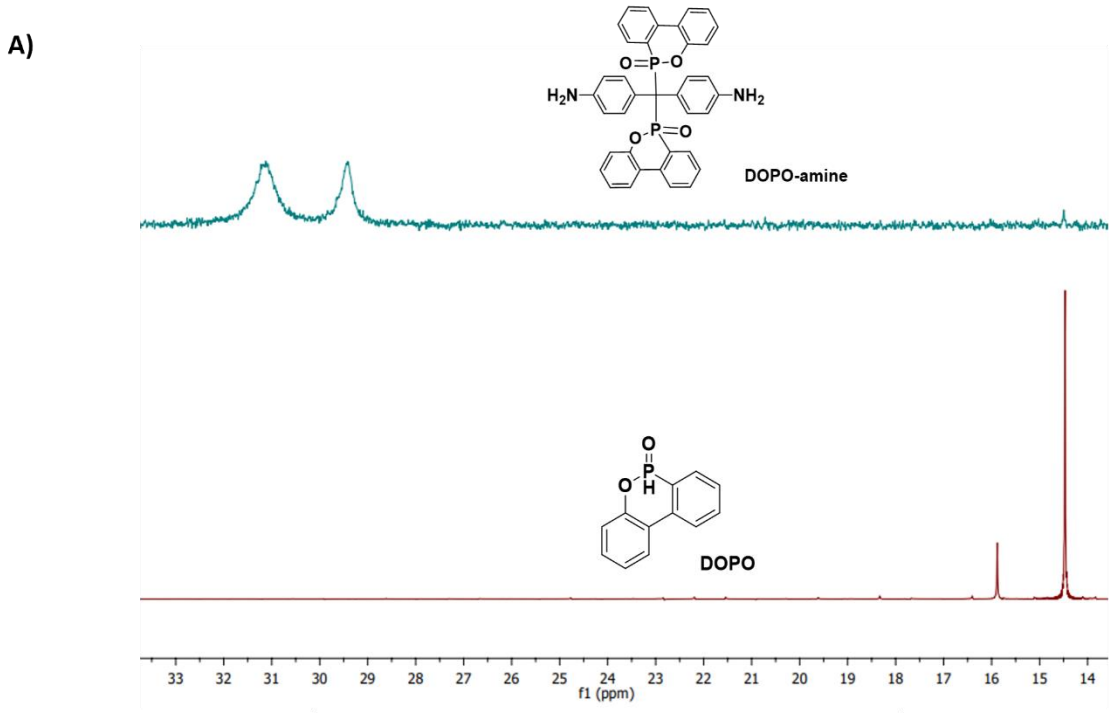

Figure V.1. A) ^{31}P NMR spectra of DOPO-diamine (synthesized) and DOPO. ***B*)** TGA thermogram of DOPO-diamine.

2.2. Reactivity of DOPO-diamine towards 5 membered cyclic carbonate (TMPTC)

Once the DOPO-diamine was characterized in the last section, the next step was to investigate its reactivity with 5-membered cyclic carbonates. DOPO-diamine was reacted with TMPTC under stoichiometric conditions ([CC]/[DOPO-NH_2] = 1). Differential scanning calorimetry (DSC) was employed to study the exothermicity about the reaction between the monomers and a temperature ramp from room temperature to 210°C. The thermogram obtained is shown in Figure V.2B. This study is particularly important to understand the reactivity of TMPTC with DOPO-diamine, given that 5-membered cyclic carbonates are generally characterized by inherently low reactivity. Furthermore, the presence of aromatic ring in the synthesized DOPO-diamine is expected to further reduce its nucleophilicity.

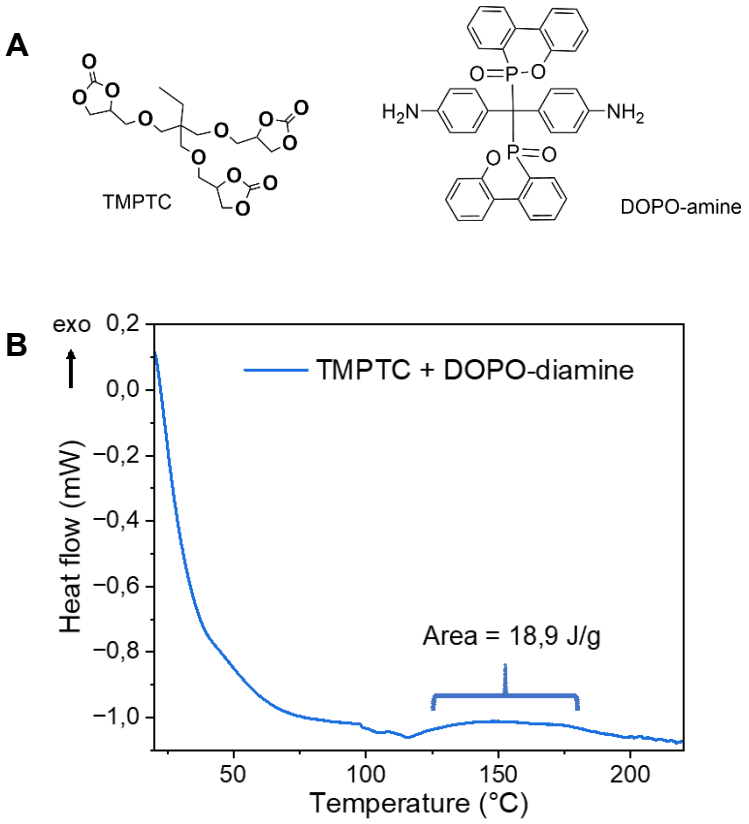

Figure V.2. A) TMPTC and DOPO-diamine chemical structures. **B)** DSC thermogram of the 1st heating ramp showing the exothermic reaction temperature range between TMPTC and DOPO-diamine in stoichiometric ratios of 1/1 from room temperature to 210°C.

From figure V.2.B, an exothermic peak is observed within the temperature range of 120 and 200°C, indicating that the reaction occurs within this temperature interval. Temperature range in which both reagents are thermally stable. This confirmed that the primary amino groups of DOPO-diamine can react with the cyclic carbonate within a temperature window compatible with a subsequent foaming process under $scCO_2$

Based on these findings, a solvent-free reaction was conducted at 180°C for 2 hours with the same stoichiometric ratio equal to 1, ([CC]/[DOPO-NH_2] = 1), expressed in equivalent functional groups. This reaction yielded a brown solid resin with voids and a gel content of 72% (Figure V.3). The chemical structure of the reactive monomers and the resulting material were analyzed by means of FTIR technique. The corresponding FTIR spectra are presented in Figure V.2.B.

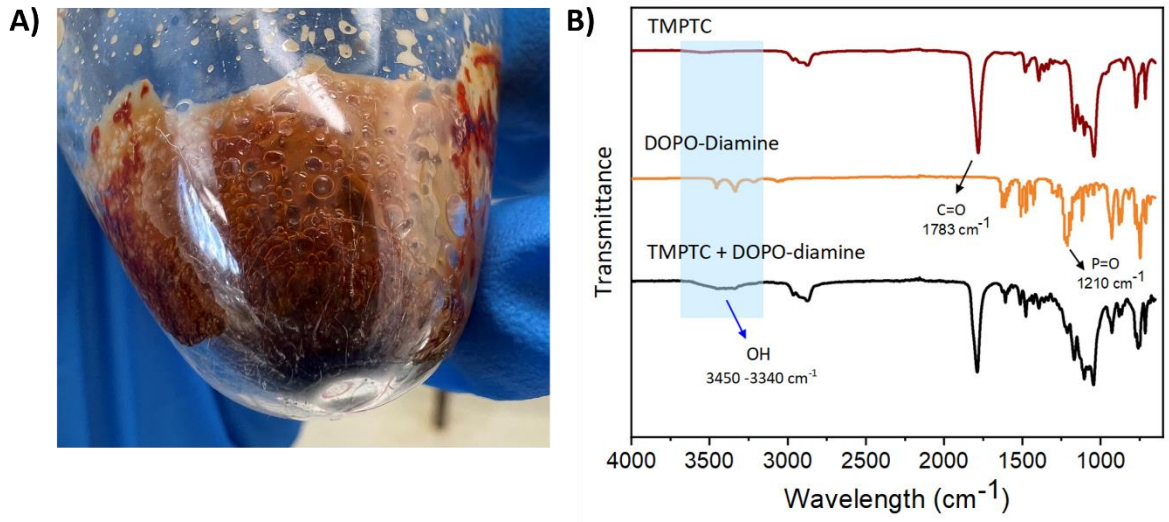

Figure V.3. A) Resulting product from the reaction of the synthesized DOPO-diamine and TMPTC at 180°C in solvent free conditions. **B)** FTIR spectra of the reactive monomers, TMPTC, DOPO-Diamine and the resulting material after reacting in stoichiometric ratio ([CC]/[DOPO- NH_2] = 1) for 2 hours at 180 °C in solvent-free conditions.The blue band corresponds to the are where -OH groups appear after the ring-opening reaction.

Figure V.3.B) illustrates the characteristic peaks of the reactive monomers. The carbonyl group (C=O) band, characteristic of cyclic carbonates in TMPTC, appears at 1780 cm^{-1} , while the peaks at 3300 and 3400 cm^{-1} correspond the primary amines (NH_2) vibrations, and the phosphoryl group (P=O) band at 1280 cm^{-1} in DOPO-Diamine. 5-membered cyclic carbonates,

similar to dialkylcarbonates, contain two electrophilic sites: i) the carbonyl group and ii) the methylene carbons. These electrophilic centers can react selectively depending on the nucleophile's nature (soft or hard).[243] Thiols and aromatic amines, such as DABP, are considered as soft nucleophiles, and thus preferentially attack the methylene carbons in five-membered cyclic carbonates, releasing CO_2 as by-product.[146]

In agreement with this mechanism, the FTIR spectrum of the resulting resin (TMPTC+DOPO-diamine) exhibits a characteristic alcohol band between 3330 and 3450 cm^{-1}, indicating the decarboxylation of TMPTC by DOPO-diamine. Notably, no band appears at around 1700 cm^{-1} which would correspond to the formation of urethane groups, further supporting the selective methylene attack of soft nucleophiles. The proposed mechanism reaction is represented in scheme V.2. In the initial step, the primary amine from DOPO-diamine attacks the non-substituted position of the 5-membered cyclic carbonate, leading to the decarboxylation of the cyclic carbonate and the subsequent release of CO_2.

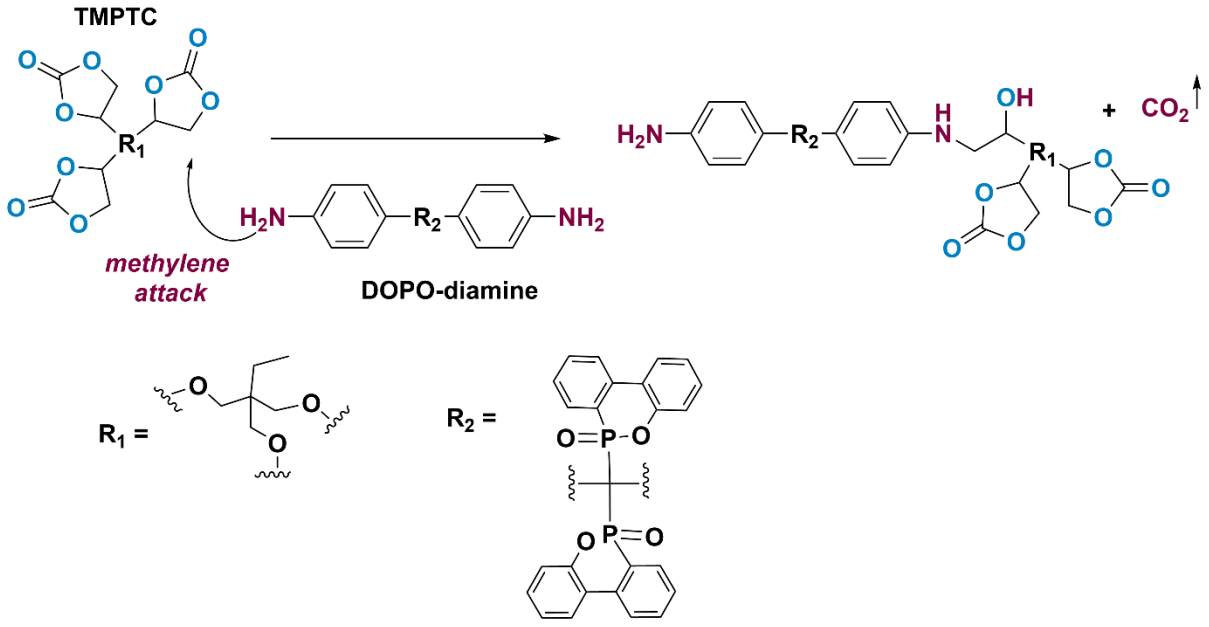

Scheme V.2. Proposed reaction mechanism for the attack of DOPO-diamine on 5-membered cyclic carbonate TMPTC.

Therefore, DOPO-diamine can effectively react with 5-membered cyclic carbonates like TMPTC, confirming its suitability as a co-curing monomer for the synthesis of NIPUs (Non-isocyanate polyurethanes). This reaction enables DOPO-diamine to become covalently bonded within the polymer network, ensuring the integration of the flame-retardant functionality.

2.3. NIPU Foam preparation with DOPO-diamine using supercritical CO_2 as blowing agent

After confirming the ability of DOPO-diamine to react selectively with 5-membered cyclic carbonates like TMPTC, the next step was to investigate its incorporation into foam formulations. In this second part of the chapter, rigid NIPU foams were prepared by introducing DOPO-diamine as a reactive co-monomer within the $scCO_2$ foaming platform as established in the previous chapter. This new step would validate the covalent integration of the DOPO-diamine into the foams and also evaluate the influence on morphology, density, crosslinking and ultimately fire performance.

To this end, a series of rigid NIPU foams incorporating the DOPO-diamine as a co-curing monomer was fabricated using the optimized formulation established in the previous chapter. Two 5-membered cyclic carbonates and two amines were employed. A mixture of a triscarbonate trimethylolpropane triscarbonate (TMPTC), and a bi(cyclic carbonate), poly(propylene oxide) biscarbonate (PPOBC), was used in a mass fraction between the cyclic carbonates of 80/20 (TMPTC/PPOBC) (Figure V.4.).

This cyclic carbonate mixture was reacted with a combination of two primary amines, m-xylylenediamine (MXDA) and DOPO-diamine, using the following ratio: [TMPTC +

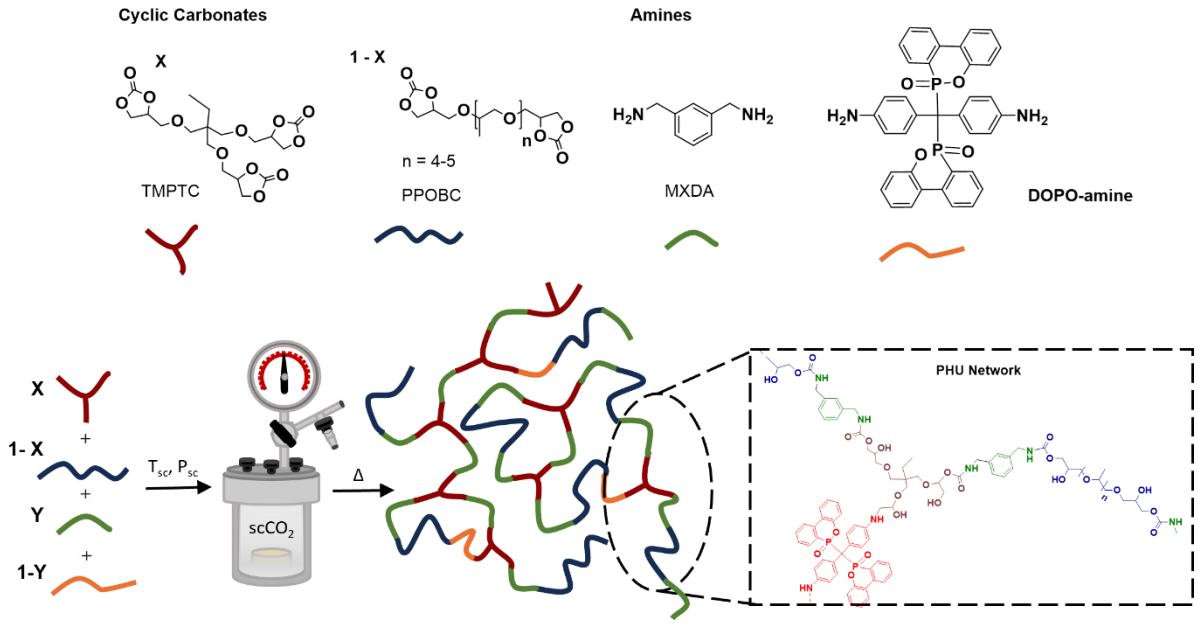

Figure V.4. Chemical structure of the reactive monomers used to fabricate NIPU Foams under $scCO_2$ conditions in batch mode and schematic representation of the resulting thermosetting network. Conditions for $scCO_2$ saturation: T_{sc}= 45°C ; P_{sc}= 100 bar and saturated for 90 min.

PPOBC]/[MXDA + DOPO-diamine] = 1/1, expressed in equivalent functional groups. The MXDA/DOPO-diamine ratio was adjusted to achieve varying phosphorous content in the final formulation. Three foams were fabricated, each containing phosphorous at levels of 0.5, 1 and 2 wt% and one foam without any phosphorous content.

The NIPU Foams were fabricated using supercritical CO_2 as physical blowing agent. The reactive monomers mixtures were saturated under supercritical CO_2 at T_{sc} = 45°C and P_{sc} = 100 bar for 90 minutes and then the CO_2-saturated sample was foamed at moderate temperature 100°C for 3 hours and post-cured for 2 hours at 180°C.

NIPU foams containing the phosphorous-amine (DOPO-diamine) were successfully synthesized and the obtained foams are observed in Figure V.5. The morphological structure of the foams and cell size were determined by optical microscope and Scanning electron microscopy (SEM). All foams present mostly spherical closed pores with slightly open pores. The cell size of the foams is summarized in table V.1. Overall, the cell size of the NIPU foams exhibits slight variations across the different formulations with varying phosphorous content, ranging from 0.32 ± 0.18 to 0.48 ± 0.29 mm. The NIPU Foam synthesized without DOPO-diamine, entry 1, presents a cell size average of 0.42 ± 0.25 mm. The foams containing 0.5 wt% and 2 wt% phosphorus (entries 2 and 4, respectively) exhibit the same average cell size range, measuring 0.48 ± 0.25 mm and 0.48 ± 0.29 mm, respectively. In contrast, the foam containing 1 wt% phosphorus shows a smaller average cell size of 0.32 ± 0.18 mm. Notably, these foams present a wide range of pore dispersion, which can be attributed to the absence of surfactants or additives that would have otherwise enhanced the homogeneity of the foam morphology and the viscosity change when DOPO-diamine is added into the formulation. The density of the foams was also determined and are presented in table V.1. The density of the foams ranges from 0.274 to 0.217 $g.cm^{-3}$. Entry 1, foam without DOPO-diamine, presents the highest density value of the series, 0.274 $g.cm^{-3}$. Upon incorporation of DOPO-diamine to the formulations, a slight decrease in density is observed. The densities of the foams containing 0.5, 1 and 2wt% phosphorus (entries 2, 3 and 4 respectively) are 0.217, 0.242 and 0.228 $g.cm^{3}$. The overall reduction in density could be attributed to the decarboxylation of the cyclic carbonate by DOPO-diamine, resulting in increased CO_2 release.

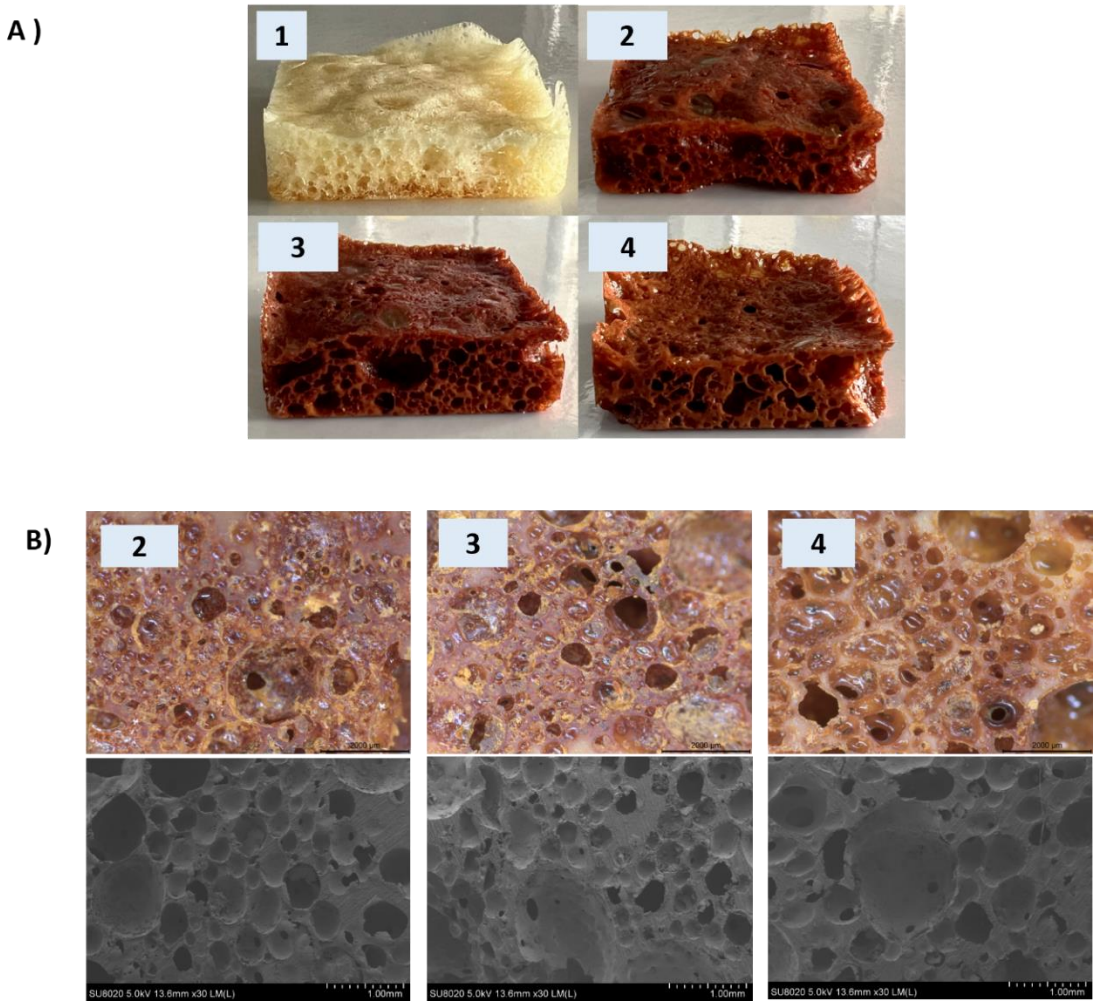

Figure V.5. A) NIPU Foams synthesized under supercritical CO_2 with DOPO-Diamine with different Phosphorous content. B) Optical microscope pictures and SEM images from the NIPU foams synthesized with 0.5, 1 and 2wt% Phosphorous. Conditions: All foams were saturated under $scCO_2$ for 1h30min at Tsc: 45°C and Psc: 100 bar in the reactor.

Consequently, the gel content was measured to check the crosslinking content and determine whether the DOPO-diamine was covalently bonded into the polymer network. The results, summarized in table V.1, demonstrate the effective crosslinking network, with gel contents exceeding 90%. Specifically, entries 2,3 and 4 exhibit values of 92, 94, 93%, respectively. The chemical structure of the NIPU foams was analyzed by FTIR. The spectra are shown in figure V.6. The urethane group formation is confirmed by the presence of the characteristic bands at 1689 cm^{-1}. Despite the high gel content values and conversion of the cyclic carbonate, a small residue peak at 1792 cm^{-1} is observed. This small peak has been previously reported in the literature. It could be attributed to the formation of the hydrogen bonds and due to the functional groups blocked within the polymer matrix. [99,244]

Table V.1. NIPU Foaming conditions and formulations, with morphological characterization of various foams with differing phosphorous content

Entry	Phosphorous content (wt.%)	Foaming temperature (°C)/ Time	Density ($g.cm^{-3}$)	Cell size (mm)	Gel content (%)
1	0% Control	100°C/3h	0.274	0.42 ± 0.26	90
2	0.5wt% P	100°C/3h +180°C/2h	0.217	0.48 ± 0.25	92
3	1wt % P	100°C/3h +180°C/2h	0.242	0.32 ± 0.18	94
4	2wt% P	100°C/3h +180°C/2h	0.228	0.480 ± 29	93

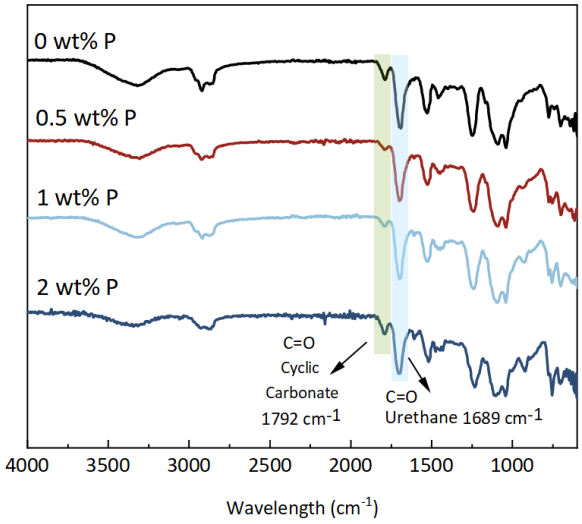

Figure V.6. FTIR spectra of NIPU foams synthesized under $scCO_2$ in a batch process with varying content of Phosphorous (0.5, 1 and 2wt% P). **Conditions:** All foams were saturated under scCO2 for 1h30min at T_{sc}= 45°C and P_{sc}= 100 bar. Foams containing 0.5, 1 and 2wt% P were foamed at 100 °C for 3 hours and then at 180°C for 2 hours. Foam without phosphorous was foamed for 3 hours at 100 °C.

2.3.1 Thermal properties

Thermal properties were also investigated to study the influence of DOPO-diamine on the NIPU foam formulations. Firstly, the glass transition temperature (T_g) of the foams containing varying phosphorous content was measured by means of DSC and the results are summarized in Table V.2 and the DSC thermograms are shown in Figure V.7. A clear effect of the DOPO-diamine is observed on the glass transition temperature. When DOPO-diamine is incorporated into the NIPU formulations, the T_g increased due to the aromaticity present in the DOPO-diamine which impart rigidity to the final polymeric material. The T_g increases by at least 10°C from Entry 1 (foam without DOPO-diamine, characterized in Chapter IV) to entry 4, foam containing 2 wt% of phosphorous. Specifically, Entry 2, 3 and 4 (0.5, 1 and 2 wt% phosphorous, respectively) exhibit T_{gs} of 50, 51 and 47 °C.

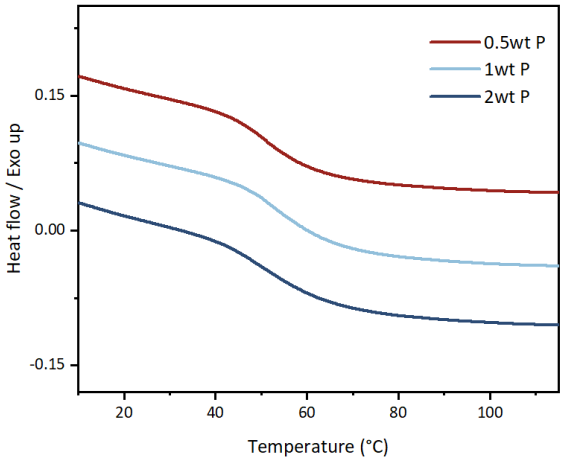

Figure V. 7. DSC Thermograms of the synthesized foams with different wt% P using supercritical CO_2 (T= 45°C; P = 100 bar; t = 1h30min) and inducing foaming at 100°C for 3 hours and 180°C for 2 hours.

Thermogravimetric analyses were also conducted under nitrogen atmosphere to determine the thermal decomposition behaviour of the NIPU foams containing DOPO-diamine. The main thermal parameters, such as thermal degradation temperature at 5% weight loss ($T_{d5\%}$), thermal degradation at 50% weight loss ($T_{d50\%}$), temperature at the maximum of the TG derivatives ($T_{d\,max}$) and the residual yield (Y_c) at 800°C are summarized in Table V.2.

The incorporation of DOPO-diamine significantly improved the thermal stability of the foams. In particular, when comparing ebtre 1 and entry 4 (2%wt), it is observed that the the thermal degradation temperature at 5wt% of weight loss ($T_{d5\%}$) increased by 46°C), rising from 252°C

for the phosphorous-free foam (Entry 1) to 298°C. All phosphorus-containing formulations exhibited comparable $Td_5\%$ values, ranging between 296 and 299°C. A similar trend was observed for the thermal degradation temperature at 50% of weight loss ($T_{d50\%}$), which increased by 36°C upon incorporating DOPO-diamine into the formulation with 1wt% of phosphorous content (Entry 3). In general, foams containing phosphorous displayed $T_{d50\%}$ values in the range of 387-395°C.

Figure V.8B shows the decomposition steps for the foams. Entries 1 and 2 exhibit double $T_{d\ max}$ peaks and entries 3 and 4 present triple peaks. The temperatures at the maxima of the TG derivatives were 300 and 362°C for entry 1, and 321 and 385°C for Entry 2. Entry 3 exhibits three distinct peaks at 316, 377 and 496°C, while Entry 4 has three peaks at 319, 381 and 500°C. This behaviour of double and triple peaks has been previously reported for NIPU and PU foams.[143] Overall, the addition of DOPO-diamine enhances the stability of the NIPU foams, as evidenced by the increased $T_{d5\%}$,$T_{d50\%}$ and T_{dmax} values in the formulations with phosphorus.

The residual yield at 800°C of the phosphorous-free foam (Entry 1) is 16% in contrast to the phosphorous containing foams, which exhibit 18% of char formation for entries 2 and 3 (0.5 and 1wt%), and 19% for entry 4 (with 2wt% P). The char formation increased by only 2-3% upon the addition of phosphorous. DOPO-diamine contains aromatic rings that may have contributed to the slight improvement in char formation. However, it is well established that DOPO, a phosphorous-based flame-retardant molecule, primarily acts in the gas phase and is a weak promoter of char formation.[245]

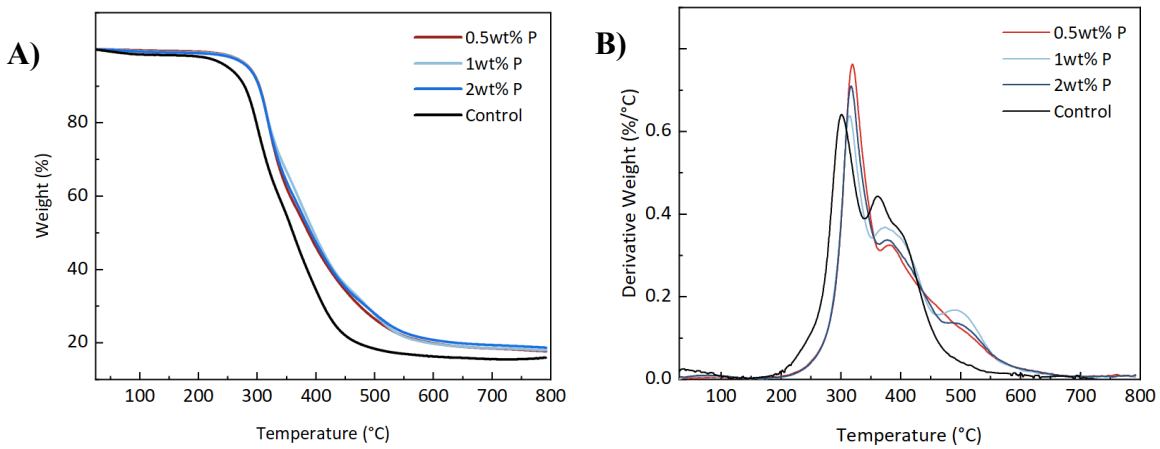

Figure 8. **A)** TGA **B)** DTG curves of the NIPU foams containing different phosphorous content.

Table V.2. Thermal characteristics of the NIPU foams synthesized containing different amounts of phosphorous.

Entry	Phosphorous content (wt%)	T_g (°C)	$T_{d5\%}$ [a]	$T_{d50\%}$ [a]	$T_{dmax\%}$ [a]	Y_c at 800°C (%) [a]
1	0% Control	37	252	359	300 and 362	16
2	0.5wt% P	50	299	387	321 and 385	18
3	1wt % P	51	296	395	316; 377 and 496	18
4	2wt% P	47	298	390	319; 381 and 500	19

[a] Under nitrogen atmosphere – $T_{d\,max}$ read on the TG derivatives

2.4. Flame retardant properties of NIPU foams

In the last part of this chapter, the flame-retardant properties were evaluated and cone calorimetry tests were performed to study the fire behaviour of the NIPU Foam materials, particularly to evaluate the influence of the phosphorus-based molecule on their flame-retardant properties. The results are summarized in table V.3. The heat release rate (HRR) *vs.* time curves is presented in Figure V.7. The parameters studied in this section include time to ignition (TTI), peak of heat release (pHRR), average of heat release (average HRR) and total heat release (THR) the parameters studied in this section.

Overall, the time to ignition (TTI) was not significantly improved by the addition of Phosphorous, remaining in the range of 9-11 seconds for all NIPU foams. As shown in Figure V.7, the peak of heat release rate (pHRR) of all the materials is within the range of 245 – 177 kW.m-^{2}. The highest peak heat release rate (pHRR) of 245 kW.m-^{2} is observed for the NIPU foam without any content of phosphorous (Entry 1). This value decreases significantly to 181 kW.m-^{2} when 2 wt% phosphorous was incorporated into the NIPU foam formulation (Entry 4). For Entries 2 and 3, which contain 1 and 2wt% phosphorus, respectively, the pHRR ranges between 177 and 179 kW.m-^{2}.

The HRR *vs.* Time curves exhibit a similar trend for all the NIPU foams. Initially, the HRR increases rapidly, accompanied by a high release of heat over a short period. This is followed

by an abrupt decrease in heat release. This behaviour provides insight into the predominant flame retardant mechanism. Flame retardants typically operate through two primary mechanisms: condensed phase action, which involves char formation that creates a protective thermal barrier on the material surface, thereby insulating the underlying polymer and sustaining a prolonged phase of low heat release; and gas phase action, which involves the release of active species that interrupt the combustion chemistry in the flame zone. The absence of significant char residue in the DOPO-containing foams, combined with the sharp HRR profile, suggests that DOPO-diamine predominantly functions through a gas phase mechanism. In this mode, phosphorus-containing radicals (such as PO• and HPO•) are released upon thermal decomposition and act as radical scavengers, quenching the highly reactive H• and OH• radicals that propagate the combustion chain reaction. This interruption of the radical chain mechanism effectively reduces the flame intensity, even without the formation of a substantial protective char layer.[178,246,247]

The avgHRR for the phosphorous-free NIPU foam (entry 1) is 150 kW,m- ^{2}. A significant reduction is observed with the addition of phosphorous, reducing to 110, 90 and 80 kW.m^{-2} for Entries 2, 3 and 4, respectively. Regarding the THR, the foam without any DOPO-diamine (Entry 1) exhibits a total heat release of 35 MJ.m^{-2}. A decrease in THR is also evidenced for foams containing phosphorous, except for Entry 2, which remains in the same range (39 MJ.m^{-2}) as Entry 2. For Entries 3 and 4, the THR is strongly reduced to 13 and 12 MJ.m^{-2}, respectively. In Figure V.7.B, the residual foam material after the cone calorimetry test is presented. In accordance with TGA results, some char formation is observed for all foams.

Table V.3. Results of the cone calorimetry test performed on the NIPU foams synthesized by supercritical CO_2 conditions containing 0.5, 1 and 2wt% of phosphorous

Entry	Phosphorous content (wt%)	TTI (s)	pHRR [KW.m^{-2}]	Average HRR [KW.m^{-2}]	THR [MJ.m^{-2}]
1	0	11	245	150	35
2	0.5	9	177	110	39
3	1	10	179	90	13
4	2	11	181	80	12

The residual foam materials were also analyzed using SEM-EDX to determine their elemental composition. This elemental analysis provides insights into the flame-retardant mechanism and the surface chemistry of each foam. The composition in terms of C, O, N and P is presented in table 4. For all foams, carbon was the predominant element in the residue, followed by oxygen, nitrogen and phosphorous. The EDX analysis indicates that Entries 2, 3 and 4 contain residual phosphorous contents of 7, 1 and 4wt%, respectively. Based on the char formation from TGA curves (Table V.2), the fraction of phosphorous retained in the residue can be roughly estimated. For Entries 3 and 4, the majority of the phosphorous is released into the gas phase, with only 18 and 24 wt% of the initial phosphorous remaining in the residual mass. In contrast, Entry 2 shows an enrichment of the phosphorous in the residual mass. Overall, given the low char formation (Y_c), the low phosphorous retention in Entries 3 and 4, and the HRR curves of all foams, it could be inferred that the DOPO-diamine exhibits limited efficiency as char promotor and primarily acts in the gas phase.

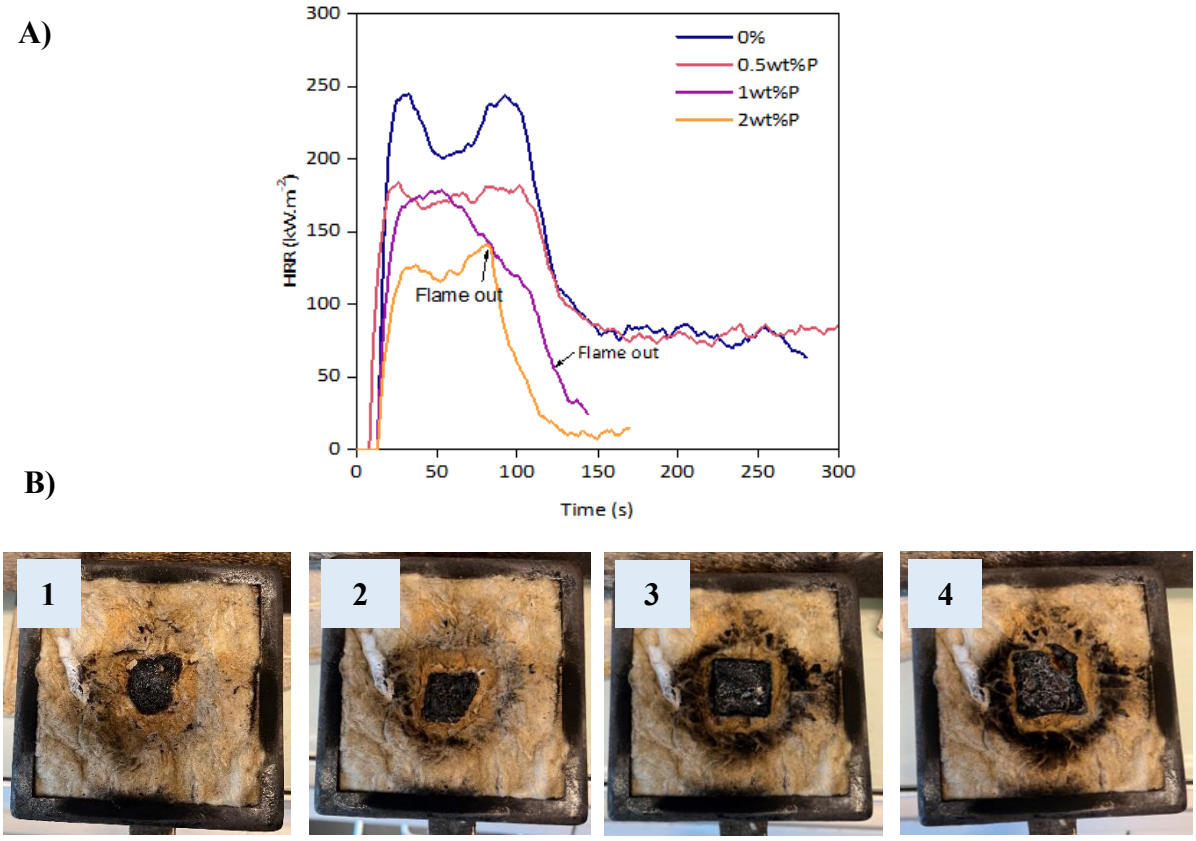

Figure V.9. A) HRR curves of the NIPU foams in cone calorimeter (33 kW/m^2) . B) Residual aspects of the foams after performing cone calorimetry tests.

Table V.4. Elemental analysis of the NIPU foam residual mass

Entry	C (%)	N (%)	O (%)	P (%)
1	64	15	20	-
2	47	8	35	7
3	64	13	19	1
4	60	11	25	4

The UL94 rating is one of the most widely used fire tests for evaluating the relative flammability of plastic materials. In this test, a specimen is held vertically while a burner flame is applied to its lower edge for 10 seconds; after removal, the after flame time (t_1) is recorded until self-extinguishment, then a second 10-second flame application is performed and the after flame time (t_2) is again recorded. Additionally, any occurrence of flaming drips that ignite the cotton indicator placed below the specimen is noted. The classification (V-0, V-1, V-2, or Not Rated) is assigned based on afterflame times, total combustion time, and dripping behaviour.Therefore, this test was performed to analyse the flammability behaviour of the different NIPU foams with varying phosphorous content. The UL 94 classification is presented in Table V.5. The flammability behaviour of each sample after 2 consecutive 10-second flame applications is presented in Figure V.10. Entry 1, NIPU foam without phosphorous content is not rated due to its prolonged flammability (>40 s). Entry 2, the foam containing 0.5 wt% phosphorus, achieves a V-1 classification due to its moderate combustion time (30 s) after the first flame application and the absence of dripping. Entries 3 and 4, containing 1 wt% and 2 wt% phosphorus, respectively, exhibit excellent flame-retardant properties due to their self-extinguishing behavior. They extinguish after just 1 and 2 seconds, respectively. Even after the second flame application, Entry 3 extinguishes within 2 seconds, while Entry 4 does not ignite at all. These foams are classified as V-0.

Table V.5. UL 94 test results of all NIPU foams

Entry	Phosphorous content (wt%)	Rating	Dripping/Cotton ignition	t_1/t_2 (s)
1	0	NC	N	>40
2	0.5	V-1	N	30/5
3	1	V-0	N	1/2
4	2	V-0	N	1/0

These preliminary results, obtained using small disc-shaped specimens, represent a promising step towards flame-retardant NIPU foam applications. Although further testing with standardized specimen geometries is required to confirm the classification, the observed self-extinguishing behaviour at phosphorus contents as low as 1 wt% suggests potential for this approach. To the best of our knowledge, such rapid flame extinction leading to potential V-0 classification has not been previously reported for NIPU foams, which are typically highly flammable without additives.[248] Moreover, conventional isocyanate-based polyurethane foams generally require 7.5–25 wt% of flame retardant additives to achieve UL-94 V-0 ratings.[249] These findings suggest that the reactive DOPO-diamine approach holds significant potential for developing flame-retardant NIPU foams suitable for construction and insulation applications, warranting further investigation under standardized testing conditions."

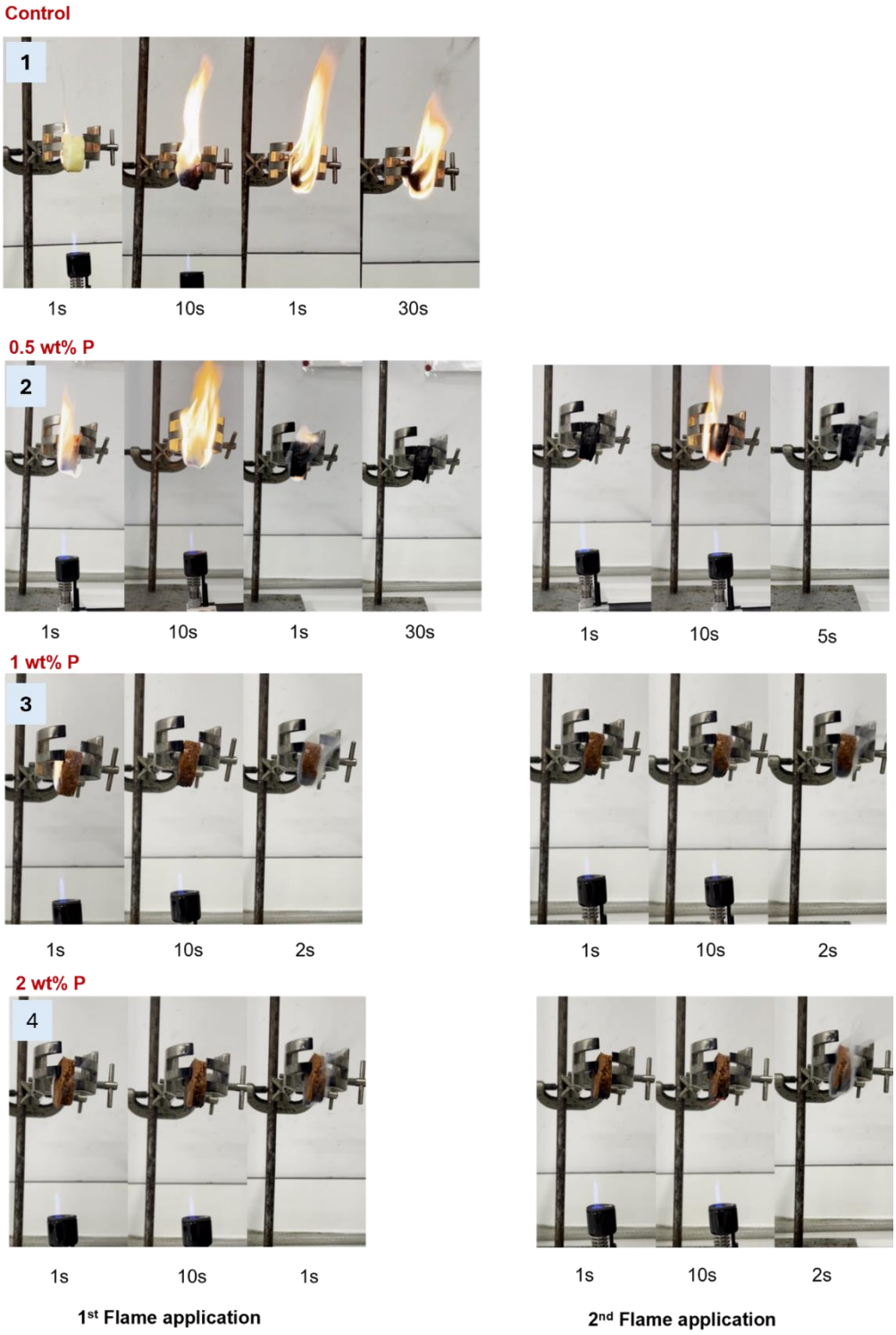

Figure V.10. Results of UL 94 rating

3. Conclusions

In conclusion, a phosphorus-based amine molecule, DOPO-diamine, was successfully synthesized to employ it as a co-curing flame-retardant monomer for the production of Non-Isocyanate Polyurethane Foams using supercritical CO_2 as physical blowing agent. In the first part of the chapter, the reactivity of DOPO-diamine toward the 5-membered cyclic carbonate, TMPTC, was studied by differential scanning calorimetry (DSC). The DSC thermogram showed that the exothermic reaction occurred within a temperature range of 120–200°C. The reaction between TMPTC and DOPO-diamine at high temperatures revealed that DOPO-diamine behaves as a soft nucleophile, promoting the decarboxylation of the 5-membered cyclic carbonate via a methylene attack.

In the second part of the chapter, DOPO-diamine was incorporated as a co-monomer into the NIPU formulation to achieve different phosphorous contents (0.5, 1 and 2wt%). Four different NIPU foams were successfully fabricated by using supercritical CO_2 as a physical blowing agent. The covalent bonding of the phosphorous-based co-monomer was confirmed by the high gel content values (>92%). The morphological and physical properties of the foams were characterized. In general, varying phosphorous content slightly decreased the foam density while increasing the cell size in comparison to the phosphorous-free foam. Moreover, the T_g of the foams increased by approximately 12°C in all formulations due to the presence of aromatic rings in DOPO-diamine.

Finally, in the last part of this chapter, the thermal and fire behavior of the cellular materials were analyzed employing TGA, cone calorimetry and the UL94 rating. All the DOPO-diamine foams exhibited better thermal stability, with a slight increase in the char formation compared to the DOPO-free foam. The incorporation of DOPO-diamine led to a 66% reduction in total heat release (THR) and achieved a V-0 rating in the UL-94 test when the phosphorous content was 1 and 2wt% compared to the DOPO-diamine free foam. These results demonstrate the effectiveness of DOPO-diamine-crafted NIPU foams in enhancing flame retardancy. Furthermore, this approach provides new insights into the development of advanced foam applications.

Appendix A.V

Tables

Table A.V.1. Formulations of the synthesized NIPU foams with different phosphorous content.

	Formulation		
Monomers	**0.5 wt% P**	**1 wt% P**	**2 wt% P**
TMPTC	1.41 g	1.48 g	1.68 g
PPOBC	0.43 g	0.54 g	0.51 g
MXDA	0.60 g	0.60 g	0.60 g
DOPO-Diamine	0.14 g	0.280 g	0.68 g

Chapter VI

Water-blown NIPU foams reinforced with bio-based nano-particles

1. Introduction

In Chapters IV and V, the feasibility of using supercritical carbon dioxide ($scCO_2$) as a sustainable physical blowing agent for the fabrication of thermosetting NIPU foams was demonstrated. The processing conditions, fundamental parameters, and functionalization strategies through reactive flame retardants were successfully established, providing a solid platform for the development of rigid NIPU foams with enhanced properties. These promising results opened new avenues to explore alternative foaming strategies and expand the scope of NIPU foam technology towards more sustainable and industrially relevant formulations.

Building upon the knowledge acquired from rigid foam fabrication, this chapter introduces an additional layer of complexity by targeting the development of flexible NIPU foams. While rigid foams find applications primarily in thermal insulation and structural components, flexible foams represent a significantly larger market segment, valued at approximately USD 5.91 billion in 2024 and projected to reach USD 10.86 billion by 2030, with diverse applications including cushioning, packaging, automotive interiors, and biomedical devices.[3] Expanding the NIPU foam portfolio to include flexible formulations is therefore essential to broaden their industrial relevance and potential for replacing conventional isocyanate-based polyurethane foams across multiple sectors.

However, the transition from rigid to flexible foams poses significant challenges in terms of monomer reactivity and formulation design. Flexible foams require lower crosslinking densities and the incorporation of soft segments to achieve the desired mechanical response, which must be carefully balanced with the foaming kinetics to ensure successful cell formation and stabilization. The inherently slow reactivity of five-membered cyclic carbonates, as established by Cornille et al.[78] and Tomita et al.[250], while being advantageous for processing rigid thermosets, becomes a critical factor when designing flexible systems where network formation must be precisely synchronized with gas generation. This challenge is further compounded when using water as a chemical blowing agent. As demonstrated by Bourguignon et al.,[17] water reacts with cyclic carbonates under basic conditions to generate CO_2 in situ, competing with the amine curing agent for reaction with the cyclic carbonate groups, effectively altering both the crosslinking kinetics and the final network architecture.

While $scCO_2$ foaming offers significant advantages in terms of environmental impact and process control, chemical blowing agents (CBAs) remain widely employed in industrial foam production due to their simplicity and lower equipment requirements. Among CBAs, water

represents a particularly attractive option for NIPU systems, as its reaction with cyclic carbonates generates CO_2 *in situ* while simultaneously participating in network formation. [17,251] This dual role of water as both blowing agent and reactive component offers unique opportunities for process design and property optimization, albeit requiring careful control to achieve the desired foam characteristics.

Beyond the choice of blowing agent, the incorporation of renewable nano-particles into polymer foams has emerged as a promising strategy to enhance mechanical performance while maintaining sustainability principles. Chitin and cellulose nanoparticles, derived from abundant natural sources, offer exceptional reinforcement potential due to their high aspect ratio, mechanical strength, and surface functionality, [252,253] as well as their abundant availability in nature. Recent studies have demonstrated that CNCs can provide up to threefold improvement in mechanical strength when incorporated into rigid NIPU foams.[254]

However, while bio-based nanoparticles have demonstrated significant reinforcing effects in conventional polymer matrices, including traditional polyurethanes, their behavior in poly(hydroxyurethane) systems remains largely unexplored. The unique chemical structure of PHUs, characterized by pendant hydroxyl groups capable of extensive hydrogen bonding, may lead to fundamentally different matrix-filler interactions compared to conventional polymers. Whether bio-nanofillers would provide reinforcement, remain inert, or even disrupt the PHU network through competitive hydrogen bonding has not been systematically investigated. For this reason, throughout this chapter we deliberately adopt the term "bio-nanofillers" rather than "bio-reinforcements", as the latter would presuppose a mechanical enhancement that cannot be assumed *a priori* in PHU systems.

Recently, Trojanowska et al.,[251] demonstrated that moisture-containing biofillers can serve as water reservoirs for self-foaming NIPU formulations, exploiting the in-situ hydrolysis of cyclic carbonates to generate CO_2. Their study employed micro-scale fillers (microcrystalline cellulose, proteins, chitosan) primarily as foaming promoters rather than structural reinforcements, and reported minimal influence on the glass transition temperature of the resulting rigid foams. The incorporation of true nanoscale bio-based particules, with their significantly higher specific surface area and enhanced potential for matrix-filler interactions, into water-blown flexible NIPU foams, and their consequent effects on foam properties, has not been reported.

This chapter presents a systematic investigation of the effects of bio-based nanofillers on the structure and properties of water-blown flexible NIPU foams. Rather than assuming reinforcement, this work aims to elucidate the nature of matrix-nanofiller interactions in flexible PHU systems. Chitin nanocrystals (Ch-NC), chitin nanofibers (Ch-NF), and cellulose nanofibers (C-NF) are incorporated at varying concentrations (0.5, 1, and 2 wt%) to evaluate: (i) whether nanoscale bio-fillers can provide reinforcement in flexible PHU matrices; (ii) how nanoparticle morphology (crystals vs. fibers) and surface chemistry (chitin vs. cellulose) influence foam properties; and (iii) the underlying mechanisms governing matrix-nanofiller interactions. Inorganic fillers (Laponite and $CaCO_3$) are included as benchmarks for comparison.

The first part of this chapter focuses on the formulation optimization and rheological characterization of the reactive system. The selection of monomers, particularly the use of liquid m-xylylenediamine (MXDA), is discussed in terms of its importance for achieving adequate dispersion of the nano-particles. Rheological measurements are conducted to investigate the influence of water content on gel point and viscosity evolution, establishing the processing window for successful foam formation. The effect of a pre-curing step on viscosity build-up is also examined as a strategy to prevent cell collapse during foaming.

The second part of this chapter addresses the fabrication and characterization of water-blown NIPU foams with varying water content. The morphology, density, and thermal properties of the resulting foams are evaluated to identify the optimal water concentration for subsequent filler incorporation.

The third part of this chapter presents the systematic incorporation of bio-based nano-particles and inorganic fillers into the optimized foam formulation. Chitin nanocrystals, chitin nanofibers, and cellulose nanofibers are incorporated at concentrations of 0.5, 1, and 2 wt%, while Laponite and $CaCO_3$ are evaluated at 5 wt%. The resulting foams are comprehensively characterized in terms of morphology, gel content, density, thermal stability, and mechanical properties under both dry and humid conditions. Finally, water uptake behavior is investigated to assess the hygroscopic nature of the modified foams.

2. Results and Discussion

2.1. Formulation design and monomer selection

The formulation strategy for water-blown flexible NIPU foams was designed considering two main requirements: (i) achieving adequate reactivity at moderate temperatures to enable CO_2 generation and network formation while maintaining sufficient flexibility in the final foam, and (ii) ensuring the dispersion of the nano-particles within the reactive mixture. To meet these objectives, trimethylolpropane triscarbonate (TMPTC) was selected as the primary cyclic carbonate monomer due to its trifunctionality and demonstrated reactivity in previous chapters. Another cyclic carbonate, EO-TMPTC, was also synthesized to introduce flexible segments into the network, which is essential for achieving the desired flexible foam characteristics.

The choice of amine curing agent was particularly critical for this study. m-Xylylenediamine (MXDA) was selected as the primary amine due to its liquid state at room temperature, which facilitates the homogeneous dispersion of nano-particles prior to mixing with the cyclic carbonate. This is in contrast to solid amines that would require dissolution in solvents, potentially compromising the foaming process and final material properties. Furthermore, MXDA has demonstrated suitable reactivity with five-membered cyclic carbonates, as established in Chapters IV and V, while its aromatic character provides a balance between reactivity and final material properties. Prior to this final formulation, different amines were tested, however, the lower reactivity limited their utilization. Some of the amines that were tested were: TMPTAE, D2000, Jeffamine D600 and Jeffamine D900.The formulation used is presented in Figure VI.1.

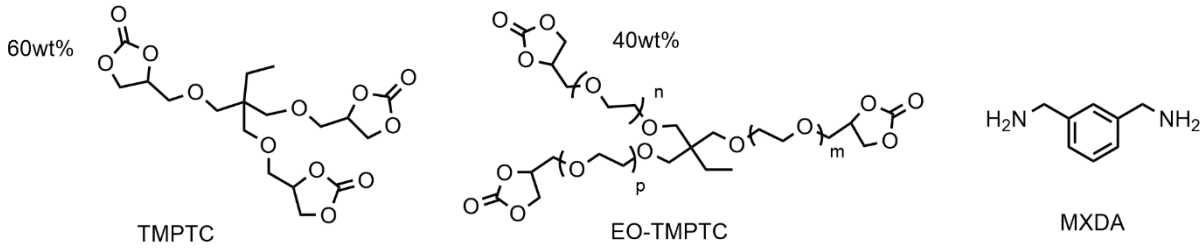

Figure VI.1. Chemical structure of monomers used in the formulation for NIPU foams

The dispersion protocol consisted of first incorporating the nano-particles (Ch-NC or Ch-NF) into liquid MXDA under mechanical stirring, followed by tip sonication to break up agglomerates and achieve uniform distribution. This pre-dispersion step was essential to ensure that the nanoparticles were distributed throughout the final foam structure. Additionally, this

avoids the use of solvents to dissolve the nanocrystals and nanofibers, and further purification processes to evaporate the remaining solvent in the material.

2.2. Rheological characterization

Understanding the rheological behavior of the reactive system is crucial for optimizing the foaming process. When water is incorporated into the NIPU formulation, it hydrolyzes the cyclic carbonate group. Generating a vicinal diol group and CO_2. This reaction effectively increases the functional group ratio [NH_2]/[CC], which in turn affects the gelation kinetics and network formation. Rheological measurements were therefore conducted to elucidate the relationship between amine content and gel point behavior, providing essential information for establishing the processing window for flexible foam fabrication, as already discussed in Chapter IV.

2.2.1. Effect of functional group ratio on gel point

To simulate the effect of water consumption on the reactive system, formulations with varying [NH_2]/[CC] molar ratios (1, 0.85, 0.75, and 0.70) were prepared and characterized by oscillatory rheometry at 80°C. The evolution of storage modulus (G') and loss modulus (G") as a function of time is presented in Figure VI.2. The gel point, defined as the crossover of G' and G", provides a direct measure of the time required for network formation.

As shown in Figure VI.2, the stoichiometric formulation ([NH_2]/[CC] = 1) exhibited the fastest gelation, with the gel point occurring at approximately 25 minutes. Decreasing the amine ratio progressively delayed the gel point: formulations with ratios of 0.85, 0.75, and 0.70 showed gel points at approximately 40, 70, and beyond 100 minutes, respectively. This trend is consistent with the reduced availability of reactive amine groups, which slows down the crosslinking reaction and extends the time required to reach the critical conversion for network formation.[94,151]

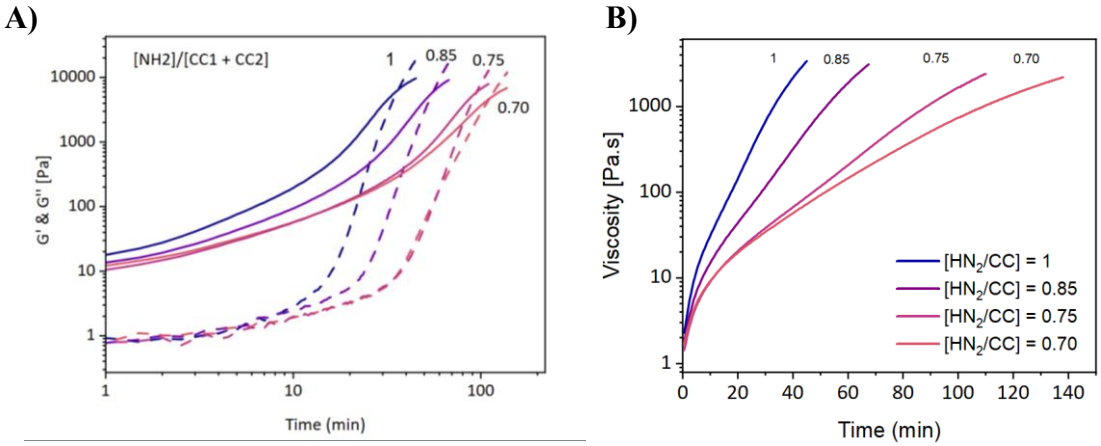

Figure VI.2. A) G' & G" vs Time. **B)** Viscosity vs time at different [NH_2]/[CC] ratios at 80°C.

The viscosity evolution during curing was also monitored and is presented in Figure VI.2. The stoichiometric formulation reached a viscosity of approximately 2000 Pa.s within 60 minutes, while the formulation with [NH_2]/[CC] = 0.70 required nearly 140 minutes to achieve similar values. This extended processing window at lower amine ratios has important implications for foam fabrication, as it determines the time available for gas generation and cell expansion before the matrix vitrifies.

2.2.2. Effect of temperature and pre-curing on gel point

The influence of curing temperature on gel point behavior was investigated at 80°C and 100°C, as well as with a pre-curing protocol consisting of 5 minutes at 80°C followed by curing at 100°C. The results are presented in Figure VI.3. At 80°C, the gel point was significantly delayed, occurring at approximately 50-60 minutes due to the lower reaction rate. In contrast, curing at 100°C accelerated the gelation to approximately 20 minutes.

Interestingly, the pre-curing protocol (5 min at 80°C + 100°C) resulted in the fastest gel point, occurring at approximately 10-15 minutes. This behavior can be attributed to the viscosity build-up achieved during the pre-curing step, which advances the conversion degree before the foaming temperature is reached.

The effect of pre-curing on the initial viscosity was further examined by comparing the viscosity evolution of formulations with [NH_2]/[CC] = 0.85, with and without the pre-curing step (Figure VI.3.B). Without pre-curing, the initial viscosity was approximately 1.5 Pa.s, while the pre-cured sample exhibited an initial viscosity of approximately 4 Pa.s. This increase in starting viscosity is critical for foam stabilization, as it provides sufficient matrix strength to

trap the CO_2 bubbles generated during the water-carbonate reaction and prevent cell collapse during expansion.

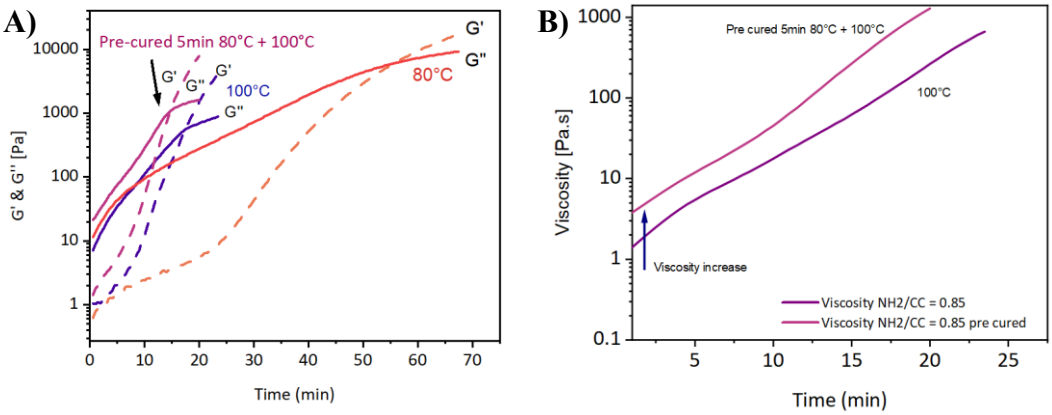

Figure VI.3. A) G' & G" vs Time. **B)** Viscosity vs time at $[NH_2]/[CC] = 0.85$ at different temperatures.

Based on these rheological studies, a pre-curing step of 5 minutes at 80°C was established as a standard protocol for all subsequent foam fabrication experiments. This approach ensures adequate viscosity build-up to stabilize the cellular structure while maintaining sufficient fluidity for gas expansion and cell growth.

2.3. Water content optimization

Following the rheological optimization, a series of foams was fabricated with varying water equivalents to determine the optimal concentration for achieving well-defined cellular morphology. Four water concentrations were investigated: 0.15, 0.25, 0.3, and 0.4 molar equivalents relative to the cyclic carbonate groups. All samples were subjected to the pre-curing protocol (5 min at 80°C) prior to adding water and then foaming at 100°C. In this case, water hydrolyses the cyclic carbonates in presence of a catalyst (DBU, in our case) to then generate CO_2, which will serve as the blowing agent [17] (Figure VI.4).

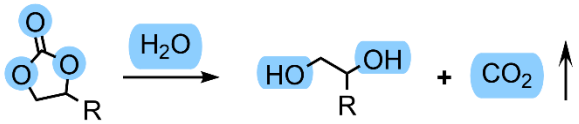

Figure VI.4. Hydrolysis of cyclic carbonates.[17]

The optical photographs of the resulting foams are presented in Figure VI.5. A clear correlation between water content and foam morphology was observed. The formulation containing 0.15 eq. H_2O produced a foam with homogeneous and smooth surface appearance. In contrast, increasing the water content to 0.25 eq. resulted in partial cell coalescence and surface irregularities. At higher water concentrations (0.3 and 0.4 eq.), the foams exhibited significant structural collapse, open-cell morphology, and irregular surfaces.

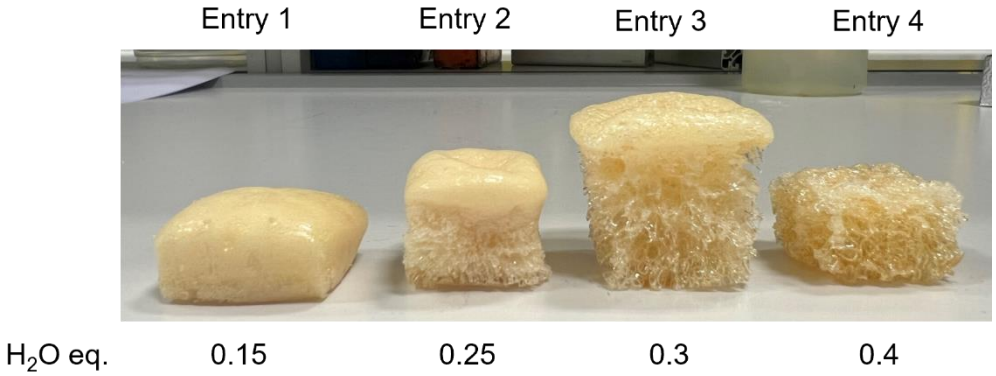

Figure VI.5.Optical photographs of foams with varying water content (0.15, 0.25, 0.3, 0.4 eq) synthesized with TMPTC, EO-TMPTC, MXDA and Water). Conditions: Pre-curing 5CC mixture with MXDA at 80°C for 5min and then adding H_2O and inducing foaming at 100°C for 5h.

The morphological differences can be rationalized in terms of the competition between gas generation rate and matrix viscosity build-up. At low water content (0.15 eq.), the CO_2 generation is moderate and well-matched with the crosslinking kinetics, allowing the matrix to stabilize the growing cells before they coalesce or collapse. At higher water concentrations, excessive gas generation occurs before the matrix has developed sufficient strength, leading to cell rupture, coalescence, and structural collapse.

The physical and thermal properties of the foams are summarized in Table VI.1. A clear trend was observed in gel content values, which decreased from 96% for Entry 1 (0.15 eq. H_2O) to 71% for Entry 4 (0.4 eq. H_2O). This decrease suggests that water hydrolyzes cyclic carbonate groups, reducing the number of CC groups available to react with amines, which in turn decreases the effective crosslinking density and network formation efficiency. The glass transition temperature (T_g) followed a similar trend, decreasing from 23°C for Entry 1 to only

1°C for Entry 4. This significant reduction in T_g is attributed to the lower crosslinking density. Notably, the low T_g values obtained, particularly for Entry 1 (23°C), confirm the flexible nature of these foams, in contrast to the rigid foams developed in previous chapters which exhibited T_g values above 50°C. All DSC thermograms are shown in Figure VI.6.

Table VI.1. Physical and thermal properties of NIPU foams with varying water content.

Entry	H_2O (eq.)	GC (%)	Density ($g.cm^{-3}$)	T_g (°C)	T_{d5} (°C)	Residue (%)
1	0.15	96 ± 1	0.321 ± 0.023	23	291	10
2	0.25	91 ± 1	0.344 ± 0.009	13	287	10
3	0.3	87 ± 1	0.164 ± 0.012	7	284	9
4	0.4	71 ± 1	n/d	1	267	8

Thermal stability, assessed by the temperature at 5% weight loss (T_{d5}) and char residue at 600°C, showed modest variations across the series. TGA curves are shown in Figure VI.6. Entries 1-3 exhibited T_{d5} values above 280°C, while Entry 4 (highest water content) exhibited lower T_{d5} around 267 °C. This could be explained by the lower formation of urethane linkages and crosslinking network. Char residues range between 8-10%.

Additionally, the urethane linkage was confirmed through FTIR (Figure VI.6) by the appearance of the characteristic peak around 1694 cm^{-1} and the disappearance of the cyclic carbonate band at 1790 cm^{-1}. Based on the combined assessment of morphology, gel content, and thermal properties, Entry 1 (0.15 eq. H_2O) was selected as the optimal formulation for subsequent studies involving nano-filler incorporation.

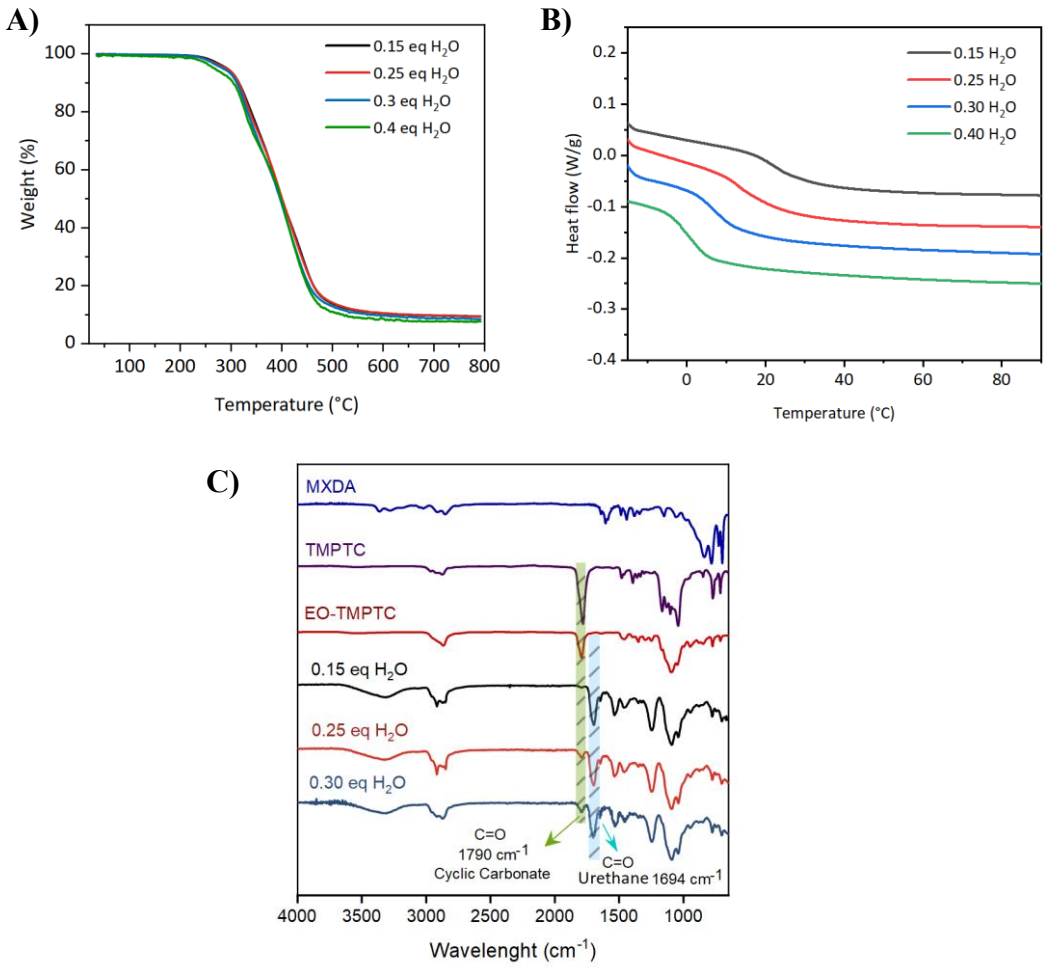

Figure VI.6. A) TGA curves. **B)** DSC thermograms. **C)** FTIR spectra of NIPU foams synthesized at different water content. Conditions: Pre-curing 5CC mixture with MXDA at 80°C for 5min and then adding H_2O and inducing foaming at 100°C for 5h.

2.4. Incorporation of bio-based nano-particles and inorganic fillers

2.4.1. Dispersion strategy and nano-particle selection

Following the optimization of water content, the next step was to incorporate bio nano-fillers into the foam formulation. Three types of bio-based nanoparticles were selected for this study: chitin nanocrystals (Ch-NC), chitin nanofibers (Ch-NF), and cellulose nanofibers (C-NF) (Figure IV.7 and Table VI.2).

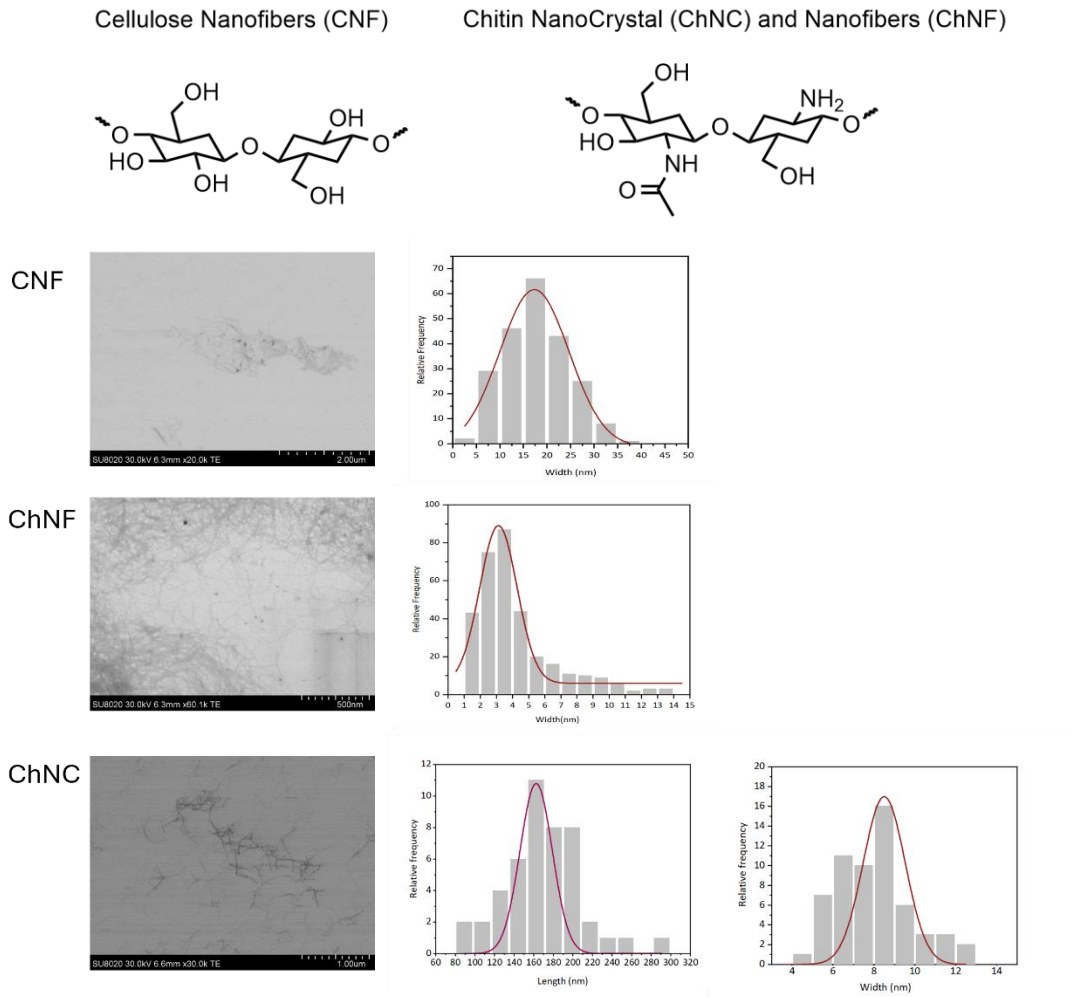

Figure VI.7. Chemical structure and size of chitin (partially deacetylated) and cellulose nanofillers.

These types of fillers were chosen based on their renewable origin, high aspect ratio, and potential for mechanical reinforcement. For comparison purposes, two inorganic fillers were also investigated.[252,253] Laponite nanoclay and Calcium Carbonate ($CaCO_3$). Laponite has been already used in Chapter IV, and has proved the improvement in the morphology of NIPU Foams. Calcium Carbonate has been also used in Polyurethane foams in the industrial sector.[255]

Table VI.2. Morphological and chemical characteristics of bio-based nanofillers

Nanofiller	Source	Width (nm)	Length (nm)	Deacetylation degree % (DDA)
ChNC (Chitin nanocrystals)	Shrimp shell	9-11	210	35
ChNF (Chitin nanofibers)	Squid	3-4	>500	14
CNF (Cellulose nanofibers)	Silvergrass (Miscanthus)	15	>500	N/A

The dispersion of bio-based nanoparticles in thermoset systems represents a significant challenge due to their tendency to agglomerateand , due to the use of solvents that need further purification processes and generate waste. [256–258] In this work, the liquid nature of MXDA at room temperature was exploited to achieve dispersion of the nano-fillers prior to mixing with the cyclic carbonate component. The nanoparticles were incorporated into liquid MXDA and subjected to tip sonication for a few seconds to break up agglomerates and ensure distribution. Upon sonication, the initially low-viscosity amine transformed into a paste-like consistency as shown in Figure VI.8.

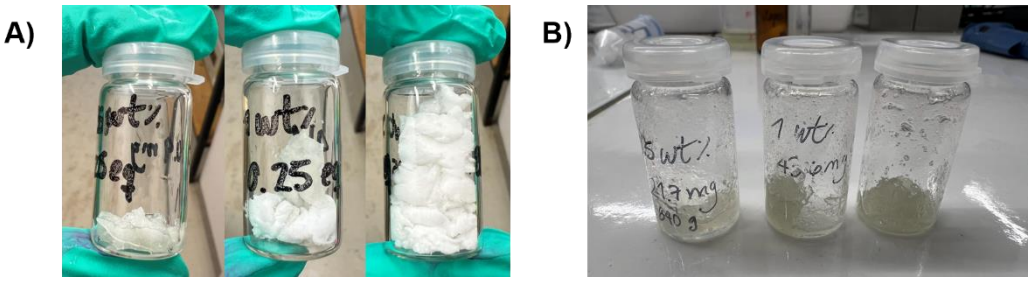

Figure VI.8. A) Photographs of chitin nanocrystals (ChNC) in MXDA. **B)** ChNC dispersed in liquid MXDA after tip sonication, showing the paste-like consistency

However, the maximum concentration of nanofillers that could be effectively incorporated was limited by the presence of the fillers themselves, which increased the viscosity of the mixture and compromised the quality of dispersion at higher loadings. Beyond 2 wt% loading, the mixture became excessively viscous and difficult to process, compromising the subsequent mixing with the cyclic carbonate and the foaming process. Therefore, the bio-based nano-fillers

(Ch-NC, Ch-NF, and C-NF) were incorporated at concentrations of 0.5, 1, and 2 wt% relative to the total formulation mass.

A different dispersion approach was employed for the CNF and inorganic fillers. CNF, Laponite and $CaCO_3$ were dispersed directly into the cyclic carbonate mixture (TMPTC + EO-TMPTC) prior to the addition of the amine component. This approach was chosen due to the different surface chemistry of these inorganic materials and their compatibility with the carbonate phase. Both inorganic fillers were incorporated at 5 wt%, a concentration commonly employed in the literature.[146] The complete list of foam formulations and their corresponding entry numbers is presented in Table VI.3.

2.4.2. Foam fabrication and morphological characterization

Using the optimized formulation (Entry 1, 0.15 eq. H_2O) and the pre-curing protocol established in section 2.2, a series of NIPU foams with bio-fillers, $CaCO_3$ and Laponite was fabricated, following the reaction depicted in Figure VI.9. All foams were successfully produced, exhibiting well-defined cellular structures regardless of the type or concentration of nano-filler employed. The optical photographs of the resulting foams are presented in Figures VI.10 and V.11.

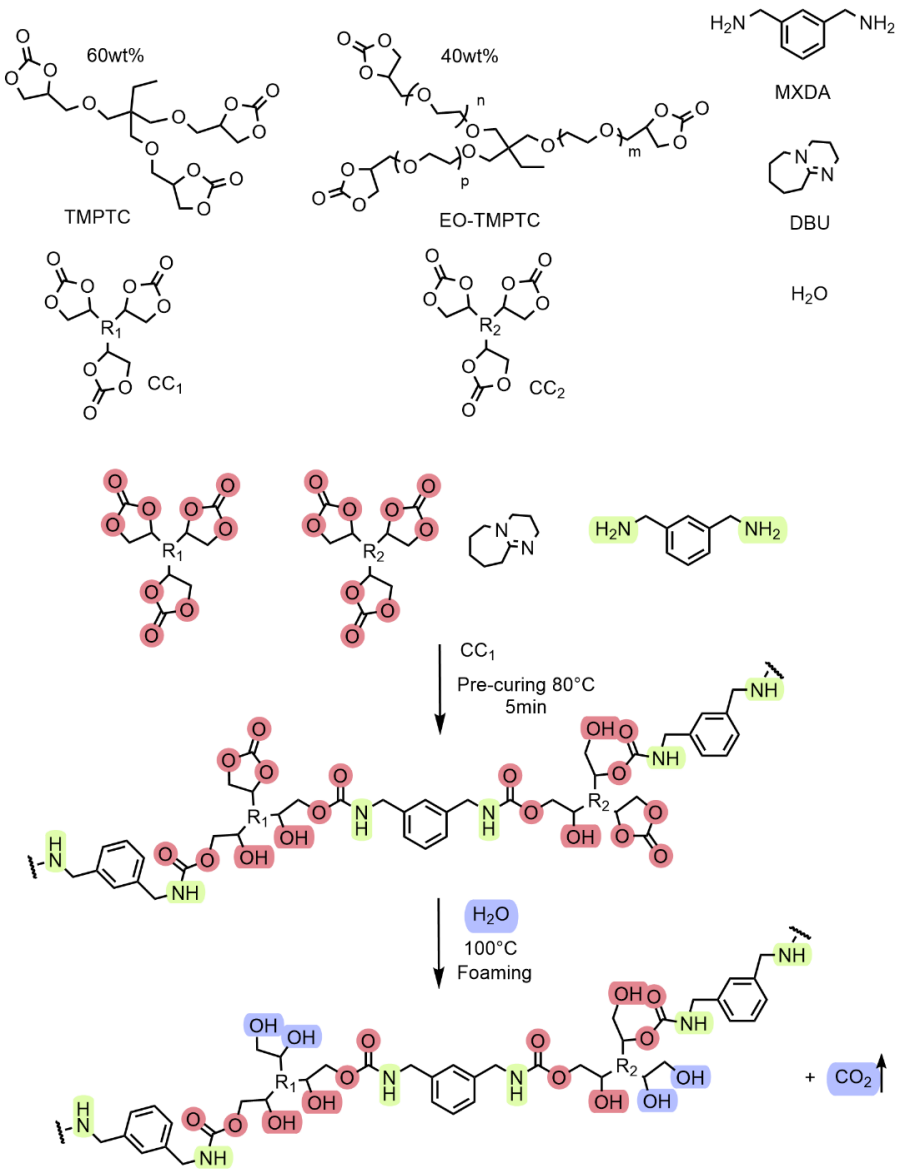

Figure VI.9. Schematic reaction of the NIPU foams synthesized with TMPTC, EO-TMPTC, MXDA and water. Conditions: Pre-curing for 5 min at 80_C. Then, adding water and inducing foaming at 100°C for 5h.

The cellular morphology of the flexible NIPU foams was examined by scanning electron microscopy (SEM). Figure VI.10 presents the cross-sectional micrographs of the foams containing bio-nanofillers: cellulose nanofibers (Entries 5–7), chitin nanofibers (Entries 8–10), while Figure VI.11 displays the foams incorporating chitin nanocrystals (Entries 11–13), inorganic fillers, namely $CaCO_3$ (Entry 14) and Laponite (Entry 15). Differences in cell size and morphology among the various filler types and concentrations were observed and are discussed in the following sections.

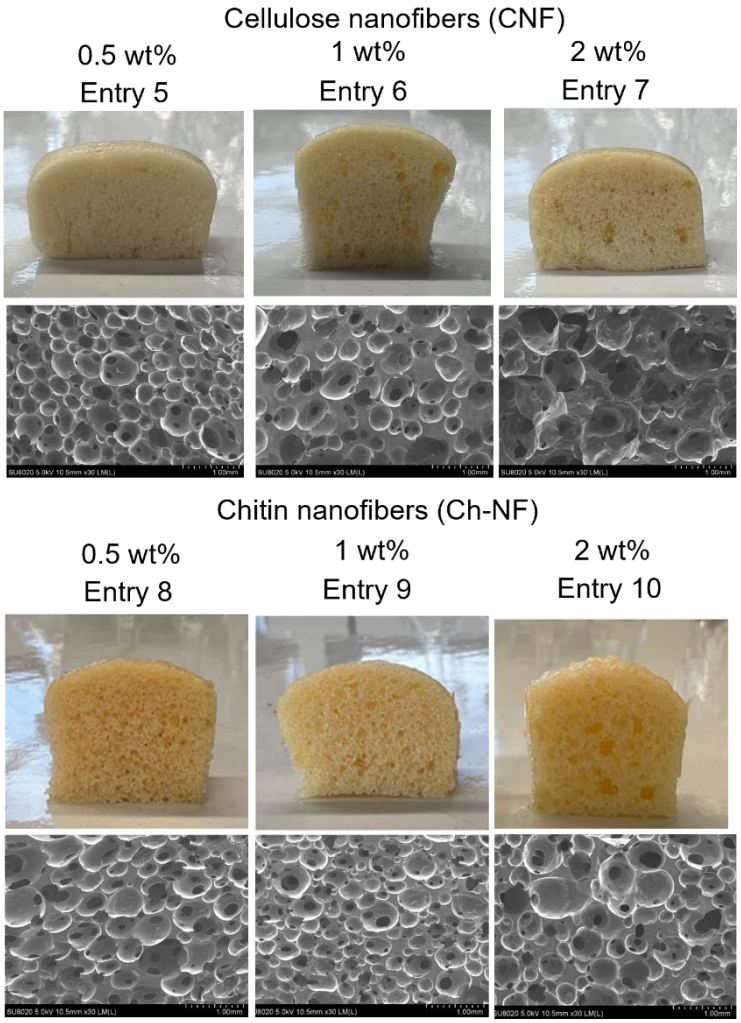

Figure VI.10. Optical pictures and SEM micrographs of NIPU foams loaded with cellulose nanofibers (CNF) and chitin nanofibers (ChNF)

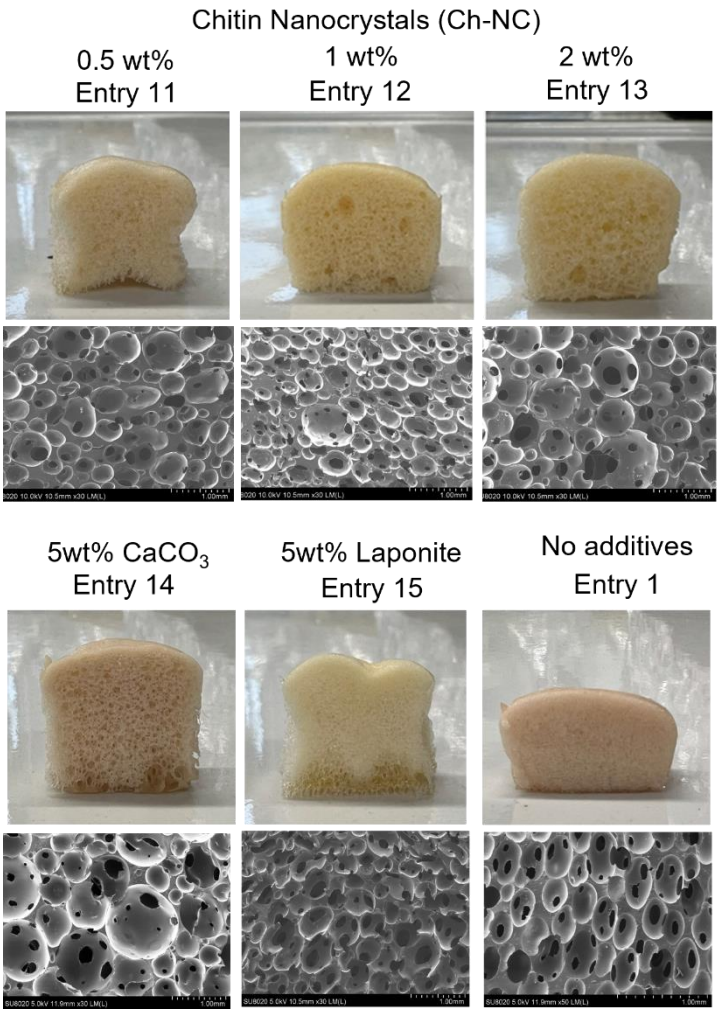

Figure VI.11. Optical pictures and SEM micrographs of NIPU foams loaded with chitin nanocrystals (ChNC), $CaCO_3$, Laponite and no fillers.

The chemical structure of the NIPU foams containing bio-nanofillers was verified by FTIR spectroscopy (Figure VI.12). All formulations exhibited the characteristic urethane carbonyl absorption band at approximately 1694 cm^{-1}, while the cyclic carbonate band at 1790 cm^{-1} disappeared, confirming the successful ring-opening reaction and network formation. The small remaining peak at 1790 cm^{-1} suggests that not all cyclic carbonates reacted.

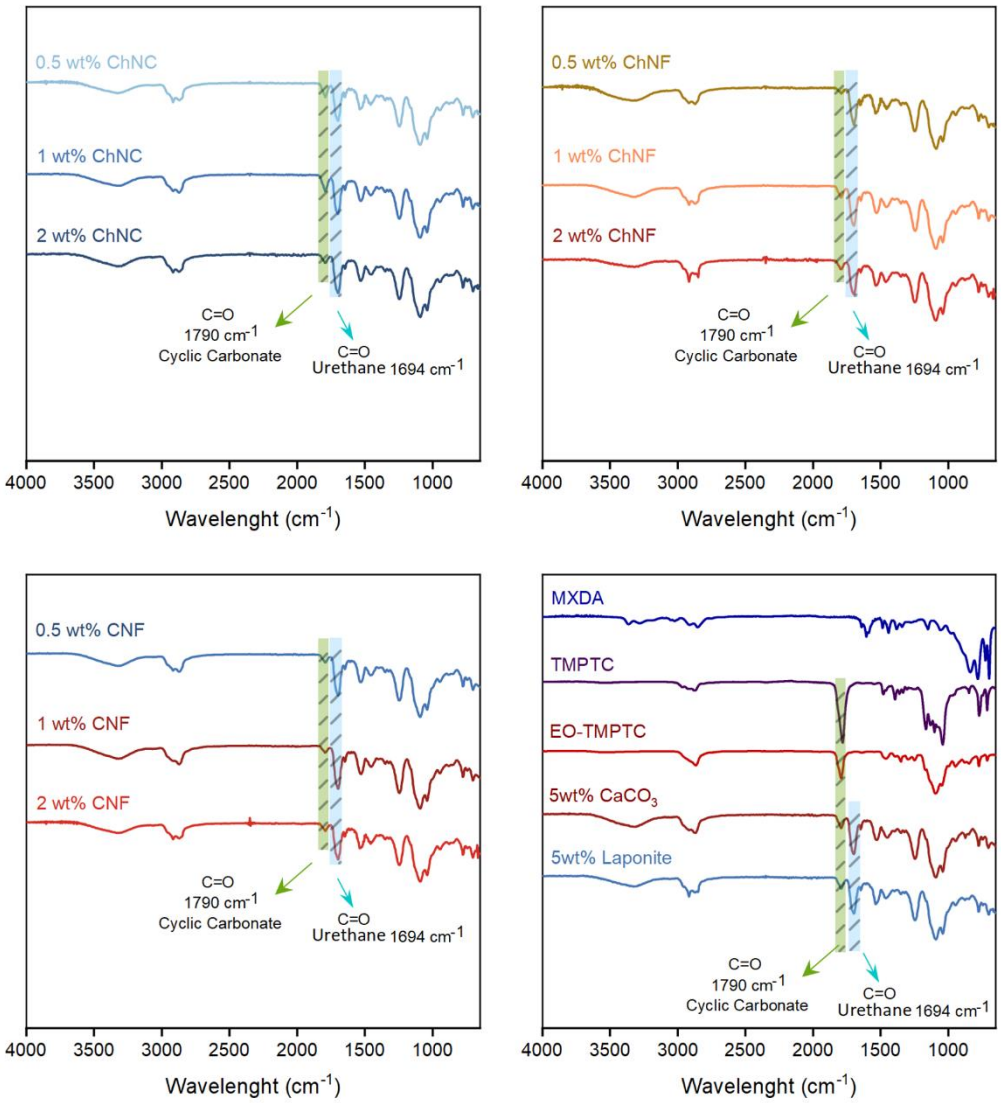

Figure VI.12. FTIR Spectra of all NIPU foams containing ChNF, CNF, ChNC, CaCO3 and Laponite. The green line corresponds to the disappearance of the cyclic carbonate C=O stretching band (~1790 cm^{-1}), indicating cyclic carbonate conversion, while the blue line represents the presence of the urethane C=O stretching band (~1700 cm^{-1})

2.5. Physical and thermal properties

The physical and thermal properties of the nano-particle reinforced foams were systematically characterized. All samples were evaluated in terms of gel content, density, glass transition temperature (T_g), thermal degradation temperature (T_{d5}), and char residue. The complete data are summarized in Table VI.3.

Table VI.3. Physical and thermal properties of NIPU foams synthesized with 0.15eq of H_2O loaded with bio-based nano-fillers and inorganic fillers

Entry	Sample	%wt	GC (%)	Density	T_g (°C) dried	$T_{d5\%}$	Residue 600 °C	Cell size (mm)
1	No additives	-	96 ± 1	0.321 ± 0.023	23	291	10	0.285 ± 0.035
5		0.5	95 ± 1	0.240 ± 0.008	18	286	9	0.343 ± 0.075
6	C NF	1	92 ± 1	0.234 ± 0.023	17	289	10	0.494 ± 0.150
7		2	94 ± 1	0.228 ± 0.009	18	287	10	0.525 ± 0.253
8		0.5	90 ± 3	0.306 ± 0.017	13	277	10	0.509 ± 0.108
9	Ch NF	1	92 ± 2	0.321 ± 0.015	14	277	10	0.362 ± 0.106
10		2	92 ± 1	0.318 ± 0.004	15	288	11	0.431 ± 0.107
11		0.5	91 ± 1	0.279 ± 0.023	7	269	9	0.411 ± 0.108
12	Ch NC	1	88 ± 1	0.273 ± 0.015	11	266	9	0.422 ± 0.097
13		2	92 ± 1	0.279 ± 0.013	15	292	10	0.518 ± 0.152
14	CaCO3	5	87 ± 1	0.231 ± 0.011	10	274	15	0.693 ± 0.209
15	Laponite	5	91 ± 1	0.32 ± 0.015	15	290	13	0.280 ± 0.131

The average cell size of the foams varied depending on the type and concentration of nano-filler incorporated. Entry 1 (without fillers) exhibited an average cell size of 0.285 ± 0.035 mm. Cellulose nanofibers (Entries 5-7) showed cell sizes ranging from 0.362 to 0.509 mm. Chitin nanofibers (Entries 8-10) displayed cell sizes between 0.343 and 0.525 mm. Chitin nanocrystals (Entries 11-13) exhibited cell sizes from 0.411 to 0.518 mm. Entry 14 ($CaCO_3$) showed the

largest cell size at 0.693 ± 0.209 mm, while Entry 15 (Laponite) exhibited 0.280 ± 0.131 mm. The summary of the densities and average cell size are shown in Figure VI.13.

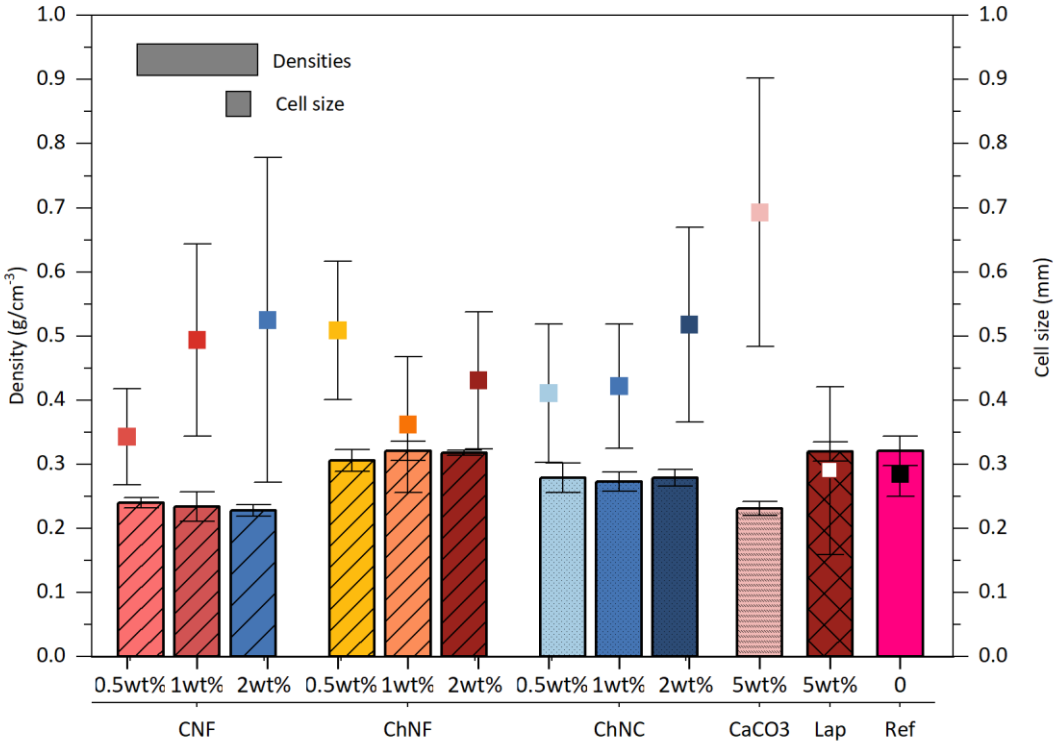

Figure VI.13. Density (columns) and average cell size (scatter) of flexible NIPU foams containing bio-based nanofillers (CNF, ChNF, ChNC) at varying loadings (0.5, 1, and 2 wt%) and inorganic fillers (Laponite and $CaCO_3$) at 5 wt%

The increase in cell size upon bio-nanofiller incorporation, contrary to the nucleating effect typically expected from nanoparticles in foam systems, can be attributed to several interconnected mechanisms. Firstly, the significant viscosity increase caused by nanofiller dispersion in MXDA, as evidenced by the paste-like consistency observed after tip sonication, may have exceeded the optimal range for efficient nucleation. According to Liu et al.,[259] when viscosity increases beyond a critical threshold, the resistance to bubble expansion decreases the nucleation rate, leading to fewer but larger cells. Secondly, the surface chemistry and wettability of the nanoparticles strongly influence their role as nucleating agents. According to classical nucleation theory, efficient heterogeneous nucleation requires favorable interfacial interactions between the particle surface and the gas phase.[260] The hydrophilic nature of cellulose and chitin nanoparticles, rich in surface hydroxyl groups, results in poor compatibility

with CO_2, reducing their efficiency as heterogeneous nucleating agents. Thirdly, at higher concentrations, nanofiller agglomeration can create interfacial dilution effects that further reduce nucleation efficiency. The significantly smaller cell size observed for Entry 15 (Laponite) supports this interpretation, as the nanoclay particules have different surface chemistry (silicate layers with lower hydrophilicity) and high aspect ratio that may promote more efficient heterogeneous nucleation compared to the bio-nanofillers.

The gel content values remained high for all formulations, ranging from 87% to 96%, indicating successful network formation regardless of the nano-particle type. Entry 1 (reference) exhibited the highest gel content at 96 ± 1%. Cellulose nanofiber foams (Entries 5-7) showed gel content values between 92-95%, while chitin nanofibers (Entries 8-10) ranged from 90-92%. Chitin nanocrystals (Entries 11-13) displayed values between 88-92%. Among the inorganic fillers, Entry 14 ($CaCO_3$) showed the lowest gel content at 87 ± 1%, while Entry 15 (Laponite) maintained a value of 91 ± 1%. The slight decrease in gel content upon nanofiller incorporation suggests that the nanoparticles may partially interfere with the crosslinking reaction, either by increasing local viscosity that hinders molecular mobility or by competing for reactive groups through interfacial interactions.

The foam density varied depending on the type of nano-filler incorporated. Entry 1 exhibited a density of 0.321 ± 0.023 $g.cm^{-3}$. Cellulose nanofibers (Entries 5-7) resulted in lower density foams, with values between 0.228 and 0.240 $g.cm^{-3}$. Chitin nanofibers (Entries 8-10) produced foams with densities ranging from 0.306 to 0.321 $g.cm^{-3}$. Chitin nanocrystals (Entries 11-13) yielded densities around 0.273-0.279 $g.cm^{-3}$. Entry 14 ($CaCO_3$) produced foams with density of 0.231 ± 0.011 $g.cm^{-3}$, while Entry 15 (Laponite) exhibited 0.320 ± 0.015 $g.cm^{-3}$. The variation in foam density reflects the complex interplay between nanofiller-induced viscosity changes, gas generation efficiency, and cell stabilization during the foaming process.

The glass transition temperature (T_g) of all foams was determined by differential scanning calorimetry (DSC). The DSC thermograms for all foam formulations are presented in Figure VI.14. Entry 1 (without nanofillers) exhibited a T_g of 23°C, confirming the flexible nature of the base formulation. Contrary to the typical reinforcing behavior reported for bio-nanofillers/reinforcement in conventional polymer nanocomposites, the incorporation of chitin and cellulose nano-biofillers into water-blown flexible NIPU foams resulted in a systematic decrease in glass transition temperature. Cellulose nanofibers (Entries 5-7) showed T_g values

of 17-18°C, representing a reduction of 5-6°C compared to the neat foam. Chitin nanofibers (Entries 8-10) exhibited lower T_g values from 13°C to 15°C, corresponding to a reduction of 8-10°C. Chitin nanocrystals displayed the most pronounced effect with a wider range: Entry 11 (0.5 wt%) showed 7°C, Entry 12 (1 wt%) showed 11°C, and Entry 13 (2 wt%) reached 15°C. Interestingly, for chitin nanocrystals, T_g increased with increasing nanofiller concentration, suggesting a concentration-dependent transition in the dominant interaction mechanism. In contrast, cellulose nanofibers, which lack amino groups, exhibited a stable plasticizing effect independent of concentration T_g = 17-18°C across all loadings).The inorganic fillers also reduced T_g, with values of 10°C for Entry 14 ($CaCO_3$) and 15°C for Entry 15 (Laponite).

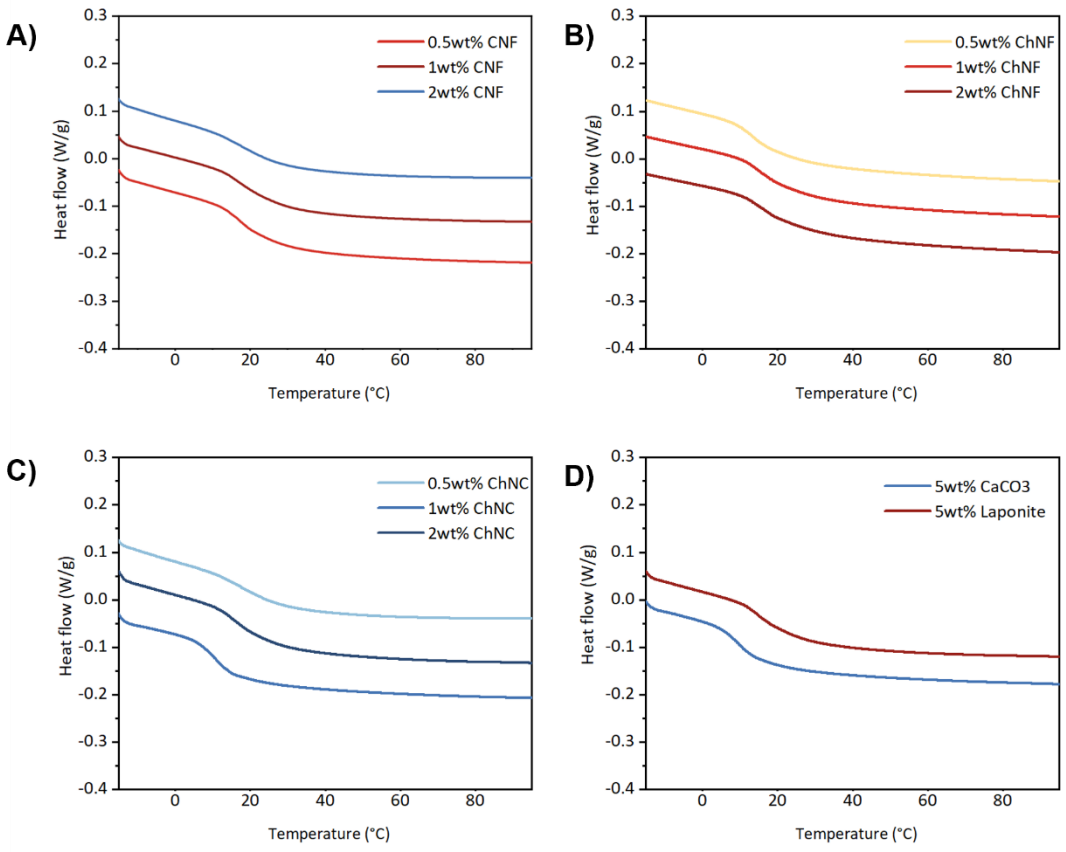

Figure VI.14. DSC thermograms of NIPU foams loaded with the different bio-nanofillers (ChNF, CNF, ChNC), Laponite and $CaCO_3$.

The overall reduction in T_g can be rationalized through the concept of competitive hydrogen bonding. Poly(hydroxyurethane)s presents a unique chemical structure characterized by pendant hydroxyl groups adjacent to each urethane linkage. These hydroxyl groups establish an extensive intra- and intermolecular hydrogen bonding network that restricts chain mobility

and contributes to the material's glass transition temperature. The introduction of bio-nanofillers, which are rich in surface hydroxyl groups (cellulose) or hydroxyl, amines and acetamide groups (chitin), creates a competitive scenario for hydrogen bond formation. The nanofiller surface groups can interact with both the pendant -OH groups and the carbonyl moieties of the PHU matrix, effectively disrupting the internal hydrogen bonding network of the polymer. This disruption increases free volume and chain mobility, consequently lowering the glass transition temperature. This phenomenon has been reported in other nanocomposite systems, where the introduction of nanofillers can either increase or decrease T_g depending on the nature of interfacial interactions.[261]

Interestingly, chitin nanocrystals exhibited a concentration-dependent behavior distinct from the other bio-nanofillers (Figure VI.15). While cellulose nanofibers showed a stable plasticizing effect independent of concentration (T_g = 17-18°C across all loadings), ChNC displayed T_g values that increased with increasing nanofiller content. This behavior can be attributed to the high degree of deacetylation of ChNC (DDA ≈ 35%, corresponding to 1.85 mmol NH_2/g), which is significantly higher than that of ChNF (DDA ≈ 14%, ~0.74 mmol NH_2/g). At low loadings (0.5 wt%), well-dispersed nanocrystals maximize the available surface area for hydrogen bond competition with the PHU matrix, resulting in pronounced plasticization (T_g = 7°C). However, at higher loadings (2 wt%), two counteracting phenomena emerge: (i) nanocrystal agglomeration reduces the effective surface area available for matrix interaction, and (ii) the increased absolute quantity of primary amino groups may react with cyclic carbonate groups in the matrix, forming additional hydroxyurethane crosslinks that restrict chain mobility. This dual functionality, plasticization through hydrogen bond disruption at low concentrations versus crosslinking through amine-carbonate reaction at higher concentrations, is consistent with the well-established reactivity between primary amines and five-membered cyclic carbonates.[262]

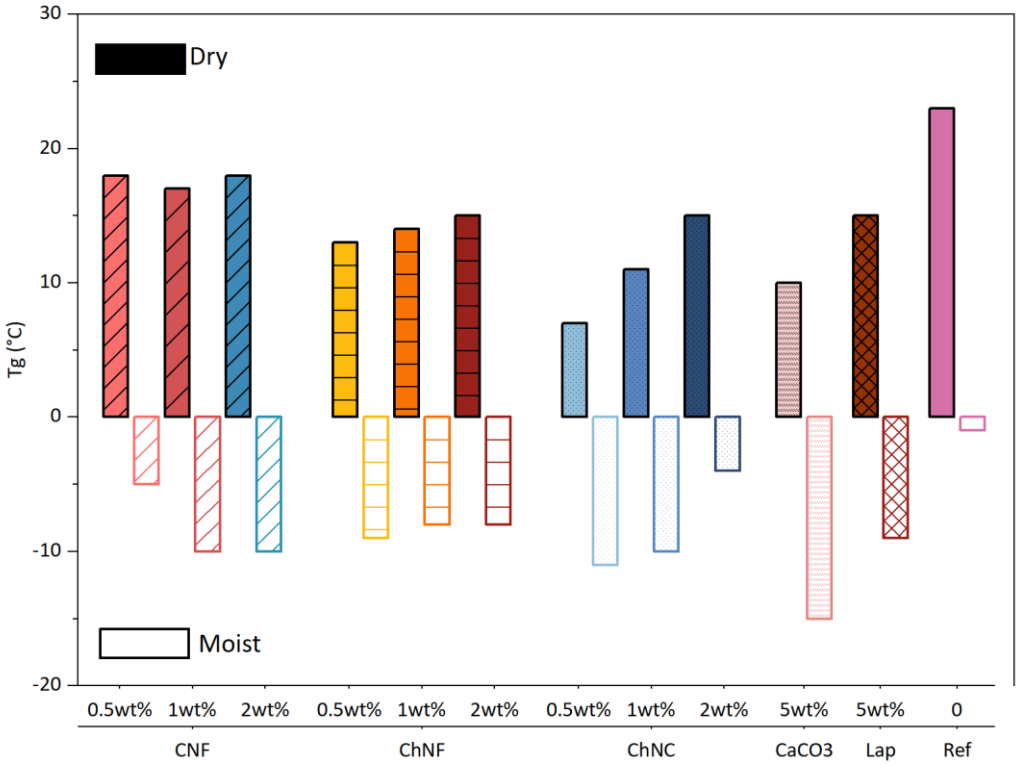

Figure VI.15. T_g of flexible NIPU foams containing bio-based nanofillers (CNF, ChNF, ChNC) at varying loadings (0.5, 1, and 2 wt%) and inorganic fillers (Laponite and $CaCO_3$) at 5 wt% in dry state (plain columns) and moist state (hollow columns).

An additional contributing factor is the hygroscopic nature of bio-nanofillers. Despite drying procedures, chitin and cellulose nanoparticles typically retain 4-8 wt% of bound water due to their hydrophilic surface chemistry. Furthermore, the hydrophilic nanofillers may compete with the foaming reaction by adsorbing water molecules that would otherwise hydrolyze cyclic carbonates to generate CO_2, potentially affecting both the foaming kinetics and the final network architecture.[251,262]

It should be noted that direct comparison of properties between bio-nanofiller-containing foams and the neat reference foam (Entry 1) is complicated by the significant differences in foam density, cell size, and morphology. The incorporation of bio-nanofillers fundamentally altered the foam structure, making it more appropriate to compare properties within each nanofiller series (i.e., between different concentrations of the same nanofiller type) rather than against the

unfilled reference. This limitation underscores the complex interplay between nanofiller incorporation, foaming kinetics, and final material properties in water-blown NIPU systems.

The thermal stability of the foams was evaluated by thermogravimetric analysis (TGA). The TGA curves are presented in Figure VI.16. Entry 1 exhibited Td5 of 291°C. Chitin nanofibers (Entries 5-7) showed Td5 values between 277-288°C, while cellulose nanofibers (Entries 8-10) ranged from 286-289°C. Chitin nanocrystals (Entries 11-13) displayed Td5 values between 266-292°C. Entry 14 ($CaCO_3$) exhibited Td5 of 274°C, and Entry 15 (Laponite) showed 290°C. The char residue at 600°C ranged from 9-15%, with the highest values for Entry 14 (15%) and Entry 15 (13%).

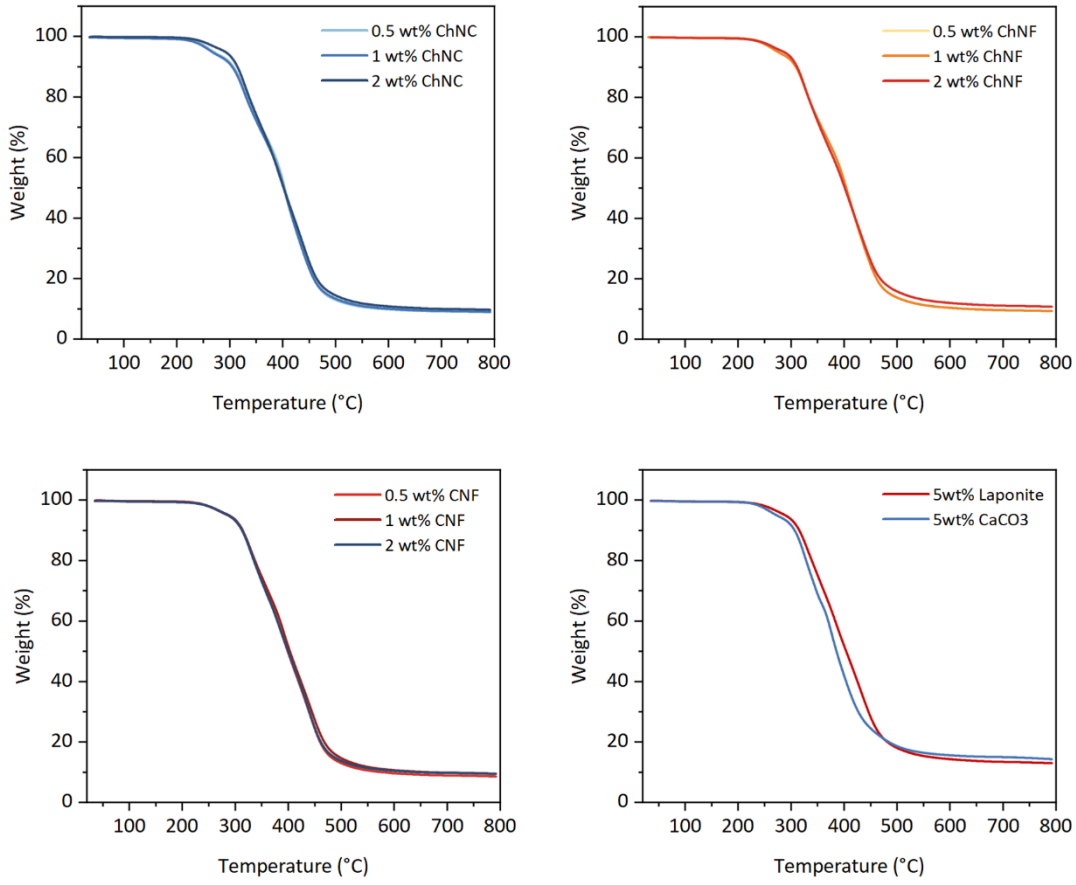

Figure VI.16. TGA curves of NIPU foams loaded with the different bio-nanofillers (ChNF, 0.35CNF, ChNC), Laponite and $CaCO_3$.

2.4.4. Mechanical properties

The compressive mechanical behavior of the flexible NIPU foams containing bio-nanofillers, CaCO3 and Laponite was evaluated through compression testing. The compressive modulus (Ec) and stress values at 50% and 70% strain were determined from these curves, and the results are summarized in Table VI.3. Summary of the mechanical properties are presented in Figure V.16. and representative stress-strain curves are presented in Figure VI.17.

Table VI.3. Mechanical properties and moisture sensitivity of NIPU foams with bio-based nano-particles and inorganic fillers.

Entry	Sample	%wt	Ec (kPa)	Stress @50%	Stress @70%	T_g (°C) moisted	Ec (kPa) Moisted	Water uptake (%)
1	No additives	-	3.4 ± 1	150 ± 51	761 ± 350	-1	1 ± 0.1	7.8 ± 0.1
5		0.5	0.99 ± 0.27	58 ± 7.5	172 ± 35	-5	0.72 ± 0.11	7.2 ± 0.2
6	C NF	1	1.24 ± 0.21	58 ± 5.2	217 ± 41	-10	0.57 ± 0.05	7.5 ± 0.1
7		2	1.21 ± 0.06	60 ± 2.3	196 ± 23	-10	0.6 ± 0.06	7.6 ± 0.1
8		0.5	0.78 ± 0.08	40 ± 4	139 ± 15	-9	0.51 ± 0.06	6.9 ± 0.2
9	Ch NF	1	0.91 ± 0.28	58 ± 5.6	188 ± 11	-8	0.66 ± 0.08	7.1 ± 0.2
10		2	2.07 ± 0.11	99 ± 13	352 ± 56	-8	1.06 ± 0.16	7.5 ± 0.2
11		0.5	0.55 ± 0.06	26 ± 4	81 ± 13	-11	0.5 ± 0.05	7.9 ± 0.1
12	Ch NC	1	0.58 ± 0.02	27 ± 1	105 ± 6	-10	0.5 ± 0.03	7.7 ± 0.1
13		2	0.93 ± 0.16	51 ± 1	167 ± 7	-4	0.82 ± 0.04	7.6 ± 0.4
14	CaCO3	5	0.375 ± 0.06	9.63 ± 0.5	36.3 ± 4	-15	0.35 ± 0.06	7.5 ± 0.1
15	Laponite	5	0.75 ± 0.12	32.5 ± 7	110 ± 33	-9	0.71 ± 0.10	8.1 ± 0.1

As previously discussed, a direct comparison between the bio-nanofiller-containing foams and the neat NIPU foam is not straightforward, since the incorporation of nanofillers significantly affects the system viscosity, nucleation behavior, and resulting cellular morphology. Therefore, the mechanical properties are analyzed by comparing the trends within each bio-nanofiller

series as a function of filler concentration. Summary of the mechanical performance and all stress-strain curves are presented in Figure VI.16. and 17

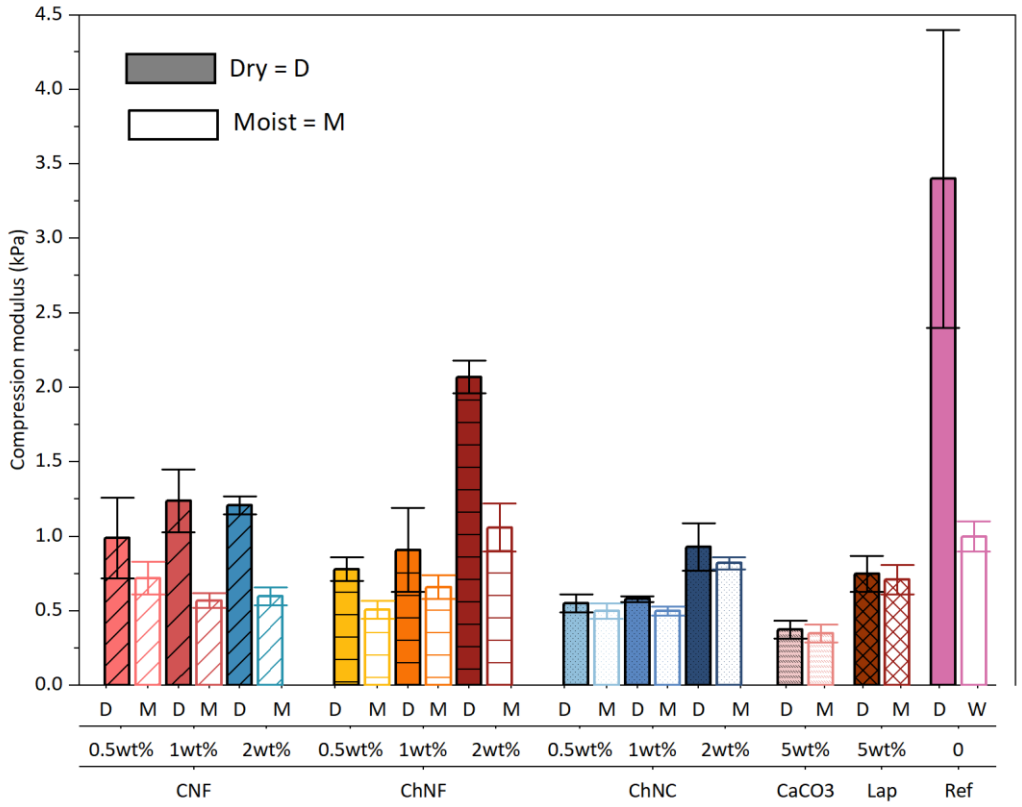

Figure V.16. Mechanical performance of water-blown NIPU foams under dry and moist state. Compressive modulus as a function of filler type, bio-based nanofillers (CNF, ChNF, ChNC) at varying loadings (0.5–2 wt%) and inorganic fillers (Laponite, $CaCO_3$) at 5 wt%.

Cellulose nanofiber series (C-NF): Within the C-NF series (Entries 5–7), the compressive modulus increased from 0.99 ± 0.27 kPa at 0.5 wt% to 1.24 ± 0.21 kPa at 1 wt%, representing a 25%-enhancement. However, further increasing the C-NF content to 2 wt% did not yield additional improvement, with the modulus remaining essentially constant at 1.21 ± 0.06 kPa. A similar trend was observed for the stress at 70% strain, which reached a maximum value of 217 ± 41 kPa at 1 wt% loading before slightly decreasing to 196 ± 23 kPa at 2 wt%. This plateau behavior suggests that an optimal C-NF concentration exists at around 1 wt%, beyond which nanofiller agglomeration may limit further mechanical enhancement.

Chitin nanofiber series (Ch-NF): The Ch-NF series (Entries 8–10) exhibited the most pronounced reinforcement effect among all bio-nanofillers studied. The compressive modulus progressively increased from 0.78 ± 0.08 kPa at 0.5 wt% to 0.91 ± 0.28 kPa at 1 wt%, and reached 2.07 ± 0.11 kPa at 2 wt%, representing a remarkable 165% increase compared to the lowest concentration. The stress at 70% strain followed the same trend, increasing from 139 ± 15 kPa to 352 ± 56 kPa over the same concentration range, a 2.5-fold enhancement. This substantial mechanical improvement at higher Ch-NF loadings indicates effective stress transfer between the PHU matrix and the chitin nanofibers, likely facilitated by hydrogen bonding interactions between the acetamide, amine and hydroxyl groups of chitin and the urethane linkages of the matrix.

Chitin nanocrystal series (Ch-NC): The Ch-NC series (Entries 11–13) displayed a more gradual increase in mechanical properties with increasing filler content. The compressive modulus rose from 0.55 ± 0.06 kPa at 0.5 wt% to 0.93 ± 0.16 kPa at 2 wt%, corresponding to a 69%-improvement. Similarly, the stress at 70% strain increased from 81 ± 13 kPa to 167 ± 7 kPa. Despite this positive trend, the absolute values remained consistently lower than those observed for Ch-NF at equivalent loadings. This difference can be attributed to the distinct morphology of the two chitin nanomaterials: while Ch-NF possesses high aspect ratio fibrillar structures capable of forming entangled networks, Ch-NC consists of shorter, rod-like crystals with lower aspect ratios, resulting in less efficient stress transfer and network formation within the foam matrix.

When comparing the three bio-nanofiller series at equivalent 2 wt% loading, a clear hierarchy in reinforcement efficiency emerges: Ch-NF (Ec = 2.07 kPa) > C-NF (Ec = 1.21 kPa) > Ch-NC (Ec = 0.93 kPa). The superior performance of chitin nanofibers over chitin nanocrystals highlights the importance of nanofiller morphology and aspect ratio in determining the mechanical response of flexible foams.[263,264] The intermediate behavior of cellulose nanofibers, despite their fibrillar morphology, may be related to differences in surface chemistry and interfacial compatibility with the PHU matrix.

Inorganic fillers: For comparison purposes, foams containing inorganic fillers were also evaluated. The $CaCO_3$-filled foam (Entry 14, 5 wt%) exhibited a compressive modulus of 0.375 ± 0.06 kPa and a stress at 70% strain of 36.3 ± 4 kPa, while the Laponite-containing foam

(Entry 15, 5 wt%) showed Ec = 0.75 ± 0.12 kPa and stress at 70% strain of 110 ± 33 kPa. Despite the higher filler loading (5 wt% vs. 0.5–2 wt% for bio-nanofillers), these inorganic fillers yielded lower mechanical properties compared to the bio-nanofiller series at 2 wt%, consistent with the weak mechanical adhesion reported for $CaCO_3$ in PU matrices.[265] This highlights the effectiveness of the chemical interactions between the bio-based nanofillers and the PHU matrix in mechanical reinforcement

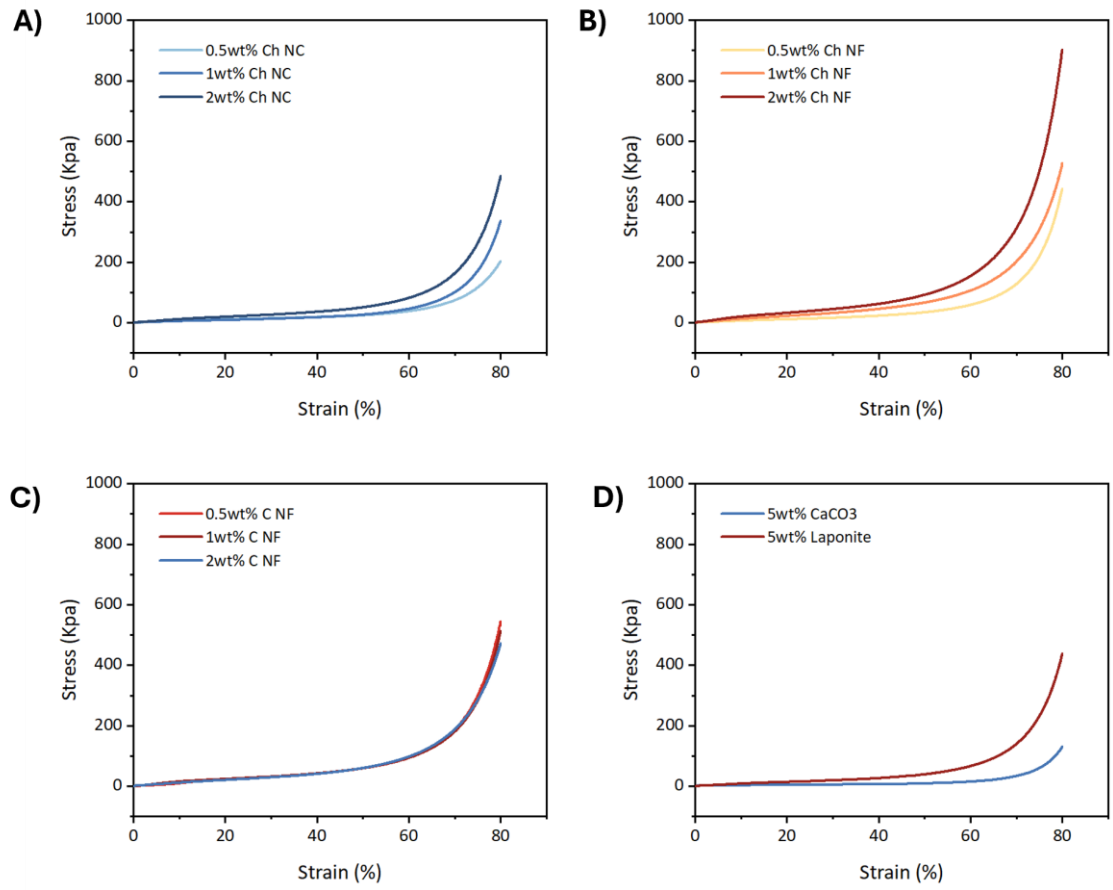

Figure VI.17. Stress vs Strain curves of NIPU foams loaded with the different bio-nanofillers (ChNF, CNF, ChNC), Laponite and $CaCO_3$.

The moisture sensitivity of the NIPU foams was evaluated by conditioning the samples at controlled humidity and subsequently measuring their thermal properties (T_g), mechanical properties and water uptake. As shown in Table VI.3, all foams exhibited water uptake values ranging from 6.9% to 8.1%, with relatively uniform absorption across the different nanofiller types. This behavior is consistent with NIPU foams developed in Chapter IV.

The effect of moisture on the thermal and mechanical properties was significant. Upon moisture conditioning, all samples exhibited a substantial decrease in glass transition temperature, shifting from positive values in the dry state (7–18°C) to negative values in the moisted state (−4 to −15°C). This pronounced plasticizing effect of absorbed water is attributed to the disruption of hydrogen bonding within the PHU network, as water molecules compete for the available hydrogen bonding sites on the pendant hydroxyl groups and urethane linkages.

The compressive modulus in the moisted state (Ec moisted) followed the same trend observed in dry conditions, with Ch-NF at 2 wt% retaining the highest value (1.06 kPa) among the bio-nanofillers (Figure VI.18). However, the extent of mechanical property retention varied significantly among the different nanofiller types. Chitin nanocrystals (Ch-NC) exhibited the best moisture resistance, with modulus reductions of only 9–14% compared to dry values. In contrast, cellulose nanofibers (C-NF) and chitin nanofibers (Ch-NF) showed greater sensitivity to moisture, with reductions ranging from 27% to 54%. Notably, the inorganic fillers (CaCO3 and Laponite) demonstrated the lowest sensitivity to moisture, with modulus reductions of only 5–7%, likely due to their lower capacity for water-mediated plasticization compared to polysaccharide-based nanofillers.

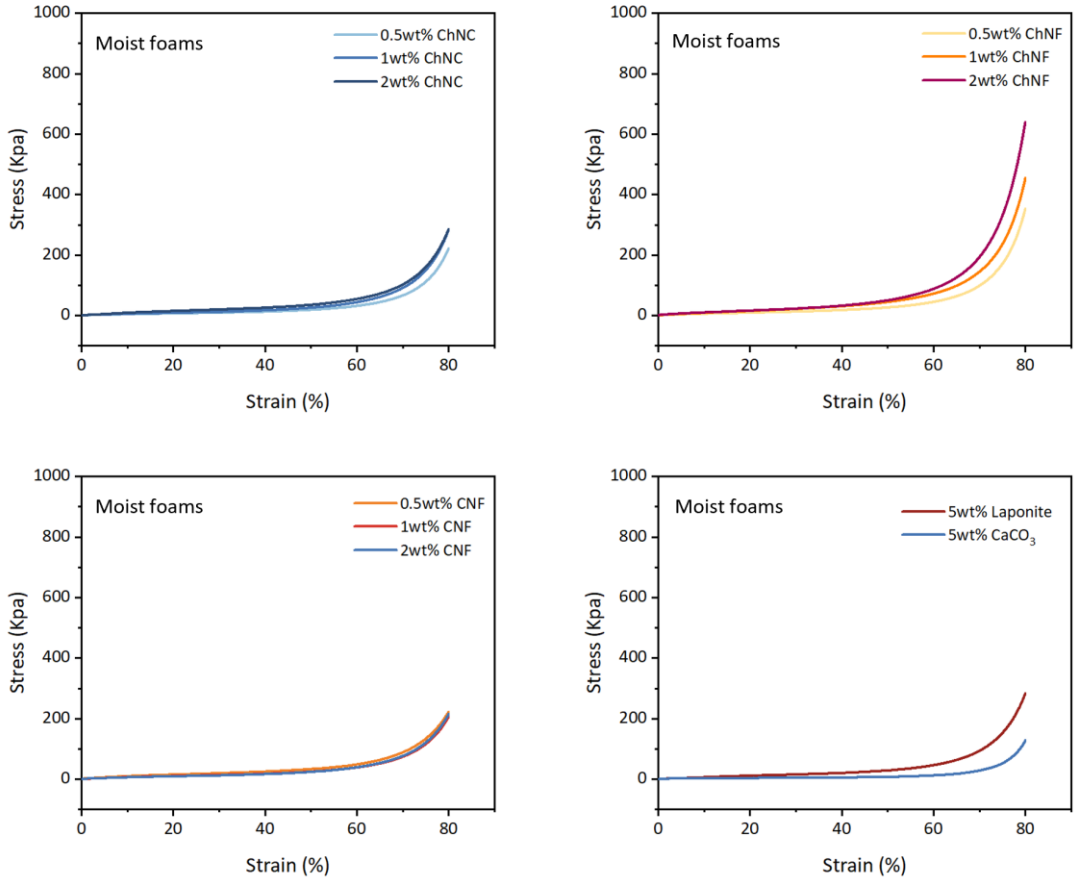

Figure VI.17.Stress vs Strain curves of NIPU foams loaded with the different bio-nanofillers (ChNF, CNF, ChNC), Laponite and $CaCO_3$ in moist conditions.

3. Conclusions

This chapter demonstrated the successful fabrication of flexible water-blown non-isocyanate polyurethane (NIPU) foams and systematically investigated the effects of bio-based nanofillers and inorganic fillers on their structure and properties. The formulation strategy, based on the combination of TMPTC and EO-TMPTC cyclic carbonates with liquid m-xylylenediamine (MXDA), enabled the direct dispersion of chitin nanocrystals (Ch-NC), chitin nanofibers (Ch-NF), and cellulose nanofibers (C-NF) without the need for organic solvents. Rheological studies revealed that the functional group ratio $[NH_2]/[CC]$ significantly affects the gelation time and, consequently, the processing window for foam fabrication. Additionally, it was found that increasing the initial viscosity of the formulation through a pre-curing step (5 min at 80°C) promoted the formation of more stable cellular structures by providing sufficient matrix strength to prevent cell collapse during gas expansion. The optimal water content was determined to be 0.15 equivalents, which provided the best balance between CO_2 generation

and network formation, yielding foams with homogeneous cellular morphology and high gel content (96%).

A key finding of this work was the plasticizing effect of bio-nanofillers on the thermal properties of the flexible PHU foam matrix. The incorporation of chitin and cellulose nanoparticles resulted in a systematic decrease in glass transition temperature, from 23°C for the neat foam to 7–18°C for bio-nanofiller-containing foams. This phenomenon was attributed to competitive hydrogen bonding between the hydroxyl-rich nanofiller surfaces and the pendant -OH groups of the PHU matrix, which disrupts the internal hydrogen bonding network and increases chain mobility, consequently lowering T_g.

The mechanical characterization revealed concentration-dependent reinforcement within each bio-nanofiller series. Chitin nanofibers demonstrated the most pronounced enhancement, with the compressive modulus increasing by 165% and the stress at 70% strain increasing 2.5-fold when comparing 0.5 and 2 wt% loadings. The hierarchy of reinforcement efficiency at 2 wt% followed the order Ch-NF > C-NF > Ch-NC, highlighting the importance of nanofiller morphology and aspect ratio over surface chemistry in determining mechanical response. These findings demonstrate that the plasticizing effect on T_g and the mechanical reinforcement are independent phenomena, and that bio-nanofillers can serve as effective reinforcements in flexible NIPU foams when appropriately designed. As a perspective, from a solid-state physics point of view, future work could explore the influence of filler geometry on mechanical reinforcement efficiency. Parameters such as aspect ratio and percolation threshold could play a significant role in the stress transfer mechanisms.

Appendix A.VI

Figures

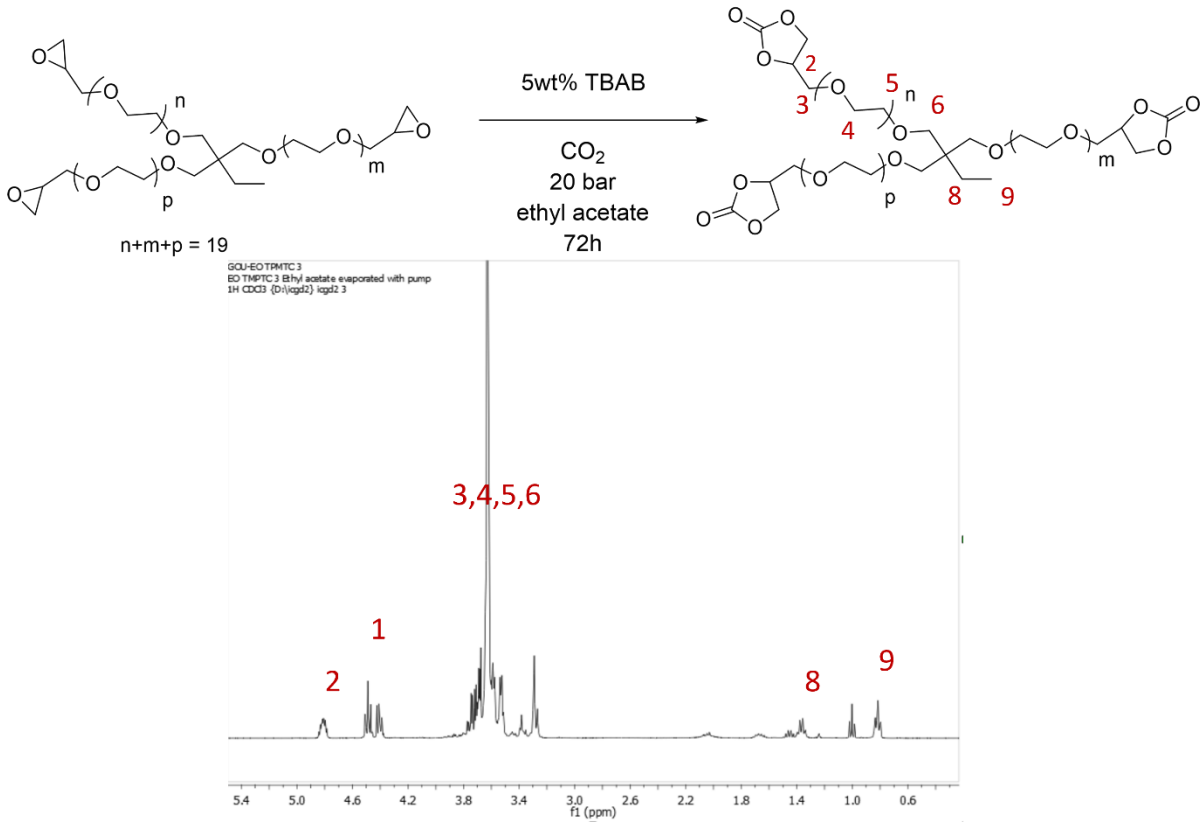

Figure A.VI.1. Synthesis of EO-TMPTC and ^{1}HNMR spectrum of EO-TMPTC. CEW = 470 g/mol.

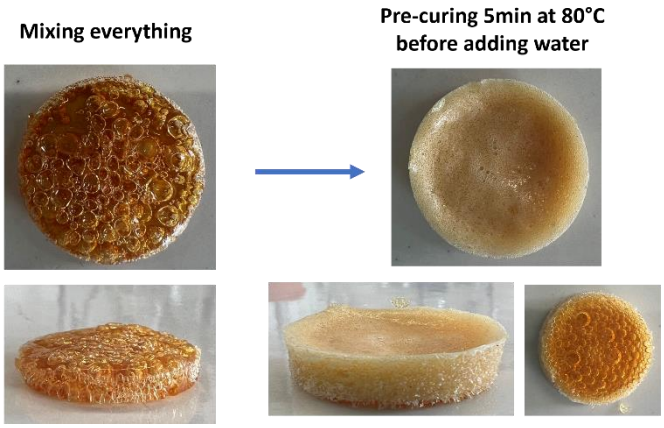

Figure A.VI.2. Preliminary tests: Effect of pre-curing 5min at 80°C before adding water to induce foaming at 100°C.

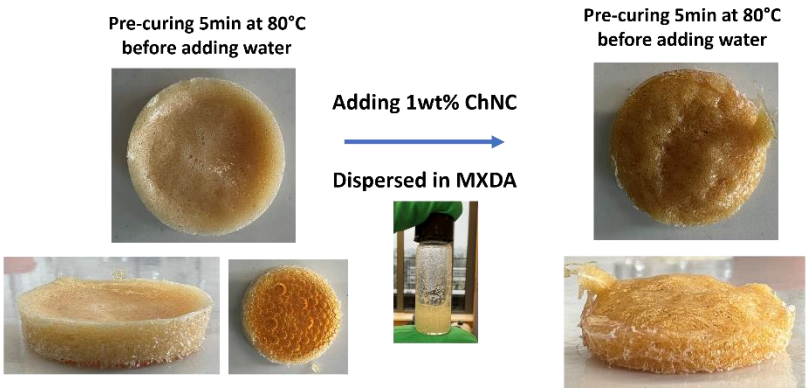

Figure A.VI.3. Preliminary tests: Effect of adding and dispersing ChNC in MXDA in the resulting NIPU foam. Conditions: Pre-curing 80°C for 5min, followed by water addition and foaming at 100°C for 5h.

Tables

Table A.VI.1 Quantity in grams used for each component in the formulation.

Compound	Mass (g)
TMPTC	2.000
EO-TMPTC	1.336
MXDA	0.840
DBU	0.110
H_2O	0.039
Total	4.326

Procedure A.VI.1 Equation to calculate the biofiller mass

For 0.5wt% Chitin nanocrystals:

$$wt\% = \frac{x}{(\mathrm{x} + \mathrm{m1})} x100$$

$$0.5 = \frac{x}{(\mathrm{x} + 4.326\ \mathrm{g})} x100$$

$x = 0.022$ g

Where m_1 = sum of the all precursors; wt% = Biofiller content desired in the formulation

Bio-filler content (wt%)	Mass (g)
0.5	0.022
1	0.044
2	0.088

Chapter VII

Conclusions and Perspectives

Polyurethane foams have become indispensable materials in modern society, dominating the market for thermal insulation, construction, transportation, packaging, and comfort goods due to their exceptional versatility and tuneable properties. However, their conventional production presents inherent drawbacks related with increasingly difficulties to reconcile with contemporary environmental and health standards. On one hand, the PU synthesis is relied on the use of isocyanates, compounds associated with occupational health hazards that have prompted increasingly stringent European regulations. On the other hand, the foaming process has historically employed physical blowing agents such as chlorofluorocarbons and hydrofluorocarbons, whose their detrimental environmental impact has driven the search for greener alternatives. While significant progress has been made toward identifying more sustainable blowing agents, the reliance on isocyanates persists as a pressing challenge for industries. In this context, polyhydroxyurethanes (PHU), synthesized through the aminolysis of cyclic carbonates, have emerged as one of the most promising candidates to address these concerns. Despite significant advances in PHU chemistry over the past decade, the translation of these materials into industrially relevant foam products has remained limited.

Therefore, this thesis addresses these concerns and proposes breakthrough strategies for the sustainable fabrication of thermosetting NIPU foams, addressing the dual challenge of eliminating hazardous precursors while establishing viable processing routes for NIPU cellular materials. Rather than focusing on a single foaming approach, this research explored both physical and chemical blowing strategies, by incorporating functional enhancements and sustainable bio-based nano-fillers to modulate foam properties and expand the application scope of NIPU foam technology.

The first part of this thesis established a foaming platform exploiting supercritical carbon dioxide as physical blowing agent. The principal challenge resided in identifying the processing parameters that would enable the efficient fabrication of thermosetting NIPU foams. Rheological analysis proved essential in identifying the processing window where the resin remained sufficiently fluid for expansion yet crosslinked enough to stabilize the cellular structure. The successful fabrication of rigid foams through this batch absorption-desorption approach validated the compatibility between PHU chemistry and $scCO_2$ processing, a combination that had not been previously demonstrated for thermosetting systems. Additionally, these foams exhibited humidity-responsive shape memory behavior arising from water-induced plasticization of the hydroxyl-rich PHU network, illustrating how the unique chemical structure of polyhydroxyurethanes can enable stimuli-responsive functionalities.

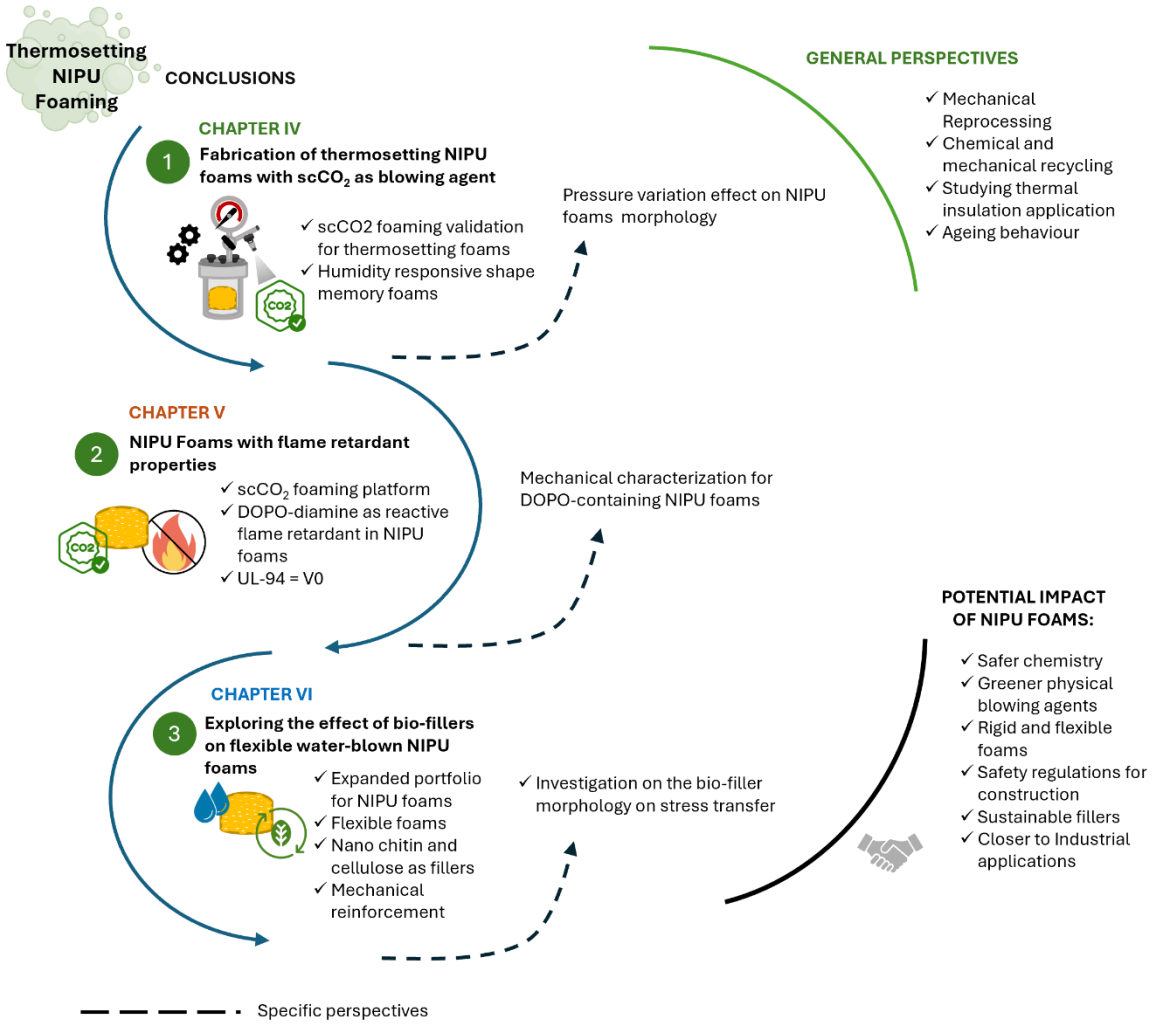

Figure VIII. 1. Conclusions and perspectives of this work

Building upon this established platform, the second part of this thesis addressed flame retardancy through a reactive strategy wherein a DOPO-derived diamine was employed as a reactive flame retardant, ensuring intimate incorporation of phosphorus moieties into the NIPU polymer backbone. The mechanistic investigation of DOPO-diamine reactivity toward five-membered cyclic carbonates revealed that this sterically hindered aromatic amine behaves as a soft nucleophile, promoting decarboxylative pathways at elevated temperatures. This understanding could establish selection criteria for functional amine co-monomers in future NIPU formulations. The thermal and fire characterization confirmed the effectiveness of the gas-phase radical scavenging mechanism, achieving significant reductions in heat release and self-extinguish behaviour in less than 2 seconds, achieving a V-0 classification in UL-94 testing. These findings demonstrated a viable pathway toward regulatory compliance in

construction applications, where fire safety requirements represent a prerequisite for material adoption.

The third part of this thesis expanded the material portfolio toward flexible water-blown foams, addressing a significantly larger market segment while exploring the incorporation of renewable bio-based nanofillers into NIPU foams. The systematic study of chitin and cellulose nano-particles revealed that these bio-nanofillers exhibited a pronounced plasticizing effect on the PHU matrix. This behavior was attributed to competitive hydrogen bonding between the hydroxyl-rich filler surfaces and the pendant hydroxyl groups of the polymer chains, disrupting the internal network of secondary interactions that governs the thermal properties of neat PHU materials. Mechanical characterization demonstrated that reinforcement in terms of compression modulus occurred in a concentration-dependent manner, independently of the thermal plasticization, with nanofiller morphology emerging as the dominant factor governing mechanical response.

In conclusion, this thesis successfully demonstrated the development of novel thermosetting NIPU foams through isocyanate-free strategies, complementing sustainable processing routes with a new portfolio of functional materials. The progression from $scCO_2$-blown rigid foams with shape memory properties, through flame-retardant formulations for construction applications, to flexible water-blown foams reinforced with bio-based nanofillers, illustrates the capacity of PHU chemistry to address diverse material requirements. These contributions provide a foundation toward narrowing the gap between emerging NIPU foam technology and industrially relevant applications.

The findings of this thesis open several avenues for future research that merit consideration. With respect to $scCO_2$-blown foams, further investigation into the effect of saturation pressure on cell size and morphology would provide greater control over foam microstructure. In parallel, optimization of impregnation time could significantly reduce processing cycles, thereby enhancing the industrial viability of this approach.

Concerning flame-retardant NIPU foams, the influence of DOPO-diamine incorporation on mechanical properties warrants systematic evaluation, as the rigid aromatic structure may affect network flexibility. Moreover, long-term stability studies under accelerated aging conditions, including thermal, hydrolytic and UV aging, would be essential to validate the durability of reactive approach for construction applications.

With regard to bio-nanofiller-reinforced flexible foams, a more comprehensive investigation into the role of nanoparticle morphology on stress transfer mechanisms from a physical standpoint would further elucidate the structure-property relationships governing mechanical reinforcement in PHU matrices.

From a broader perspective, reprocessing studies of the developed foams would contribute to understanding the effect of DOPO-diamine and bio-nanofillers on the dynamic network rearrangements characteristic of PHU systems. In this regard, exploring both mechanical and chemical recycling approaches would further align NIPU foam technology with the sustainability goals and circular economy principles. Additionally, the study of thermal insulating performance for building applications should be addressed, including the assessment of aging behaviour related to gas release and long-term mechanical and chemical stability. Finally, a significant challenge that remains to be addressed is the reduction of foam density. Achieving lower densities comparable to conventional PU foams has not yet been accomplished with PHU networks and represents a critical milestone toward industrial competitiveness.

Chapter VIII

Experimental part

1. Materials

Trimethylolpropane triglycidyl ether (TMPT) and Tetrabutylammonium bromide (TBAB) (purity 99 %) were purchased from Sigma-Aldrich (Darmstadt,Germany). Polypropylene glycol, α,ωbis(cyclocarbonate) (PPOBC) was acquired from Specific Polymers (France). Polyglycidyl ether of ethoxylated trimethylolpropane (EO-TMPTE or IPOX CL60) was kindly supplied by Ipox chemicals. *M*-Xylylenediamine (MXDA) was purchased from TCI. Laponite, Tegostab E-8930, Tegostab E-8158 were kindly supplied by Evonik. Ethyl acetate and tetrahydrofuran were purchased from VWR international S.A.S. 4.4'-diaminobenzophenone (DABP) was purchased at Sigma and 9,10-Dihydro-oxa-10-phosphaphenanthrene-10-oxide (DOPO) was purchased at TCi. Cellulose nanofibers were obtained from Celabor. Ethyl acetate and tetrahydrofuran were purchased by VWR international S.A.S. The NMR solvent $CDCl_3$ was from Eurisotop. The NMR solvent $CDCl_3$ was from Eurisotop. CO_2 (Alphagaz CO_2 SFC, ≥ 99.998%) was purchased from Air Liquide.

2. Syntheses

2.1. Synthesis of 4,4'-(((2-ethyl-2-(((2-oxo-1,3-dioxolan-4-yl)methoxy)methyl)propane-1,3-diyl)bis(oxy))bis(methylene))bis(1,3-dioxolan-2-one) (TMPTC)

Trimethylolpropane triglycidyl ether (TMPTE; 150 g, 0.50 mol) was poured into a 600 mL hastelloy pressure reactor (Parr Instrument Company) with tetrabutylammonium bromide (TBAB; 3.75 g, 0.012 mol) and solubilized in 150 mL of ethyl acetate. The reaction was performed at 80 °C for 96 h at a constant CO_2 pressure of 20 bar. The crude solution was washed 3 times with water and 2 times with brine to remove TBAB. Magnesium sulphate was added to remove the residual water and, ethyl acetate was removed under vacuum at room temperature to obtain a yellowish viscous liquid (yield = 95%). CEW = 191 $eq.mol^{-1}$. ^{1}HNMR (400 MHz, $CDCl_3$, ppm): δ = 0.84 (t, 3H, CH_3), 1.41 (m, 2H, CH_2-CH_3), 3.28-4.03 (m, 6H, Cq-CH_2), 4.46 (m, 3H, CH_2-O(C=O)-O), 4.49 (t, 3H, CH_2-O(C=O)-O), 4.85 (m, 3H, CH-O(C=O)-O).

2.2 Synthesis of ethoxylated trimethylolpropane cyclic carbonate (EO-TMPTC)

Polyglycidyl ether of ethoxylated trimethylolpropane (101 g) was introduced into a 600 mL hastelloy pressure reactor (Parr Instrument Company) along with tetrabutylammonium bromide (TBAB; 5wt% relative to the epoxy, 5.075g) and dissolved in ethyl acetate. The reactor was placed in the appropriate heating jacket and heated to 80 °C. CO_2 was then injected into the reactor until a pressure of 20 bar was reached. The reaction was carried out for approximately 96 h, with periodic CO_2 reloading to maintain the pressure at 20 bar when any

decrease was observed. After completion, the crude product was recovered and washed three times with water, followed by two washing steps with brine to ensure complete removal of the catalyst. Residual water was removed by addition of anhydrous magnesium sulfate. The ethyl acetate was evaporated using a rotary evaporator, and the final product was placed under high vacuum to remove trace solvent, yielding a viscous liquid. CEW = 470 $g.eq^{-1}$. ^{1}HNMR (400 MHz, $CDCl_3$) = δ /ppm = 4.75 (2-CH), 4.43 (1-CH_2), 4.37 (1′-CH_2), 4.00–3.18 (3/4/5/6-CH_2), 1.30 (8-CH_2), 0.76 (9-CH_3).

2.3. Synthesis of DOPO-diamine

In a 25 mL two-necked flask, 0.5 g of 4.4'-diaminobenzophenone (DABP) (2.36 mmol), 3.06 g of 9,10-dihydro-9-oxa-10-phosphaphenanthrene10-oxide DOPO (14.13 mmol) were stirred under a nitrogen atmosphere for 4 hours at 180°C. The product obtained was cooled to 100°C and then 20mL of toluene was added. Consequently, the mixture was filtered and the powder product obtained was recrystallized from THF, filtered and washed with ethanol. The product was dried under vacuum overnight at 40°C. Finally, a white/yellowish powder was obtained with a 72% yield. ^{1}HNMR (400 MHz, DMSO-d_6, δ ppm): 4.86 (b, 4H), 5.77(s, 1H), 5.82-5.95 (m, 3H), 6.63-6.87 (m, 5H), 7.05-7.13 (m, 3H)m 7.25-7.30 (m, 2H), 7.54 (m, 2H), 7.65-7.70 (m, 3H), 7.76-7.79 (m, 1H), 7.91-7.93 (m, 2H), 8.17 (s, 1H), 8.63 (s, 1H). ^{31}P NMR (400 MHz, DMSO-d_6, δ ppm): 31.78, 30.12.

2.4. Preparation of Partially Deacetylated Chitin Nanocrystals (ChNCs)

Partially deacetylated chitin nanocrystals were prepared from squid pen through a multistep process from the methodology reported by Wijeratne et al.[262] Firstly, raw powdered squid pen was demineralized by immersion in 1 M HCl at room temperature for 12 h, followed by thorough rinsing with deionized water. Subsequently, the sample was treated in 1 M NaOH at room temperature for 12 h to remove residual proteins, and then rinsed again with deionized water. This acid-base treatment cycle was repeated three times to ensure complete purification. The isolated β-chitin was then dried at 60 °C in a vacuum oven prior to partial deacetylation.

To increase the content of amine groups on the chitin surface, 1 g of the isolated β-chitin was suspended in 25 mL of 33 wt% NaOH aqueous solution and heated at 90 °C for 4 h under continuous stirring. The partially deacetylated chitin was collected and thoroughly washed with deionized water through repeated centrifugation cycles at 4100g for 15 min until a neutral pH was reached. Finally, the deacetylated chitin was suspended in water and mechanically disintegrated through repeated ultrasonication (Branson SFX550 Sonifier) until a stable turbid

aqueous suspension of chitin nanocrystals was obtained. The suspension was freeze-dried to obtain dry ChNC.

The degree of deacetylation (DDA) was determined by conductometric titration to be approximately 35%, corresponding to an amine group content of 1.85 mmol/g.

2.5. Preparation of chitin nanofibers (ChNF)

Chitin nanofibers (ChNF) were prepared from lobster exoskeleton (*Homarus Americanus*) following the procedure described by Mushi et al.[266]

The extraction process consisted of three sequential steps. Firstly, demineralization of the exoskeleton was performed by treatment with 2M HCl for 2 hours at room temperature, using a ratio of 15 mL of acid per gram of material. Subsequently, depigmentation was carried out by immersing the material in 96% ethanol for 12 hours under stirring. Finally, deproteinization was accomplished by treatment with 20% (w/w) NaOH for 2 weeks at room temperature (23°C). Between each step, the material was thoroughly washed with deionized water until neutral pH was reached.

For mechanical disintegration, the treated material was suspended in 1-4% (v/v) acetic acid and stirred for 12 hours to obtain a 1% (w/w) colloidal suspension at pH 3. The suspension was pre-homogenized using a high-speed blender and subsequently processed through a high-pressure homogenizer (Microfluidizer M-110EH, Microfluidics Inc., USA). The homogenization process comprised five passes through 400 and 200 µm interaction chambers at a pressure of 900 bar, followed by five additional passes through 200 and 100 µm chambers at 1600 bar.

The aqueous ChNF suspension was freeze-dried to obtain dry chitin nanofibers, which were subsequently dispersed in the amine component for foam preparation.

The nanofibers exhibited an average diameter of 3-4 nm, lengths between 700-1000 nm, and an aspect ratio of approximately 250. The residual protein content was 4.7% and the degree of acetylation was 86%.

3. Foam preparation

3.1. General procedure for thermoset NIPU foam fabrication using supercritical CO_2 as a blowing agent in batch mode

Typically, a carbonate mixture (trifunctional and bifunctional) and additives (5wt% of Laponite relative to the total resin mass or 0.5wt% (relative to the cyclic carbonate mixture mass) were weighed and placed in a 5 mL plastic pot. This mixture was mixed for 3 minutes at room temperature in a speed mixer at 2500 rpm to obtain a homogeneous mixture. Then, the diamine was added to the carbonate mixture and mixed again in the speed mixer for 3 minutes at room temperature at 2500 rpm. The formulation was then transferred to a 27 mm diameter, and 12 mm height open circular silicon mold (wall thickness = 1mm). The mold was placed in a 100 mL stainless steel reactor (Parr Instrument Company) equipped with a 130-bar rupture disk, and sealed. The reactor was then filled at room temperature (liquid CO_2) with 73 ml of CO_2 (vapor pressure of liquid CO_2 of about P=59 ± 1 bar at T=22 ± 1 °C in the reactor) using an ISCO syringe pump (model 260D) thermostated at 40°C and operating under the constant pressure mode set at 150 bar (77 mL of CO_2 at 40°C and 150 bar, thus a CO_2 density of 0.78023 g/mL, corresponding to a delivered mass of CO_2 of 60.07 g [267]) (Figure VIII.1). Subsequently, the reactor was heated up to 45°C to reach supercritical CO_2 domain with a final pressure of 100 bar. The sample was saturated with $scCO_2$ for about 90 min under these conditions. Then, the reactor was cooled down to 0°C with an ice bath and quickly depressurized (in about 2 minutes). Finally, the CO_2-saturated sample was heated in an oven under air at 80, 100 or 140°C to tune up the simultaneous temperature-induced CO_2 desorption and crosslinking processes.

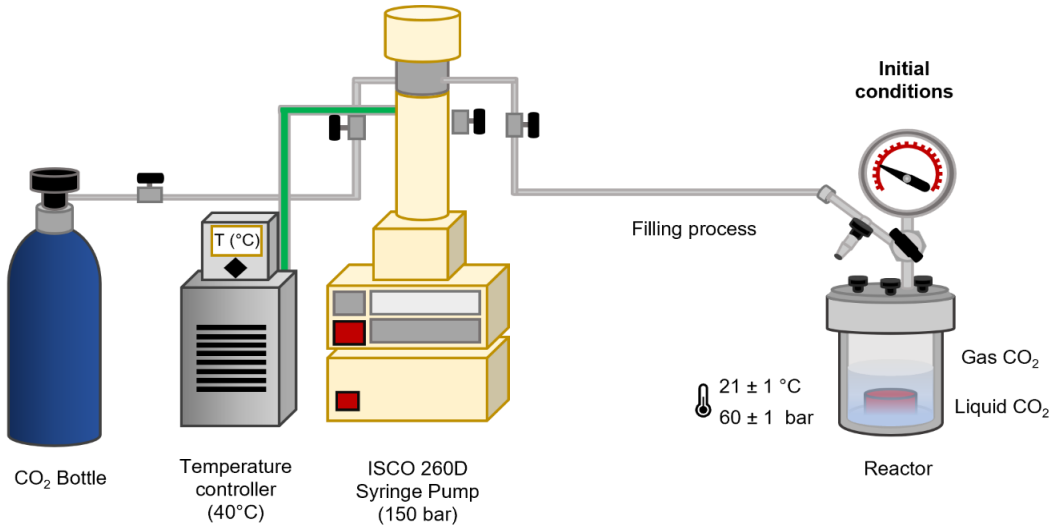

Figure VIII.1. Experimental set-up conditions to fill up the reactor with CO_2

3.2 General procedure for batch fabrication of thermoset NIPU foams with DOPO using supercritical CO_2 as a blowing agent

A carbonate mixture (trifunctional and bifunctional) was weighed and poured in a 5mL plastic pot and mixed for 3 minutes at room temperature in the speed mixer at 2500 rpm to ensure a homogeneous mixture. Then, the diamines (MXDA and DOPO-Diamine) were mixed together and then added to the carbonate mixture and mixed again in the speed mixer for 3 minutes at room temperature at 2500 rpm. The formulation was then transferred to a 27 mm diameter, and 12 mm height open circular silicon mold (wall thickness = 1mm). The mold was placed in a 100 mL stainless steel reactor (Parr Instrument Company) equipped with a 130-bar rupture disk, and sealed. The reactor was then filled at room temperature (liquid CO_2) with 73 ml of CO_2 (vapor pressure of liquid CO_2 of about P=59 ± 1 bar at T=22 ± 1 °C in the reactor) using an ISCO syringe pump (model 260D) thermostated at 40°C and operating under the constant pressure mode set at 150 bar (77 mL of CO_2 at 40°C and 150 bar, thus a CO_2 density of 0.78023 g/mL, corresponding to a delivered mass of CO_2 of 60.07 g [267]). Subsequently, the reactor was heated up to 45°C to reach supercritical CO_2 domain with a final pressure of 100 bar. The sample was saturated with scCO_2 for about 90 min under these conditions. Then, the reactor was cooled down to 0°C with an ice bath and quickly depressurized (in about 2 minutes). Finally, the CO_2-saturated sample was heated in an oven at 100°C for 3 hours and 180°C for 2 hours to tune up the simultaneous temperature-induced CO_2 desorption and crosslinking processes.

3.3. General procedure for batch fabrication of flexible water-blown NIPU foams using bio-based nanofillers (ChNC, ChNF, CNF) and inorganic fillers.

For the fabrication of flexible water-blown foams, a cyclic carbonate mixture consisting of EO-TMPTC (40 wt%) and TMPTC (60 wt%) was weighed and transferred into a cubic aluminum mold. The mixture was manually stirred for approximately 1 min. Subsequently, the catalyst (DBU) and diamine (MXDA) were added to the cyclic carbonate blend and mixed for an additional minute to ensure homogeneity. The resulting monomer mixture was pre-cured at 80 °C for 5 min. Water was then added as a chemical blowing agent and manually mixed for 1 min. Finally, the formulation was cured and foamed at 100 °C for 5 h.

For foams containing chitin nanocrystals (ChNC) or chitin nanofibers (ChNF) at loadings of 0.5, 1, or 2 wt% (relative to the total formulation), the chitin-based nanofillers were first dispersed in MXDA using tip sonication until a paste-like consistency was achieved with no visible white particles. This nanofiller-MXDA dispersion was then used in place of neat MXDA, following the procedure described above.

For foams loaded with cellulose nanofibers (CNF) at 0.5, 1, or 2 wt%, or with Laponite or $CaCO_3$ at 5 wt%, the fillers were directly incorporated into the cyclic carbonate mixture prior to the addition of catalyst and diamine, and the foaming protocol proceeded as previously described.

4. Characterizations

4.1.Nuclear Magnetic resonance

Nuclear Magnetic Resonance (^1H, ^{31}P, ^{13}C NMR) analyses were performed using a Bruker Avance 400 MHz Spectrometer at 25°C. All ^1H-NMR samples were dissolved in $CDCl_3$. Shifts are given in ppm.

4.2.TMPTC Titration of the carbonate equivalent weight by ^{1}HNMR

The Carbonate Equivalent Weight (CEW, $g.eq^{-1}$)) was calculated by ^{1}HNMR technique. Benzophenone was used as an internal standard. In an NMR tube, both known masses in monomer and benzophenone were introduced and dissolved in 600 µL of $CDCl_3$. Then, the CEW was determined using the following equation:

$$CEW = \frac{I1 \text{ x } H_{carbonate}}{I2 \text{ x } H_{PhCOPh}} \times \frac{m_{carbonate}}{m_{PhCOPh}} \times M_{PhCOPh}$$

Where I1 is the integration of the signal corresponding to CH of benzophenone (7.4 ppm); I2 is the integration of the signal corresponding to CH of carbonate (4.8 ppm); $H_{carbonate}$ is the number of carbonate protons; H_{PhCOPh} is the number of protons related to benzophenone; $m_{carbonate}$ is the product mass; m_{PhCOPh} is the benzophenone mass; and M_{PhCOPh} is the Benzophenone molar mass. CEW = 191 $g.eq^{-1}$

4.3. EO-TMPTC titration of the carbonate equivalent weight by ^{1}HNMR

The Carbonate Equivalent Weight (CEW, $g.eq^{-1}$)) was calculated by ^{1}HNMR technique. Benzophenone was used as an internal standard. In an NMR tube, known mass of monomer and benzophenone were introduced and dissolved in 600 µL of $CDCl_3$. Then, the CEW was determined using the following equation:

$$CEW = \frac{I1 \text{ x } H_{carbonate}}{I2 \text{ x } H_{PhCOPh}} \times \frac{m_{carbonate}}{m_{PhCOPh}} \times M_{PhCOPh}$$

Where I1 is the integration of the signal corresponding to CH of benzophenone (7.4 ppm); I2 is the integration of the signal corresponding to CH of carbonate (4.75 ppm); $H_{carbonate}$ is the number of carbonate protons; H_{PhCOPh} is the number of protons related to benzophenone;

$m_{carbonate}$ is the product mass; m_{PhCOPh} is the benzophenone mass; and M_{PhCOPh} is the Benzophenone molar mass. CEW = 470 $g.eq^{-1}$

4.4.Fourier transform infrared spectroscopy

Infrared spectroscopy spectra were recorded on a Bruker IFS 66v/S spectrometer equipped with an attenuated total reflectance cell (ATR). Spectra were obtained in transmission mode with 32 scans and 4 cm^{-1} resolution in the 600-4000 cm^{-1} range.

4.5.Differential scanning calorimetry

Differential scanning calorimetry (DSC) analyses were performed using a thermal analyzer NETZSCH DSC200F3 for samples from Chapter V. Calibration was performed using Indium under N_2 flow. Approximately, samples of 5-6 mg were introduced in a pierced lid aluminum pan. The analyses were conducted at a heating rate of 10°C/min between -40°C and 150°C. The dried foams were conditioned using a first ramp from 25°C to 80°C and a 5-minute isothermal treatment at 80 °C. Then the T_g of the dried foams were measured from the second ramp.

To study the reactivity of DOPO-diamine and TMPTC (Chapter VI), the monomers were mixed and a sample of approximately 5 mg was introduced in a high-pressure pan and the analysis was recorded from room temperature to 220°C at 10°C.min^{-1}.

DSC analyses for NIPU foams with DOPO-diamine (Chapter VI) and water-blown NIPU foams (Chapter VII) were recorded on a Q2000 thermal analyzer from TA instruments calibrated with high purity Indium and operating under N_2. Samples of 5-6 mg were introduced in a pierced lid aluminum pan. The analyses were conducted at a heating rate of 10°C/min between -40°C and 80°C. The dried foams were conditioned using a first ramp from 25°C to 80°C and a 5-minute isothermal treatment at 80 °C. Then the T_g of the dried foams were measured from the second ramp.

4.6.Gel content

Three samples of approximately 300 mg of the same foam, were weighed and immersed in THF for 24 hours. Consequently, the samples were dried under vacuum at 70°C for 16 hours. The gel content (GC) was calculated using the following equation:

$$GC\ (\%) = 100\ \times \frac{m_1}{m_0}$$

Where m_0 is the initial mass of the foam sample before immersion and m_1 is the mass after immersion and drying

4.7.Effective or apparent Density

Effective density was assessed using a gravimetric method by cutting cubes of approximately 10 mm^3. They were measured and weighed. The density* was calculated by dividing the mass by the volume. Each foam density was measured in triplicate and the density reported is the mean of the three measurements.

4.8. Water uptake

Three samples of each foam were previously dried under vacuum at 80°C overnight and weighed (m_2). Then, the foams were placed in a desiccator with a saturated KCl solution with approximately 85% relative humidity for 48 hours and weighed again (m_3). The water content (WC) percentage absorbed by the foams was calculated by the following equation:

$$WC = \frac{m_3 - m_2}{m_2} \times\ 100$$

The water content uptake overtime in the shape memory material section was measured using thermogravimetric analysis, and the average value of three measurements is reported.

4.9. Scanning electron microscopy

NIPU foam cell morphology images were analyzed using scanning electron microscopy (SEM). All the images were acquired using a FEI QUANTA 200 FEG. The pore sizes of around 100 cells were measured using imageJ software.

4.10. Thermogravimetric analysis

Thermogravimetric analyses were performed on a Netzsch TG 209TG 209F1 with a nitrogen flow of 40 $mL.min^{-1}$ for the sample atmosphere (and 20 $mL.min^{-1}$ nitrogen flow of protective

*The term “density” will be used throughout the main text.

gas for the balance protection) for all samples obtained in Chapter V and VI. Q500 thermal analyzer from TA instruments under N_2 flow

Samples of around 10 mg were placed in an aluminum pan and the weight loss was analyzed upon heating the samples from room temperature to 600°C at a heating rate of 10°C.min^{-1}.

4.11.Compression test

The compression tests were performed using an INSTRON machine for Chapter IV, and ZweckRoell tensile Z2.5 for Chapter VI. Compression was done on cubic samples of around 1cm^3 at a fixed rate of 10%.min^{-1} at room temperature. The compression modulus was calculated using the beginning of the linear range (0-10% strain) of stress-strain curve slope.

4.12 .Recovery ratio percentage

The recovery ratio (Rr) of the NIPU foams was calculated from the different heights of the foam before and after recovery using the initial height (initial temporary shape) and recovered height upon exposure to humidity. The recovery ratio was calculated using the following equation:

$$Rr\ (\%) = \frac{H_{recovered} - H_{compressed}}{H_{original} - H_{compressed}}$$

Where $H_{recovered}$ is the height of the foam exposed to humidity overtime; $H_{compressed}$ is the height of the foam after compression and before exposure to humidity. $H_{original}$ is the original height of the foam before being compressed.

4.13. Rheological measurements

The rheological behavior of the reactive mixtures during curing was investigated using an Anton Paar Modular Compact Rheometer MCR 302. Measurements were performed in oscillatory mode using a parallel plate geometry with 25 mm diameter disposable aluminum plates and a gap of 1 mm. Small amplitude oscillatory shear (SAOS) tests were conducted at a constant strain amplitude of 2% and an angular frequency of 6.28 rad/s (1 Hz). Approximately 2 g of monomer mixture was loaded onto the preheated lower plate, and the upper plate was lowered to the measurement position. Isothermal time sweep experiments were performed at selected temperatures to monitor the evolution of the storage modulus (G'), loss modulus (G''), and complex viscosity (η*) as a function of curing time. The gel point was determined from the crossover of G' and G''

4.14. UL-94

Vertical burning tests (UL-94) were performed using a butane torch with 2.5cm inner blue flame. Samples were placed 2.5 cm from the torch and the flame was held for 10 seconds. After the first flame application, a second flame was held for other 10 seconds. All foams were round with a diameter of 27 mm and approximately 10 mm height.

4.15. Cone calorimetry

Flammability tests were performed using a cone calorimetry to study the fire behaviour. NIPU foams dimensions were 35x35 mm^2 and weighed around 3g. All samples were embedded in a 'rockwool mold' in each test. The samples were placed around 2.5 cm below the conic heater and then exposed to a 33 $kW.m^{-2}$ heat flux in ventilated conditions.[99] The ignition was produced by a spark igniter. Tests were performed in duplicate.

References

1. Steffen, W.; Richardson, K.; Rockström, J.; Cornell, S. E.; Fetzer, I.; Bennett, E. M.; Biggs, R.; Carpenter, S. R.; de Vries, W.; de Wit, C. A.; Folke, C.; Gerten, D.; Heinke, J.; Mace, G. M.; Persson, L. M.; Ramanathan, V.; Reyers, B.; Sörlin, S. Planetary Boundaries: Guiding Human Development on a Changing Planet. *Science (80-.).* **2015**, *347* (6223). https://doi.org/10.1126/science.1259855
2. Rockström, J.; Steffen, W.; Noone, K.; Persson, Å.; Chapin, F. S.; Lambin, E. F.; Lenton, T. M.; Scheffer, M.; Folke, C.; Schellnhuber, H. J.; Nykvist, B.; de Wit, C. A.; Hughes, T.; van der Leeuw, S.; Rodhe, H.; Sörlin, S.; Snyder, P. K.; Costanza, R.; Svedin, U.; Falkenmark, M.; Karlberg, L.; Corell, R. W.; Fabry, V. J.; Hansen, J.; Walker, B.; Liverman, D.; Richardson, K.; Crutzen, P.; Foley, J. A. A Safe Operating Space for Humanity. *Nature* **2009**, *461* (7263), 472–475. https://doi.org/10.1038/461472a
3. Research, G. V. *Polyurethane (PU) Foam Market Size, Share & Trends Analysis Report By Type (Flexible, Rigid, Spray), By End-use (Furniture & Bedding, Automotive, Construction), By Region, And Segment Forecasts, 2024 - 2030*. https://www.grandviewresearch.com/industry-analysis/polyurethane-foam-market (accessed 2025-04-20)
4. Research, I. *Polyurethane Foam Market Size, Share, Growth, and Industry Analysis, By Type (Rigid Foam,Flexible Foam), By Application (Bedding & Furniture,Transportation,Packaging,Construction,Others), Regional Insights and Forecast to 2034*. https://www.industryresearch.biz/market-reports/polyurethane-foam-market-111903 (accessed 2025-10-24)
5. Delavarde, A.; Savin, G.; Derkenne, P.; Boursier, M.; Morales-Cerrada, R.; Nottelet, B.; Pinaud, J.; Caillol, S. Sustainable Polyurethanes: Toward New Cutting-Edge Opportunities. *Prog. Polym. Sci.* **2024**, *151*, 101805. https://doi.org/10.1016/j.progpolymsci.2024.101805
6. Gama, N. V.; Ferreira, A.; Barros-Timmons, A. Polyurethane Foams: Past, Present, and Future. *Materials (Basel).* **2018**, *11* (10), 1841. https://doi.org/10.3390/ma11101841
7. Santos, M.; Mariz, M.; Tiago, I.; Alarico, S.; Ferreira, P. Bio-Based Polyurethane Foams: Feedstocks, Synthesis, and Applications. *Biomolecules* **2025**, *15* (5), 680.

https://doi.org/10.3390/biom15050680

8. Borowicz, M.; Paciorek-Sadowska, J.; Lubczak, J.; Czupryński, B. Biodegradable, Flame-Retardant, and Bio-Based Rigid Polyurethane/Polyisocyanurate Foams for Thermal Insulation Application. *Polymers (Basel).* **2019**, *11* (11). https://doi.org/10.3390/polym11111816
9. Hadała, B.; Zygmunt-Kowalska, B.; Kuźnia, M.; Szajding, A.; Telejko, T. Thermal Insulation Properties of Rigid Polyurethane Foam Modified with Fly Ash- a Comparative Study. *Thermochim. Acta* **2024**, *731* (June 2023). https://doi.org/10.1016/j.tca.2023.179659
10. Naldzhiev, D.; Mumovic, D.; Strlic, M. Polyurethane Insulation and Household Products – A Systematic Review of Their Impact on Indoor Environmental Quality. *Build. Environ.* **2020**, *169* (July 2019), 106559. https://doi.org/10.1016/j.buildenv.2019.106559
11. Szycher, M. *Szycher's Handbook of Polyurethanes*; CRC press, 1999.
12. European commission. REACH Regulation.
13. Anastas, P.; Eghbali, N. Green Chemistry: Principles and Practice. *Chem. Soc. Rev.* **2010**, *39* (1), 301–312. https://doi.org/10.1039/b918763b
14. Martínez de Sarasa Buchaca, M.; de la Cruz-Martínez, F.; Francés-Poveda, E.; Fernández-Baeza, J.; Sánchez-Barba, L. F.; Garcés, A.; Castro-Osma, J. A.; Lara-Sánchez, A. Synthesis of Nonisocyanate Poly(Hydroxy)Urethanes from Bis(Cyclic Carbonates) and Polyamines. *Polymers (Basel).* **2022**, *14* (13), 2719. https://doi.org/10.3390/polym14132719
15. Eaves (role)edt, D. *Handbook of Polymer Foams*; Shawbury, 2004.
16. *Natural Foam Blowing Agents Sustainable Ozone-and Climate-Friendly Alternatives to HCFCs*; Hasse, V., Ederberg, L., Croiset, I., Usinger, J., Eds.; Proklima International, 2012.
17. Bourguignon, M.; Grignard, B.; Detrembleur, C. Water-Induced Self-Blown Non-Isocyanate Polyurethane Foams. *Angew. Chemie Int. Ed.* **2022**, *61* (51). https://doi.org/10.1002/anie.202213422
18. Costanza, G.; Solaiyappan, D.; Tata, M. E. Properties, Applications and Recent Developments of Cellular Solid Materials: A Review. *Materials (Basel).* **2023**, *16* (22), 7076. https://doi.org/10.3390/ma16227076
19. Nizam, P. A.; Thomas, S. Innovations in Polymeric Foams and New Application Opportunities Including Energy and Energy Devices. In *Multifunctional Polymeric*

Foams; CRC Press, 2023; pp 181–196.

20. Reynolds, J. I.; Chrysler, L.; By, I. Automotive Cushioning through the Ages. **2008**.
21. G. Ron Blair; John I. Reynolds; Mark D. Weierstall. Automotive Cushioning Through The Ages: A Review. *Molded Polyurethane Foam Ind. Panel* **2008**, No. September, 1–64.
22. Wang, Z.; Wang, C.; Gao, Y.; Li, Z.; Shang, Y.; Li, H. Porous Thermal Insulation Polyurethane Foam Materials. *Polymers (Basel).* **2023**, *15* (18), 3818. https://doi.org/10.3390/polym15183818
23. Mistry, M.; Prajapati, V.; Dholakiya, B. Z. *Redefining Construction: An In-Depth Review of Sustainable Polyurethane Applications*; Springer US, 2024; Vol. 32. https://doi.org/10.1007/s10924-023-03161-w
24. MarketsandMarkets. *Polymer Foam Market*. https://www.marketsandmarkets.com/Market-Reports/foams-market-1011.html (accessed 2024-02-22)
25. Burgaz, E. *Polyurethane Insulation Foams for Energy and Sustainability*, 1st ed.; Advanced Structured Materials; Springer International Publishing: Cham, 2019; Vol. 111. https://doi.org/10.1007/978-3-030-19558-8
26. Alsuhaibani, A. M.; Refat, M. S.; Qaisrani, S. A.; Jamil, F.; Abbas, Z.; Zehra, A.; Baluch, K.; Kim, J.-G.; Mubeen, M. Green Buildings Model: Impact of Rigid Polyurethane Foam on Indoor Environment and Sustainable Development in Energy Sector. *Heliyon* **2023**, *9* (3), e14451. https://doi.org/10.1016/j.heliyon.2023.e14451
27. Herrington, R.; Hock, K. *Dow Polyurethanes*; 1997.
28. Chattopadhyay, D. K.; Raju, K. V. S. N. Structural Engineering of Polyurethane Coatings for High Performance Applications. *Prog. Polym. Sci.* **2007**, *32* (3), 352–418. https://doi.org/10.1016/j.progpolymsci.2006.05.003
29. Sawpan, M. A. Polyurethanes from Vegetable Oils and Applications: A Review. *J. Polym. Res.* **2018**, *25* (8), 184. https://doi.org/10.1007/s10965-018-1578-3
30. Tersac, G. Chemistry and Technology of Polyols for Polyurethanes. Milhail Ionescu. Rapra Technology, Shrewsbury, UK. *Polym. Int.* **2007**, *56* (6), 820. https://doi.org/https://doi.org/10.1002/pi.2159
31. Peyrton, J.; Avérous, L. Structure-Properties Relationships of Cellular Materials from Biobased Polyurethane Foams. *Mater. Sci. Eng. R Reports* **2021**, *145* (March). https://doi.org/10.1016/j.mser.2021.100608
32. S. N. Singh. *Blowing Agents for Polyurethanes*; Rapra Technology: Shawbury, UK,

2002.

33. UN Environment programme. *UN calls for urgent rethink as resource use skyrockets*. https://www.unep.org/news-and-stories/press-release/un-calls-urgent-rethink-resource-use-skyrockets (accessed 2025-01-21)
34. Maes, S.; Badi, N.; Winne, J. M.; Du Prez, F. E. Taking Dynamic Covalent Chemistry out of the Lab and into Reprocessable Industrial Thermosets. *Nat. Rev. Chem.* **2025**, *9* (3), 144–158. https://doi.org/10.1038/s41570-025-00686-7
35. Sardon, H.; Mecerreyes, D.; Basterretxea, A.; Avérous, L.; Jehanno, C. From Lab to Market: Current Strategies for the Production of Biobased Polyols. *ACS Sustain. Chem. Eng.* **2021**, *9* (32), 10664–10677. https://doi.org/10.1021/acssuschemeng.1c02361
36. Bakkali-Hassani, C.; Berne, D.; Ladmiral, V.; Caillol, S. Transcarbamoylation in Polyurethanes: Underestimated Exchange Reactions? *Macromolecules* **2022**, *55* (18), 7974–7991. https://doi.org/10.1021/acs.macromol.2c01184
37. Bothare, V. *Natural Oils Polyols Market Size: Industry Analysis & Forecast 2033*; 2024. https://straitsresearch.com/report/natural-oils-polyols-market
38. Li, Y.; Luo, X.; Hu, S. *Bio-Based Polyols and Polyurethanes*; SpringerBriefs in Molecular Science; Springer International Publishing: Cham, 2015. https://doi.org/10.1007/978-3-319-21539-6
39. Dworakowska, S.; Bogdal, D.; Prociak, A. Microwave-Assisted Synthesis of Polyols from Rapeseed Oil and Properties of Flexible Polyurethane Foams. *Polymers (Basel).* **2012**, *4* (3), 1462–1477. https://doi.org/10.3390/polym4031462
40. Seydibeyoğlu, M. Ö.; Misra, M.; Mohanty, A.; Blaker, J. J.; Lee, K.-Y.; Bismarck, A.; Kazemizadeh, M. Green Polyurethane Nanocomposites from Soy Polyol and Bacterial Cellulose. *J. Mater. Sci.* **2013**, *48* (5), 2167–2175. https://doi.org/10.1007/s10853-012-6992-z
41. Malani, R. S.; Malshe, V. C.; Thorat, B. N. Polyols and Polyurethanes from Renewable Sources : Past , Present and Future — Part 1 : Vegetable Oils and Lignocellulosic Biomass. *J. Coatings Technol. Res.* **2022**, *19* (1), 201–222. https://doi.org/10.1007/s11998-021-00490-0
42. Ha, M.; Eun, T.; Lee, Y. Production of Polyols and Polyurethane from Biomass : A Review. *Environ. Chem. Lett.* **2023**, *21* (4), 2199–2223. https://doi.org/10.1007/s10311-023-01592-4
43. Hu, S.; Luo, X.; Li, Y. Polyols and Polyurethanes from the Liquefaction of

Lignocellulosic Biomass. *ChemSusChem* **2014**, *7* (1), 66–72. https://doi.org/10.1002/cssc.201300760

44. Maisonneuve, L.; Chollet, G.; Grau, E.; Cramail, H. Vegetable Oils: A Source of Polyols for Polyurethane Materials. *OCL* **2016**, *23* (5), D508. https://doi.org/10.1051/ocl/2016031
45. Paananen, H.; Alvila, L.; Pakkanen, T. T. Hydroxymethylation of Softwood Kraft Lignin and Phenol with Paraformaldehyde. *Sustain. Chem. Pharm.* **2021**, *20* (September 2020), 100376. https://doi.org/10.1016/j.scp.2021.100376
46. Voirin, C.; Caillol, S.; Sadavarte, N. V; Tawade, B. V; Boutevin, B.; Wadgaonkar, P. P. Functionalization of Cardanol: Towards Biobased Polymers and Additives. *Polym. Chem.* **2014**, *5* (9), 3142–3162. https://doi.org/10.1039/C3PY01194A
47. Zhang, M.; Zhang, J.; Chen, S.; Zhou, Y. Synthesis and Fire Properties of Rigid Polyurethane Foams Made from a Polyol Derived from Melamine and Cardanol. *Polym. Degrad. Stab.* **2014**, *110*, 27–34. https://doi.org/10.1016/j.polymdegradstab.2014.08.009
48. Hu, Y.; Tian, Y.; Cheng, J.; Zhang, J. Synthesis of Eugenol-Based Polyols via Thiol–Ene Click Reaction and High-Performance Thermosetting Polyurethane Therefrom. *ACS Sustain. Chem. Eng.* **2020**, *8* (10), 4158–4166. https://doi.org/10.1021/acssuschemeng.9b06867
49. Vijayan, S. P.; John, B.; Sahoo, S. K. Modified Cardanol Based Colorless, Transparent, Hydrophobic and Anti-Corrosive Polyurethane Coating. *Prog. Org. Coatings* **2022**, *162*, 106586. https://doi.org/10.1016/j.porgcoat.2021.106586
50. Vahabi, H.; Rastin, H.; Movahedifar, E.; Antoun, K.; Brosse, N.; Saeb, M. R. Flame Retardancy of Bio-Based Polyurethanes: Opportunities and Challenges. *Polymers (Basel).* **2020**, *12* (6), 1234. https://doi.org/10.3390/polym12061234
51. Usman, A.; Zia, K. M.; Zuber, M.; Tabasum, S.; Rehman, S.; Zia, F. Chitin and Chitosan Based Polyurethanes: A Review of Recent Advances and Prospective Biomedical Applications. *Int. J. Biol. Macromol.* **2016**, *86*, 630–645. https://doi.org/10.1016/j.ijbiomac.2016.02.004
52. Ge, J.; Wu, R.; Shi, X.; Yu, H.; Wang, M.; Li, W. Biodegradable Polyurethane Materials from Bark and Starch. II. Coating Material for Controlled-release Fertilizer. *J. Appl. Polym. Sci.* **2002**, *86* (12), 2948–2952. https://doi.org/10.1002/app.11211
53. Zia, F.; Zia, K. M.; Zuber, M.; Kamal, S.; Aslam, N. Starch Based Polyurethanes: A Critical Review Updating Recent Literature. *Carbohydr. Polym.* **2015**, *134*, 784–798.

https://doi.org/10.1016/j.carbpol.2015.08.034

54. Lazaridou, A.; Biliaderis, C. G. Thermophysical Properties of Chitosan, Chitosan–Starch and Chitosan–Pullulan Films near the Glass Transition. *Carbohydr. Polym.* **2002**, *48* (2), 179–190. https://doi.org/https://doi.org/10.1016/S0144-8617(01)00261-2

55. Fernandes, S.; Freire, C. S. R.; Neto, C. P.; Gandini, A. The Bulk Oxypropylation of Chitin and Chitosan and the Characterization of the Ensuing Polyols. *Green Chem.* **2008**, *10* (1), 93–97. https://doi.org/10.1039/B711648A

56. National Research Council (US) Committee on Toxicology. *Emergency and Continuous Exposure Limits for Selected Airborne Contaminants: Volume 2.* https://www.ncbi.nlm.nih.gov/books/NBK208308/ (accessed 2025-02-23)

57. More, A. S.; Lebarbé, T.; Maisonneuve, L.; Gadenne, B.; Alfos, C.; Cramail, H. Novel Fatty Acid Based Di-Isocyanates towards the Synthesis of Thermoplastic Polyurethanes. *Eur. Polym. J.* **2013**, *49* (4), 823–833. https://doi.org/https://doi.org/10.1016/j.eurpolymj.2012.12.013

58. Morales-Cerrada, R.; Tavernier, R.; Caillol, S. Fully Bio-Based Thermosetting Polyurethanes from Bio-Based Polyols and Isocyanates. *Polymers (Basel).* **2021**, *13* (8), 1255. https://doi.org/10.3390/polym13081255

59. Çaylı, G.; Küsefoğlu, S. Biobased Polyisocyanates from Plant Oil Triglycerides: Synthesis, Polymerization, and Characterization. *J. Appl. Polym. Sci.* **2008**, *109* (5), 2948–2955. https://doi.org/10.1002/app.28401

60. Lemouzy, S.; Delavarde, A.; Lamaty, F.; Bantreil, X.; Pinaud, J.; Caillol, S. Lignin-Based Bisguaiacol Diisocyanate: A Green Route for the Synthesis of Biobased Polyurethanes. *Green Chem.* **2023**, *25* (12), 4833–4839. https://doi.org/10.1039/D3GC00704A

61. Olivito, F.; Jagdale, P.; Oza, G. Synthesis and Biodegradation Test of a New Polyether Polyurethane Foam Produced from PEG 400, L-Lysine Ethyl Ester Diisocyanate (L-LDI) and Bis-Hydroxymethyl Furan (BHMF). *Toxics* **2023**, *11* (8), 698. https://doi.org/10.3390/toxics11080698

62. Golling, F. E.; Pires, R.; Hecking, A.; Weikard, J.; Richter, F.; Danielmeier, K.; Dijkstra, D. Polyurethanes for Coatings and Adhesives – Chemistry and Applications. *Polym. Int.* **2019**, *68* (5), 848–855. https://doi.org/10.1002/pi.5665

63. Li, W.; Li, H.; Wu, C.; Han, B.; Ouyang, P.; Chen, K. An Effective Synthesis of Bio-Based Pentamethylene Diisocyanate in a Jet Loop Reactor. *Chem. Eng. J.* **2021**, *425*,

131527. https://doi.org/10.1016/j.cej.2021.131527

64. Das, S.; Pandey, P.; Mohanty, S.; Nayak, S. K. Influence of NCO/OH and Transesterified Castor Oil on the Structure and Properties of Polyurethane: Synthesis and Characterization. *Mater. Express* **2015**, *5* (5), 377–389. https://doi.org/10.1166/mex.2015.1254
65. Sahoo, S.; Kalita, H.; Mohanty, S.; Nayak, S. Synthesis and Characterization of Vegetable Oil Based Polyurethane Derived from Biobased Isocyanate. *J. Polym. Mater.* **2017**, *34*, 647–661.
66. Covestro. *High Performance Enabled by Nature: First Bio-Based Crosslinker*; 2019.
67. Malewska, E.; Prociak, T.; Michałowski, S.; Barczewski, M.; Banaś, J.; Kurańska, M.; Prociak, A. Environmentally Friendly Shape Memory Biofoams. *Biomass Convers. Biorefinery* **2025**, *15* (11), 17697–17714. https://doi.org/10.1007/s13399-024-06385-5
68. Ihata, O.; Kayaki, Y.; Ikariya, T. Synthesis of Thermoresponsive Polyurethane from 2-Methylaziridine and Supercritical Carbon Dioxide. *Angew. Chemie* **2004**, *116* (6), 735–737. https://doi.org/10.1002/ange.200352215
69. Zhang, D.; Zhang, Y.; Fan, Y.; Rager, M.-N.; Guérineau, V.; Bouteiller, L.; Li, M.-H.; Thomas, C. M. Polymerization of Cyclic Carbamates: A Practical Route to Aliphatic Polyurethanes. *Macromolecules* **2019**, *52* (7), 2719–2724. https://doi.org/10.1021/acs.macromol.9b00436
70. Neffgen, S.; Keul, H.; Höcker, H. Ring-Opening Polymerization of Cyclic Urethanes and Ring-Closing Depolymerization of the Respective Polyurethanes. *Macromol. Rapid Commun.* **1996**, *17* (6), 373–382. https://doi.org/10.1002/marc.1996.030170602
71. Gérard, D.; Méchin, F.; Saint-Loup, R.; Fleury, E.; Pascault, J.-P. Study of the Carbamate/Aldehyde Reaction, a New Pathway towards NIPU Materials. *Prog. Org. Coatings* **2022**, *165* (October 2021), 106728. https://doi.org/10.1016/j.porgcoat.2022.106728
72. Silbert, S. D.; Serum, E. M.; Lascala, J.; Sibi, M. P.; Webster, D. C. Biobased, Nonisocyanate, 2K Polyurethane Coatings Produced from Polycarbamate and Dialdehyde Cross-Linking. *ACS Sustain. Chem. Eng.* **2019**, *7* (24), 19621–19630. https://doi.org/10.1021/acssuschemeng.9b04713
73. Unverferth, M.; Kreye, O.; Prohammer, A.; Meier, M. A. R. Renewable Non-Isocyanate Based Thermoplastic Polyurethanes via Polycondensation of Dimethyl

Carbamate Monomers with Diols. *Macromol. Rapid Commun.* **2013**, *34* (19), 1569–1574. https://doi.org/https://doi.org/10.1002/marc.201300503

74. Sharma, B.; Keul, H.; Höcker, H.; Loontjens, T.; Benthem, R. van. Synthesis and Characterization of Alternating Poly(Amide Urethane)s from ε-Caprolactone, Diamines and Diphenyl Carbonate. *Polymer (Guildf).* **2005**, *46* (6), 1775–1783. https://doi.org/10.1016/j.polymer.2004.11.024
75. Zheng, L.; Yang, G.; Liu, J.; Hu, X.; Zhang, Z. Metal-Free Catalysis for the One-Pot Synthesis of Organic Carbamates from Amines, CO2, and Alcohol at Mild Conditions. *Chem. Eng. J.* **2021**, *425* (August), 131452. https://doi.org/10.1016/j.cej.2021.131452
76. Kébir, N.; Nouigues, S.; Moranne, P.; Burel, F. Nonisocyanate Thermoplastic Polyurethane Elastomers Based on Poly(Ethylene Glycol) Prepared through the Transurethanization Approach. *J. Appl. Polym. Sci.* **2017**, *134* (45), 44991. https://doi.org/https://doi.org/10.1002/app.44991
77. Cornille, A.; Blain, M.; Auvergne, R.; Andrioletti, B.; Boutevin, B.; Caillol, S. A Study of Cyclic Carbonate Aminolysis at Room Temperature: Effect of Cyclic Carbonate Structures and Solvents on Polyhydroxyurethane Synthesis. *Polym. Chem.* **2017**, *8* (3), 592–604. https://doi.org/10.1039/C6PY01854H
78. Cornille, A.; Auvergne, R.; Figovsky, O.; Boutevin, B.; Caillol, S. A Perspective Approach to Sustainable Routes for Non-Isocyanate Polyurethanes. *Eur. Polym. J.* **2017**, *87*, 535–552. https://doi.org/10.1016/j.eurpolymj.2016.11.027
79. Cornille, A.; Michaud, G.; Simon, F.; Fouquay, S.; Auvergne, R.; Boutevin, B.; Caillol, S. Promising Mechanical and Adhesive Properties of Isocyanate-Free Poly(Hydroxyurethane). *Eur. Polym. J.* **2016**, *84*, 404–420. https://doi.org/10.1016/j.eurpolymj.2016.09.048
80. Mhd. Haniffa, M. A. C.; Munawar, K.; Ching, Y. C.; Illias, H. A.; Chuah, C. H. Bio-based Poly(Hydroxy Urethane)s: Synthesis and Pre/Post-Functionalization. *Chem. – An Asian J.* **2021**, *16* (11), 1281–1297. https://doi.org/10.1002/asia.202100226
81. Rayung, M.; Ghani, N. A.; Hasanudin, N. A Review on Vegetable Oil-Based Non Isocyanate Polyurethane: Towards a Greener and Sustainable Production Route. *RSC Adv.* **2024**, *14* (13), 9273–9299. https://doi.org/10.1039/D3RA08684D
82. Tomita, H.; Sanda, F.; Endo, T. Reactivity Comparison of Five- and Six-Membered Cyclic Carbonates with Amines: Basic Evaluation for Synthesis of Poly(Hydroxyurethane). *J. Polym. Sci. Part A Polym. Chem.* **2001**, *39* (1), 162–168.

https://doi.org/10.1002/1099-0518(20010101)39:1<162::AID-POLA180>3.0.CO;2-O

83. Tomita, H.; Sanda, F.; Endo, T. Polyaddition Behavior of Bis(Five- and Six-Membered Cyclic Carbonate)s with Diamine. *J. Polym. Sci. Part A Polym. Chem.* **2001**, *39* (6), 860–867. https://doi.org/https://doi.org/10.1002/1099-0518(20010315)39:6<860::AID-POLA1059>3.0.CO;2-2

84. Burk, R.; ROOF, M. A Safe and Efficient Method for Conversion of 1,2- and 1,3-Diols to Cyclic Carbonates Utilizing Triphosgene. *ChemInform* **2010**, *24*. https://doi.org/10.1002/chin.199322115

85. Pescarmona, P. P. Cyclic Carbonates Synthesised from CO2: Applications, Challenges and Recent Research Trends. *Curr. Opin. Green Sustain. Chem.* **2021**, *29*, 100457. https://doi.org/https://doi.org/10.1016/j.cogsc.2021.100457

86. Aomchad, V.; Cristòfol, À.; Della Monica, F.; Limburg, B.; D'Elia, V.; Kleij, A. W. Recent Progress in the Catalytic Transformation of Carbon Dioxide into Biosourced Organic Carbonates. *Green Chem.* **2021**, *23* (3), 1077–1113. https://doi.org/10.1039/D0GC03824E

87. Guo, L.; Lamb, K. J.; North, M. Recent Developments in Organocatalysed Transformations of Epoxides and Carbon Dioxide into Cyclic Carbonates. *Green Chem.* **2021**, *23* (1), 77–118. https://doi.org/10.1039/D0GC03465G

88. Alves, M.; Grignard, B.; Mereau, R.; Jerome, C.; Tassaing, T.; Detrembleur, C. Organocatalyzed Coupling of Carbon Dioxide with Epoxides for the Synthesis of Cyclic Carbonates: Catalyst Design and Mechanistic Studies. *Catal. Sci. Technol.* **2017**, *7* (13), 2651–2684. https://doi.org/10.1039/C7CY00438A

89. Mundo, F.; Caillol, S.; Ladmiral, V.; Meier, M. A. R. On Sustainability Aspects of the Synthesis of Five-Membered Cyclic Carbonates. *ACS Sustain. Chem. Eng.* **2024**, *12* (17), 6452–6466. https://doi.org/10.1021/acssuschemeng.4c01274

90. Liu, X.-F.; Zhang, S.; Song, Q.-W.; Liu, X.-F.; Ma, R.; He, L.-N. Cooperative Calcium-Based Catalysis with 1,8-Diazabicyclo[5.4.0]-Undec-7-Ene for the Cycloaddition of Epoxides with CO 2 at Atmospheric Pressure. *Green Chem.* **2016**, *18* (9), 2871–2876. https://doi.org/10.1039/C5GC02761F

91. Steinbauer, J.; Spannenberg, A.; Werner, T. An in Situ Formed Ca2+–Crown Ether Complex and Its Use in CO2-Fixation Reactions with Terminal and Internal Epoxides. *Green Chem.* **2017**, *19* (16), 3769–3779. https://doi.org/10.1039/C7GC01114H

92. Kim, Y.; Hyun, K.; Ahn, D.; Kim, R.; Park, M. H.; Kim, Y. Efficient Aluminum Catalysts for the Chemical Conversion of CO 2 into Cyclic Carbonates at Room Temperature and Atmospheric CO 2 Pressure. *ChemSusChem* **2019**, *12* (18), 4211–4220. https://doi.org/10.1002/cssc.201901661

93. Quienne, B.; Poli, R.; Pinaud, J.; Caillol, S. Enhanced Aminolysis of Cyclic Carbonates by β-Hydroxylamines for the Production of Fully Biobased Polyhydroxyurethanes. *Green Chem.* **2021**, *23* (4), 1678–1690. https://doi.org/10.1039/d0gc04120c

94. Purwanto, N. S.; Chen, Y.; Wang, T.; Torkelson, J. M. Rapidly Synthesized, Self-Blowing, Non-Isocyanate Polyurethane Network Foams with Reprocessing to Bulk Networks via Hydroxyurethane Dynamic Chemistry. *Polymer (Guildf).* **2023**, *272* (November 2022), 125858. https://doi.org/10.1016/j.polymer.2023.125858

95. Gomez-Lopez, A.; Ayensa, N.; Grignard, B.; Irusta, L.; Calvo, I.; Müller, A. J.; Detrembleur, C.; Sardon, H. Enhanced and Reusable Poly(Hydroxy Urethane)-Based Low Temperature Hot-Melt Adhesives. *ACS Polym. Au* **2022**, *2* (3), 194–207. https://doi.org/10.1021/acspolymersau.1c00053

96. Zareanshahraki, F.; Mannari, V. Formulation and Optimization of Radiation-Curable Nonisocyanate Polyurethane Wood Coatings by Mixture Experimental Design. *J. Coatings Technol. Res.* **2021**, *18* (3), 695–715. https://doi.org/10.1007/s11998-020-00453-x

97. Pierrard, A.; Aqil, A.; Detrembleur, C.; Jérôme, C. Thermal and UV Curable Formulations of Poly(Propylene Glycol)-Poly(Hydroxyurethane) Elastomers toward Nozzle-Based 3D Photoprinting. *Biomacromolecules* **2023**, *24* (10), 4375–4384. https://doi.org/10.1021/acs.biomac.2c00860

98. Gomez-Lopez, A.; Grignard, B.; Calvo, I.; Detrembleur, C.; Sardon, H. Accelerating the Curing of Hybrid Poly(Hydroxy Urethane)-Epoxy Adhesives by the Thiol-Epoxy Chemistry. *ACS Appl. Polym. Mater.* **2022**, *4* (12), 8786–8794. https://doi.org/10.1021/acsapm.2c01195

99. Coste, G.; Denis, M.; Sonnier, R.; Caillol, S.; Negrell, C. Synthesis of Reactive Phosphorus-Based Carbonate for Flame Retardant Polyhydroxyurethane Foams. *Polym. Degrad. Stab.* **2022**, *202* (April), 110031. https://doi.org/10.1016/j.polymdegradstab.2022.110031

100. Seychal, G.; Ocando, C.; Bonnaud, L.; De Winter, J.; Grignard, B.; Detrembleur, C.; Sardon, H.; Aramburu, N.; Raquez, J.-M. Emerging Polyhydroxyurethanes as

Sustainable Thermosets: A Structure–Property Relationship. *ACS Appl. Polym. Mater.* **2023**, *5* (7), 5567–5581. https://doi.org/10.1021/acsapm.3c00879

101. Poussard, L.; Mariage, J.; Grignard, B.; Detrembleur, C.; Jéroîme, C.; Calberg, C.; Heinrichs, B.; De Winter, J.; Gerbaux, P.; Raquez, J. M.; Bonnaud, L.; Dubois, P. Non-Isocyanate Polyurethanes from Carbonated Soybean Oil Using Monomeric or Oligomeric Diamines to Achieve Thermosets or Thermoplastics. *Macromolecules* **2016**, *49* (6), 2162–2171. https://doi.org/10.1021/acs.macromol.5b02467
102. Tamami, B.; Sohn, S.; Wilkes, G. L. Incorporation of Carbon Dioxide into Soybean Oil and Subsequent Preparation and Studies of Nonisocyanate Polyurethane Networks. *J. Appl. Polym. Sci.* **2004**, *92* (2), 883–891. https://doi.org/https://doi.org/10.1002/app.20049
103. Javni, I.; Hong, D. P.; Petrović, Z. S. Polyurethanes from Soybean Oil, Aromatic, and Cycloaliphatic Diamines by Nonisocyanate Route. *J. Appl. Polym. Sci.* **2013**, *128* (1), 566–571. https://doi.org/https://doi.org/10.1002/app.38215
104. Lee, A.; Deng, Y. Green Polyurethane from Lignin and Soybean Oil through Non-Isocyanate Reactions. *Eur. Polym. J.* **2015**, *63*, 67–73. https://doi.org/10.1016/j.eurpolymj.2014.11.023
105. Dong, J.; Liu, B.; Ding, H.; Shi, J.; Liu, N.; Dai, B.; Kim, I. Bio-Based Healable Non-Isocyanate Polyurethanes Driven by the Cooperation of Disulfide and Hydrogen Bonds. *Polym. Chem.* **2020**, *11* (47), 7524–7532. https://doi.org/10.1039/D0PY01249A
106. Das, M.; Mandal, B.; Katiyar, V. Environment-Friendly Synthesis of Sustainable Chitosan-Based Nonisocyanate Polyurethane: A Biobased Polymeric Film. *J. Appl. Polym. Sci.* **2020**, *137* (36), 49050. https://doi.org/https://doi.org/10.1002/app.49050
107. Doley, S.; Bora, A.; Saikia, P.; Ahmed, S.; Dolui, S. K. Blending of Cyclic Carbonate Based on Soybean Oil and Glycerol: A Non-Isocyanate Approach towards the Synthesis of Polyurethane with High Performance. *J. Polym. Res.* **2021**, *28* (5), 146. https://doi.org/10.1007/s10965-021-02485-2
108. Yang, X.; Wang, S.; Liu, X.; Huang, Z.; Huang, X.; Xu, X.; Liu, H.; Wang, D.; Shang, S. Preparation of Non-Isocyanate Polyurethanes from Epoxy Soybean Oil: Dual Dynamic Networks to Realize Self-Healing and Reprocessing under Mild Conditions. *Green Chem.* **2021**, *23* (17), 6349–6355. https://doi.org/10.1039/D1GC01936H
109. Helbling, P.; Hermant, F.; Petit, M.; Tassaing, T.; Vidil, T.; Cramail, H. Unveiling the Reactivity of Epoxides in Carbonated Epoxidized Soybean Oil and Application

in the Stepwise Synthesis of Hybrid Poly(Hydroxyurethane) Thermosets. *Polym. Chem.* **2023**, *14* (4), 500–513. https://doi.org/10.1039/D2PY01318E

110. Lei, Y.-F.; Wang, X.-L.; Liu, B.-W.; Ding, X.-M.; Chen, L.; Wang, Y.-Z. Fully Bio-Based Pressure-Sensitive Adhesives with High Adhesivity Derived from Epoxidized Soybean Oil and Rosin Acid. *ACS Sustain. Chem. Eng.* **2020**, *8* (35), 13261–13270. https://doi.org/10.1021/acssuschemeng.0c03451
111. Piyataksanon, N.; Suttiruengwong, S.; Seadan, M. Bio-Based Polyurethane Derived from Carbon Dioxide and Epoxidized Soybean Oil. *Suan Sunandha Sci. Technol. J.* **2022**, *9* (2), 8–14. https://doi.org/10.53848/ssstj.v9i2.229
112. Gholami, H.; Yeganeh, H. Soybean Oil-Derived Non-Isocyanate Polyurethanes Containing Azetidinium Groups as Antibacterial Wound Dressing Membranes. *Eur. Polym. J.* **2021**, *142*, 110142. https://doi.org/10.1016/j.eurpolymj.2020.110142
113. Dhore, N.; Prasad, E.; Narayan, R.; Rao, C. R. K.; Palanisamy, A. Studies on Biobased Non-Isocyanate Polyurethane Coatings with Potential Corrosion Resistance. *Sustain. Chem.* **2023**, *4* (1), 95–109. https://doi.org/10.3390/suschem4010008
114. Mahendran, A. R.; Aust, N.; Wuzella, G.; Müller, U.; Kandelbauer, A. Bio-Based Non-Isocyanate Urethane Derived from Plant Oil. *J. Polym. Environ.* **2012**, *20*, 926–931. https://doi.org/10.1007/s10924-012-0491-9
115. Bähr, M.; Mülhaupt, R. Linseed and Soybean Oil-Based Polyurethanes Prepared via the Non-Isocyanate Route and Catalytic Carbon Dioxide Conversion. *Green Chem.* **2012**, *14* (2), 483–489. https://doi.org/10.1039/C2GC16230J
116. Dong, T.; Dheressa, E.; Wiatrowski, M.; Pereira, A. P.; Zeller, A.; Laurens, L. M. L.; Pienkos, P. T. Assessment of Plant and Microalgal Oil-Derived Nonisocyanate Polyurethane Products for Potential Commercialization. *ACS Sustain. Chem. Eng.* **2021**, *9* (38), 12858–12869. https://doi.org/10.1021/acssuschemeng.1c03653
117. Wang, T.; Deng, H.; Zeng, H.; Shen, J.; Xie, F.; Zhang, C. Self-Blowing Non-Isocyanate Polyurethane Foams from Cyclic Carbonate Linseed Oil. *ACS Sustain. Resour. Manag.* **2024**, *1* (3), 462–470. https://doi.org/10.1021/acssusresmgt.3c00103
118. Wang, T.; Deng, H.; Li, N.; Xie, F.; Shi, H.; Wu, M.; Zhang, C. Mechanically Strong Non-Isocyanate Polyurethane Thermosets from Cyclic Carbonate Linseed Oil. *Green Chem.* **2022**, *24* (21), 8355–8366. https://doi.org/10.1039/D2GC02910C
119. Doley, S.; Dolui, S. K. Solvent and Catalyst-Free Synthesis of Sunflower Oil Based Polyurethane through Non-Isocyanate Route and Its Coatings Properties. *Eur. Polym.*

J. **2018**, *102*, 161–168. https://doi.org/10.1016/j.eurpolymj.2018.03.030

120. Farhadian, A.; Ahmadi, A.; Omrani, I.; Miyardan, A. B.; Varfolomeev, M. A.; Nabid, M. R. Synthesis of Fully Bio-Based and Solvent Free Non-Isocyanate Poly (Ester Amide/Urethane) Networks with Improved Thermal Stability on the Basis of Vegetable Oils. *Polym. Degrad. Stab.* **2018**, *155*, 111–121. https://doi.org/10.1016/j.polymdegradstab.2018.07.010
121. Boyer, A.; Cloutet, E.; Tassaing, T.; Gadenne, B.; Alfos, C.; Cramail, H. Solubility in CO2 and Carbonation Studies of Epoxidized Fatty Acid Diesters: Towards Novel Precursors for Polyurethane Synthesis. *Green Chem.* **2010**, *12* (12), 2205. https://doi.org/10.1039/c0gc00371a
122. Rodrigues, J. D. O.; Andrade, C. K. Z.; Quirino, R. L.; Sales, M. J. A. Non-Isocyanate Poly(Acyl-Urethane) Obtained from Urea and Castor (Ricinus Communis L.) Oil. *Prog. Org. Coatings* **2022**, *162*, 106557. https://doi.org/10.1016/j.porgcoat.2021.106557
123. Pathak, R.; Kathalewar, M.; Wazarkar, K.; Sabnis, A. Non-Isocyanate Polyurethane (NIPU) from Tris-2-Hydroxy Ethyl Isocyanurate Modified Fatty Acid for Coating Applications. *Prog. Org. Coatings* **2015**, *89*, 160–169. https://doi.org/10.1016/j.porgcoat.2015.08.015
124. Hambali, R. A.; Faiza, M. A.; Zuliahani, A. Non-Isocyanate Polyurethane (NIPU) Based on Rubber Seed Oil Synthesized via Low-Pressured Carbonization Reaction. *Sains Malaysiana* **2021**, *50* (8), 2407–2417. https://doi.org/10.17576/jsm-2021-5008-22
125. Haniffa, M. A. C. M.; Ching, Y. C.; Chuah, C. H.; Kuan, Y. C.; Liu, D.-S.; Liou, N.-S. Synthesis, Characterization and the Solvent Effects on Interfacial Phenomena of Jatropha Curcas Oil Based Non-Isocyanate Polyurethane. *Polymers (Basel).* **2017**, *9* (5), 162. https://doi.org/10.3390/polym9050162
126. Fache, M.; Darroman, E.; Besse, V.; Auvergne, R.; Caillol, S.; Boutevin, B. Vanillin, a Promising Biobased Building-Block for Monomer Synthesis. *Green Chem.* **2014**, *16* (4), 1987–1998. https://doi.org/10.1039/C3GC42613K
127. Ménard, R.; Caillol, S.; Allais, F. Chemo-Enzymatic Synthesis and Characterization of Renewable Thermoplastic and Thermoset Isocyanate-Free Poly(Hydroxy)Urethanes from Ferulic Acid Derivatives. *ACS Sustain. Chem. Eng.* **2017**, *5* (2), 1446–1456. https://doi.org/10.1021/acssuschemeng.6b02022
128. Chen, Q.; Gao, K.; Peng, C.; Xie, H.; Zhao, Z. K.; Bao, M. Preparation of

Lignin/Glycerol-Based Bis(Cyclic Carbonate) for the Synthesis of Polyurethanes. *Green Chem.* **2015**, *17* (9), 4546–4551. https://doi.org/10.1039/C5GC01340B

129. Furtwengler, P.; Avérous, L. From D-Sorbitol to Five-Membered Bis(Cyclo-Carbonate) as a Platform Molecule for the Synthesis of Different Original Biobased Chemicals and Polymers. *Sci. Rep.* **2018**, *8* (1), 9134. https://doi.org/10.1038/s41598-018-27450-w
130. Mazurek-Budzyńska, M. M.; Rokicki, G.; Drzewicz, M.; Guńka, P. A.; Zachara, J. Bis(Cyclic Carbonate) Based on d-Mannitol, d-Sorbitol and Di(Trimethylolpropane) in the Synthesis of Non-Isocyanate Poly(Carbonate-Urethane)S. *Eur. Polym. J.* **2016**, *84*, 799–811. https://doi.org/10.1016/j.eurpolymj.2016.04.021
131. Bähr, M.; Bitto, A.; Mülhaupt, R. Cyclic Limonene Dicarbonate as a New Monomer for Non-Isocyanate Oligo- and Polyurethanes (NIPU) Based upon Terpenes. *Green Chem.* **2012**, *14* (5), 1447–1454. https://doi.org/10.1039/c2gc35099h
132. Camara, F.; Benyahya, S.; Besse, V.; Boutevin, G.; Auvergne, R.; Boutevin, B.; Caillol, S. Reactivity of Secondary Amines for the Synthesis of Non-Isocyanate Polyurethanes. *Eur. Polym. J.* **2014**, *55* (1), 17–26. https://doi.org/10.1016/j.eurpolymj.2014.03.011
133. Stemmelen, M.; Pessel, F.; Lapinte, V.; Caillol, S.; Habas, J.-P.; Robin, J.-J. A Fully Biobased Epoxy Resin from Vegetable Oils: From the Synthesis of the Precursors by Thiol-ene Reaction to the Study of the Final Material. *J. Polym. Sci. Part A Polym. Chem.* **2011**, *49* (11), 2434–2444. https://doi.org/10.1002/pola.24674
134. Türünç, O.; Firdaus, M.; Klein, G.; Meier, M. A. R. Fatty Acid Derived Renewable Polyamides via Thiol–Ene Additions. *Green Chem.* **2012**, *14* (9), 2577–2583. https://doi.org/10.1039/C2GC35982K
135. Destaso, F. C.; Libretti, C.; Le Coz, C.; Grau, E.; Cramail, H.; Meier, M. A. R. Optimized Synthesis of a High Oleic Sunflower Oil Derived Polyamine and Its Lignin-Based NIPUs. *Green Chem.* **2025**, *27* (5), 1440–1450. https://doi.org/10.1039/D4GC05645K
136. Attanasi, O. A.; Berretta, S.; Fiani, C.; Filippone, P.; Mele, G.; Saladino, R. Synthesis and Reactions of Nitro Derivatives of Hydrogenated Cardanol. *Tetrahedron* **2006**, *62* (25), 6113–6120. https://doi.org/10.1016/j.tet.2006.03.105
137. Metkar, P. S.; Scialdone, M. A.; Moloy, K. G. Lysinol: A Renewably Resourced Alternative to Petrochemical Polyamines and Aminoalcohols. *Green Chem.* **2014**, *16* (10), 4575–4586. https://doi.org/10.1039/C4GC01167H

138. Kind, S.; Wittmann, C. Bio-Based Production of the Platform Chemical 1,5-Diaminopentane. *Appl. Microbiol. Biotechnol.* **2011**, *91*, 1287–1296. https://doi.org/10.1007/s00253-011-3457-2

139. Cok, B.; Tsiropoulos, I.; Roes, A. L.; Patel, M. K. Succinic Acid Production Derived from Carbohydrates: An Energy and Greenhouse Gas Assessment of a Platform Chemical toward a Bio-based Economy. *Biofuels, Bioprod. Biorefining* **2014**, *8* (1), 16–29. https://doi.org/10.1002/bbb.1427

140. Brasse, C.; Haas, T.; Weber, R.; Neuroth, J. Method of Producing Hexamethylene Diamine from Butadiene. U.S. Patent Application US20030212298A1, 2003. https://patents.google.com/patent/US20030212298A1

141. Scheelje, F. C. M.; Destaso, F. C.; Cramail, H.; Meier, M. A. R. Nitrogen-Containing Polymers Derived from Terpenes: Possibilities and Limitations. *Macromol. Chem. Phys.* **2023**, *224* (3), 2200403. https://doi.org/https://doi.org/10.1002/macp.202200403

142. Cornille, A.; Dworakowska, S.; Bogdal, D.; Boutevin, B.; Caillol, S. A New Way of Creating Cellular Polyurethane Materials: NIPU Foams. *Eur. Polym. J.* **2015**, *66*, 129–138. https://doi.org/10.1016/j.eurpolymj.2015.01.034

143. Cornille, A.; Guillet, C.; Benyahya, S.; Negrell, C.; Boutevin, B.; Caillol, S. Room Temperature Flexible Isocyanate-Free Polyurethane Foams. *Eur. Polym. J.* **2016**, *84*, 873–888. https://doi.org/10.1016/j.eurpolymj.2016.05.032

144. Coste, G.; Berne, D.; Ladmiral, V.; Negrell, C.; Caillol, S. Non-Isocyanate Polyurethane Foams Based on Six-Membered Cyclic Carbonates. *Eur. Polym. J.* **2022**, *176* (May), 111392. https://doi.org/10.1016/j.eurpolymj.2022.111392

145. Sternberg, J.; Pilla, S. Materials for the Biorefinery: High Bio-Content, Shape Memory Kraft Lignin-Derived Non-Isocyanate Polyurethane Foams Using a Non-Toxic Protocol. *Green Chem.* **2020**, *22* (20), 6922–6935. https://doi.org/10.1039/d0gc01659d

146. Monie, F.; Grignard, B.; Thomassin, J.; Mereau, R.; Tassaing, T.; Jerome, C.; Detrembleur, C. Chemo- and Regioselective Additions of Nucleophiles to Cyclic Carbonates for the Preparation of Self-Blowing Non-Isocyanate Polyurethane Foams. *Angew. Chemie* **2020**, *132* (39), 17181–17189. https://doi.org/10.1002/ange.202006267

147. El Khezraji, S.; Gonzalez Tomé, S.; Thakur, S.; Ablouh, E.-H.; Ben Youcef, H.; Raihane, M.; Lopez-Manchado, M. A.; Verdejo, R.; Lahcini, M. Fast Synthesis of

Crosslinked Self-Blowing Poly(β-Hydroxythioether) Foams by Decarboxylative-Alkylation of Thiols at Room Temperature. *Eur. Polym. J.* **2023**, *189*, 111960. https://doi.org/https://doi.org/10.1016/j.eurpolymj.2023.111960

148. Monie, F.; Grignard, B.; Detrembleur, C. Divergent Aminolysis Approach for Constructing Recyclable Self-Blown Nonisocyanate Polyurethane Foams. *ACS Macro Lett.* **2022**, *11* (2), 236–242. https://doi.org/10.1021/acsmacrolett.1c00793
149. Coste, G.; Negrell, C.; Caillol, S. Cascade (Dithio)Carbonate Ring Opening Reactions for Self-Blowing Polyhydroxythiourethane Foams. *Macromol. Rapid Commun.* **2022**, *43* (13). https://doi.org/10.1002/marc.202100833
150. Purwanto, N. S.; Chen, Y.; Torkelson, J. M. Reprocessable, Bio-Based, Self-Blowing Non-Isocyanate Polyurethane Network Foams from Cashew Nutshell Liquid. *ACS Appl. Polym. Mater.* **2023**, *5* (8), 6651–6661. https://doi.org/10.1021/acsapm.3c01196
151. Purwanto, N. S.; Chen, Y.; Torkelson, J. M. Biobased, Reprocessable, Self-Blown Non-Isocyanate Polyurethane Foams: Influence of Blowing Agent Structure and Functionality. *Eur. Polym. J.* **2024**, *206* (November 2023), 112775. https://doi.org/10.1016/j.eurpolymj.2024.112775
152. Bourguignon, M.; Thomassin, J.-M.; Grignard, B.; Jerome, C.; Detrembleur, C. Fast and Facile One-Pot One-Step Preparation of Nonisocyanate Polyurethane Hydrogels in Water at Room Temperature. *ACS Sustain. Chem. Eng.* **2019**, *7* (14), 12601–12610. https://doi.org/10.1021/acssuschemeng.9b02624
153. Bourguignon, M.; Grignard, B.; Detrembleur, C. Cascade Exotherms for Rapidly Producing Hybrid Nonisocyanate Polyurethane Foams from Room Temperature Formulations. *J. Am. Chem. Soc.* **2024**, *146* (1), 988–1000. https://doi.org/10.1021/jacs.3c11637
154. Choong, P. Sen; Hui, Y. L. E.; Lim, C. C. CO 2 -Blown Nonisocyanate Polyurethane Foams. *ACS Macro Lett.* **2023**, *12* (8), 1094–1099. https://doi.org/10.1021/acsmacrolett.3c00334
155. Wypych, G. *Handbook of Foaming and Blowing Agents*; 2017.
156. Kharbas, H. A.; McNulty, J. D.; Ellingham, T.; Thompson, C.; Manitiu, M.; Scholz, G.; Turng, L.-S. Comparative Study of Chemical and Physical Foaming Methods for Injection-Molded Thermoplastic Polyurethane. *J. Cell. Plast.* **2017**, *53* (4), 373–388. https://doi.org/10.1177/0021955X16652107
157. Olang, F. N. Hybrid Polyurethane Spray Foams Made with Urethane Pre Polymers

and Rheology Modifiers. US 2012/0183694 A1, 2012.

158. Figovsky, O.; Potashnikov, R.; Leykin, A.; Shapovalov, L.; Sivokon, S. Method for Forming a Sprayable Nonisocyanate Polymer Foam Composition. **2015**, *1* (19), 19, U.S. Patent Application No. 13/770,319.

159. Blattmann, H.; Lauth, M.; Mülhaupt, R. Flexible and Bio-Based Nonisocyanate Polyurethane (NIPU) Foams. *Macromol. Mater. Eng.* **2016**, *301* (8), 944–952. https://doi.org/10.1002/mame.201600141

160. Gunasekaran, H. B.; Ponnan, S.; Thirunavukkarasu, N.; Laroui, A.; Wu, L.; Wang, J. Rapid Carbon Dioxide Foaming of 3D Printed Thermoplastic Polyurethane Elastomers. *ACS Appl. Polym. Mater.* **2022**, *4* (2), 1497–1511. https://doi.org/10.1021/acsapm.1c01846

161. Belmonte, P.; Ramos, M. J.; Rodríguez, J. F.; Garrido, I.; García, M. T.; García-Vargas, J. M. Transformation of TPU Elastomers into TPU Foams Using Supercritical CO2. A New Reprocessing Approach. *J. Supercrit. Fluids* **2023**, *192* (November 2022), 105806. https://doi.org/10.1016/j.supflu.2022.105806

162. Wang, G.; Wan, G.; Chai, J.; Li, B.; Zhao, G.; Mu, Y.; Park, C. B. Structure-Tunable Thermoplastic Polyurethane Foams Fabricated by Supercritical Carbon Dioxide Foaming and Their Compressive Mechanical Properties. *J. Supercrit. Fluids* **2019**, *149*, 127–137. https://doi.org/10.1016/j.supflu.2019.04.004

163. Villamil Jiménez, J. A.; Le Moigne, N.; Bénézet, J.-C.; Sauceau, M.; Sescousse, R.; Fages, J. Foaming of PLA Composites by Supercritical Fluid-Assisted Processes: A Review. *Molecules* **2020**, *25* (15), 3408. https://doi.org/10.3390/molecules25153408

164. Grignard, B.; Thomassin, J. M.; Gennen, S.; Poussard, L.; Bonnaud, L.; Raquez, J. M.; Dubois, P.; Tran, M. P.; Park, C. B.; Jerome, C.; Detrembleur, C. CO2-Blown Microcellular Non-Isocyanate Polyurethane (NIPU) Foams: From Bio- and CO2-Sourced Monomers to Potentially Thermal Insulating Materials. *Green Chem.* **2016**, *18* (7), 2206–2215. https://doi.org/10.1039/c5gc02723c

165. Mao, H.; Chen, C.; Yan, H.; Rwei, S. Synthesis and Characteristics of Nonisocyanate Polyurethane Composed of Bio-based Dimer Diamine for Supercritical <scp> CO $_2$ </Scp> Foaming Applications. *J. Appl. Polym. Sci.* **2022**, *139* (35). https://doi.org/10.1002/app.52841

166. Kirchberg, A.; Khabazian Esfahani, M.; Röpert, M. C.; Wilhelm, M.; Meier, M. A. R. Sustainable Synthesis of Non-Isocyanate Polyurethanes Based on Renewable 2,3-Butanediol. *Macromol. Chem. Phys.* **2022**, *223* (13), 1–8.

https://doi.org/10.1002/macp.202200010

167. Valette, V.; Kébir, N.; Burel, F.; Lecamp, L. Design of Biobased Non-Isocyanate Polyurethane (NIPU) Foams Blown with Water and/or Ethanol. *Express Polym. Lett.* **2023**, *17* (9), 974–990. https://doi.org/10.3144/expresspolymlett.2023.72

168. Valette, V.; Kébir, N.; Tiavarison, F. B.; Burel, F.; Lecamp, L. Preparation of Flexible Biobased Non-Isocyanate Polyurethane (NIPU) Foams Using the Transurethanization Approach. *React. Funct. Polym.* **2022**, *181*, 105416. https://doi.org/10.1016/j.reactfunctpolym.2022.105416

169. Datta Sarma, A.; Zubkevich, S. V.; Addiego, F.; Schmidt, D. F.; Shaplov, A. S.; Berthé, V. Synthesis of High-Tg Nonisocyanate Polyurethanes via Reactive Extrusion and Their Batch Foaming. *Macromolecules* **2024**, *57* (7), 3423–3437. https://doi.org/10.1021/acs.macromol.4c00222

170. Zhang, H.; Wang, H.; Wang, T.; Han, S.; Zhang, X.; Wang, J.; Sun, G. Polyurethane Foam with High-Efficiency Flame Retardant, Heat Insulation, and Sound Absorption Modified By Phosphorus-Containing Graphene Oxide. *ACS Appl. Polym. Mater.* **2024**, *6* (3), 1878–1890. https://doi.org/10.1021/acsapm.3c02706

171. Basinska, M.; Kaczorek, D.; Koczyk, H. Building Thermo-Modernisation Solution Based on the Multi-Objective Optimisation Method. *Energies* **2020**, *13* (6), 1–19. https://doi.org/10.3390/en13061433

172. Jelle, B. P. Traditional, State-of-the-Art and Future Thermal Building Insulation Materials and Solutions - Properties, Requirements and Possibilities. *Energy Build.* **2011**, *43* (10), 2549–2563. https://doi.org/10.1016/j.enbuild.2011.05.015

173. Müller, A. Energy Performance Evaluation of Internal Insulation as a Measure for the Modernization of Existing Buildings. In *Energy-Efficient Retrofit of Buildings by Interior Insulation*; Wakili, K. G., Stahl, T. B. T.-E.-E. R. of B. by I. I., Eds.; Elsevier, 2022; pp 467–490. https://doi.org/10.1016/B978-0-12-816513-3.00005-8

174. Tinti, A.; Tarzia, A.; Passaro, A.; Angiuli, R. Thermographic Analysis of Polyurethane Foams Integrated with Phase Change Materials Designed for Dynamic Thermal Insulation in Refrigerated Transport. *Appl. Therm. Eng.* **2014**, *70* (1), 201–210. https://doi.org/10.1016/j.applthermaleng.2014.05.003

175. Fu, K.; Zhang, L.; Zhang, W.; Ma, Q.; Zheng, X.; Chang, C. Sustainable Production and Evaluation of Bio-Based Flame-Retardant PU Foam via Liquefaction of Industrial Biomass Residues. *Ind. Crops Prod.* **2024**, *210*, 118100. https://doi.org/10.1016/j.indcrop.2024.118100

176. Grignard, B.; Thomassin, J.-M.; Gennen, S.; Poussard, L.; Bonnaud, L.; Raquez, J.-M.; Dubois, P.; Tran, M.-P.; Park, C. B.; Jerome, C.; Detrembleur, C. CO 2 -Blown Microcellular Non-Isocyanate Polyurethane (NIPU) Foams: From Bio- and CO 2 -Sourced Monomers to Potentially Thermal Insulating Materials. *Green Chem.* **2016**, *18* (7), 2206–2215. https://doi.org/10.1039/C5GC02723C

177. Pau, D. S. W.; Fleischmann, C. M.; Spearpoint, M. J.; Li, K. Y. Thermophysical Properties of Polyurethane Foams and Their Melts. *Fire Mater.* **2014**, *38* (4), 433–450. https://doi.org/https://doi.org/10.1002/fam.2188

178. Parcheta-Szwindowska, P.; Habaj, J.; Krzemińska, I.; Datta, J. A Comprehensive Review of Reactive Flame Retardants for Polyurethane Materials: Current Development and Future Opportunities in an Environmentally Friendly Direction. *Int. J. Mol. Sci.* **2024**, *25* (10), 5512. https://doi.org/10.3390/ijms25105512

179. Singh, H.; Jain, A. K. Ignition, Combustion, Toxicity, and Fire Retardancy of Polyurethane Foams: A Comprehensive Review. *J. Appl. Polym. Sci.* **2009**, *111* (2), 1115–1143. https://doi.org/https://doi.org/10.1002/app.29131

180. Alaee, M.; Arias, P.; Sjödin, A.; Bergman, Å. An Overview of Commercially Used Brominated Flame Retardants, Their Applications, Their Use Patterns in Different Countries/Regions and Possible Modes of Release. *Environ. Int.* **2003**, *29* (6), 683–689. https://doi.org/10.1016/S0160-4120(03)00121-1

181. Chen, M.-J.; Shao, Z.-B.; Wang, X.-L.; Chen, L.; Wang, Y.-Z. Halogen-Free Flame-Retardant Flexible Polyurethane Foam with a Novel Nitrogen–Phosphorus Flame Retardant. *Ind. Eng. Chem. Res.* **2012**, *51* (29), 9769–9776. https://doi.org/10.1021/ie301004d

182. Thirumal, M.; Khastgir, D.; Singha, N. K.; Manjunath, B. S.; Naik, Y. P. Effect of Expandable Graphite on the Properties of Intumescent Flame-Retardant Polyurethane Foam. *J. Appl. Polym. Sci.* **2008**, *110* (5), 2586–2594. https://doi.org/https://doi.org/10.1002/app.28763

183. Thirumal, M.; Singha, N. K.; Khastgir, D.; Manjunath, B. S.; Naik, Y. P. Halogen-Free Flame-Retardant Rigid Polyurethane Foams: Effect of Alumina Trihydrate and Triphenylphosphate on the Properties of Polyurethane Foams. *J. Appl. Polym. Sci.* **2010**, *116* (4), 2260–2268. https://doi.org/https://doi.org/10.1002/app.31626

184. Shao, Z.-B.; Zhang, J.; Jian, R.-K.; Sun, C.-C.; Li, X.-L.; Wang, D.-Y. A Strategy to Construct Multifunctional Ammonium Polyphosphate for Epoxy Resin with Simultaneously High Fire Safety and Mechanical Properties. *Compos. Part A Appl.*

Sci. Manuf. **2021**, *149* (June), 106529. https://doi.org/10.1016/j.compositesa.2021.106529

185. Yuan, Y.; Yang, H.; Yu, B.; Shi, Y.; Wang, W.; Song, L.; Hu, Y.; Zhang, Y. Phosphorus and Nitrogen-Containing Polyols: Synergistic Effect on the Thermal Property and Flame Retardancy of Rigid Polyurethane Foam Composites. *Ind. Eng. Chem. Res.* **2016**, *55* (41), 10813–10822. https://doi.org/10.1021/acs.iecr.6b02942
186. Xu, J.; Wu, Y.; Zhang, B.; Zhang, G. Synthesis and Synergistic Flame-retardant Effects of Rigid Polyurethane Foams Used Reactive <scp>DOPO</Scp> -based Polyols Combination with Expandable Graphite. *J. Appl. Polym. Sci.* **2021**, *138* (16). https://doi.org/10.1002/app.50223
187. *ECHA identifies certain brominated flame retardants as candidates for restriction*. https://echa.europa.eu/-/echa-identifies-certain-brominated-flame-retardants-as-candidates-for-restriction (accessed 2024-10-01)
188. Rao, W.-H.; Zhu, Z.-M.; Wang, S.-X.; Wang, T.; Tan, Y.; Liao, W.; Zhao, H.-B.; Wang, Y.-Z. A Reactive Phosphorus-Containing Polyol Incorporated into Flexible Polyurethane Foam: Self-Extinguishing Behavior and Mechanism. *Polym. Degrad. Stab.* **2018**, *153*, 192–200. https://doi.org/10.1016/j.polymdegradstab.2018.04.029
189. Bhoyate, S.; Ionescu, M.; Kahol, P. K.; Chen, J.; Mishra, S. R.; Gupta, R. K. Highly Flame-retardant Polyurethane Foam Based on Reactive Phosphorus Polyol and Limonene-based Polyol. *J. Appl. Polym. Sci.* **2018**, *135* (21), 46224. https://doi.org/10.1002/app.46224
190. Qian, X.; Liu, Q.; Zhang, L.; Li, H.; Liu, J.; Yan, S. Synthesis of Reactive DOPO-Based Flame Retardant and Its Application in Rigid Polyisocyanurate-Polyurethane Foam. *Polym. Degrad. Stab.* **2022**, *197*, 109852. https://doi.org/10.1016/j.polymdegradstab.2022.109852
191. Yang, S.; Wang, J.; Huo, S.; Wang, M.; Wang, J. Preparation and Flame Retardancy of a Compounded Epoxy Resin System Composed of Phosphorus/Nitrogen-Containing Active Compounds. *Polym. Degrad. Stab.* **2015**, *121*, 398–406. https://doi.org/10.1016/j.polymdegradstab.2015.10.006
192. Lopez-Cuesta, J. M. Flame-Retardant Polymer Nanocomposites. In *Advances in Polymer Nanocomposites*; Elsevier, 2012; pp 540–566. https://doi.org/10.1533/9780857096241.3.540
193. Babushok, V.; Tsang, W. Inhibitor Rankings for Alkane Combustion. *Combust. Flame* **2000**, *123* (4), 488–506. https://doi.org/10.1016/S0010-2180(00)00168-1

194. Wang, P.; Cai, Z. Highly Efficient Flame-Retardant Epoxy Resin with a Novel DOPO-Based Triazole Compound: Thermal Stability, Flame Retardancy and Mechanism. *Polym. Degrad. Stab.* **2017**, *137*, 138–150. https://doi.org/10.1016/j.polymdegradstab.2017.01.014

195. Lin, C. H.; Wang, C. S. Synthesis and Property of Phosphorus-Containing Bismaleimide by a Novel Method. *J. Polym. Sci. Part A Polym. Chem.* **2000**, *38* (12), 2260–2268. https://doi.org/https://doi.org/10.1002/(SICI)1099-0518(20000615)38:12<2260::AID-POLA150>3.0.CO;2-R

196. Seibold, S.; Schäfer, A.; Lohstroh, W.; Walter, O.; Döring, M. Phosphorus-Containing Terephthaldialdehyde Adducts—Structure Determination and Their Application as Flame Retardants in Epoxy Resins. *J. Appl. Polym. Sci.* **2008**, *108* (1), 264–271. https://doi.org/https://doi.org/10.1002/app.27550

197. Sag, J.; Kukla, P.; Goedderz, D.; Roch, H.; Kabasci, S.; Döring, M.; Schönberger, F. Synthesis of Novel Polymeric Acrylate-Based Flame Retardants Containing Two Phosphorus Groups in Different Chemical Environments and Their Influence on the Flammability of Poly (Lactic Acid). *Polymers (Basel).* **2020**, *12* (4), 778. https://doi.org/10.3390/polym12040778

198. Wu, Y.; Xu, J.; Zhang, J.; Xie, Y.; Zhang, G. Effects of Innovative Aromatic Phosphorus Containing Flame-Retardant Polyols on Rigid Polyurethane Foams. *Chem. Pap.* **2021**, *75* (7), 3373–3385. https://doi.org/10.1007/s11696-021-01571-5

199. Wang, J.; Xu, B.; Wang, X.; Liu, Y. A Phosphorous-Based Bi-Functional Flame Retardant for Rigid Polyurethane Foam. *Polym. Degrad. Stab.* **2021**, *186*, 109516. https://doi.org/10.1016/j.polymdegradstab.2021.109516

200. Vakili, M.; Nikje, M. M. A.; Hajibeygi, M. The Effects of a Phosphorus/Nitrogen-Containing Diphenol on the Flammability, Thermal Stability, and Mechanical Properties of Rigid Polyurethane Foam. *Colloid Polym. Sci.* **2024**, *302* (1), 79–90. https://doi.org/10.1007/s00396-023-05182-2

201. Pascarella, A.; Recupido, F.; Lama, G. C.; Sorrentino, L.; Campanile, A.; Liguori, B.; Berthet, M.; Rollo, G.; Lavorgna, M.; Verdolotti, L. Design and Development of Sustainable Polyurethane Foam: A Proof-of-Concept as Customizable Packaging for Cultural Heritage Applications. *Adv. Eng. Mater.* **2024**, *26* (7), 1–12. https://doi.org/10.1002/adem.202301888

202. Kolgesiz, S.; Berksun, E.; Tas, C. E.; Unal, S.; Unal, H. Flexible Waterborne Polyurethane Nanocomposite Foams Incorporated with Halloysites as Fresh-Keeping

Packaging Inserts for Fresh Fruits. *Food Packag. Shelf Life* **2023**, *40* (January), 101204. https://doi.org/10.1016/j.fpsl.2023.101204

203. Kafalı, H.; Tunca, E. Investigation of the Mechanical Properties of Polyurethane Foam-Filled FDM-Printed Honeycomb Core Sandwich Composites for Aircraft. *Aeronaut. J.* **2024**, *128* (1321), 577–597. https://doi.org/10.1017/aer.2023.85
204. Schönfeld, D.; Chalissery, D.; Wenz, F.; Specht, M.; Eberl, C.; Pretsch, T. Actuating Shape Memory Polymer for Thermoresponsive Soft Robotic Gripper and Programmable Materials. *Molecules* **2021**, *26* (3), 522. https://doi.org/10.3390/molecules26030522
205. Walter, M.; Friess, F.; Krus, M.; Zolanvari, S.M.H.; Grün, G.; Kröber, H.; Pretsch, T. Shape Memory Polymer Foam with Programmable Apertures. *Polymers (Basel).* **2020**, *12* (9), 1–23. https://doi.org/https://doi.org/10.3390/polym12091914
206. Wang, R.; Tan, Z.; Zhong, W.; Liu, K.; Li, M.; Chen, Y.; Wang, W.; Wang, D. Polypyrrole (PPy) Attached on Porous Conductive Sponge Derived from Carbonized Graphene Oxide Coated Polyurethane (PU) and Its Application in Pressure Sensor. *Compos. Commun.* **2020**, *22*, 100426. https://doi.org/10.1016/j.coco.2020.100426
207. Wang, X.; Li, H.; Wang, T.; Niu, X.; Wang, Y.; Xu, S.; Jiang, Y.; Chen, L.; Liu, H. Flexible and High-Performance Piezoresistive Strain Sensors Based on Multi-Walled Carbon Nanotubes@polyurethane Foam. *RSC Adv.* **2022**, *12* (22), 14190–14196. https://doi.org/10.1039/D2RA01291J
208. Huang, W.; Dai, K.; Zhai, Y.; Liu, H.; Zhan, P.; Gao, J.; Zheng, G.; Liu, C.; Shen, C. Flexible and Lightweight Pressure Sensor Based on Carbon Nanotube/Thermoplastic Polyurethane-Aligned Conductive Foam with Superior Compressibility and Stability. *ACS Appl. Mater. Interfaces* **2017**, *9* (48), 42266–42277. https://doi.org/10.1021/acsami.7b16975
209. Wang, C.; Du, L.; Xing, X.; Feng, D.; Yang, D. Lightweight Porous Polyurethane Foam Integrated with Graphene Oxide for Flexible and High-Concentration Hydrogen Sensing. *ACS sensors* **2022**, *7* (8), 2420–2428.
210. Ghosh, A.; Chowdhury, S. R.; Dutta, R.; Babu, R.; Rumbo, C.; Dasgupta, N.; Mukherjee, P.; Das, N. C.; Ranjan, S. Polyurethane Chemistry for the Agricultural Applications – Recent Advancement and Future Prospects. In *Polyurethanes: Preparation, Properties, and Applications Volume 3: Emerging Applications*; ACS Publications, 2023; pp 1–36. https://doi.org/10.1021/bk-2023-1454.ch001
211. Li, H.; Wang, B.; Shui, H.; Wei, Q.; Xu, C. C. Preparation of Bio-Based Polyurethane

Hydroponic Foams Using 100% Bio-Polyol Derived from Miscanthus through Organosolv Fractionation. *Ind. Crops Prod.* **2022**, *181*, 114774. https://doi.org/10.1016/j.indcrop.2022.114774

212. Estellano, V. H.; Pozo, K.; Efstathiou, C.; Pozo, K.; Corsolini, S.; Focardi, S. Assessing Levels and Seasonal Variations of Current-Use Pesticides (CUPs) in the Tuscan Atmosphere, Italy, Using Polyurethane Foam Disks (PUF) Passive Air Samplers. *Environ. Pollut.* **2015**, *205*, 52–59. https://doi.org/10.1016/j.envpol.2015.05.002
213. Huang, W. M.; Yang, B.; Fu, Y. Q. *Polyurethane Shape Memory Polymers*; CRC press Boca Raton, FL, 2012.
214. Singhal, P.; Rodriguez, J. N.; Small, W.; Eagleston, S.; Van De Water, J.; Maitland, D. J.; Wilson, T. S. Ultra Low Density and Highly Crosslinked Biocompatible Shape Memory Polyurethane Foams. *J. Polym. Sci. Part B Polym. Phys.* **2012**, *50* (10), 724–737. https://doi.org/10.1002/polb.23056
215. Chung, K.; Feng, X.; Jiang, Y.; Li, K.; Chen, J.; Han, Y.; Tan, L.; Du, Z. Shape Memory Polyurethane Foams With Tunable Mechanical Properties and Radiation Tolerance for Breast Repair and Reconstruction. *J. Biomed. Mater. Res. Part A* **2025**, *113* (1), e37821. https://doi.org/10.1002/jbm.a.37821
216. Poser, A.; Pretsch, T. FOIM: Thermal Foaming of Shape Memory Polyurethane Foil. *Macromol. Rapid Commun.* **2025**, *46* (8), 2401103. https://doi.org/10.1002/marc.202401103
217. Tam, E. K. W.; Chong, N. X.; Choong, P. Sen; Sana, B.; Seayad, A. M.; Jana, S.; Seayad, J. Phosphate Functionalized Nonisocyanate Polyurethanes with Bio-Origin, Water Solubility and Biodegradability. *Green Chem.* **2024**, *26* (2), 1007–1019.
218. Pierrard, A.; Melo, S. F.; Thijssen, Q.; Van Vlierberghe, S.; Lancellotti, P.; Oury, C.; Detrembleur, C.; Jérôme, C. Design of 3D-Photoprintable, Bio-, and Hemocompatible Nonisocyanate Polyurethane Elastomers for Biomedical Implants. *Biomacromolecules* **2024**, *25* (3), 1810–1824. https://doi.org/10.1021/acs.biomac.3c01261
219. Schimpf, V.; Heck, B.; Reiter, G.; Mülhaupt, R. Triple-Shape Memory Materials via Thermoresponsive Behavior of Nanocrystalline Non-Isocyanate Polyhydroxyurethanes. *Macromolecules* **2017**, *50* (9), 3598–3606. https://doi.org/10.1021/acs.macromol.7b00500
220. Melo, S. F.; Nondonfaz, A.; Aqil, A.; Pierrard, A.; Hulin, A.; Delierneux, C.;

Ditkowski, B.; Gustin, M.; Legrand, M.; Tullemans, B. M. E.; Brouns, S. L. N.; Nchimi, A.; Carrus, R.; Dejosé, A.; Heemskerk, J. W. M.; Kuijpers, M. J. E.; Ritter, J.; Steinseifer, U.; Clauser, J. C.; Jérôme, C.; Lancellotti, P.; Oury, C. Design, Manufacturing and Testing of a Green Non-Isocyanate Polyurethane Prosthetic Heart Valve. *Biomater. Sci.* **2024**, *12* (8), 2149–2164. https://doi.org/10.1039/d3bm01911j

221. Liang, C.; Gracida-Alvarez, U. R.; Gallant, E. T.; Gillis, P. A.; Marques, Y. A.; Abramo, G. P.; Hawkins, T. R.; Dunn, J. B. Material Flows of Polyurethane in the United States. *Environ. Sci. Technol.* **2021**, *55* (20), 14215–14224. https://doi.org/10.1021/acs.est.1c03654
222. Rossignolo, G.; Malucelli, G.; Lorenzetti, A. Recycling of Polyurethanes: Where We Are and Where We Are Going. *Green Chem.* **2023**, *26* (3), 1132–1152. https://doi.org/10.1039/d3gc02091f
223. Zia, K. M.; Bhatti, H. N.; Ahmad Bhatti, I. Methods for Polyurethane and Polyurethane Composites, Recycling and Recovery: A Review. *React. Funct. Polym.* **2007**, *67* (8), 675–692. https://doi.org/10.1016/j.reactfunctpolym.2007.05.004
224. Sheel, A.; Pant, D. Chemical Depolymerization of Polyurethane Foams via Glycolysis and Hydrolysis. In *Recycling of Polyurethane Foams*; Elsevier, 2018; pp 67–75. https://doi.org/10.1016/B978-0-323-51133-9.00006-1
225. Deng, Y.; Dewil, R.; Appels, L.; Ansart, R.; Baeyens, J.; Kang, Q. Reviewing the Thermo-Chemical Recycling of Waste Polyurethane Foam. *J. Environ. Manage.* **2021**, *278*, 111527. https://doi.org/10.1016/j.jenvman.2020.111527
226. Swartz, J. L.; Sheppard, D. T.; Haugstad, G.; Dichtel, W. R. Blending Polyurethane Thermosets Using Dynamic Urethane Exchange. *Macromolecules* **2021**, *54* (23), 11126–11133. https://doi.org/10.1021/acs.macromol.1c01910
227. Sun, M.; Sheppard, D. T.; Brutman, J. P.; Alsbaiee, A.; Dichtel, W. R. Green Catalysts for Reprocessing Thermoset Polyurethanes. *Macromolecules* **2023**, *56* (17), 6978–6987. https://doi.org/10.1021/acs.macromol.3c01116
228. Unal, K.; Maes, D.; Stricker, L.; Lorenz, K.; Du Prez, F. E.; Imbernon, L.; Winne, J. M. Foam-to-Elastomer Recycling of Polyurethane Materials through Incorporation of Dynamic Covalent TAD-Indole Linkages. *ACS Appl. Polym. Mater.* **2024**, *6* (5), 2604–2615. https://doi.org/10.1021/acsapm.3c02791
229. Bakkali-Hassani, C.; Berne, D.; Bron, P.; Irusta, L.; Sardon, H.; Ladmiral, V.; Caillol, S. Polyhydroxyurethane Covalent Adaptable Networks: Looking for Suitable Catalysts. *Polym. Chem.* **2023**, *14* (31), 3610–3620.

https://doi.org/10.1039/D3PY00579H

230. Chen, X.; Li, L.; Wei, T.; Venerus, D. C.; Torkelson, J. M. Reprocessable Polyhydroxyurethane Network Composites: Effect of Filler Surface Functionality on Cross-Link Density Recovery and Stress Relaxation. *ACS Appl. Mater. Interfaces* **2019**, *11* (2), 2398–2407. https://doi.org/10.1021/acsami.8b19100

231. Chen, X.; Li, L.; Jin, K.; Torkelson, J. M. Reprocessable Polyhydroxyurethane Networks Exhibiting Full Property Recovery and Concurrent Associative and Dissociative Dynamic Chemistry via Transcarbamoylation and Reversible Cyclic Carbonate Aminolysis. *Polym. Chem.* **2017**, *8* (41), 6349–6355. https://doi.org/10.1039/C7PY01160A

232. Hu, S.; Chen, X.; Bin Rusayyis, M. A.; Purwanto, N. S.; Torkelson, J. M. Reprocessable Polyhydroxyurethane Networks Reinforced with Reactive Polyhedral Oligomeric Silsesquioxanes (POSS) and Exhibiting Excellent Elevated Temperature Creep Resistance. *Polymer (Guildf).* **2022**, *252*, 124971. https://doi.org/10.1016/j.polymer.2022.124971

233. Hu, S.; Chen, X.; Torkelson, J. M. Biobased Reprocessable Polyhydroxyurethane Networks: Full Recovery of Crosslink Density with Three Concurrent Dynamic Chemistries. *ACS Sustain. Chem. Eng.* **2019**, *7* (11), 10025–10034. https://doi.org/10.1021/acssuschemeng.9b01239

234. Seychal, G.; Ximenis, M.; Lemaur, V.; Grignard, B.; Lazzaroni, R.; Detrembleur, C.; Sardon, H.; Aranburu, N.; Raquez, J. Synergetic Hybridization Strategy to Enhance the Dynamicity of Poorly Dynamic CO2-derived Vitrimers Achieved by a Simple Copolymerization Approach. *Adv. Funct. Mater.* **2025**, *35* (2), 2412268.

235. Bacsik, Z.; Ahlsten, N.; Ziadi, A.; Zhao, G.; Garcia-Bennett, A. E.; Martín-Matute, B.; Hedin, N. Mechanisms and Kinetics for Sorption of CO 2 on Bicontinuous Mesoporous Silica Modified with N-Propylamine. *Langmuir* **2011**, *27* (17), 11118–11128. https://doi.org/10.1021/la202033p

236. Didas, S. A.; Sakwa-Novak, M. A.; Foo, G. S.; Sievers, C.; Jones, C. W. Effect of Amine Surface Coverage on the Co-Adsorption of CO2 and Water: Spectral Deconvolution of Adsorbed Species. *J. Phys. Chem. Lett.* **2014**, *5* (23), 4194–4200. https://doi.org/10.1021/jz502032c

237. Bose, M.; Dhaliwal, G.; Chandrashekhara, K.; Nam, P. Role of Additives in Fabrication of Soy-based Rigid Polyurethane Foam for Structural and Thermal Insulation Applications. *J. Appl. Polym. Sci.* **2021**, *138* (45), 1–10.

https://doi.org/10.1002/app.51325

238. Pronoitis, C.; Hakkarainen, M.; Odelius, K. Structurally Diverse and Recyclable Isocyanate-Free Polyurethane Networks from CO 2 -Derived Cyclic Carbonates. *ACS Sustain. Chem. Eng.* **2022**, *10* (7), 2522–2531. https://doi.org/10.1021/acssuschemeng.1c08530

239. Leng, J.; Lu, H.; Liu, Y.; Huang, W. M.; Du, S. Shape-Memory Polymers - A Class of Novel Smart Materials. *MRS Bull.* **2009**, *34* (11), 848–855. https://doi.org/10.1557/mrs2009.235

240. Huang, W. M.; Ding, Z.; Wang, C. C.; Wei, J.; Zhao, Y.; Purnawali, H. Shape Memory Materials. *Mater. Today* **2010**, *13* (7–8), 54–61. https://doi.org/10.1016/S1369-7021(10)70128-0

241. Sessini, V.; Arrieta, M. P.; Fernández-Torres, A.; Peponi, L. Humidity-Activated Shape Memory Effect on Plasticized Starch-Based Biomaterials. *Carbohydr. Polym.* **2018**, *179* (July 2017), 93–99. https://doi.org/10.1016/j.carbpol.2017.09.070

242. Sessini, V.; Raquez, J.; Lourdin, D.; Maigret, J.; Kenny, J. M.; Dubois, P.; Peponi, L. Humidity-Activated Shape Memory Effects on Thermoplastic Starch/EVA Blends and Their Compatibilized Nanocomposites. *Macromol. Chem. Phys.* **2017**, *218* (24), 1–12. https://doi.org/10.1002/macp.201700388

243. Tundo, P.; Musolino, M.; Aricò, F. The Reactions of Dimethyl Carbonate and Its Derivatives. *Green Chem.* **2018**, *20* (1), 28–85. https://doi.org/10.1039/c7gc01764b

244. Blain, M.; Cornille, A.; Boutevin, B.; Auvergne, R.; Benazet, D.; Andrioletti, B.; Caillol, S. Hydrogen Bonds Prevent Obtaining High Molar Mass PHUs. *J. Appl. Polym. Sci.* **2017**, *134* (45), 44958. https://doi.org/10.1002/app.44958

245. Wang, H.; Liu, Q.; Zhao, X.; Jin, Z. Synthesis of Reactive DOPO-Based Flame Retardant and Its Application in Polyurethane Elastomers. *Polym. Degrad. Stab.* **2021**, *183*, 109440. https://doi.org/10.1016/j.polymdegradstab.2020.109440

246. Salmeia, K. A.; Fage, J.; Liang, S.; Gaan, S. An Overview of Mode of Action and Analytical Methods for Evaluation of Gas Phase Activities of Flame Retardants. *Polymers (Basel).* **2015**, *7* (3), 504–526. https://doi.org/10.3390/polym7030504

247. Liu, C.; Zhang, P.; Shi, Y.; Rao, X.; Cai, S.; Fu, L.; Feng, Y.; Wang, L.; Zheng, X.; Yang, W. Enhanced Fire Safety of Rigid Polyurethane Foam via Synergistic Effect of Phosphorus/Nitrogen Compounds and Expandable Graphite. *Molecules* **2020**, *25* (20), 4741. https://doi.org/10.3390/molecules25204741

248. Stachak, P.; Łukaszewska, I.; Hebda, E.; Pielichowski, K. Recent Advances in

Fabrication of Non-Isocyanate Polyurethane-Based Composite Materials. *Materials (Basel).* **2021**, *14* (13), 3497. https://doi.org/10.3390/ma14133497

249. Zhu, M.; Ma, Z.; Liu, L.; Zhang, J.; Huo, S.; Song, P. Recent Advances in Fire-Retardant Rigid Polyurethane Foam. *J. Mater. Sci. Technol.* **2022**, *112*, 315–328. https://doi.org/10.1016/j.jmst.2021.09.062
250. Tomita, H.; Sanda, F.; Endo, T. Model Reaction for the Synthesis of Polyhydroxyurethanes from Cyclic Carbonates with Amines: Substituent Effect on the Reactivity and Selectivity of Ring-opening Direction in the Reaction of Five-membered Cyclic Carbonates with Amine. *J. Polym. Sci. Part A Polym. Chem.* **2001**, *39* (21), 3678–3685. https://doi.org/10.1002/pola.10009
251. Trojanowska, D.; Monie, F.; Perotto, G.; Athanassiou, A.; Grignard, B.; Grau, E.; Vidil, T.; Cramail, H.; Detrembleur, C. Valorization of Waste Biomass for the Fabrication of Isocyanate-Free Polyurethane Foams. *Green Chem.* **2024**, *26* (14), 8383–8394. https://doi.org/10.1039/D4GC01547A
252. Bai, L.; Liu, L.; Esquivel, M.; Tardy, B. L.; Huan, S.; Niu, X.; Liu, S.; Yang, G.; Fan, Y.; Rojas, O. J. Nanochitin: Chemistry, Structure, Assembly, and Applications. *Chem. Rev.* **2022**, *122* (13), 11604–11674. https://doi.org/10.1021/acs.chemrev.2c00125
253. Moon, R. J.; Martini, A.; Nairn, J.; Simonsen, J.; Youngblood, J. Cellulose Nanomaterials Review: Structure, Properties and Nanocomposites. *Chem. Soc. Rev.* **2011**, *40* (7), 3941. https://doi.org/10.1039/c0cs00108b
254. Ren, H.; Liao, Q.; Zhou, Z.; Gao, S.; Wang, Y.; Du, X.; Yuan, B.; Zhang, H. Cellulose Nanocrystal/Phytic Acid-Enhanced Non-Isocyanate Polyurethane Foams. *Polymer (Guildf).* **2025**, *334*, 128740. https://doi.org/10.1016/j.polymer.2025.128740
255. Choe, H.; Lee, J. H.; Kim, J. H. Polyurethane Composite Foams Including CaCO3 Fillers for Enhanced Sound Absorption and Compression Properties. *Compos. Sci. Technol.* **2020**, *194*, 108153. https://doi.org/10.1016/j.compscitech.2020.108153
256. Zhao, F.; Tian, P.-X.; Li, Y.-D.; Weng, Y.; Zeng, J.-B. Fabrication of Well-Dispersed Cellulose Nanocrystal Reinforced Biobased Epoxy Composites Using Reversibility of Covalent Adaptable Network. *Int. J. Biol. Macromol.* **2023**, *244*, 125202. https://doi.org/10.1016/j.ijbiomac.2023.125202
257. Viet, D.; Beck-Candanedo, S.; Gray, D. G. Dispersion of Cellulose Nanocrystals in Polar Organic Solvents. *Cellulose* **2007**, *14* (2), 109–113. https://doi.org/10.1007/s10570-006-9093-9

258. Rueda, L.; Saralegui, A.; Fernández d'Arlas, B.; Zhou, Q.; Berglund, L. A.; Corcuera, M. A.; Mondragon, I.; Eceiza, A. Cellulose Nanocrystals/Polyurethane Nanocomposites. Study from the Viewpoint of Microphase Separated Structure. *Carbohydr. Polym.* **2013**, *92* (1), 751–757. https://doi.org/https://doi.org/10.1016/j.carbpol.2012.09.093

259. Liu, S.; Eijkelenkamp, R.; Duvigneau, J.; Vancso, G. J. Silica-Assisted Nucleation of Polymer Foam Cells with Nanoscopic Dimensions: Impact of Particle Size, Line Tension, and Surface Functionality. *ACS Appl. Mater. Interfaces* **2017**, *9* (43), 37929–37940. https://doi.org/10.1021/acsami.7b11248

260. Zhai, W.; Yu, J.; Wu, L.; Ma, W.; He, J. Heterogeneous Nucleation Uniformizing Cell Size Distribution in Microcellular Nanocomposites Foams. *Polymer (Guildf).* **2006**, *47* (21), 7580–7589. https://doi.org/https://doi.org/10.1016/j.polymer.2006.08.034

261. Rittigstein, P.; Torkelson, J. M. Polymer–Nanoparticle Interfacial Interactions in Polymer Nanocomposites: Confinement Effects on Glass Transition Temperature and Suppression of Physical Aging. *J. Polym. Sci. Part B Polym. Phys.* **2006**, *44* (20), 2935–2943. https://doi.org/https://doi.org/10.1002/polb.20925

262. Wijeratne, P. M.; Ocando, C.; Grignard, B.; Berglund, L. A.; Raquez, J.-M.; Zhou, Q. Synthesis, Thermal and Mechanical Properties of Nonisocyanate Thermoplastic Polyhydroxyurethane Nanocomposites with Cellulose Nanocrystals and Chitin Nanocrystals. *Biomacromolecules* **2025**, *26* (6), 3481–3494. https://doi.org/10.1021/acs.biomac.5c00113

263. Xu, X.; Liu, F.; Jiang, L.; Zhu, J. Y.; Haagenson, D.; Wiesenborn, D. P. Cellulose Nanocrystals vs. Cellulose Nanofibrils: A Comparative Study on Their Microstructures and Effects as Polymer Reinforcing Agents. *ACS Appl. Mater. Interfaces* **2013**, *5* (8), 2999–3009. https://doi.org/10.1021/am302624t

264. Salaberria, A. M.; Diaz, R. H.; Labidi, J.; Fernandes, S. C. M. Role of Chitin Nanocrystals and Nanofibers on Physical, Mechanical and Functional Properties in Thermoplastic Starch Films. *Food Hydrocoll.* **2015**, *46*, 93–102. https://doi.org/10.1016/j.foodhyd.2014.12.016

265. Donate-Robles, J.; Martín-Martínez, J. M. Addition of Precipitated Calcium Carbonate Filler to Thermoplastic Polyurethane Adhesives. *Int. J. Adhes. Adhes.* **2011**, *31* (8), 795–804. https://doi.org/https://doi.org/10.1016/j.ijadhadh.2011.07.008

266. Mushi, N. E.; Butchosa, N.; Salajkova, M.; Zhou, Q.; Berglund, L. A. Nanostructured

Membranes Based on Native Chitin Nanofibers Prepared by Mild Process. *Carbohydr. Polym.* **2014**, *112*, 255–263. https://doi.org/10.1016/j.carbpol.2014.05.038

267. Lemmon, E. W.; Bell, I. H.; Huber, M. L.; McLinden, M. O. Thermophysical Properties of Fluid Systems. In *NIST Chemistry WebBook*; Linstrom, P. J., Mallard, W. G., Eds.; National Institute of Standards and Technology (NIST): Gaithersburg MD. https://doi.org/https://doi.org/10.18434/T4D303

List of publications

Peer-reviewed article

- Gouveia, K., Vauloup, J., Colpaert, M., Ocando, C., Lacroix-Desmazes, P., Ladmiral, V., Caillol, S., & Raquez, J.-M.. Sustainable CO_2 Utilization as a Blowing Agent in Thermoset PHU Foam Production with Humidity-Responsive Shape Memory. *ACS Appl. Polym. Mater.* **7**, 6113–6124 (2025).

Oral presentations

- Gouveia jovel, K., Vauloup, J., Ocando, C., Lacroix-Desmazes, P., Ladmiral, V., Caillol, S., & Raquez, J.-M. "Supercritical CO_2 as an ecofriendly physical blowing agent for tailoring properties in non-isocyanate polyurethane thermoset foams". IUPAC Macro 2024, Warwick, United Kingdom. (04 July 2024).

- Gouveia, K., Vauloup, J., Ocando, C., Lacroix-Desmazes, P., Ladmiral, V., Caillol, S., & Raquez, J.-M. "Sustainable non-isocyanate polyurethane thermoset foam's design: harnessing the power of supercritical CO_2 as a blowing agent". BPG annual meeting, Blankenberge, Belgium. (31 May 2024).

Poster presentations

- Gouveia Jovel, K., Chevret L., Vauloup J., Laoutid Fouad, Ocando Connie, Lacroix-Desmazes P., Ladmiral V., Caillol S., & Raquez, J.-M. "Supercritical CO_2 as blowing agent for the eco-design of NIPU foams with superior flame retardant properties. Mardi des chercheurs, Mons, Belgium. (26 March 2024).

- Gouveia jovel, K., Ocando Cordero, C., Ladmiral V., Caillol, S., & Raquez, J.-M. "Study of the kinetics for the synthesis of novel NIPUs by continuous reactive extrusion". GEP-SLAP, San Sebastian, Spain. (12 May 2022).

- Gouveia Jovel, K., Ocando Cordero, C., Ladmiral V., Caillol S., & Raquez, J.-M. "Sustainable processes for the synthesis of non-isocyanate polyurethanes". MCAA Annual Conference, Lisbon, Portugal. (27 March 2022).